The road not taken:

Lineage bias and restriction of haematopoietic stem and progenitor cells



Joana Isabel de Teixeira Carrelha

A thesis submitted for the degree of

Doctor of Philosophy

St Cross College

Michaelmas Term 2016

I am often asked, “What made *you* become a scientist?” But I can’t stand far enough away from myself to give a really satisfactory answer, for I cannot distinctly remember a time when I did not think that a scientist was the most exciting possible thing to be.

Sir Peter B. Medawar, “Advice to a Young Scientist”, 1979

ABSTRACT

The mammalian haematopoietic system is a progressively lineage-restricted branching hierarchy that replenishes mature blood cells throughout the life of an organism. Self-renewing haematopoietic stem cells (HSCs) reside at the apex of the hierarchy and give rise to multipotent progenitors that undergo increasingly restricted lineage commitments, until they finally assume a single cell fate at the exclusion of all others. Several competing models of the haematopoietic hierarchy have been proposed, and it is yet unclear if all mechanisms of lineage commitment in definitive haematopoiesis are identical between foetal liver (FL) and adult bone marrow (BM). Herein we explored early lineage fate decisions in the first branches of the lymphoid-primed multipotent progenitor (LMPP) model of haematopoiesis.

We prospectively isolated the earliest known immune-restricted progenitor from early FL and yolk sac, prior to the establishment of definitive haematopoiesis in the embryo. These progenitors express early lymphoid-affiliated genes – recombination-activating gene 1 (*Rag1*), interleukin-7 receptor (*Il7r*), and Fms-like tyrosine kinase 3 (*Flt3*) – and were shown to be equivalent to the adult BM LMPP compartment, having robust combined lympho-myeloid potentials but little or no megakaryocyte/erythroid potentials. Moreover, the physiological contribution of this immune-restricted progenitor to embryonic myelopoiesis was conclusively demonstrated, supporting the relevance of the LMPP model of the haematopoietic hierarchy in early embryonic lymphoid commitment.

In other studies pertaining to the myeloid/megakaryocyte/erythroid branch of the LMPP model, we characterised the function of individual platelet-biased and platelet-restricted HSCs in adult BM. Based on our findings we propose a revised model of the LMPP hierarchy, with the addition of a primitive megakaryocyte-restricted pathway of HSC differentiation. In contrast, we found that platelet-biased reconstitution behaviour is very rare in FL HSCs, but is promptly acquired by FL-derived adult HSCs. Therefore, the megakaryocyte-restricted differentiation branch proposed might be exclusive to adult haematopoiesis.

ACKNOWLEDGEMENTS

I am thankful to my supervisor Professor Sten Eirik Jacobsen for the opportunity to carry out my DPhil studies in his lab, and for introducing me to the fascinating field of haematopoiesis and cutting-edge science in general.

I am also thankful to all my colleagues at the Weatherall Institute of Molecular Medicine for teaching me and helping me throughout these four years. Thank you for putting up with me during these four crazy years of hard work. Thank you especially to my closest collaborators, Dr. Charlotta Böiers, Dr. Michael Lutteropp, Dr. Tiago Luis, and Dr. Adriana Gambardella.

I am most grateful to my family and friends for always making me feel right at home even after long periods of absence.

Mãe, Pai, Vó, Mana… aqui fica uma obra para a História. Obrigada por tudo. Amo-vos muito!

TABLE OF CONTENTS

ABSTRACT **3**

ACKNOWLEDGEMENTS **4**

TABLE OF CONTENTS **5**

LIST OF FIGURES **9**

LIST OF TABLES **10**

COMMONLY USED ABBREVIATIONS **11**

COMMONLY USED ABBREVIATIONS (CONTINUED) **12**

CHAPTER 1: INTRODUCTION **13**

1.1. HAEMATOLOGY 13

1.2. HAEMATOPOIESIS 13

1.3. HAEMATOPOIETIC STEM CELLS 15

1.3.1. Haematopoietic stem cell transplantation *15*

1.3.2. Functional definition of haematopoietic stem cells *16*

1.3.3. Prospective isolation and purification of haematopoietic stem and progenitor cells *18*

1.3.4. In vitro culture of haematopoietic stem and progenitor cells *23*

1.3.5. In vivo transplantation of haematopoietic stem and progenitor cells *24*

1.3.6. In vivo tracing of the lineage potentials of haematopoietic stem cells *26*

1.4. EMBRYONIC HAEMATOPOIESIS 27

1.5. LINEAGE COMMITMENT IN THE ADULT BONE MARROW HAEMATOPOIETIC SYSTEM 31

1.5.1. The classical model of the haematopoietic hierarchy *32*

1.5.2. The myeloid-biased and LMPP models of the haematopoietic hierarchy *33*

1.5.3. Regulation of haematopoietic lineage commitment by transcription factors *38*

1.5.4. Regulation of haematopoietic lineage commitment by cytokines *38*

1.6. HETEROGENEITY OF HAEMATOPOIETIC STEM CELLS 41

1.6.1. Single cell lineage tracing by time-lapse microscopy *42*

1.6.2. Single cell lineage tracing by paired daughter cell assays *44*

1.6.3. Single cell lineage tracing by transplantation: limiting dilution *45*

1.6.4. Single cell lineage tracing by transplantation: LSK^{SP} compartment *47*

1.6.5. Single cell lineage tracing by transplantation: LSK^{SP} Rho- compartment *48*

1.6.6. Single cell lineage tracing by transplantation: comparison of lineage-bias classifications *50*

1.6.7. Single cell lineage tracing by genetic barcoding *51*
1.7. ANALYSIS OF PLATELET RECONSTITUTION 53
1.7.1. Platelet-biased LT-HSCs *53*
1.7.2. Myeloid-restricted repopulating progenitors (MyRPs) in the HSC compartment *55*
1.8. AIMS OF THE PRESENT WORK 57
CHAPTER 2: MATERIALS AND METHODS 58
2.1 MICE 58
2.1.1. Husbandry *58*
2.1.2. Mouse strains *58*
2.1.3. Timed matings *59*
2.1.4. Genotyping and phenotyping of experimental mice *60*
2.2. CELL PREPARATIONS 61
2.2.1. Embryonic tissues *61*
2.2.2. Adult tissues *62*
2.2.3. c-Kit enrichment of adult bone marrow *62*
2.2.4. Peripheral blood *63*
2.3. FLOW CYTOMETRY AND FLUORESCENCE ACTIVATED CELL SORTING 64
2.3.1 Antibody stainings *64*
2.3.2 Instruments and analysis *64*
2.4. *IN VIVO* RECONSTITUTION ASSAYS 71
2.4.1. Single cell transplantation of bone marrow and foetal liver cells *71*
2.4.2. Secondary bone marrow transplantation *72*
2.4.3. Unfractionated foetal liver transplantation *73*
2.5. *IN VITRO* CELL CULTURE ASSAYS 73
2.5.1. Lymphoid lineage potentials in stromal co-cultures *73*
2.5.2. Myeloid, megakaryocyte, and erythroid lineage potentials in liquid culture *74*
2.5.3. Myeloid, megakaryocyte, and erythroid lineage potentials in semi-solid culture *75*
2.5.4. Combined lineage potentials in switch-culture *76*
2.6. CYTOSPINS AND CELL MORPHOLOGY ANALYSIS 77
2.7. GENE EXPRESSION ANALYSIS 77
2.7.1. RNA sequencing *77*
2.7.2. Single cell RNA sequencing *78*
2.7.3. Multiplexed quantitative PCR *79*
2.8. STATISTICAL ANALYSIS 80

CHAPTER 3: LYMPHO-MYELOID HAEMATOPOIETIC PROGENITORS IN EARLY FOETAL LIVER AND YOLK SAC 83

3.1. INTRODUCTION 83

3.2. RESULTS 86

3.2.1. Early embryonic progenitors with combined lymphoid and myeloid lineage potentials in vitro 86

3.2.2. Transcriptional profile of embryonic lympho-myeloid progenitors 97

3.2.3. Expression of paired immunoglobulin-like receptors in embryonic lympho-myeloid progenitors excludes B cell potential 101

3.3. DISCUSSION 105

CHAPTER 4: PHYSIOLOGICAL CONTRIBUTION OF LYMPHOID-PRIMED HAEMATOPOIETIC PROGENITORS TO EMBRYONIC MYELOPOIESIS 108

4.1. INTRODUCTION 108

4.2. RESULTS 110

4.2.1. Rag1-expressing progenitors contribute robustly to embryonic myelopoiesis in vivo 110

4.2.2. Embryonic tissue-resident macrophages are mainly not derived from Rag1-expressing progenitors 118

4.3. DISCUSSION 122

CHAPTER 5: FUNCTIONAL AND MOLECULAR CHARACTERISATION OF PLATELET-BIASED HAEMATOPOIETIC STEM CELLS IN ADULT BONE MARROW 127

5.1. INTRODUCTION 127

5.2. RESULTS 130

5.2.1. Investigating the in vivo reconstitution behaviour of individual bone marrow Vwf+ long-term haematopoietic stem cells 130

5.2.2. In vivo lineage outputs of single Vwf^{high} LT-HSCs follow a systematic and predictable pattern 136

5.2.3. Platelet-biased peripheral blood reconstitution patterns reflect equally biased haematopoietic hierarchies 142

5.2.4. Vwf+ haematopoietic stem cells and early multipotent progenitors are expanded in the LSK compartment of platelet-biased hierarchies 150

5.2.5. Long-term haematopoietic stem cells lacking lymphoid output in vivo show lymphoid potential in vitro 157

5.2.6. Long-term haematopoetic stem cells lacking myeloid output in vivo show myeloid potential in vitro 162

5.2.7. Gene expression profile of platelet-biased haematopoetic stem cells 166
5.3. DISCUSSION 171
CHAPTER 6: IDENTIFICATION OF RARE PLATELET-BIASED HAEMATOPOIETIC STEM CELLS IN FOETAL LIVER 182
6.1. INTRODUCTION 182
6.2. RESULTS 183
6.2.1. Vwf expression in E14.5 foetal liver haematopoietic stem cells 183
6.2.2. Haematopoietic stem cells with in vivo platelet-biased behaviour are rare in E14.5 foetal liver 187
6.2.3. Balanced foetal liver haematopoietic stem cells generate bone marrow platelet-biased haematopoietic stem cells 191
6.2.4. Platelet-biased reconstitution activity in early foetal liver 194
6.3. DISCUSSION 197
CHAPTER 7: CONCLUSIONS 200
7.1. IMMUNE-RESTRICTED EMBRYONIC PROGENITORS 200
7.2. PLATELET-BIASED/RESTRICTED HAEMATOPOIETIC STEM CELLS 201
BIBLIOGRAPHY 202

LIST OF FIGURES

FIGURE 1.1. FLOW CYTOMETRY AND FLUORESCENCE ACTIVATED CELL SORTING. 21

FIGURE 1.2. SUCCESSIVE HAEMATOPOIETIC SITES DURING DEVELOPMENT OF MAMMALIAN EMBRYOS. 30

FIGURE 1.3. COMPETING MODELS OF THE HAEMATOPOIETIC HIERARCHY. 37

FIGURE 3.1. EXPRESSION OF LYMPHOID COMMITMENT MARKERS IN EARLY EMBRYONIC CD45+ C-KIT+ PROGENITORS. ...90

FIGURE 3.2. IL7RA+ FLT3+ EMBRYONIC PROGENITORS SHOW LYMPHOID AND MYELOID POTENTIALS BUT LACK MEGAKARYOCYTE AND ERYTHROID POTENTIALS *IN VITRO*. 94

FIGURE 3.3. TRANSCRIPTIONAL PRIMING OF LYMPHO-MYELOID EMBRYONIC PROGENITORS. 100

FIGURE 3.4. PAIRED IMMUNOGLOBULIN-LIKE RECEPTORS IN FOETAL LIVER PROGENITORS. 104

FIGURE 4.1. LINEAGE TRACING IN *RAG1*-CRE/*R26*R-EYFP EMBRYOS AND ADULT MICE. 114

FIGURE 4.2. EMBRYONIC *RAG1*-EXPRESSING PROGENITORS GENERATE BOTH MONOCYTES AND GRANULOCYTES *IN VIVO* AND *IN VITRO*. 117

FIGURE 4.3. EMBRYONIC *RAG1*-EXPRESSING PROGENITORS DO NOT CONTRIBUTE SIGNIFICANTLY TO TISSUE-RESIDENT MACROPHAGES. 121

FIGURE 5.1. THE VWF-TDTOMATO/GATA1-EGFP DOUBLE REPORTER MOUSE. 132

FIGURE 5.2. SINGLE CELL TRANSPLANTATION OF BONE MARROW *VWF*^{HIGH} LONG-TERM HAEMATOPOIETIC STEM CELLS AND PERIPHERAL BLOOD ANALYSIS BY FLOW CYTOMETRY. 134

FIGURE 5.3. RESTRICTION OF LINEAGE OUTPUTS IN MICE RECONSTITUTED BY SINGLE *VWF*^{HIGH} LONG-TERM HAEMATOPOIETIC STEM CELLS FOLLOWS A SYSTEMATIC AND PREDICTABLE ORDER. 141

FIGURE 5.4. FLOW CYTOMETRIC ANALYSIS OF THE DONOR-DERIVED HAEMATOPOIETIC HIERARCHY IN RECIPIENTS OF SINGLE *VWF*^{HIGH} LONG-TERM HAEMATOPOIETIC STEM CELLS. 148

FIGURE 5.5. *VWF*+ HAEMATOPOIETIC STEM CELLS AND EARLY MULTIPOTENT PROGENITORS ARE EXPANDED IN THE DONOR-DERIVED LIN- SCA-1+ C-KIT+ COMPARTMENT OF MICE WITH PLATELET-BIASED RECONSTITUTION PATTERNS. 154

FIGURE 5.6. HAEMATOPOIETIC STEM CELLS LACKING T CELL OUTPUT *IN VIVO* SHOW T CELL POTENTIAL *IN VITRO*. 161

FIGURE 5.7. HAEMATOPOIETIC STEM CELLS LACKING MYELOID OUTPUT *IN VIVO* SHOW MYELOID POTENTIAL *IN VITRO*. ...165

FIGURE 5.8. GENE EXPRESSION PROFILE OF PLATELET-BIASED HAEMATOPOETIC STEM CELLS BY SINGLE CELL RNA SEQUENCING. 169

FIGURE 5.9. PROPOSED MODEL FOR THE ESTABLISHMENT OF PLATELET-BIASED HIERARCHIES BY *VWF*+ HAEMATOPOETIC STEM CELLS THROUGH A NOVEL BRANCH OF MEGAKARYOCYTE LINEAGE DIFFERENTIATION. 181

FIGURE 6.1. *VWF* EXPRESSION IN E14.5 FOETAL LIVER HAEMATOPOIETIC STEM CELLS. 186

FIGURE 6.2. PLATELET-BIASED HAEMATOPOIETIC STEM CELLS ARE RARE IN E14.5 FOETAL LIVER. 190

FIGURE 6.3. PLATELET-BIASED RECONSTITUTION BEHAVIOUR BY ADULT BONE MARROW *VWF+* FOETAL LIVER-DERIVED HAEMATOPOIETIC STEM CELLS. 193

FIGURE 6.4. PLATELET-BIASED REPOPULATION ACTIVITY IN EARLY FOETAL LIVER. 196

LIST OF TABLES

TABLE 1.1. PHENOTYPIC DEFINITIONS OF MURINE BONE MARROW HAEMATOPOIETIC STEM CELLS. 22
TABLE 2.1. ANTIBODIES USED IN FLOW CYTOMETRY. 66
TABLE 2.2. LINEAGE MARKERS USED FOR LINEAGE EXCLUSION GATING IN FLOW CYTOMETRY. 69
TABLE 2.3. OPTICAL SYSTEM SETTINGS FOR FLOW CYTOMETRY. 70
TABLE 2.4. TAQMAN ASSAYS USED IN MULTIPLEXED QUANTITATIVE PCR. 81
TABLE 5.1. DONOR-DERIVED RECONSTITUTION BIASES AND PATTERNS DERIVED FROM SINGLE CELL TRANSPLANTATION OF *VWF*^{HIGH} LONG-TERM HAEMATOPOIETIC STEM CELLS. 139
TABLE 5.2. RECONSTITUTION OF HAEMATOPOIETIC CELL COMPARTMENTS IN BLOOD, SPLEEN, THYMUS AND BONE MARROW OF RECIPIENTS OF SINGLE *VWF*^{HIGH} LONG-TERM HAEMATOPOIETIC STEM CELLS. 149
TABLE 5.3. PROPAGATION OF PLATELET-BIASED RECONSTITUTION IN SECONDARY TRANSPLANTATION. 156
TABLE 6.1. PLATELET-BIASED RECONSTITUTION BEHAVIOUR UPON SECONDARY TRANSPLANTATION OF BALANCED FOETAL LIVER–DERIVED HAEMATOPOIETIC STEM CELLS. 192
TABLE 6.2. RECONSTITUTION PATTERNS OBTAINED FROM TRANSPLANTATION OF EARLY FOETAL LIVERS. 195

COMMONLY USED ABBREVIATIONS

7AAD: 7-amino-actinomycin D

AGM: aorta-gonad-mesonephros

BFU-E: burst forming unit-erythroid

BM: bone marrow

Bi: bias

CD: cluster of differentiation

CFU-GM: colony forming unit-granulocyte-macrophage

CFU-G: colony forming unit-granulocyte

c-Kit: proto-oncogene c-Kit / CD117 antigen

CLP: common lymphoid progenitor

CMP: common myeloid progenitor

DAPI: 4', 6-diamidine-2-phenylidole dihydrochloride

DN: double negative

DP: double positive

E: embryonic day (for example E11.5)

FACS: fluorescence-activated cell sorting

FL: foetal liver

Flt3: fms-like tyrosine kinase 3 / CD135 antigen

GFP: green fluorescent protein

GM: granulocyte-macrophage

GMP: granulocyte-macrophage progenitor

HSC: haematopoietic stem cell

HSPCs: haematopoietic stem and progenitor cells

IL-7Rα: interleukin-7 receptor alpha

COMMONLY USED ABBREVIATIONS (CONTINUED)

Lin: collection of mature lineage markers

LMPP: lymphoid-primed multipotent progenitor

LSK: cell compartment phenotypically defined as Lin- Sca1+ cKit+

LT-HSC: long-term repopulating haematopoietic stem cell

Ly: lymphoid

Mk: megakaryocyte

Mk/E: megakaryocyte-erythroid

MkP: megakaryocyte progenitor

MPP: multipotent progenitor

mRNA: messenger ribonucleic acid

My: myeloid

PB: peripheral blood

Plt: platelet

Pre-CFU-E: pre-colony forming unit-erythroid progenitor

Pre-GM: pre-granulocyte-macrophage progenitor

Pre-MegE: pre-megakaryocyte-erythroid progenitor

Rag1: recombination-activating gene 1

qPCR: quantitative polymerase chain reaction

Vwf: von Willebrand factor

EYFP: enhanced yellow fluorescent protein

YS: yolk sac

CHAPTER 1: Introduction

1.1. Haematology

Haematology – the study of blood, its components and its diseases – is a long-standing field of study. Macroscopic analysis of the blood and bloodletting were practiced as forms of disease treatment as far back as ancient Egypt and ancient Greece. The ancient Greek physician Galen published the first observations regarding blood circulation in the 2nd century A.D., but it was only in the early 17th century that William Harvey and Marcello Malpighi produced a more accurate and detailed description of the cardiovascular system. Later in the 17th century, Jan Swammerdam and Antoni van Leeuwenhoek first observed and described blood erythrocytes at a microscopic level. By the end of the 19th century, platelets and leucocytes had also been identified, and Paul Ehrlich had developed staining techniques to distinguish between the different leucocyte lineages. The foundations for the field of haematology were thus established, and the origin of the different cellular components of the blood became a major scientific question.

1.2. Haematopoiesis

Blood is constituted by several cellular components with distinct specialised functions. Erythrocytes transport oxygen to the tissues, platelets (derived from megakaryocytes) mediate blood clotting in the case of injury, and leucocytes (myeloid cells, lymphoid cells, and dendritic cells) constitute the immune system (Wickrema and Kee, 2009). Monocytes/macrophages, granulocytes (basophils, eosinophils, and the more abundant neutrophils) and mast cells are the myeloid cells that comprise the innate immune system. This system provides an immediate first line of defence against infection from bacteria,

fungi, and parasites, and mediates inflammatory and allergic responses. T cells, B cells, and natural killer (NK) cells are the lymphoid cells that comprise the adaptive immune system. This system mounts a more sophisticated and targeted response against different types of pathogens including viruses, and also against deregulated cancerous cells. Adaptive immune responses take longer to develop than innate responses, but they result in long-lasting enhanced protection against repeated re-infection by the same pathogens (immunological memory) (Murphy, 2014). At the interface between the two immune systems are dendritic cells (DC), which play a critical role in the activation of adaptive immune responses (Mildner and Jung, 2014; Iwasaki and Medzhitov, 2015). Recently identified innate lymphoid cells (ILC) have also been shown to play important parts in the regulation of the adaptive immune system and in tissue homeostasis after infection (Spits and Cupedo, 2012; Walker et al., 2013; Hepworth and Sonnenberg, 2014).

Blood is one of the most dynamic and highly regenerative tissues. The life span of the majority of mature blood cells is relatively limited, and they need to be frequently replenished throughout the life of an organism. It is estimated that one trillion blood cells are replaced every day in the body of an adult human (Ogawa, 1993).

Haematopoiesis is the process by which all blood cells are formed. The main anatomic haematopoietic sites of vertebrates change sequentially throughout development (Zon, 1995). In adult mammals, normal haematopoiesis occurs primarily in the bone marrow (BM) and, to a much lesser extent, in liver and spleen (Nijhof et al., 1993; Broudy et al., 1996; Taniguchi et al., 1996). Surges of increased extramedullary haematopoiesis are commonly associated with disease (Johns and Christopher, 2012).

Haematopoiesis is carried out through a complex cellular hierarchy arising from a common cell precursor: the haematopoietic stem cell (HSC).

1.3. Haematopoietic stem cells

A major advancement in the field of haematology, and arguably one of the greatest biological discoveries of the 20th century, was the identification of HSCs. Artur Pappenheim, Wera Dantschakoff, and Alexander Maximow were early proponents of the existence of a common precursor for all blood cell types (unitarian theory of haematopoiesis) at the turn of the century (Ramalho-Santos and Willenbring, 2007; Maehle, 2011), but the hallmark properties of HSCs – multilineage differentiation and sustained self-renewal – were only demonstrated 50 years later, in the 1950-60's.

1.3.1. Haematopoietic stem cell transplantation

Following the atomic bomb explosions in Japan at the end of World War II, it was recognised that exposure to radiation resulted in compromised ability to regenerate blood leucocytes and platelets, which eventually became lethal. Biomedical research efforts were then directed towards the understanding of the biological effects of ionizing radiation exposure, and how to treat them.

Early studies of inbred mice showed that shielding the spleen or one femur with lead conferred protection against the lethal effects of whole body X-irradiation (Jacobson et al., 1949; Jacobson et al., 1951). Shortly after it was demonstrated that intravenous or intra-peritoneal injection of spleen or BM cell suspensions from healthy mice also conferred the same protection on irradiated mice (Lorenz et al., 1951). It was at first debated if the protective effect observed was due to secreted factors produced by spleen and BM that promoted repair of irradiation damage in endogenous cells (Jacobson et al., 1951), or instead due to a direct blood-forming ability from cellular components of these tissues (Barnes and Loutit, 1954). Through the use of techniques that allowed the distinction

between endogenous cells of the recipient mouse and injected cells of the donor mouse, it was demonstrated that the blood system of irradiated animals was directly regenerated by transplanted cells, rather than by repaired endogenous cells (Ford et al., 1956; Nowell et al., 1956; Vos et al., 1956).

1.3.2. Functional definition of haematopoietic stem cells

In the 1960's the use of X-irradiation was being evaluated in the treatment of metastatic cancer, as a method to eliminate highly proliferative cancer cells. It was therefore necessary to quantitatively compare the sensitivity of cancer cells and normal cells to this treatment.

The ground-breaking studies for the field of stem cell research that were conducted by James Till and Ernest McCulloch began as a quantification of the radiation sensitivity of limiting numbers of normal BM cells, using the radiation-protective transplantation method. They discovered that irradiated mice that were injected with less than a fully protective dose of BM cells, and consequently died within approximately 2 weeks, developed spleen colonies comprised of myeloid cells, erythrocytes, and megakaryocytes. The number of these spleen colonies was directly correlated to the number of BM cells transplanted, which suggested that each heterogeneous colony could be derived from a single BM precursor (Till and McCulloch, 1961). To investigate the clonality of spleen colonies (whether all blood cells in a colony were derived from the same precursor), the donor cells were marked before transplantation. This was accomplished by irradiation-induced chromosome breaks, which lead to the formation of unique DNA lesions when repaired, lesions that are passed down to all progeny of a dividing cell. With this method it was confirmed that all different types of blood cells found in a single spleen colony were marked by the same unique chromosome repair lesion, and therefore were generated by the same blood-forming cell (Becker et al., 1963). These studies provided the first example of a short-term quantitative *in vivo* assay for

the proliferation and differentiation capacity of HSCs, a technique now commonly known as colony-forming unit-spleen (CFU-S) assay.

In further studies the cells from individual spleen colonies were re-transplanted into new lethally irradiated mice. By counting the spleen colonies generated in both primary and secondary recipients the numbers of CFU in the original BM cell suspension and within the primary spleen colonies were estimated. Cells from several primary spleen colonies were able to give rise to secondary spleen colonies, and it was concluded that CFU cells have self-renewal ability (Siminovitch et al., 1963), although it was also noted that functional self-renewal can be exhausted over the course of multiple re-transplantations (Siminovitch et al., 1964). A few years later it was also demonstrated that CFU cells were not only able to generate myeloid, erythroid, and megakaryocytic progeny, but also lymphoid progeny (Wu et al., 1968).

Together the above studies demonstrated the existence of BM CFUs with the capacity, at the single cell level, for extensive proliferation (formation of macroscopic colonies from a single cell), multipotent differentiation (production of many differentiated blood cell types), and self-renewal (re-generation of colonies in re-transplantation), the three hallmark characteristics of HSCs. Because of these characteristics, a single HSC is capable of sustaining long-term repopulation of the entire haematopoietic system (Osawa et al., 1996).

With the advent of HSC purification techniques it was later clarified that the majority of spleen colonies analysed at 8-12 days post-transplantation are derived from more mature haematopoietic progenitors, rather than HSCs (Jones et al., 1990; Na Nakorn et al., 2002). This is not unexpected considering the short-term nature of the CFU-S assay, and nevertheless a fraction of the later spleen colonies does correspond to the activity of real HSCs. The key conclusions drawn from the 1960's CFU-S studies remain sound, and those experiments helped pave the way for modern stem cell research (Weissman, 2006).

1.3.3. Prospective isolation and purification of haematopoietic stem and progenitor cells

HSCs were first identified retrospectively by their function, but the rarity of these cells – only 0.01% to 0.05% of total nucleated BM cells (Domen and Weissman, 1999) – makes prospective isolation imperative for further characterisation and eventual clinical use.

The first attempts at HSC isolation through sedimentation were pursued following the discoveries from the CFU-S assay (Miller and Phillips, 1969; Worton et al., 1969a, b). Isolation of purer fractions of cells with HSC activity from mouse (Morstyn et al., 1980; Müller-Sieburg et al., 1986; Spangrude et al., 1988) and human (Sutherland et al., 1989; Baum et al., 1992; Bhatia et al., 1997) based on the expression of specific cell surface antigens was developed much later, in the 1980-90's (Weissman and Shizuru, 2008). This was largely driven by increased availability of monoclonal antibodies, as well as advances in flow cytometry and fluorescence activated cell sorting (FACS) technology. Flow cytometry and FACS have become an integral part of the haematopoiesis research field, allowing for the isolation of many highly purified populations of haematopoietic stem and progenitor cells (HSPCs) and differentiated blood cell populations for biological and biochemical studies. Other cell sorting methods, such as magnetic activated cell sorting (MACS) (Miltenyi et al., 1990), are also commonly used in order to quickly achieve an enrichment of the cell type of interest in a heterogeneous cell suspension, and thus increase the speed and efficiency of the subsequent high level purification step performed by FACS.

Combinations of several cell surface antigens can be simultaneously targeted by fluorophore-conjugated monoclonal antibodies (fluorochromes) in order to distinguish between different HSPC populations. Expression of fluorescent proteins in reporter mouse lines, such as *Vwf*-EGFP (Sanjuan-Pla et al., 2013), can also be used for HSPC identification. In

flow cytometry, emission of fluorescence by fluorochromes and fluorescent proteins is stimulated by laser beams, and these emission signals are quantified for each individual cell, together with the information regarding cell size and granularity that is conveyed by forward scatter (FSC) and side-scatter (SSC) of light, respectively. These signals can be used to identify cells of interest in a heterogeneous cell suspension, and then an electrostatic charge can be selectively applied to sort them into a chosen collection tube or plate (Figure 1.1).

HSPC populations are most commonly identified by their expression or lack of expression of 4-6 cell surface antigens, and simultaneous absence of lineage markers for differentiated cells (lineage negative, Lin-). In mouse BM, HSCs and multipotent progenitors (MPP) reside within the Lin-, proto-oncogene c-Kit positive (c-Kit+ or CD117+), stem cell antigen-1 positive (Sca-1+ or Ly-6A/E+) compartment (LSK or KSL compartment). Other commonly used HSC/MPP cell surface antigens include CD90.1 (Thy1.1), CD93 (AA4.1), CD41, CD34, CD150, CD48, CD244, and Fms-like tyrosine kinase 3 (Flt3, Flk2, CD135). Another characteristic used to prospectively isolate HSCs is their capacity for retention or efflux of cell-permeant dyes, such as Rhodamine (Bertoncello et al., 1985; Spangrude and Johnson, 1990) and Hoechst (which defines the so-called side population, SP) (Goodell et al., 1996; Goodell et al., 1997). An overview of the phenotypic definitions of murine BM HSC populations over the years is presented in Table 1.1. Importantly, although modern strategies for prospective isolation of murine HSCs yield highly purified populations that are homogeneous in regards to cell surface phenotype and total long-term self-renewal ability *in vivo* (Goodell et al., 1996; Camargo et al., 2006), they do not yet provide the ability to dissect the full heterogeneity of HSC populations in regards to their differentiation ability (Schroeder, 2010; Copley et al., 2012; Müller-Sieburg et al., 2012; Ema et al., 2014; Krieger and Simons, 2015). Populations of prospectively isolated MPPs and more committed progenitors also still contain considerable functional heterogeneity that requires further investigation (Lai et al., 2005;

Paul et al., 2015; Pietras et al., 2015). Single cell level approaches for the dissection of differentiation heterogeneity within HSCs are discussed in section 1.6.

The diversity of marker combinations for HSPCs frequently leads to an inability to accurately compare data from different studies regarding the same cell type, because the definition of the cell type of interest is not identical between different research groups. A consensus phenotypic definition for each HSPC population would enable more meaningful data comparisons between studies (Akashi et al., 2005). Importantly, the expression of some antigens, such as CD34, can fluctuate with cell cycle and metabolic state (Ogawa, 2002). Moreover, due to variation in haematopoietic gene expression throughout development, phenotypic definitions do not correspond perfectly between adult BM and embryonic tissues, such as the aorta-gonad-mesonephros region (AGM) and foetal liver (FL) (Matsuoka, 2001; Mikkola and Orkin, 2006; McKinney-Freeman et al., 2009).

The different cell compartments involved in human haematopoiesis are not as well characterised as in mouse. Although mouse and human HSPCs share some known cell surface markers, there are many differences between the definitions used to identify equivalent cell populations in the two species (Majeti et al., 2007; Doulatov et al., 2012; Yokota et al., 2012).

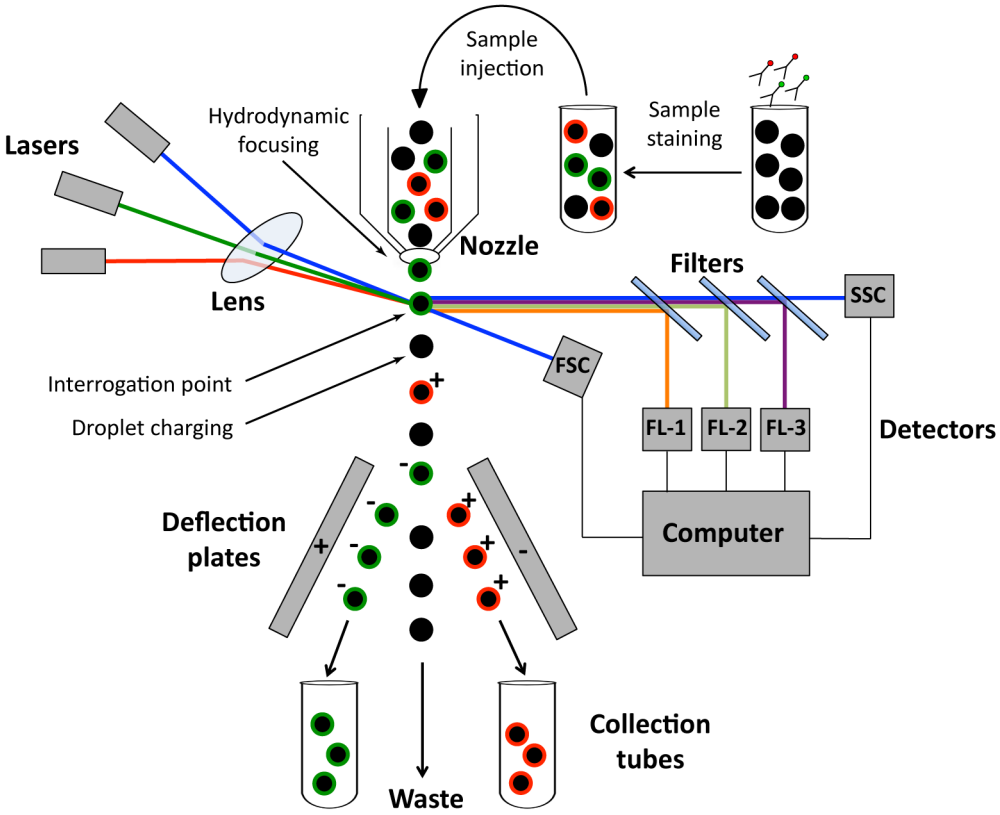

Figure 1.1. Flow cytometry and fluorescence activated cell sorting.

Heterogeneous cell suspensions labelled by fluorochromes are injected into the flow cytometer by the fluidics system. Passage through a nozzle produces a stream of droplets containing single cells that can be interrogated by the detection system, in a process called hydrodynamic focusing. Each hydrodynamically focused cell is probed by beams of light from lasers of single wavelength. Light scattering and fluorescence signals from fluorochromes are emitted by the interrogated cell in a mixture of wavelengths and captured by several photodetectors, each corresponding to separate fluorescence channels. The specificity of detection in each channel is controlled by optical filters that absorb (block) specific wavelengths of emitted light and transmit others. In a cell sorter, the scatter and fluorescence signals detected for each cell are compared to the selection criteria defined by the user. If a cell matches the sort criteria, the fluid droplet containing it is charged when exiting the nozzle of the fluidics system. Droplets then pass through an electrostatic field and, based on their charge, are deflected at a set angle into collection tubes or plates.

Table 1.1. Phenotypic definitions of murine bone marrow haematopoietic stem cells.

Population	Phenotype	Reference
LT-HSC	Thy-1.1^{low} Lin- Sca-1+	Spangrude et al. (1988)
	LSK CD34$^{-/low}$	(Osawa et al., 1996)
	LSK SP	(Goodell et al., 1996)
	LSK Flt3-	(Adolfsson et al., 2001)
	Lin- CD45^{mid} Rho^{low} SP	(Uchida et al., 2003)
	LSK CD150+ CD244- CD48-	(Kiel et al., 2005)
	LSK CD150+ CD34- CD48- CD41-	(Wilson et al., 2008)
	CD45+ CD150+ CD48- EPCR+	(Kent et al., 2009)
	LSK CD34- CD150^{high}	(Morita et al., 2010)
	LSK CD150+ CD48- Flt3-	(Pietras et al., 2015)
	EPCR^{high} CD48- CD150+ Sca1^{high}	(Wilson et al., 2015)
ST-HSC	LSK CD34+ Flt3-	(Yang et al., 2005)
	LSK CD150- CD34+	(Morita et al., 2010)
	LSK CD150- CD48- Flt3-	(Pietras et al., 2015)

HSC, haematopoietic stem cell. LT, long-term. ST, short-term. LSK, Lineage- c-Kit+ Sca-1+. Rho, rhodamine. SP, side population.

1.3.4. *In vitro* culture of haematopoietic stem and progenitor cells

In vitro cultures were early on identified as surrogate methods of testing the clonogenic activity and lineage differentiation abilities of HSPCs (Pluznick and Sachs, 1965; Bradley and Metcalf, 1966), as well as the effects of external factors on the function of these cells (Curry and Trentin, 1967a, b; Wolf and Trentin, 1968). Many *in vitro* differentiation assays are now well established in the field (Pereira et al., 2007), but maintenance of full HSC self-renewal capacity *in vitro*, which is especially relevant for future clinical applications, still requires extensive optimisation (Sauvageau et al., 2004; Chou et al., 2010).

Standard *in vitro* differentiation systems consist of culturing enriched cell suspensions or highly purified cell populations in commercially available semi-solid matrices or liquid media supplemented with appropriate cocktails of cytokines and growth factors, for time periods that range from a few days to several weeks, depending on assay purpose. The specific media formulation for each assay is based on our increasing understanding of the factors that regulate proliferation and differentiation of HSPCs (Lotem and Sachs, 2002; Kaushansky, 2006). While myeloerythroid lineage potential is commonly assessed in semi-solid or liquid cultures, B and T lymphocyte differentiation typically requires the use of specialised co-culture systems (Whitlock and Witte, 1982; Nakano et al., 1994; Schmitt and Zúñiga-Pflücker, 2002). *In vitro* co-culture can also be used for selective expansion of rare primitive HSPC populations for subsequent assays requiring large cell numbers (Lu et al., 1996). The majority of *in vitro* assays are designed to generate lineage-restricted output or mixed myeloerythroid outputs, but some methods have also been developed for the analysis of combined lymphoid and myeloid lineage potentials at the single cell level (Kawamoto et al., 1997; Mansson et al., 2007). Differentiated cells produced in *in vitro* cultures are commonly assessed by immunostaining coupled with flow cytometry or fluorescence microscopy, or by histochemical staining coupled with bright field microscopy for morphological analysis.

1.3.5. *In vivo* transplantation of haematopoietic stem and progenitor cells

Animal models, and especially mice, are critical tools for *in vivo* analysis of the haematopoietic system. The gold-standard for detection of long-term HSC self-renewal activity is *in vivo* reconstitution of haematopoiesis in pre-conditioned mice (Domen and Weissman, 1999). Pre-conditioning typically consists of whole body irradiation and is used to ablate endogenous haematopoiesis before transplantation of the donor cells of interest, which can be heterogeneous cell mixtures or highly purified populations, and can be as few as a single cell (Osawa et al., 1996).

After transplantation, the presence of donor-derived cells is assessed at several time points in peripheral blood and/or other haematopoietic tissues of recipient mice. Reconstitution of circulating granulocytes, due to their short life span, is considered to be the best reflection of HSC self-renewal ability. The contribution of donor cells and recipient cells to haematopoiesis can be distinguished by the expression of distinct markers. These markers are commonly different allelic versions of the same protein-coding gene (congenic markers), which can be detected by different monoclonal antibodies. Another common method of distinction is the detection of fluorescent proteins that are only expressed by the donor cells or the host cells. Older methods also include induction of unique marks in the non-coding DNA of donor cells that can be detected by molecular techniques, and also detection of the Y-chromosome in male donor cells transplanted into a female recipient.

In transplantation assays, the cells of interest must be transplanted along with a known source of HSCs (typically unfractionated BM cells) that can ensure recipient survival in the absence or delay of repopulation activity from the test sample. The number and type of support cells used depends on experimental design (Purton and Scadden, 2007). When assaying a highly purified cell population or performing limiting dilutions of an HSC source, the smallest possible amount of wild-type cells, or cells with diminished competitive ability,

may be used as support. These assays are highly sensitive in the detection of HSC activity, and are especially useful when transplanting single purified HSCs, but they are not designed for direct comparison of the functional differences between the population of interest and a known competitive standard of HSCs (Camargo et al., 2006). In competitive assays, in which the objective is to compare the functional potential of an unknown or modified source of HSCs (such as BM from mutated mouse models) to the potential of a normal wild-type source of HSCs, a standard amount of donor and competitor cells is used (Harrison, 1980; Harrison et al., 1993). If relevant, support/competitor cells can be distinguished from donor cells and recipient cells in the reconstitution analysis, but very frequently the same markers are used for both support/competitors cells and recipient cells.

Serial reconstitution, in which the tissues of a reconstituted recipient are used as the source of HSCs for a subsequent transplantation, can be used to further test the lifespan and expansion limits of HSCs. HSCs are historically classified as long-term (LT-HSC) and short-term (ST-HSC) based on the duration of their repopulation of irradiated mice. ST-HSCs are commonly defined as contributing to granulocyte reconstitution for only 2 months (8 weeks), and are not serially transplantable. LT-HSCs are defined as contributing to granulocyte reconstitution for at least 4 months (16 weeks), and are serially transplantable. However, intermediate-term HSCs (IT-HSCs) phenotypically defined as LSK CD34- Rho^{low} CD49b+ were recently proposed to contribute to granulocyte reconstitution for up to 8 months (32 weeks). This suggests a need to analyse blood reconstitution more than 8 months post-transplantation in order to identify true LT-HSCs (Benveniste et al., 2010). In contrast to highly purified populations of HSCs, multipotent progenitors further downstream have very limited repopulating ability *in vivo* (Oguro et al., 2013).

1.3.6. *In vivo* tracing of the lineage potentials of haematopoietic stem cells

Cell isolation and subsequent transplantation into lethally irradiated mice involves the induction of non-physiological signals within the recipient and within the transplanted donor cells, and therefore the lineage potentials expressed by HSCs in transplantation assays may not always reflect their normal physiological activity, meaning the lineage outputs that these cells naturally produce in unperturbed conditions. Genetic lineage tracing assays allow the tracking of the lineage outputs of a cell population in unperturbed steady-state conditions *in vivo*. The most commonly used lineage tracing method in the haematopoiesis field consists of intracellular labelling of a cell population of interest and all its progeny through Cre/Lox recombination (Sauer and Henderson, 1988), typically Cre recombinase-driven expression of fluorescent proteins. In this method the Cre recombinase gene is placed under the control of an endogenous promoter specifically expressed by the cell population of interest, and a fluorescent protein gene baring a floxed transcriptional stop sequence is inserted into a ubiquitously expressed endogenous locus, such as ROSA26 (Srinivas et al., 2001a). When the promoter is activated in the cells of interest, Cre recombinase is expressed and mediates the irreversible excision of the floxed stop sequence in the fluorescent protein gene. The recombined fluorescent protein gene is transmitted to daughter cells upon cell division, thus both the population of interest and its progeny are fluorescently labelled, and can be analysed by flow cytometry and fluorescence microscopy.

A variety of mouse models with constitutive or inducible (Hayashi and McMahon, 2002; Belteki et al., 2005; Yu et al., 2005; Feil et al., 2009) haematopoietic Cre/Lox systems have been developed, namely with pan-haematopoietic promoters – such as *Vav*-Cre and *Mx1*-Cre (Georgiades et al., 2002; Siegemund et al., 2015) – or lineage-specific promoters – such as *Csf1r*-Cre and *LysM*-Cre for the myeloid lineage (Hume, 2011), CD2-Cre for the B and T cell

lineages (de Boer et al., 2003), *Mb1*-Cre and *CD19*-Cre for the B cell lineage (Rickert et al., 1997; Hobeika et al., 2006), and *Pf4*-Cre for the megakaryocyte lineage (Tiedt et al., 2007). However, the early expression of lineage-affiliated genes in upstream HSPC multipotent or oligopotent compartments can limit the use of the so-called lineage-specific promoters, and this must be taken into account in experimental design (Calaminus et al., 2012; Siegemund et al., 2015). For many discrete progenitor compartments unique promoters able to faithfully and specifically drive Cre recombinase-mediated labelling in the cells of interest have not yet been identified.

Lineage tracing of single cells can be accomplished *in vitro* by time-lapse microscopy (Wu et al., 2007; Schroeder, 2011; Kokkaliaris et al., 2012) and by analysis of daughter and granddaughter cell pairs (Ema et al., 2000; Takano et al., 2004). Novel methods of single cell level lineage tracing *in vivo* through genetic barcoding have also been developed (Gerrits et al., 2010; Lu et al., 2011; Grosselin et al., 2013; Sun et al., 2014; Zanatta et al., 2014; Busch et al., 2015). These methods are discussed in section 1.6.7.

1.4. Embryonic haematopoiesis

Ontogeny of the mammalian haematopoietic system is characterised by two waves of haematopoiesis in the embryo. The first wave starts at embryonic day E7-7.5 and consists of transient cell populations that ensure survival of the early embryo. The second wave depends on definitive HSCs (dHSCs) that emerge at E10.5 and later establish adult haematopoiesis (Medvinsky et al., 2011). Both waves of haematopoietic cells migrate to the FL, but only dHSCs are believed to also subsequently colonise BM and give rise to adult haematopoiesis. The production and expansion of haematopoietic cells throughout the two waves occurs in temporally successive but partially overlapping sites, including yolk sac (YS),

placenta, AGM, and FL (Figure 1.2) (Dzierzak and Speck, 2008; Ottersbach et al., 2010; Medvinsky et al., 2011).

The first haematopoietic cells detected in the mouse are large nucleated erythrocytes formed from YS mesoderm at E7-7.5, in structures called blood islands, and slightly later primitive megakaryocyte and macrophages are also generated there (Palis et al., 1999; Palis and Yoder, 2001; Bertrand et al., 2005; Tober et al., 2007; Baron, 2013). These early cells were termed "primitive" due to the fact that they are morphologically more immature than their BM-derived counterparts, and resemble blood cells from lower vertebrates. It is not known whether the primitive lineages that emerge in the YS are part of a hierarchical program, similarly to adult haematopoiesis, or whether they develop independently from subsets of mesoderm cells (McGrath and Palis, 2005). Nevertheless, YS-derived haematopoiesis does not consist only of primitive cells. YS also generates definitive-like haematopoietic lineages, including lymphoid cells, that transiently populate the FL starting at around E9.5 (Lux et al., 2008; Frame et al., 2013; McGrath et al., 2015).

In the 1970's, early *in vitro* colony assays and transplantations of tissues from the murine embryo suggested that the YS was the ultimate source of the adult haematopoietic system (Moore and Metcalf, 1970; Weissman et al., 1978; Cumano and Godin, 2007; Dzierzak and Speck, 2008). In contrast, inter-species and intra-species tissue-grafting experiments in avian and amphibian embryos demonstrated that YS is not the source of adult haematopoiesis in non-mammalian vertebrates (Godin and Cumano, 2005; Dzierzak and Medvinsky, 2008; Dzierzak and Speck, 2008). The controversy regarding this subject remained for over 20 years, until advances in tissue culture and transplantation techniques allowed the demonstration that HSCs with substantial long-term multilineage repopulating activity emerge around E10.5 in the AGM region of the embryo proper, and in the vitelline and

umbilical arteries (Medvinsky et al., 1993; Müller et al., 1994; Medvinsky and Dzierzak, 1996). Only after E10.5 are dHSCs also found in placenta, YS, and FL (Müller et al., 1994; Medvinsky and Dzierzak, 1996; Ottersbach and Dzierzak, 2005). Connection between embryonic and yolk-sac vasculatures and formation of a beating heart tube occurs by E8.25-E8.5 (Delassus and Cumano, 1996; McGrath et al., 2003), thus allowing circulation of haematopoietic cells between different intra-embryonic and extra-embryonic sites. Studies of embryonic and extra-embryonic tissues explanted pre-circulation suggest that only intra-embryonic haematopoietic cells are capable of long-term multilineage repopulation of lethally irradiated adult recipients (Cumano et al., 2001; Cumano and Godin, 2001). Although FL environment may promote expansion of AGM-derived HSC numbers (Ema and Nakauchi, 2000; Takeuchi et al., 2002), additional spatial and temporal considerations suggest that both YS and placenta also strongly contribute to the FL HSC pool (Kumaravelu et al., 2002; Alvarez-Silva et al., 2003; Ottersbach and Dzierzak, 2005). This could occur through expansion of AGM-derived HSCs as in FL, or by *de novo* generation of HSCs. There is no direct evidence of dHSC emergence in YS, but the placental vasculature has been shown to be a true site of multipotent HSC generation in the absence of circulation (Rhodes et al., 2008; Ottersbach and Dzierzak, 2010). The allantois and the chorion, extra-embryonic membranes which contribute to the formation of the placenta and umbilical cord, have also been shown to have intrinsic haematopoietic potential, although it is unknown if this potential reflects HSC or progenitor activity (Zeigler et al., 2006; Corbel et al., 2007).

Importantly, it was recently proposed that tissue resident macrophages in the adult are predominantly YS-derived (Samokhvalov et al., 2007; Gomez Perdiguero et al., 2015), suggesting that dHSCs are not the sole source of the adult haematopoietic system. However, contradictory data have also been published (Hoeffel et al., 2015; Hoeffel and Ginhoux, 2015), and these competing observations require further investigation.

YS and placenta-derived haematopoietic progenitors start colonising the FL around E9.5 (Alvarez-Silva et al., 2003; Cumano and Godin, 2007), but AGM-derived dHSCs only seed the FL at E11-E11.5 (Medvinsky et al., 1993; Sanchez et al., 1996; Kumaravelu et al., 2002). Additionally, a recent study has suggested that phenotypically distinct immature HSCs (imHSC), which acquire dHSC properties in the FL, constitute a wave of FL colonisation that precedes the arrival of AGM-derived dHSCs (Kieusseian et al., 2012). The dHSC pool undergoes massive expansion in FL between E11.5 and E15.5, and these cells acquire the characteristic cell surface markers of adult HSCs (Morrison et al., 1995) before colonising the foetal BM at E15.5-E17.5 (Christensen and Weissman, 2004).

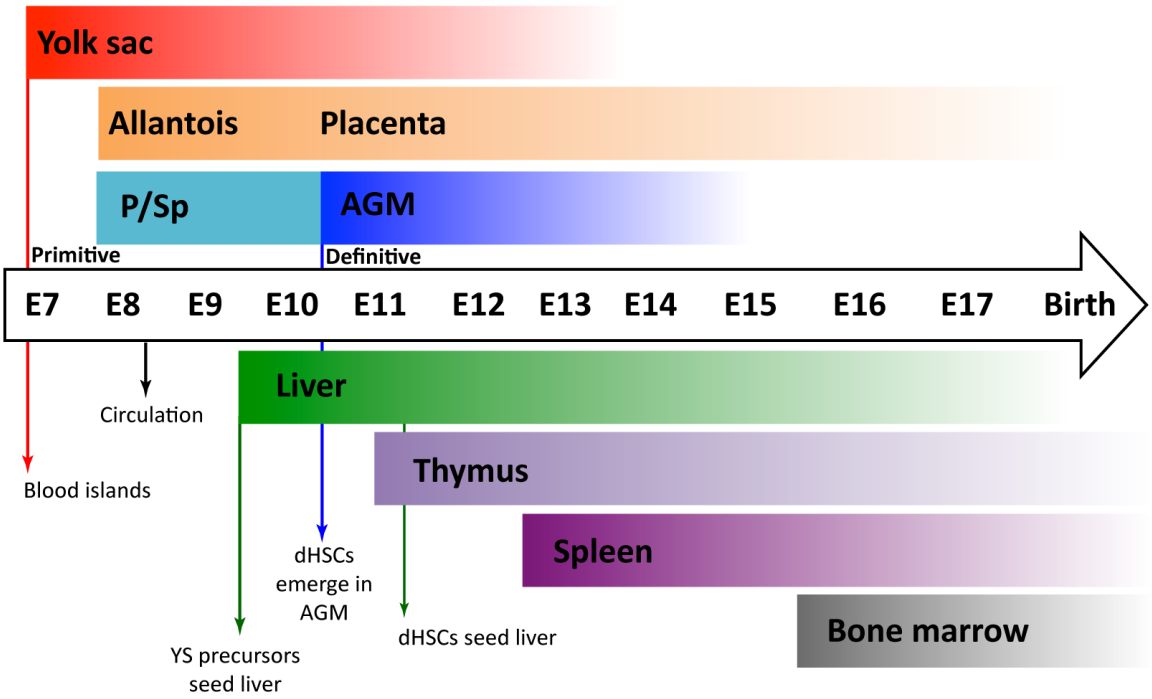

Figure 1.2. Successive haematopoietic sites during development of mammalian embryos. The first primitive haematopoietic cells emerge at embryonic day E7 in yolk sac (YS) blood islands. Definitive haematopoietic stem cells (dHSCs) emerge at E10.5 in the aorta-gonad-mesonephros region (AGM) and subsequently seed the foetal liver at E11-E11.5. Bone marrow (BM) is seeded after E15.5. P-Sp, para-aortic splanchnopleura (prospective AGM). Adapted from Dzierzak and Speck (2008).

1.5. Lineage commitment in the adult bone marrow haematopoietic system

The haematopoietic system is a progressively lineage-restricted branching hierarchy that generates all mature blood cells throughout mammalian life. Although the haematopoietic hierarchy is very likely to be an oversimplification, a roadmap of developmental potentials is a very useful scaffold for the study of conserved cellular and molecular mechanisms of stem cell differentiation under normal and abnormal conditions (Orkin, 2000; Reya et al., 2001; Bryder et al., 2006; Orkin and Zon, 2008; Pina et al., 2012).

Over the last 20 years different models of the BM and FL haematopoietic hierarchies have been proposed and continuously revised, reflecting the growing knowledge in the field regarding regulation of lineage fate decisions. Nevertheless, different models have in common the positioning of a relatively small pool of HSCs – capable of self-renewal, proliferation, and differentiation – at the apex of the hierarchy.

The most primitive HSCs are long-term repopulating HSCs (LT-HSC) (Morrison and Weissman, 1994), which give rise to short-term repopulating HSCs (ST-HSC) (Yang et al., 2005) and multipotent progenitors (MPP) (Morrison et al., 1997; Bryder et al., 2006) that sustain all lineage potentials but lack the long-term self-renewal ability characteristic of LT-HSCs. All of these cell populations are contained within the Lineage$^{-/low}$ Sca-1+ c-Kit+ (LSK) compartment, and can be further distinguished by their differential expression of CD34, Flt3/Flk2, and SLAM family markers (Osawa et al., 1996; Adolfsson et al., 2001; Christensen and Weissman, 2001; Kiel et al., 2005; Yang et al., 2005; Oguro et al., 2013). The first lineage fate decisions start at the level of the MPP, which give rise to the first lineage-committed progenitors. Through successive intermediate cell compartments, these progenitors undergo stepwise lineage restriction, until they finally assume a single cell lineage fate at the exclusion of all others (Orkin, 2000; Bellantuono, 2004; Luc et al., 2008b).

1.5.1. The classical model of the haematopoietic hierarchy

In the classical model of the BM haematopoietic hierarchy, the first step of lineage restriction downstream of the MPP compartment is the bifurcation of myelopoiesis and lymphopoiesis (Figure 1.3A) (Orkin, 2000; Akashi, 2009). In this model, MPPs generate both a common lymphoid progenitor (CLP), and a common myeloid progenitor (CMP). The CLP is predicted to be the common progenitor of all lymphoid cells (B, T, and NK) while lacking megakaryocyte/erythroid/myeloid potentials, and is phenotypically defined as Lin- IL7Rα+ Thy1.1- Sca-1^{low} c-Kit^{low} (Kondo et al., 1997). Conversely, the CMP is predicted to give rise to all historically termed "myeloid" lineages (granulocytes, monocytes/macrophages, erythroid cells, and megakaryocytes), and is phenotypically defined as Lin- IL7Rα- Sca-1- c-Kit+ CD34+ FcγR^{low} (Akashi et al., 2000b). Downstream of the CMP, further segregation of the "myeloid" lineages was proposed to occur through the generation of the granulocyte-macrophage progenitor (GMP, Lin- IL7Rα- Sca-1- c-Kit+ CD34- FcγR$^{high)}$, and the megakaryocyte-erythroid progenitor (MEP, Lin- IL7Rα- Sca-1- c-Kit+ CD34- FcγR^{low}) (Akashi et al., 2000b). However, the single cell level differentiation heterogeneity observed within the prospectively isolated CMP, GMP, and MEP progenitors suggests that these compartments (especially CMP) might be a heterogeneous mixture of distinct lineage-restricted progenitors (Pronk et al., 2007; Rieger et al., 2009b; Pronk and Bryder, 2011). Furthermore, sub-fractionation of the CLP compartment based on expression of Ly6D, *Rag1*-GFP and transgenic hCD25 (controlled by the λ5 promoter) was shown to separate B cell and T cell fates, again indicating that this compartment might not be a common progenitor of all lymphoid lineages but a composite of distinct lineage-restricted progenitors (Inlay et al., 2009; Mansson et al., 2010).

1.5.2. The myeloid-biased and LMPP models of the haematopoietic hierarchy

The classical hierarchical model was proposed based on the prospective isolation of the CLP and CMP populations, but it does not exclude the possibility of alternative or additional commitment routes that are parallel or upstream of the dichotomy between lymphopoiesis and myelopoiesis. (Luc et al., 2008b; Orkin and Zon, 2008; Seita and Weissman, 2010). Shortly after the proposal of the classical model, and based on findings regarding sustained myeloid potential from lymphoid precursors, a myeloid-based model was also proposed (Figure 1.3B) (Katsura and Kawamoto, 2001; Kawamoto et al., 2010). In this model, the first lineage restriction step in the hierarchy is segregation between CMP and a common myelo-lymphoid progenitor (CMLP). The CMLP is proposed to further diverge into bi-potential myeloid-T cell progenitors (MTP) and myeloid-B cell progenitors (MBP), and so the CLP does not feature in this model. While the classical model was based on prospective isolation of cell populations through schemes of cell surface markers, the myeloid-biased model was initially based on *in vitro* analysis of clonal differentiation.

Importantly, the experiments that led to the classical model were performed with adult BM cells, while the experiments that led to the myeloid-biased model were performed with mid-gestation FL cells. Moreover, in agreement with the myeloid-biased model, the prospective isolation of the CLP equivalent in FL demonstrated that these cells sustain myeloid potential (Mebius et al., 2001). This resulted in initial speculation that one hierarchy model might apply to adult haematopoiesis, while the other might apply to foetal haematopoiesis (Kincade et al., 2002). However, shortly after myeloid potential was shown to be sustained by *Rag1*-expressing early lymphoid progenitors in the adult BM (Igarashi et al., 2002), and a CMLP-like compartment was also prospectively isolated from adult BM (Adolfsson et al., 2005). This CMLP identified in BM was phenotypically defined as LSK Flt3^{high} (25% of LSK cells with highest Flt3 expression) and renamed lymphoid-primed multipotent progenitor (LMPP)

(Adolfsson et al., 2005). Concomitantly with Flt3 up-regulation, LMPPs were shown to lack long-term self-renewal ability (Adolfsson et al., 2001), as expected for a MPP compartment. LMPPs were further demonstrated to have combined lympho-myeloid lineage potentials at the single cell level, but little or no megakaryocyte/erythroid potential. Transcriptionally, single LMPPs up-regulate expression of genes associated with early lymphoid regulation (such as *Rag1, Rag2,* and *IL7r*), while also sustaining expression of myeloid-affiliated genes (such as *Csfr3*, *Sfpi1* and *Cebpa)* (Adolfsson et al., 2005; Mansson et al., 2007). Alternative isolation of LMPPs based on expression of the Ikaros family zinc finger protein 1 transcription factor (*Ikzf1*), which correlates with (and regulates) Flt3 expression, was also proposed (Yoshida et al., 2006).

Prospective isolation of the BM LMPP led to the proposal of a new revised haematopoietic roadmap, similar but distinct from the previously proposed myeloid-biased model (Figure 1.3C) (Luc et al., 2008b). This new model positions the LMPP compartment downstream of ST-HSCs, in parallel to CMPs, and upstream of CLPs. Unlike the studies associated with the myeloid-biased model, the LMPP studies did not address CLP heterogeneity, and so the existence of this compartment was not specifically questioned as before (Kawamoto et al., 2010). Studies showing retention of myeloid potential and loss of B cell potential in adult thymus T cell progenitors support the MT-MB dichotomy specifically proposed in the myeloid-biased model (Bell and Bhandoola, 2008; Wada et al., 2008), but contradictory findings have also been reported (Schlenner et al., 2010; Schlenner and Rodewald, 2010; De Obaldia et al., 2013). Therefore, it remains controversial if thymus T cell progenitors represent a T/myeloid-restricted progenitor compartment (MT) or full T cell restricted progenitors that could be the progeny of either CLP or CMLP.

Transcriptional regulation of the proposed LMPP-CMP dichotomy has been further investigated. The transcription factors PU.1 (Iwasaki et al., 2005b) and GATA-1 (Ferreira et

al., 2005) are key regulators of myeloid/lymphoid commitment, and megakaryocyte/erythroid commitment, respectively. In agreement with their known roles, within the MPP compartment up-regulation of PU.1 expression was shown to determine myelo-lymphoid lineage specification, and up-regulation of GATA-1 expression was shown to determine myelo-erythroid lineage specification (Arinobu et al., 2007). In this study, mouse lines in which GFP expression correlates with the level of PU.1 and GATA-1 mRNA and protein were used (Back et al., 2005; Iwasaki et al., 2005a). *Gata1*-GFP+ MPPs, which express Sca-1 at an intermediate level between Sca-1^{high} MPPs and the classical Sca-1- CMP, were shown to have granulocyte/monocyte and megakaryocyte/erythroid potential but to lack lymphoid potential. These cells represent a more primitive and more proliferative fraction of the classical CMP. Although heterogeneity of the differentiation potentials of the two CMP compartments was again reported, a considerable fraction of single *Gata1*-GFP+ CMPs showed mixed myeloid/megakaryocyte/erythroid potential *in vitro*. These findings support the previously questioned existence of a real CMP compartment, although it also suggests that the classically defined CMP might already represent a group of increasingly restricted progenitors derived from the real *Gata1*-GFP+ CMP (Arinobu et al., 2007).

PU.1-GFP+ MPPs, which express Flt3 but in contrast to LMPP are Sca-1^{low}, were shown to have granulocyte/monocyte and lymphoid potential but to strictly lack megakaryocyte/erythroid potential. These cells represent a more restricted fraction of the classical LMPP, and were termed *granulocyte*–monocyte–lymphoid progenitors (GMLP) (Arinobu et al., 2007).

Furthermore, down-regulation of cell surface expression of the thrombopoietin receptor MPL in LMPPs – a regulator of HSC and megakaryocyte development (Kaushansky, 2006; de Graaf and Metcalf, 2011) – was also shown to coincide with further loss of the already low megakaryocyte/erythroid potential observed in the LMPP compartment. Down-regulation of MPL expression is also associated with decreased myeloid output and increased lymphoid-

priming (Luc et al., 2008a; Luc et al., 2008b). Similarly, further restriction of the LMPP compartment into the lymphoid lineage has been shown to be associated with down-regulation of cell surface expression of the vascular cell adhesion molecule VCAM-1. Both VCAM1+ and VCAM1- LMPPs show the same low level of megakaryocyte/erythroid potential, but while VCAM1+ LMPPs have robust lympho-myeloid potentials, VCAM1- LMPPs have reduced myeloid potential and increased lymphoid-priming (Lai et al., 2005; Lai and Kondo, 2006).

Transplantation of high cell doses of LMPPs into lethally irradiated mice led to robust dose-dependent short-term reconstitution of the megakaryocyte/erythroid lineages *in vivo* (Forsberg et al., 2006), and the authors concluded that either all LMPPs have low megakaryocyte/erythroid potential or a fraction of LMPPs is still fully multipotent. The different degrees of lympho-myeloid and lymphoid restriction identified within sub-fractions of the LMPP compartment, and especially the finding that megakaryocyte/erythroid potential is almost exclusively restricted to LSK Flt3^{high} MPL^{high} cells corresponding to >60% of the total LMPP population (Luc et al., 2008a), supports the latter conclusion.

Overall, the findings described above regarding lympho-myeloid progenitor heterogeneity indicate that there is a need for further dissection of lineage restriction regulation between the MPP, LMPP, CMP, and CLP compartments, with corresponding revision of the haematopoietic hierarchy model (Figure 1.3D) (Iwasaki and Akashi, 2007a, b; Akashi, 2009).

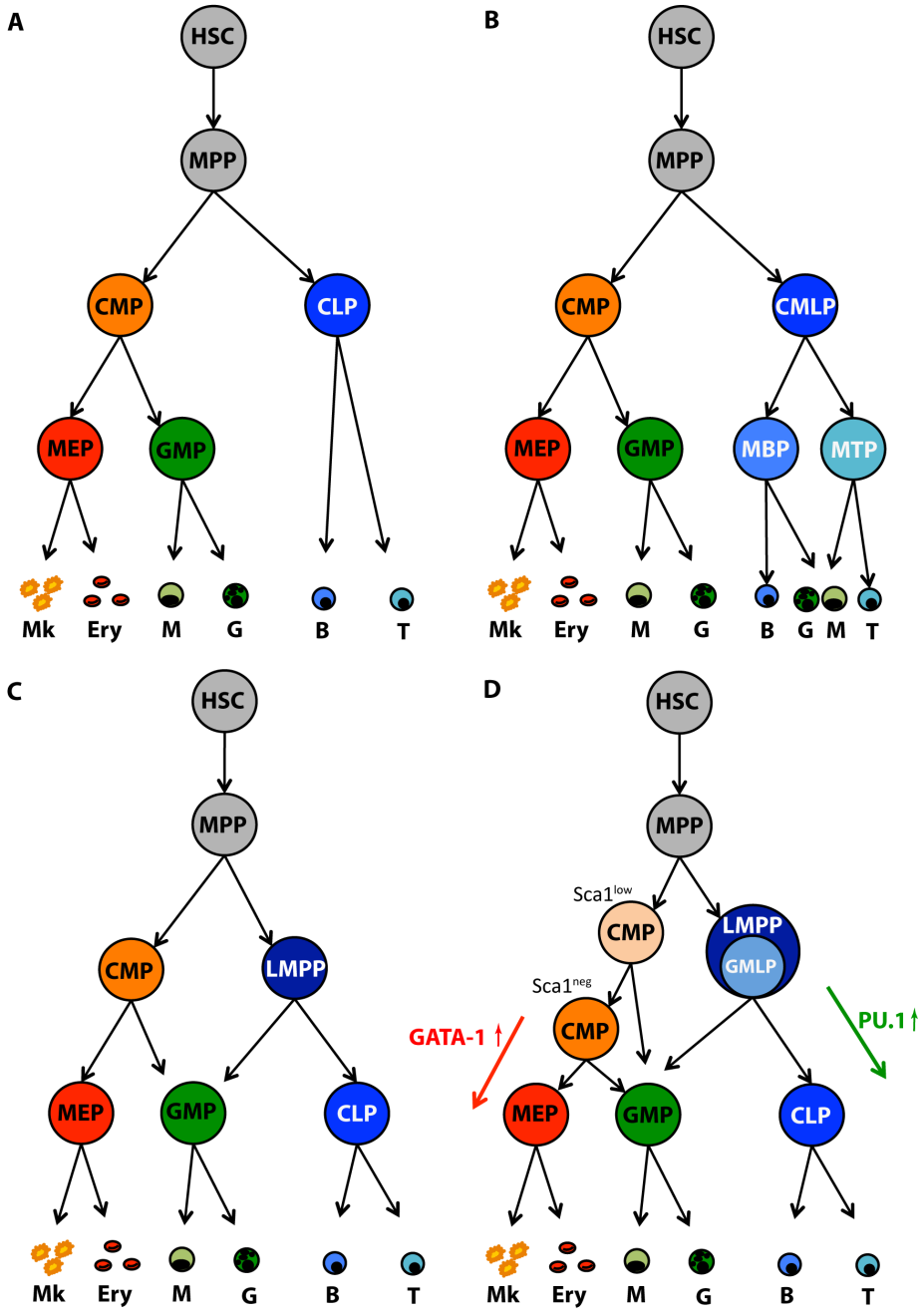

Figure 1.3. Competing models of the haematopoietic hierarchy.

(A) The classical model. **(B)** The myeloid-biased model. **(C)** The LMPP model. **(D)** A revised LMPP model. HSC, haematopoietic stem cell. MPP, multipotent progenitor. CMP, common myeloid progenitor. CLP, common lymphoid progenitor. MEP, megakaryocyte-erythroid progenitor. GMP, granulocyte-macrophage progenitor. LMPP, lymphoid-primed multipotent progenitor. GMLP, granulocyte-macrophage-lymphoid progenitor. MTP, myeloid-T cell progenitors. MBP, myeloid-B cell progenitors. Adapted from Arinobu et al. (2007) and Iwasaki and Akashi (2007).

1.5.3. Regulation of haematopoietic lineage commitment by transcription factors

Maintenance of mature blood cell production depends on accurate lineage commitment throughout the haematopoietic hierarchy at all stages of development. This process is, therefore, highly regulated, both intrinsically and extrinsically, and both in steady-state conditions and during situations of emergency haematopoiesis, when the production of specific lineages needs to be acutely increased (Zhu and Emerson, 2002; Kaushansky, 2006; Robb, 2007; Takizawa et al., 2012).

The brief discussion above regarding the reciprocal interaction between PU.1 and GATA-1 at the earliest branching point in the LMPP model of the haematopoietic hierarchy (Arinobu et al., 2007) highlighted the instructive role of cell intrinsic transcription factors (TFs). Individual TFs have lineage-specific roles, but they are also part of connected networks that simultaneously integrate the signals from several TFs and from cell extrinsic cues. Commitment to each cell lineage is ultimately determined by the balance of activating and repressive time-sensitive interactions between combinations of several TFs (Zhu and Emerson, 2002; Iwasaki et al., 2006; Laiosa et al., 2006; Mercer et al., 2011). Nevertheless, forced down-regulation or overexpression of individual cornerstone factors in a network may be sufficient to completely induce, repress, or reprogram commitment to a specific lineage, which underlines the strong instructive role of key TFs (Iwasaki et al., 2003; Iwasaki-Arai et al., 2003; Iwasaki et al., 2005b).

1.5.4. Regulation of haematopoietic lineage commitment by cytokines

Haematopoietic lineage fate decisions are also regulated by the micro-environment occupied by the cell, and this extrinsic regulation is mediated by lineage-specific cytokines and their respective receptors (Kaushansky, 2006; Robb, 2007). Identification of the first haematopoietic cytokines resulted from colony forming unit (CFU) cell culture assays

developed in the 1960-80's, which revealed the biological activity of colony-stimulating factors (CSFs) and led to the cloning of their receptors (Nicola, 1989). Early *in vitro* culture systems also suggested that some haematopoietic cytokines are associated with commitment to a specific lineage, while others have broader roles in the commitment of multiple lineages. These observations led to the theory that a hierarchical system of cytokines mimics the haematopoietic hierarchy, with some cytokines acting at the level of HSCs and MPPs and other cytokines acting at the level of lineage-specific progenitors (Robb, 2007). However, it is currently accepted that even the cytokines originally considered to be lineage-restricted have pleiotropic effects. Similarly to TF networks, cytokine effects are likely the result of a balance between several factors: differential expression of receptors in different cell types, availability of cytokines in the micro-environment, and positive and negative regulatory interactions between combinations of cytokines (Robb, 2007).

Two main models of cytokine-mediated lineage commitment have been proposed: the permissive (or stochastic) model and the instructive model. There is experimental evidence for both, and they are also not mutually exclusive.

The permissive model was the first to be proposed based on the findings of the CFU-S assay, the first *in vivo* assay of haematopoietic self-renewal and differentiation (Till et al., 1964). This model stipulates that cytokines only regulate the proliferation and survival of cells after they have already committed intrinsically to a specific lineage. Therefore, only cells in which the TF regulatory network has already resulted in the expression of lineage-specific cytokine receptors can respond to the signal of the respective cytokine. This mode of action is supported by many findings obtained through different experimental approaches, including mouse models of cytokine expression knock-out, and models with constitutively active receptors. Among the data that support a permissive role of cytokines are observations from experiments in which mice with chimeric receptors were generated. In one case, the thrombopoietin (TPO) receptor MPL was modified with the signalling cytoplasmic domain of

the granulocyte colony stimulating factor receptor (G-CSFR), so that when the receptor bound TPO it transmitted G-CSFR signals. This chimeric receptor was able to function as a normal MPL receptor when binding TPO, and there was no change in numbers of BM megakaryocytic or granulocytic progenitors (Stoffel et al., 1999). In another case, G-CSFR was modified with the signalling cytoplasmic domain of the erythropoietin receptor (EPOR), so that when the receptor bound G-CSF it transmitted EPOR signals. Once again, the binding of G-CSF to this chimeric receptor did not alter the dynamics of myeloid or erythroid BM progenitor differentiation (Semerad et al., 1999). Overall, these and other experiments suggest that the signals generated by at least a few different cytokine receptors are non-specific survival and proliferation signals, and do not induce distinct lineage commitments (Robb, 2007).

The instructive model instead proposes that cytokine signalling plays a direct role in lineage specification. Ectopic expression of specific cytokines or their receptors in well characterised haematopoietic cell lines was shown to some times result in induction of lineage-specific transcriptional programs and cell differentiation (Just et al., 1991), but overall experimental data in favour of this model derives predominantly from observations regarding the regulation of lymphoid progenitor differentiation. In Flt3-ligand (Flt3L)-deficient and IL7Rα-deficient mice lymphoid progenitor compartments are reduced (Peschon et al., 1994; McKenna et al., 2000; Sitnicka et al., 2002). Moreover, in Flt3L-deficient mice LMPPs show reduced lymphoid-priming, whereas their myeloid transcriptional program remains unaltered (Sitnicka et al., 2007). Ectopic expression of IL-2βR or GM-CSFR in CLPs resulted in granulocyte-macrophage differentiation, rather then lymphoid differentiation, upon *in vitro* exposure to IL-2 or GM-CSF, respectively (Kondo et al., 2000). Thus, these and other similar experiments suggest that at least some cytokines can directly instruct haematopoietic differentiation.

1.6. Heterogeneity of haematopoietic stem cells

The classical view of the regulation of self-renewal and differentiation potentials of LT-HSCs was that the primitive HSC pool at the apex of the haematopoietic hierarchy constitutes a homogeneous population in which all individual cells give rise to all the different lineage-committed progenitors with equal propensity. Heterogeneity in the haematopoietic system would then be regulated by cell intrinsic stochastic variation and extrinsic cues from the micro-environment.

Over the past decade, growing experimental evidence regarding functional heterogeneity within the LT-HSC compartment suggests that distinct subsets of LT-HSCs are intrinsically primed to preferentially generate specific downstream lineages with specific generation kinetics (Sieburg et al., 2006; Dykstra et al., 2007; Beerman et al., 2010; Challen et al., 2010; Hock, 2010; Schroeder, 2010; Glotzbach et al., 2011; Copley et al., 2012). This indicates that the study of HSC function at the population level generates outputs that are a composite of the specific functions of distinct HSC subsets, and so it is crucial to analyse HSC lineage commitment at the clonal level. Little is currently known about the distinct functional properties and regulation mechanisms of the different HSC subsets proposed (Copley et al., 2012; Ema et al., 2014). Increasing efforts have been made in the development of novel *in vitro* and *in vivo* approaches for the characterisation of the self-renewal, proliferation, and differentiation abilities of individual HSCs. A brief discussion of these methods is included below.

Importantly, early functional heterogeneity might be a general property of stem cell populations in different tissues, raising the question of the evolutionary and biological significance of establishing such heterogeneity at the level of the most primitive multipotent compartment. Therefore, uncovering the principles of heterogeneous lineage priming at the level of primitive HSCs might have an impact in the direction of future studies of induced

pluripotent stem cells (iPSCs) and also in the development of future stem cell-based biomedical applications.

1.6.1. Single cell lineage tracing by time-lapse microscopy

Differentiation of haematopoietic cells *in vitro* through multiple cell divisions can be tracked with long-term time-lapse microscopy. In the absence of non-invasive *in vivo* methods of continuous tracking of an individual cell, this approach has been heralded as the most precise method of cell fate choice quantification (Kokkaliaris et al., 2012). Indeed, time-lapse microscopy has provided new insights into long-standing questions in the haematopoietic field, namely regarding the differentiation of endothelial and haematopoietic cells from haemogenic endothelium (Eilken et al., 2009), and the instructive role of haematopoietic cytokines on lineage commitment (Rieger et al., 2009a).

Single cells are deposited in culture and imaged at regular intervals over time, currently up to several weeks for mammalian cells (Schroeder, 2011). The lineage fate decisions of individual cells and their changing properties can be traced through the use of fluorescent protein expression driven by lineage-specific promoters (Stadtfeld et al., 2005) or incubation with fluorochromes for labelling of highly expressed cell surface markers. The automated imaging system allows for simultaneous quantification of multiple fluorescence and morphological parameters over time, at an intermediate to high throughput level (Schroeder, 2011).

Despite many conceptual advantages, this approach has many technical caveats that prevent it from being more widely used. The establishment of an efficient long-term automated cell tracking platform for a given cell type of interest requires in-depth

interdisciplinary expertise and extensive optimisation. Firstly, it is crucial that the *in vitro* culture conditions are appropriately optimised to sustain survival of the cells of interest for long periods of time without inducing apoptosis or changes in normal behaviour. Moreover, the culture conditions must not interfere with the detection of fluorescence signals and with general imaging quality. This requires carefully balanced compromises between different components of the culturing and imaging systems. An optimal compromise must be found for each cell tracking study, which will depend on several factors including the main biological question of the experiment, the cell of interest and its culture requirements, the rate of cell division, compatibility between cell incubation and microscope hardware, the relative brightness of fluorescent reporters and fluorochromes used to identify cell states, etc.

To obtain enough statistical power, long-term time-lapse imaging experiments will typically require the continuous tracking of a large number of cells, which increases exponentially with each cell division. This generates very large quantities of imaging data, and requires the development of specialised automated cell tracking software capable of fast and accurate interpretation of the multiple information parameters recorded with each image. An additional issue with automated imaging analysis is the fact that many cells in culture are relatively motile, and frequently come into close contact with each other. This can result in the loss of ability to track the identity of each individual cell. When imaging such cultures, very short time intervals between acquisition of sequential images might be necessary, which will drastically increase the already large amount of data generated and also further increase the software power required for subsequent processing of that data (Schroeder, 2005, 2011; Kokkaliaris et al., 2012).

1.6.2. Single cell lineage tracing by paired daughter cell assays

Another approach of *in vitro* tracking of haematopoietic lineage fate decisions at the single cell level is the paired daughter cell assay. This method was initially developed for the study of multilineage commitment in mouse spleen colonies (Suda et al., 1983; Suda et al., 1984), and was later adapted to the study of symmetrical and asymmetrical divisions of highly purified HSCs (Ema et al., 2000; Takano et al., 2004). In contrast to continuous time-lapse microscopy, this method is dedicated to the observation of a cell fate decision during a single cell division. Single cells are deposited in short-term culture until one division occurs, and the daughter cell pair generated over this division can be characterised phenotypically (expression of lineage markers, histochemical stains), molecularly (expression of transcriptional programs), or functionally (further differentiation *in vitro* or repopulating activity *in vivo*).

Analysis of daughter and granddaughter cell pairs provided evidence for lineage differentiation through asymmetrical division of HSCs, and suggested that this process is influenced by extrinsic cytokine signals (Ema et al., 2000; Takano et al., 2004). When coupled to gene expression knock-out and overexpression, this approach has also provided insight into the molecular mechanisms underlying the balance between HSC self-renewal and differentiation. Namely, the polycomb gene *Bmi-1* and the adaptor molecule *Lnk* were shown to be positive and negative regulators of HSC self-renewal, respectively (Iwama et al., 2004; Seita et al., 2007). More recently, observations from the use of paired daughter assays suggested a novel megakaryocyte lineage commitment pathway for HSCs, a pathway in which progenitors with megakaryocyte-restricted *in vivo* repopulation activity are asymmetrically generated by an HSC in a single cell division (Yamamoto et al., 2013).

1.6.3. Single cell lineage tracing by transplantation: limiting dilution

The *in vivo* repopulating activity of HSCs at the single cell level was first analysed by Osawa et al. through a limiting dilution method, and although the focus of that study was the relevance of CD34 as a cell surface marker, differences in clonal long-term reconstitution were already observed and attributed to variability of self-renewal potential or of multilineage differentiation potential (Osawa et al., 1996).

Later, the Müller-Sieburg group described in more detail the heterogeneous *in vivo* repopulation behaviour of single HSCs and proposed the existence of distinct HSC subtypes (Müller-Sieburg et al., 2002; Müller-Sieburg et al., 2004). HSC clones were generated through co-culture of limiting-dilutions of unfractionated adult BM with S17 stromal cells (Cho and Müller-Sieburg, 2000), and then transplanted. Lineage-biased long-term reconstitution of recipients was observed, as defined by a skewed lymphoid-to-myeloid ratio of donor-derived cells in peripheral blood. Although they found that the majority of HSCs appeared to be balanced in output, lineage-biased HSCs (Lin-bi) were found to comprise up to 30% of the HSC compartment, with half falling into a lymphoid-biased category (Ly-bi) and the other half into a myeloid-biased category (My-bi). In order to assess if the observed heterogeneity was an effect of the *in vitro* clonal expansion in stromal co-cultures, BM cells from primary recipients were serially transplanted and the array of Lin-bi reconstitution patterns was confirmed. Furthermore, Lin-bi patterns were maintained throughout long-term serial transplantations, suggesting that they correspond to a stable property of HSC subsets. All Lin-bi reconstitution patterns reported still included some level of both myeloid and lymphoid reconstitution throughout time. Thus, no unilineage patterns were reported, although some of the Ly-bi cases observed arguably showed very low myeloid reconstitution levels (Müller-Sieburg et al., 2002; Müller-Sieburg et al., 2004).

Muller-Sieburg et al. also analysed the reconstitution level of myeloid and lymphoid precursors generated by limiting dilutions of BM cells from primary recipients reconstituted with Lin-bi HSCs. In myeloid stromal co-cultures, BM cells derived from My-bi and from balanced HSCs produced similar levels of cells, on average 0.6-fold higher than the growth observed for BM cells derived from Ly-bi HSCs. In contrast, BM cells derived from Ly-bi and balanced HSCs produced similar levels of B-cell precursors in lymphoid stromal co-culture, 3-fold higher than the growth observed for My-bi HSCs. Moreover, BM cells derived from My-bi HSCs were found to generate reduced numbers of thymus T cell progenitors *in vivo*, although the few progenitors generated were equally functional in the production of mature T cells when compared to the ones derived from the progeny of Ly-bi HSCs.

The comparison between gene expression programs of lymphocytes derived from My-bi HSCs and balanced HSCs revealed that the gene coding for the receptor of lymphoid growth factor interleukin-7 (IL7Rα) was strongly down-regulated in the lymphoid progeny of My-bi HSCs. A corresponding down-regulation of cell surface expression of IL7Rα in the lymphoid progeny of My-bi HSCs was confirmed, and it was further demonstrated that these cells do not respond to IL-7 stimulation *in vitro*. Overall these data suggest that changes in the developmental program of My-bi HSCs lead to lymphoid progeny with a reduced response to IL-7 signalling, which indicates that long-term repopulating My-bi HSCs are programmed for inefficient lymphopoiesis (Müller-Sieburg et al., 2004).

1.6.4. Single cell lineage tracing by transplantation: LSK^{SP} compartment

Stronger evidence of stably propagated functional heterogeneity of HSCs was obtained through analysis of serial transplantations of single HSCs prospectively isolated by FACS (Dykstra et al., 2007; Kent et al., 2009; Challen et al., 2010; Morita et al., 2010).

The Goodell group proposed a HSC isolation scheme based on differential capacity for Hoechst dye efflux, which defines sub-fractions of side population (SP) (Goodell et al., 1996). Although the LSK^{SP} compartment is very homogenous in the expression of canonical stem cell markers, it was noted that cells from different SP regions have different functional potentials when repopulating activity is analysed over long periods of time (Goodell et al., 1997; Camargo et al., 2006). A gradient of HSCs with distinct phenotypic, functional, and molecular characteristics was then identified within the adult BM LSK^{SP} compartment through transplantation of single purified HSCs (Challen et al., 2010). The authors observed that My-bi HSCs were enriched in the lower SP region and were long-lived, while Ly-bi HSCs were enriched in the upper SP region and had a shorter life span. They further identified the TGF-β1 signalling pathway as a potential mechanism of differential regulation between these two different HSC subtypes (Challen et al., 2010). Moreover, they showed that the pool of lower SP My-bi HSCs expands with age, and proposed that the deficit in lymphopoiesis observed in transplantation of HSCs from old mice is due to the expansion of My-bi HSCs in BM rather than a decrease in the lymphoid potential of all individual HSCs.

Similarly to the Müller-Sieburg studies, albeit using a different phenotypic HSC definition (Müller-Sieburg et al., 2004), the Goodell group only reported Lin-bi patterns with reconstitution of both lymphoid and myeloid lineages, and did not discuss any cases of unilineage restricted reconstitution (Challen et al., 2010).

1.6.5. Single cell lineage tracing by transplantation: LSK^{SP} Rho- compartment

Single cell reconstitution studies were also performed by the Eaves group, using a different definition for prospective isolation of HSCs by FACS (Dykstra et al., 2007). Transplantation of single adult BM CD45^{mid} Lin- Rho- SP cells, either freshly purified or moderately expanded by *in vitro* culture for 4 days (Audet et al., 2002), generated different reconstitution patterns that were classified by the authors into four categories (α, β, γ, and δ), according to their lineage differentiation capacity and the length of time over which they sustained reconstitution of the transplanted mice. For comparison of reconstitution behaviour they defined a myeloid-to-lymphoid ratio (referred to as GM:(B+T)) that is not directly reciprocal to the L/M ratio previously defined by the Müller-Sieburg group. This ratio also includes recipient cell contribution, while Müller-Sieburg's L/M ratio did not.

The α type (My-bi) was defined by robust long-term myeloid potential but poor ability to produce B and T cells. The β type (balanced) was defined as making long-term significant contributions to both the myeloid and the lymphoid lineages. Ly-bi HSCs were defined by robust long-term lymphoid potential and were further subdivided into two types according to their different abilities to sustain long-term low myeloid reconstitution. Therefore, the γ subtype of Ly-bi HSCs sustains low myeloid potential in the long-term, whereas the δ subtype becomes increasingly more Ly-bi with time (Dykstra et al., 2007). For all four HSC types the authors observed that the reconstitution patterns and lineage-specific levels of peripheral blood reconstitution 4 months after secondary or tertiary transplantation were very similar, across all recipients, to what was observed in their respective primary recipients. Many α and β HSCs sustained their characteristic reconstitution pattern *in vivo* for over a year. However, change from one pattern to another was observed at 16 weeks in 50% of secondary recipients of cells from primary mice with α or β patterns. In these cases, α HSCs tended to start demonstrating lymphoid potential, thus switching to a more β

pattern in one or both secondary recipients. In contrast, β cells tended to lose myeloid potential, thus switching to a more γ or δ pattern. Furthermore, when transplanting single $CD45^{mid}$ Lin- Rho- SP cells after *in vitro* culture for up to 10 days, the authors observed that the ratio of biased patterns in primary recipient mice was different from that observed when transplanting freshly purified cells. After 4 days of culture the number of recipients with γ and δ reconstitution patterns increased and the number of recipients with α and β patterns respectively decreased by nearly 50%. After 10 days in culture, all reconstituted mice had either a γ (25%) or δ (75%) pattern. When equal portions of a clone after 10 days of culture were transplanted into multiple mice, for 45% of clones more than one recipient was reconstituted, demonstrating that multiple repopulating cells were generated in culture. The above data suggests that α cells may be able to produce β, γ and/or δ HSCs and that β HSCs may be able to produce γ and/or δ HSCs (but apparently not α) or that certain stimulating conditions can change the output bias of HSCs from one type of pattern to another (Dykstra et al., 2007).

The Eaves group also later defined a rare CD45+ EPCR+ CD48- CD150+ (E-SLAM) phenotypic population that contains highly purified functional HSCs. They isolated this population from different haematopoietic tissues of E14.5 embryos, and also from different ages of mice up to 2 years old (Benz et al., 2012). The authors reported that these cells display the same spectrum of differentiation patterns that they previously reported for adult BM HSCs defined by different phenotypic markers (Dykstra et al., 2007). They demonstrated an early origin of at least two subtypes of HSCs – α and β – both with high self-renewal potential but each displaying very different abilities to produce lymphoid cells. Both α-HSCs and β-HSCs are present in E14.5 FL, but β-HSCs are the dominant subtype. Thus, β-HSCs seem either more likely to arise from their embryonic precursors or otherwise have a growth advantage over α-HSCs in the earliest stages of embryonic HSC expansion in FL. Conversely, in old mice

(1–2 years old) α-HSCs tend to become the dominant subtype in the BM, which is in agreement with previous findings (Morrison et al., 1996; Müller-Sieburg et al., 2004; Miller and Allman, 2005; Beerman et al., 2010). At E14.5 β-HSCs represent >90% of the FL HSC compartment, and after that both α-HSCs and β-HSCs increase very rapidly. In E18.5 foetal BM the number of α-HSCs is already 3-fold higher than β-HSCs, similar to what is observed in BM of young adult mice. The stability of α-HSC abundance over β-HSCs as soon as the foetal BM is colonised suggests a potential role for the BM microenvironment in mediating this bias (Benz et al., 2012).

1.6.6. Single cell lineage tracing by transplantation: comparison of lineage-bias classifications

In a recent review (Ema et al., 2014) the authors assessed the correspondence between the different lineage-biased HSC subsets as defined by the Müller-Sieburg (My-bi, balanced, and Ly-bi) and Eaves criteria (α, β, and γ/δ) by reanalysing previously published data of 30 single HSC transplantations (Morita et al., 2010). They found that all α-cells were also classifiable as My-bi, but only 70% of My-bi cells were classifiable as α, with the majority of remaining My-bi cells being classifiable as β instead. All balanced cells were also classifiable as β-cells, but β-cells were an even mixture of both My-bi and balanced. The most comparable criteria were the ones defining lymphoid-bias, with all Ly-bi cells also being classifiable as γ and 90% of γ-cells also being classifiable as Ly-bi. Thus, the Müller-Sieburg criteria seem more prone to classify HSCs as My-bi, whereas the Eaves criteria are more conservative and classify many of Müller-Sieburg's My-bi cells as β (balanced) instead. Overall, both classifications identify similar classes of cells (Ema et al., 2014).

In regards to the longevity of reconstitution, LT-HSCs and IT-HSCs seem to be myeloid-biased or balanced, whereas ST-HSCs are more lymphoid-biased. Interestingly, the categories of Ly-bi, γ, and ST-HSC identify an almost identical population of cells (Ema et al., 2014).

Importantly, all the single HSC transplantation studies failed to prospectively isolate the different biased subsets of HSCs. These cells were only retrospectively identified based on the observed lineage outputs after single cell transplantation.

1.6.7. Single cell lineage tracing by genetic barcoding

Genetic barcoding coupled to high-throughput sequencing allows the simultaneous tracking of the repopulating activity of hundreds of individual HSCs transplanted into the same recipient mouse. With this method the clonal composition of the entire haematopoietic system reconstituted by a single HSC can be assessed (Dick et al., 1985; Lemischka et al., 1986; Jordan and Lemischka, 1990; Gerrits et al., 2010). High-throughput approaches like barcoding are very important in the study of rare or stochastic cellular events, and can be applied in both *in vitro* and *in vivo* studies of any nucleated virus-accessible cell type (Lu et al., 2011).

This method first involves the generation of a large library of semi-random synthesised DNA barcodes. This barcode library is then cloned into a lentiviral construct, and is transduced into a mixture of cells at a low titer to ensure that the majority of cells only receive a single barcode. Each barcode carried by a lentiviral construct integrates into the host cell genome and is replicated alongside it during cell division. Thus, all cells descending from a barcoded cell can be identified by the same DNA barcode.

After at least 16 weeks post-transplantation, haematopoietic populations of interest (HSCs, progenitors, mature cells) are isolated from the recipient mouse and genomic DNA is

extracted from each cell population. DNA barcodes are then amplified by PCR and sequenced. In sequencing analysis the DNA barcode sequences are distinguished by a small library ID, which identifies the library of origin.

The construction of the library is one of the critical steps of this approach, since the accurate unravelling of all the genomic sequences recovered from reconstituted cells depends on it. Many of the *in vitro* steps prior to transplantation can be multiplexed for efficiency, but all of the protocol parameters must ensure, as much as possible, that the majority of lentiviral constructs will only receive one barcode, and in turn the majority of transduced cells will only receive one lentiviral construct (Gerrits et al., 2010; Lu et al., 2011; Bystrykh et al., 2012; Bystrykh et al., 2014). Moreover, the barcode labelling process involves cell culture and lentiviral transduction prior to transplantation, which might affect the *in vivo* behaviour of the transplanted cells. Even though it has been suggested that this process does not alter HSC function *in vivo* (Gonzalez-Murillo et al., 2008), it is important to optimise the lentiviral transduction protocol for minimal manipulation of cells prior to transplantation.

The DNA barcoding approach, coupled to transplantation, has recently provided evidence of the asymmetry of HSC distribution throughout different BM niches, and has also demonstrated differences between the differentiation of young and aged HSCs (Verovskaya et al., 2013; Verovskaya et al., 2014).

A novel *in situ* barcoding system has also been developed, to eliminate the need for cell transplantation, and thus allow tracking of *in vivo* HSC differentiation under more physiological conditions. One recent approach involves a mouse model in which semi-random transposition of a tagged transposon can be induced, so that every cell that undergoes transposition acquires a unique insertion site. Recovery of the DNA tags and high-throughput sequencing are then performed similarly to the classic DNA barcoding approach.

The first, and so far only, study in which this method was used surprisingly suggested that native haematopoiesis is predominantly maintained by transient MPP compartments rather than by LT-HSCs (Sun et al., 2014). However, technical aspects such as true randomness of transposition-dependent labelling are still under debate.

1.7. Analysis of platelet reconstitution

The previous HSC transplantation studies for lineage bias analysis used the conventional CD45-congenic system to distinguish donor cells from recipient or competitor cells. But since CD45 is only expressed on leucocytes, bias of HSCs to other lineages has always been excluded from reconstitution analysis. More recently, with the development of new reporter mice, reconstitution analysis of all lineages, including erythroid and platelets, as become possible.

1.7.1. Platelet-biased LT-HSCs

Several genes strongly associated with the megakaryocytic lineage are also expressed by LT-HSCs (Mansson et al., 2007; Sanjuan-Pla et al., 2013). One of the megakaryocytic genes most highly expressed in murine LT-HSCs is the gene for von Willebrand factor (vWF), which is also expressed by endothelial cells. vWF is a blood clotting glycoprotein that acts as a carrier for anti-haemophilic factor (FVIII) and also mediates platelet aggregation and adherence to blood vessels (McGrath et al., 2010; Peyvandi et al., 2011).

Through the use of *Vwf*-EGFP transgenic reporter mice, our group recently showed that *Vwf* expression discriminates two prospectively isolatable phenotypic LT-HSC subsets (LSK CD150+ CD48- CD34-) in the BM of young adult mice (Sanjuan-Pla et al., 2013). Compared to

Vwf- HSCs, low cell numbers of transplanted *Vwf*+ HSCs (5, 10, or 50 cells) preferentially reconstituted platelets in both the short-term and long-term, and also showed a tendency for higher myeloid and lower lymphoid contributions than *Vwf*- HSCs (Sanjuan-Pla et al., 2013). The different long-term reconstitution patterns observed after transplantation of 10 *Vwf*+ or *Vwf*- HSCs were classified into five categories: platelet-biased, platelet/myeloid-biased, myeloid-biased, lymphoid-biased, and balanced/other. Transplantation of 10 *Vwf*+ HSCs into 15 recipients generated 60% platelet-biased or platelet/myeloid-biased patterns, and only 20% of lymphoid-biased patterns. Transplantation of 10 *Vwf*- HSCs into 10 recipients resulted in 100% of lymphoid-biased patterns. Thus, expression of *Vwf* enriches for platelet-biased and platelet/myeloid-biased HSCs, but it does not allow complete purification (Sanjuan-Pla et al., 2013). Importantly, the *Vwf*+ HSC subset contains not only platelet-biased HSCs, but also platelet/myeloid-biased HSCs that were likely identified as myeloid-biased in previous studies that did not analyse platelet reconstitution.

Gene expression analysis by multiplexed quantitative PCR at the single cell level showed that, in contrast to *Vwf*- cells, *Vwf*+ HSCs have a megakaryocyte-primed gene expression signature. Notably, the *Mpl* gene encoding for the thrombopoietin (THPO) receptor is more highly expressed by *Vwf*+ HSCs than by *Vwf*- HSCs. Acute platelet depletion mediated by the CD42b antibody, which increases the level of THPO in the plasma, resulted in rapid and selective activation of *Vwf*+ HSCs into S/G2M phase of the cell cycle. In *Vwf*-EGFP *Thpo*-/- mice, *Vwf*+ HSCs were very reduced, whereas *Vwf*- HSCs were not affected. Furthermore, transplantation of unfractionated BM cells from *Vwf*-EGFP *Thpo*-/- results only in lymphoid-biased reconstitution, but reconstitutes both *Vwf* + and *Vwf* - HSCs in BM. Collectively, these data suggest that maintenance of the *Vwf*+ HSC pool in BM is THPO-dependent (Sanjuan-Pla et al., 2013).

Platelet-biased reconstitution patterns generated by *Vwf*+ HSCs are sustained in secondary transplantation, and are associated with high reconstitution of *Vwf*+ HSCs in BM, which suggests that the platelet bias is stable and intrinsic to *Vwf*+ HSCs. Lymphoid-biased patterns generated by transplanted *Vwf*+ or *Vwf*- HSCs are also maintained after secondary transplantation, but are instead associated with reconstitution of BM *Vwf*- HSCs.

BM Lin- *Vwf*+ and Lin- *Vwf*- cells reconstituted by transplanted *Vwf*+ HSCs are fully functional in secondary transplantation, and respectively demonstrate the expected platelet and lymphoid bias. In contrast, *Vwf*- HSCs do not robustly reconstitute *Vwf*+ HSCs upon transplantation, and the few reconstituted Lin- *Vwf*+ cells only result in low and inconsistent multipotent reconstitution when serially transplanted. Thus, platelet-primed *Vwf*+ HSCs seem to be the more primitive HSCs, giving rise to lymphoid-biased *Vwf*- HSCs. *Vwf*- HSCs do not appear to be able to generate functional *Vwf*+ HSCs (Sanjuan-Pla et al., 2013).

The positioning of *Vwf*+ HSCs at the apex of the haematopoietic hierarchy, upstream of *Vwf*- HSCs fits with the fact that virtually all LSK CD150+ CD48- HSCs in E14.5 FL are *Vwf*-EGFP+. If *Vwf*+ HSCs behave similarly in FL and adult BM, then their abundance in FL would suggest that platelet-biased and platelet/myeloid-biased HSCs are the predominant subtypes present in the embryo. However, this was not investigated further (Sanjuan-Pla et al., 2013).

1.7.2. Myeloid-restricted repopulating progenitors (MyRPs) in the HSC compartment

The Nakauchi group generated the Kusabira Orange mouse line, which constitutively expresses a red/orange fluorescent protein in all tissues and cells, including leucocytes, platelets and erythrocytes (Hamanaka et al., 2013). Using this transgenic line as donor for isolation of single BM LSK CD34- CD150+ HSCs for transplantation, high frequency of

restricted patterns of reconstitution were observed, which the authors attributed to the activity of myeloid-restricted repopulating progenitors (MyRPs). Three sub-groups of MyRPs were identified: common myeloid repopulating progenitors (CMRP), megakaryocyte-erythroid repopulating progenitors (MERPs), and megakaryocyte repopulating progenitors (MkRPs) (Yamamoto et al., 2013).

Sustained repopulating activity of lineage-restricted outputs in some of the cases of secondary transplantation of unfractionated BM suggested that MyRPs might directly arise from HSCs. To further elucidate this the authors performed paired daughter cell micromanipulation of single LSK CD150+ CD41- cells after one cell division in culture, followed by single cell transplantation of each daughter cell. To show direct commitment of a LT-HSC to specific lineages in one cell division, asymmetric division that renews the LT-HSC (shown by long-term and serially transplantable repopulation of all lineages) and also produces one of the proposed progenitors (shown by long-term and serially transplantable repopulation of specific lineages) is essential. Out of 27 daughter cell pairs transplanted, two LT-HSC/MkRP pairs were detected, but no LT-HSC/MERP or LT-HSC/CMRP pairs. This suggests that MkRPs might be generated directly from LT-HSCs without passing through intermediate progenitor stages.

To determine if the short-term culture of the paired daughter cell assay had any effect on lymphoid and myeloid differentiation potentials of HSCs, the authors also compared the reconstitution ability of freshly isolated LSK CD150+ CD41- cells, and cells after one division *in vitro*. *In vitro* culture slightly increased the proportion of ST-HSCs and decreased the proportion of LT-HSCs, CMRPs, MERPs and MkRPs, but these differences were not statistically significant.

Donor-derived LMPPs, CLPs, and CD150- CD41- progenitors were not detected in BM of mice reconstituted with CMRP or MkRP. In mice reconstituted with MkRP, GMPs were also not

reconstituted. These data support the proposal that CMRPs and MkRPs have restricted potentials, and that they produce mature myeloid cells, platelets and erythrocytes in peripheral blood without producing lymphoid progenitor stages (Yamamoto et al., 2013).

1.8. Aims of the present work

The first bifurcation in the LMPP model of the haematopoietic hierarchy consists of the segregation between a lymphoid/myeloid branch and a myeloid/megakaryocyte/erythroid branch of lineage commitment.

The physiological contribution of the lympho-myeloid branch in the adult and embryo has been the subject of much debate since the proposal of this alternative model. Studies presented in this thesis aimed to identify the earliest lymphoid-commitment step in the mouse embryo (chapter 3), and to evaluate the extent to which myeloid potential is sustained in those early lymphoid fate decisions (chapter 4).

Recent studies have also questioned the regulation of lineage commitment within the myeloid/megakaryocyte/erythroid pathway, on the opposite side of the first branching point. Platelet-biased HSCs have been identified in adult bone marrow, and long-term repopulating HSCs have been suggested to be able to directly differentiate into megakaryocyte-restricted repopulating progenitors. Studies presented in this thesis aimed to further characterise the extent of platelet-bias or restriction of individual adult bone marrow HSCs (chapter 5), and to investigate if these early commitment steps in the myeloid/megakaryocyte/erythroid branch are also paralleled in the foetal liver haematopoietic hierarchy (chapter 6).

CHAPTER 2: Materials and methods

2.1 Mice

2.1.1. Husbandry

All mice used in these studies were bred and maintained by the University of Oxford Biomedical Services, JR Hospital. All experimental procedures were performed in accordance with UK Home Office regulations under the Animals (Scientific Procedures) Act 1986, with the approval of the Ethical Review Committee of the Oxford University Medical Sciences Division.

2.1.2. Mouse strains

C57BL/6J (CD45.2) and B6.SJL-*Ptprc*^{a} *Pepc*^{b}/BoyJ (CD45.1) mice were obtained from colonies managed by the University of Oxford Biomedical Services.

Kit$^{W41/W41}$ mice used in chapters 5 and 6 as donors of unfractionated bone marrow (BM) cells for support in single cell transplantation experiments were purchased from The Jackson Laboratory and bred homozygously in a B6.SJL-*Ptprc*^{a} *Pepc*^{b}/BoyJ genetic background for >6 generations.

Rag1-GFP knock-in mice used in chapter 3 were kindly provided by Dr. Nobuo Sakaguchi (Kuwata et al., 1999). *Rag1*-Cre/*R26*R-EYFP mice used in chapter 4 are a cross between the heterozygously bred *Rag1*-Cre strain kindly provided by Dr. Terence Rabbitts (McCormack et al., 2003b) and the homozygously bred *R26*R-EYFP strain kindly provided by Dr. Shankar Srinivas (Srinivas et al., 2001b).

Vwf-EGFP (Sanjuan-Pla et al., 2013), *Vwf*-tdTomato (unpublished) and *Gata1*-EGFP mice (unpublished) used in chapters 5 and 6 were kindly provided by Dr. Claus Nerlov. The *Vwf*-

tdTomato and *Gata1*-EGFP transgenes were generated by bacterial artificial chromosome engineering (BAC) at the EMBL Genome Engineering Core Facility. BAC constructs were produced with the endogenous genomic locus of each gene, including known regulatory elements, and the coding sequence for fluorescent protein was inserted into the second exon. Each mouse line was then generated by intracytoplasmic sperm injection (Moreira et al., 2006) at the EMBL Monterotondo Transgenic Facility. Each line was characterised as a faithful reporter of gene expression. *Vwf*-tdTomato and *Gata1*-EGFP mice were crossed to produce *Vwf-tdTomato/Gata1-EGFP* double reporter experimental mice, heterozygous for both alleles.

All the genetically modified mouse strains used were backcrossed to a C57BL/6J genetic background for >6 generations. All experimental mice and embryos of fluorescent reporter strains were heterozygous for each modified allele. All adult mice used in experiments were 6-18 weeks old. Both female and male mice were used, and care was taken to evenly distribute mice of different ages and sex between experimental groups. In single cell transplantation experiments no specific variation was noted in the outcome of transplantation when using mice of either sex.

2.1.3. Timed matings

Embryos were obtained by timed mating over night, with the morning of vaginal plug detection set as embryonic day E0.5. The E8-E10.5 embryos were additionally staged by counting of somite pairs (sp) as follows: ≤E8.25 (pre-circulation), ≤6 sp; E8.5, 4-7 sp; E9.5, 14-26 sp; E10.5, 30-38 sp.

Mice were mated to produce only heterozygous experimental embryos and negative controls. To avoid contamination from maternal/placenta GFP+ cells when dissecting early embryos the *Rag1*-GFP and *Gata1*-EGFP alleles were always inherited from the male parent.

Similarly, *Rag1*-Cre and *R26*R-EYFP alleles were never inherited together from the same parent, typically *Rag1*-Cre was inherited from the male and *R26*R-EYFP was inherited from the female. For generation of E14.5 embryos for sorting of long-term repopulating haematopoietic stem cells (LT-HSC), in which there is less possibility of contamination from maternal cells, *Vwf*-EGFP and *Vwf*-tdTomato were inherited from the male parent and *Gata1*-EGFP from the female parent.

2.1.4. Genotyping and phenotyping of experimental mice

In the first experiments with fluorescent reporters – *Rag1*-GFP, *Rag1*-Cre/*R26*R-EYFP, *Vwf*-EGFP, *Vwf*-tdTomato, *Gata1*-EGFP– experimental adult mice and embryos were genotyped by PCR of DNA extracted from ear biopsies and from embryonic tissue (limb, tail or head), respectively (Phire Animal Tissue Direct PCR Kit, Thermo Fisher Scientific; KAPA Express Extract Kit and KAPA 2G Robust HotStart Ready Mix, KAPA Biosystems). Once analysis of fluorescent signals was confirmed to allow correct inference of the genotype revealed by PCR, experimental mice and embryos >E12.5 were instead routinely phenotyped by flow cytometry. Younger embryos (≤E12.5) were always genotyped by PCR.

Megakaryocytic cells and mature platelets express both *Vwf* and *Gata1*; erythroid cells and many myeloid progenitors express *Gata1.* Therefore detection of Tomato and/or GFP signal in peripheral blood platelets and unfractionated foetal liver (FL) cells of *Vwf*-EGFP, *Vwf*-tdTomato, and *Gata1*-EGFP adult mice and embryos, respectively, reveals their phenotype. Mature B and T cells express *Rag1*, therefore detection of GFP or YFP in BM and FL of *Rag1*-GFP and *Rag1*-Cre/*R26*R-EYFP adult mice and embryos, respectively, also reveals their phenotype. Phenotyping by flow cytometry was carried out on small aliquots of unstained cells, and platelets and leucocytes were identified by FSC-A/SSC-A profile.

2.2. Cell preparations

2.2.1. Embryonic tissues

Method used in chapters 3-4 and 6. Embryo dissections and preparation of cell suspensions were carried out in Dulbecco's phosphate-buffered saline containing calcium and magnesium (DPBS, Gibco) supplemented with 10% foetal calf serum (FCS, Thermo Fisher Scientific) and 2mM ethylenediaminetetraacetic acid (EDTA, Sigma-Aldrich). Embryos were freed from the decidua and dissected under stereo microscope as previously described (Medvinsky et al., 2008).

Whole E8.5 conceptus (including yolk sac, allantois and embryo proper, without the ectoplacental cone), E9.5 yolk sac (without vitelline or umbilical cord), and E10.5 FL were treated with 1.25mg/mL collagenase type I (Sigma-Aldrich) for 10 minutes at 37°C, homogenised through gentle pipetting. E11.5 FL and E13.5-E14.5 FL were disrupted mechanically by repeated suction through 1mL syringes (Terumo) with 27G and 25G needles (BD Microlance), respectively.

For tissue-resident macrophage analysis E14.5 FL, brain and skin were incubated 30 minutes at 37°C in PBS with 0.5mg/ml Collagenase D (Roche), 2.4mg/ml Dispase (Invitrogen), 100U/mL Deoxyribonuclease I (DNAse I, Sigma-Aldrich) and 3% foetal bovine serum (FBS, Invitrogen) followed by light mechanical disruption.

For the majority of assays, especially sorting, tissues from several embryos with appropriate number of sp were pooled into the same sample. Cells in suspension were pelleted by centrifugation at 300-350x*g* for 5 minutes and antibody staining was carried out in DPBS with 10% FCS and 2mM EDTA.

2.2.2. Adult tissues

Method used in chapters 3-6. Preparation of adult cell suspensions was carried out in phosphate-buffered saline (PBS, Gibco) supplemented with 5-10% foetal calf serum (FCS, Thermo Fisher Scientific) and 2mM ethylenediaminetetraacetic acid (EDTA, Sigma-Aldrich).

BM cell suspensions were obtained from femurs, tibias, iliac crests, and sternum harvested from individual adult mice with minimal muscle tissue, crushed with pestle and mortar, homogenised through pipetting, and strained through a 70µm cell strainer (Fisher Scientific).

Spleen and thymus were harvested from individual adult mice, mushed with syringe plunger through a 70µm cell strainer and homogenised through pipetting to produce single cell suspensions.

In transplantation experiments, BM cell aliquots were stained with a solution of Trypan Blue (Sigma-Aldrich)/Zap-OGLOBIN II (Beckman Coulter) and counted manually in a Neubauer haemocytometer. The required number of cells was pelleted by centrifugation at 400-500x*g* for 5-7 minutes and resuspended in the appropriate media for transplantation.

In flow cytometry experiments, cell aliquots were counted automatically in a Sysmex KX-21N Haematology Analyser. The required number of cells was pelleted by centrifugation at 400-500x*g* for 5-7 minutes and resuspended in PBS with 5-10% FCS and 2mM EDTA for antibody staining.

2.2.3. c-Kit enrichment of adult bone marrow

Method used in chapter 3. Adult BM cells for sorting of lymphoid-primed progenitors (LMPP) for *in vitro* culture assays were enriched for c-Kit (CD117) expression by manual magnetic activated cell sorting (MACS, Miltenyi Biotec) according to manufacturer's instructions with

minor modifications. BM samples for single cell transplantation or gene expression analysis were not enriched by this method.

BM cell suspensions were centrifuged at 500x*g* for 5-7 minutes and resuspended at a concentration of $1x10^9$ cells/mL in PBS 5-10% FCS 2mM EDTA. Magnetic anti-CD117 microbeads (Miltenyi Biotec) were added 1:40 and the cell suspension was incubated for 20 minutes at 4^oC, with regular mixing to avoid sedimentation. Excess beads were washed with PBS/FCS, samples were centrifuged and resuspended, then strained and passed through equilibrated MACS LS columns mounted on a magnetic separator (Miltenyi Biotec). c-Kit- cells were removed from the columns through several washing steps and c-Kit+ cells were eluted with PBS/FCS. Eluted cells were again counted before antibody staining.

2.2.4. Peripheral blood

Method used in chapters 5 and 6. Peripheral blood (100-200µL, <10% of total blood volume) was collected from mouse tail-vein into lithium heparin-coated microvettes with capillary (Sarstedt). 2µL of unfractionated blood was used for analysis of erythroid cells. Platelets were isolated from the supernatant after centrifugation in tabletop centrifuge at 100x*g* for 10 minutes at room temperature (RT). For leucocyte separation the remaining sample was incubated 1:1 with 2% w/v Dextran (Sigma-Aldrich), 20-30 minutes at 37^oC. Excess erythrocytes were lysed from the leucocyte preparation through incubation with 1x ammonium chloride solution (Stem Cell Technologies) for 2 minutes at RT. Erythroid cells were pelleted by centrifugation for 5 minutes at 500x*g* while platelets and leucocytes were pelleted by centrifugation for 5 minutes at 1000x*g*, and antibody staining was carried out in PBS with 1-2% FCS and 0.4-0.8mM EDTA.

2.3. Flow cytometry and fluorescence activated cell sorting

2.3.1 Antibody stainings

Method used in chapters 3-6. Pelleted cells were first blocked with purified anti-CD16/32 (Fc-block, produced in-house) for 10-15 minutes at 4°C and then stained with monoclonal antibodies for 15-20 minutes at 4°C. When biotinilated antibodies requiring a second staining step were used, samples were washed and incubated again for 15-20 minutes at 4°C with the respective streptavidin conjugate. In the staining of BM myeloid progenitors, which includes CD16/32 as a marker, incubation with conjugated CD16/32 substituted the first Fc-block step. Antibody details are specified in Tables 2.1 and 2.2.

Cell suspensions were typically stained at a concentration of ≤ 1.5 x 10^8 cells/mL, and stained samples were typically resuspended at a final concentration of ≤ 5 x 10^7 cells/mL before analysis or sorting. Stained samples were filtered through 35μm cell strainer cap into polystyrene tubes (BD Falcon) for analysis and polypropylene tubes (BD Falcon) for sorting. 7-amino-actinomycin D (7-AAD, Sigma-Aldrich) or 4',6-diamidino-2-phenylindole (DAPI, Invitrogen) was added to samples to allow exclusion of non-viable cells from analysis and sorting.

2.3.2 Instruments and analysis

Method used in chapters 3-6. Appropriate sorter and analyser laser voltage settings to ensure minimal need for compensation between fluorescence channels were adjusted with Negative Control Compensation Particles Sets (CompBeads, BD Biosciences) single-stained with the fluorochromes of interest, and also fluorescent cells when applicable. Fluorescence-minus-one (FMO) controls as well as internal control populations were used as guides for

gating. Due to the variability of population sizes and strength of fluorescent signal in the tissues of different single cell reconstituted mice, in the analysis of the reconstituted haematopoietic hierarchy the same exact gates were not systematically applied to all samples but instead adjusted to the natural cell distribution of each individual mouse and according to internal population controls.

Cell sorting was performed on BD FACSAriaII, BD FACSAriaIII and BD FACSAria Fusion special order cell sorters. YS cells were sorted using 100µm nozzle, while FL cells, BM cells, and cells grown *in vitro* were sorted with 85µm nozzle. Cell sorting purity was tested before and after every experiment and ensured to be >95%. Single cell sorting was performed by an automated cell deposition unit (ACDU) providing single cells in >99% of wells and no wells with >1 cell. Single cell deposition efficiency was confirmed in all experiments with fluorescent beads (BD Biosciences).

Flow cytometry analysis was performed on BD LSRII, BD LSRFortessa and BD LSRFortessa X-20 analysers (BD Biosciences). Flow cytometry data was acquired with FACSDiva software (BD Biosciences) and subsequent analysis was performed with FlowJo software (Tree Star, Inc). Overview of optical systems (lasers and band-pass filters) is specified in Table 2.3.

Table 2.1. Antibodies used in flow cytometry.

Antibody	Clone	Conjugate	Supplier	Application
B220 (CD45R)	RA3-6B2	APC	BD	*Rag1*-Cre lineage tracing
		FITC	eBiosience	B cell cultures
		PE	BD	B cell cultures
		PE-TexasRed	BD	*Rag1*-Cre lineage tracing
		APC-eF780	eBioscience	BM B cell progenitors
CD4	RM4-5	AF700	eBioscience	*Rag1*-Cre lineage tracing
		APC-eF780	eBioScience	Peripheral blood
		BV650	BioLegend	T cell cultures; peripheral blood; thymus T cell progenitors; spleen B and T cells
	H129.19	PE	BioLegend	T cell cultures
CD8α	53-6.7	APC	eBioscence	T cell cultures; peripheral blood
		APC-eF780	eBioscence	Peripheral blood; thymus T cell progenitors; spleen B and T cells
		PE-Cy7	eBioscence	T cell cultures
CD11b (Mac-1)	M1/70	AF700	eBioscence	*Rag1*-Cre lineage tracing; B cell cultures; peripheral blood
		APC	BioLegend	Peripheral blood
		PE	eBioscence	*Rag1*-Cre lineage tracing (macrophages)
		PE-Cy5	BioLegend	T cell cultures
CD16/32 (FcγRII/III)	93	APC	eBioscience	BM myeloid progenitors
CD19	1D3	APC	BD	*Rag1*-Cre lineage tracing; BM B cell progenitors
		PE	BD	T cell cultures; *Rag1*-Cre lineage tracing
		PE-Cy7	BD	E9.5 YS, E10.5 FL and E11.5 FL progenitors; B cell, T cell and switch cultures; peripheral blood
		Pacific Blue	eBioscience	Peripheral blood; spleen B and T cells
		eF450	eBioscience	Peripheral blood; spleen B and T cells
CD25	3C7	PE	BD	T cell and switch cultures
	PC61	PerCP-Cy5.5	BD	T cell cultures
CD34	RAM34	AF700	eBioscience	BM HSC

Table 2.1. Antibodies used in flow cytometry (continued).

Antibody	Clone	Conjugate	Supplier	Application
CD41	MWReg30	PE	eBioscence	Platelets
		PE-Cy7	eBioscience	*Rag1*-Cre lineage tracing; platelets
		BV605	BD	BM myeloid progenitors
CD45	30-F11	AF700	eBioscience	E9.5 YS, E10.5 and E11.5 FL progenitors
		Pacific Orange	Invitrogen	B and T cell cultures
CD45.1	A20	Biotin	BD	*Rag1*-Cre lineage tracing
		PE	eBioScience	Reconstitution analysis: peripheral blood
		PE-Cy7	BioLegend	Reconstitution analysis: thymus, spleen, T cell cultures
		BV605	BioLegend	Reconstitution analysis: peripheral blood
		BV650	BioLegend	Reconstitution analysis: BM
CD45.2	104	AF700	BioLegend	Reconstitution analysis: peripheral blood, BM, thymus, spleen
		APC-Cy7	BD	*Rag1*-Cre lineage tracing (macrophages)
CD48	HM48-1	APC	BioLegend	E14.5 FL HSC; BM HSC and LMPP
CD90.2 (Thy1.2)	30-H12	APC	BioLegend	T cell and switch cultures
	53-2.1	APC-eF780	eBioscience	T cell cultures
CD105 (Endoglin)	MJ7/18	BV421	BD	BM myeloid progenitors
CD150	TC15-12F12.2	APC	BioLegend	Platelets; *Rag1*-Cre lineage tracing
		PE-Cy7	BioLegend	BM HSC and LMPP; platelets
c-Kit (CD117)	2B8	APC-eF780	eBioscience	E9.5 YS, E10.5 FL and E11.5 FL progenitors; E14.5 FL HSC; BM HSC, LMPP, myeloid progenitors
		PE-Cy7	BD	*Rag1*-Cre lineage tracing (macrophages); BM B cell progenitors
F4/80	BM8	e450	eBioscience	*Rag1*-Cre lineage tracing (macrophages)
Flt3 (CD135)	A2F10	Biotin	eBioscience	E11.5 FL progenitors; BM LMPP
		PE	BioLegend	BM LMPP

Table 2.1. Antibodies used in flow cytometry (continued).

Antibody	Clone	Conjugate	Supplier	Application
Gr-1 (Ly-6G/Ly-6C)	RB6-8C5	APC	BioLegend	B cell cultures; *Rag1*-Cre lineage tracing (macrophages)
		Pacific Orange	Invitrogen	Peripheral blood; *Rag1*-Cre lineage tracing
IL7Rα	A7R34	PE	eBioscience	E9.5 YS, E10.5 FL and E11.5 FL progenitors; BM LMPP
NK1.1	PK136	Pacific Blue	BioLegend	B cell and T cell cultures; peripheral blood
		PE-Cy5	BioLegend	Peripheral blood
PIR-A/B	6C1	PerCP-eF710	eBioscience	E11.5 FL and E13.5 FL progenitors
Sca-1 (Ly-6A/E)	E13-161.7	Pacific Blue	BioLegend	E9.5 YS and E10.5 FL progenitors; E14.5 FL HSC; BM HSC and LMPP
		FITC	BD	E11.5 FL progenitors; E14.5 FL HSC; BM HSC and LMPP
	D7	BV786	BD	BM myeloid progenitors
TCRβ	H57-597	APC	eBioscience	Peripheral blood; thymus T cell progenitors
TER-119	TER119	PerCP-Cy5.5	eBioscence	*Rag1*-Cre lineage tracing; platelets; erythrocytes
Streptavidin	N/A	BV605	BioLegend	BM LMPP reconstitution
		Qd655	Invitrogen	E11.5 FL progenitors
		PE-TexasRed	BD	*Rag1*-Cre lineage tracing

Table 2.2. Lineage markers used for lineage exclusion gating in flow cytometry.

Antibody	Clone	Conjugate	Supplier	Application
B220 (CD45R)	RA3-6B2	PE-Cy5	BioLegend	E14.5 FL HSC; BM HSC, LMPP, myeloid progenitors; thymus T cell progenitors
		PE-Cy7	BioLegend	E9.5 YS, E10.5 FL and E11.5 FL progenitors
CD3ε	145-2C11	APC	BD	E9.5 YS, E10.5 FL, E11.5 FL progenitors
		PE-Cy5	eBioscience	BM B cell progenitors
CD4	RM4-5	PE-Cy5	BD	BM HSC, LMPP, myeloid progenitors
CD5	53-7.3	PE-Cy5	BD	E14.5 FL HSC; BM HSC and LMPP
CD8α	53-6.7	PE-Cy5	eBioscience	E14.5 FL HSC; BM HSC, LMPP, myeloid progenitors
CD11b (Mac-1)	M1/70	PE-Cy5	BioLegend	BM HSC, LMPP, myeloid progenitors; thymus T cell progenitors; T cell cultures; spleen B and T cells
CD11c	N418	PE-Cy5	BioLegend	BM B cell progenitors; thymus T cell progenitors; spleen B and T cells
CD19	ID3	PE-Cy5	eBioscience	E9.5 YS, E10.5 FL and E11.5 FL embryonic progenitors; thymus T cell progenitors
		PE-Cy7	BD	E9.5 YS, E10.5 FL and E11.5 FL embryonic progenitors
F4/80	BM8	APC	Invitrogen	E9.5 YS, E10.5 FL, E11.5 FL progenitors
		PE-Cy5	BioLegend	BM B cell progenitors reconstitution
Gr-1 (Ly-6G/Ly-6C)	RB6-8C5	APC	BioLegend	E9.5 YS, E10.5 FL, E11.5 FL progenitors
		PE-Cy5	BioLegend	E14.5 FL HSC; BM HSC, LMPP, B cell and myeloid progenitors; thymus T cell progenitors; spleen B and T cells
NK1.1	PK136	APC	BD	E9.5 YS, E10.5 FL, E11.5 FL progenitors
		PE-Cy5	BioLegend	BM B cell progenitors; thymus T cell progenitors; spleen B and T cells
TER-119	TER119	APC	eBioscience,	E9.5 YS, E10.5 FL, E11.5 FL progenitors
		PE-Cy5	BioLegend	E14.5 FL HSC; BM HSC, LMPP, B cell and myeloid progenitors; thymus T cell progenitors; spleen B and T cells

Table 2.3. Optical system settings for flow cytometry.

Laser wavelengths	Detection channels	Band-pass optical filters
Red laser 633nm or 640nm *	APC	670/14, 660/20 or 670/20
	AF700	730/45
	APCeF780	780/60
Blue laser 488nm	FITC, GFP, YFP	525/50 or 530/30
	PerCP PerCPCy5.5	670/20 or 670/30 695/40
Violet laser 405nm	PB, DAPI, BV421	450/50
	PO, BV510	525/50
	Qd605, BV605	605/20 or 610/20
	Qd655, BV650	660/20
	BV711	710/50
	BV785	780/60
Green laser, 532nm or Yellow/Green, 561nm **	PE	575/25 or 585/15
	PETxR	610/20
	PECy5, 7AAD	685/35 or 670/14
	PECy5.5, PerCPCy5.5	710/40 or 710/50
	PECy7	780/60

* BD FACSAriaII cell sorter, BD LSRII and BD LSRFortessa X-20 analysers were fitted with the 640nm red laser. BD FACSAriaIII and BD FACSAria Fusion cell sorters were fitted with the 633nm red laser.

** BD FACSAriaII cell sorter and BD LSRII analyser were fitted with the 532nm green laser. BD FACSAriaIII and BD FACSAria Fusion cell sorters, and BD LSRFortessa X-20 analyser were fitted with the 561nm yellow/green laser.

2.4. *In vivo* reconstitution assays

2.4.1. Single cell transplantation of bone marrow and foetal liver cells

Method used in chapters 5 and 6. Single cell transplantation and peripheral blood reconstitution analysis were performed as previously published (Sanjuan-Pla et al., 2013). Single phenotypically defined *Vwf*^{high} LT-HSC (LSK CD150+ CD48- CD34-) were sorted by flow cytometry from *Vwf*-EGFP (CD45.2) or *Vwf*-tdTomato/*Gata1*-EGFP (CD45.2) adult BM or E14.5 FL, and deposited by ACDU into round-bottom 96-well plates (Corning Costar) containing 100µL per well of Iscove's Modified Dulbecco's Medium (IMDM, Gibco) supplemented with 20% BIT-9500 Serum Substitute (Stem Cell Technologies), 100U/mL Penicillin, 0.1mg/mL Streptomycin (100x Pen/Strep, PAA Laboratories), 2mM L-Glutamine (PAA Laboratories), 0.1mM 2-Mercaptoethanol (Sigma-Aldrich). 100µL of the same supplemented IMDM containing 1x10^6 unfractionated BM cells from a *Kit*$^{W41/W41}$ mouse (CD45.1) were added to each well. The contents of each well were carefully loaded into sterile 0.5mL insulin syringes with 29G needle (Terumo), and syringes were kept on ice until injection. Samples were transplanted by intravenous injection into lethally irradiated (two doses of 5 Gy, 4 hours apart) B6.SJL-*Ptprc*^{a} *Pepc*^{b}/BoyJ (CD45.1) recipient mice.

Peripheral blood reconstitution was analysed at two or three regularly spaced time points, every 4 weeks between 6 weeks and 18 weeks post-transplantation. For some recipient mice blood was analysed at one or two additional time points up to 35 weeks post-transplantation. Peripheral blood reconstitution analysis of platelets, erythrocytes, and leucocytes by flow cytometry was carefully performed to maximize sensitivity and selectivity. To increase reconstitution detection power, cell recovery and separation were prioritised in the antibody staining protocols, and as many flow cytometry events as possible were recorded for each population of interest. To ensure the highest possible specificity, our

antibody panel and gating strategy prioritised exclusion of possible staining artefacts. To ensure a clean staining background for precise detection of low reconstitution levels, peripheral blood from a non-transplanted wild-type CD45.1 mouse was regularly screened alongside blood samples of transplanted mice.

Mice were considered to be long-term reconstituted when donor contribution to at least one peripheral blood lineage was ≥0.01%. Additionally, reconstitution was only considered to be credible when ≥10 clustered donor-derived events were observed within a lineage gate. Recipients with <0.01% reconstitution of all lineages at any given time point post-transplantation were considered to not be long-term reconstituted and were not analysed further. Recipients that did not survive the entire blood follow-up period were also eliminated from analysis.

After the final peripheral blood analysis (15-35 weeks post-transplantation), reconstituted mice of interest were terminated for flow cytometric analysis of the donor-derived haematopoietic hierarchy in different tissues, for functional *in vitro* analysis of lineage potentials of donor-derived LSK cells, and for secondary transplantation of donor-derived HSCs.

2.4.2. Secondary bone marrow transplantation

Method used in chapters 5 and 6. Donor-derived CD45.2+ cells were sorted by flow cytometry from BM of single cell reconstituted recipients into eppendorf tubes with 100µL of PBS 1% FCS. Another 100µL of PBS 1%FCS containing $1x10^6$ unfractionated BM cells from a $Kit^{W41/W41}$ mouse (CD45.1) were added to each tube.

Unfractionated BM cells from single cell reconstituted recipients were counted and diluted in PBS 1% FCS to a concentration of 3.5×10^6 - 1×10^7 cells in 200µL, as required.

In both cases samples were loaded into sterile 0.5mL insulin syringes with 29G needle and transplanted by intravenous injection into lethally irradiated (two doses of 5 Gy, 4 hours apart) B6.SJL-*Ptprc*^{a} *Pepc*^{b}/BoyJ (CD45.1) recipient mice.

2.4.3. Unfractionated foetal liver transplantation

Method used in chapter 6. Individual FLs were dissected in DPS 10% FCS from *Gata1*-EGFP embryos genotyped by PCR. E11-E14.5 FLs were mechanically disrupted and E10-E10.5 FLs were digested enzymatically as described above. 5x10^{5} E14.5 FL cells and whole E10-E12 individual FLs were centrifuged at 400x*g* for 5-6 minutes and resuspended in 100µL DPBS 1% FCS. Another 100µL of PBS 1% FCS containing 1x10^{6} unfractionated BM cells from a *Kit*$^{W41/W41}$ mouse (CD45.1) was added to each sample. Samples were loaded into sterile 0.5mL insulin syringes with 29G needle and transplanted by intravenous injection into lethally irradiated (two doses of 5 Gy, 4 hours apart) B6.SJL-*Ptprc*^{a} *Pepc*^{b}/BoyJ (CD45.1) recipient mice.

2.5. *In vitro* cell culture assays

2.5.1. Lymphoid lineage potentials in stromal co-cultures

Methods used in chapters 3 and 5. One or two days before sorting the cells of interest, confluent monolayers (~80%) of OP9 or OP9-DL1 stromal cells were prepared by seeding 1.5-2x10^{3} cells in flat-bottom 96-well plates (Corning Costar) in Opti-MEM Glutamax medium (Gibco) supplemented with 10% culture-grade FCS (Sigma-Aldrich or GE Healthcare HyClone), 100U/mL Penicillin, and 0.1mg/mL Streptomycin (100x Pen/Strep, PAA Laboratories). OP9 stromal cells support differentiation of B cell and myeloid potential, while

OP9-DL1 stromal cells support differentiation of T cell potential. B and T cell cultures were analysed by flow cytometry.

Haematopoietic cells were bulk sorted and manually plated on the pre-prepared stromal layers at an average of 1 cell/well (E11.5 FL cells and adult BM LMPP, chapter 3), 4 cells/well (E10.5 FL cells, chapter 3), or 5-20 cells/well (reconstituted BM cells, chapter 5).

In the FL studies in chapter 3, OP9 co-cultures were maintained for 12-15 days and OP9-DL1 co-cultures were maintained for 21 days. Both co-cultures were supplemented with 25ng/mL mouse stem cell factor (mSCF, PreproTech) and 25ng/mL human Flt3-ligand (hFlt3-L, Amgen), and OP9 culture was additionally supplemented with 20ng/mL human interleukin 7 (hIL-7, PreproTech).

In the reconstituted BM studies in chapter 5, OP9-DL1 co-cultures were maintained for 26-37 days, and were supplemented with 5ng/mL mSCF, 5ng/mL hFlt3-L, and 4-5ng/mL hIL-7. In these cultures hIL-7 was noted to promote a higher frequency of CD4+ CD8+ T cells.

2.5.2. Myeloid, megakaryocyte, and erythroid lineage potentials in liquid culture

Methods used in chapters 3 and 5. Bulk sorted cells were manually plated at a density of 0.5cell/well or 1 cell/well in 60-well Terasaki microplates (Thermo Fisher Scientific) with X-VIVO 15 medium containing Gentamycin and L-Glutamine (Lonza BioWhittaker) supplemented with 10-20% culture-grade FCS, and 0.1mM 2-Mercaptoethanol.

For evaluation of myeloid (GM) potential in the FL studies in chapter 3 cultures were maintained for 7-11 days, and the medium was supplemented with 25-50ng/mL mSCF, 25-50ng/mL hFlt3-L, 25-50ng/mL human thrombopoietin (hTPO, PreproTech), 10-20ng/mL mouse interleukin 3 (mIL-3, PreproTech), 25-50ng/mL human granulocyte-colony stimulating factor (hG-CSF, Amgen), and 25-50ng/mL mouse granulocyte/macrophage-colony stimulating factor (mGM-CSF, PreproTech).

For evaluation of granulocyte morphology in the FL studies in chapter 3, cultures of 10 cells/well were maintained for 6 days in medium supplemented with 25-50ng/mL mSCF, 25-50ng/mL hFlt3-L, 25-50ng/mL hTPO, 10-20ng/mL mIL-3, and 25-50ng/mL hG-CSF.

For evaluation of GM potential in the reconstituted BM studies in chapter 5 cultures were maintained for 10-21 days and the medium was supplemented with 2ng/mL mSCF, 5ng/mL hFlt3-L, 5ng/mL hTPO, 5ng/mL mIL-3, 10ng/mL hG-CSF, and 10ng/mL mGM-CSF.

For evaluation of megakaryocyte/erythroid potential (Mk/E) in the FL studies in chapter 3, cultures were maintained for 7-11 days, and the medium was supplemented with 50ng/mL mSCF, 50ng/mL hFlt3-L, 20ng/mL mIL-3, 50ng/mL hTPO, and 5ng/mL human erythropoietin (hEPO, Roche). Erythroid cells in Mk/E cultures were identified by staining with 2,7-diaminofluorene (DAF, Sigma-Aldrich). This staining consists of 5 minutes incubation at room temperature in a solution of 200mM Tris-HCl (pH 7.5) with 0.3% hydrogen peroxide and 5% DAF (DAF stock solution of 10mg/mL in 90% glacial acetic acid).

2.5.3. Myeloid, megakaryocyte, and erythroid lineage potentials in semi-solid culture

Methods used in chapter 3 and 4. Colony forming unit-granulocyte/macrophage (CFU-GM) potential was evaluated in incomplete MethoCult methylcellulose-based medium (MethoCult M3134, Stem Cell Technologies) supplemented with 5ng/mL mGM-CSF, 10ng/mL hFlt3-L, 2ng/mL mIL-3, and 10ng/mL hG-CSF. Colony forming unit-granulocyte (CFU-G) potential was evaluated in MethoCult M3134 supplemented with 50 ng/mL mSCF and 10ng/mL hG-CSF.

Colony forming unit-megakaryocyte (CFU-MK) potential was evaluated in MegaCult-C collagenase-based medium (Stem Cell Technologies) supplemented with 10ng/mL mIL-3, 50ng/mL hTPO, 20ng/mL human interleukin 6 (hIL-6, PreproTech), and 50ng/mL human

interleukin 11 (hIL-11, Genetics Institute, Inc). Cultures were maintained for 7 days and analysed by staining with Acetylthiocholine iodide (Sigma-Aldrich). This staining consists of 5 minute incubation in ice cold acetone followed by 4 hours incubation in a solution of 0.45 mg/mL Acetylthiocholine iodide, 4.5 mM sodium citrate, 2.7mM copper sulphate, and 0.45mM potassium ferricyanide. Stained slides are fixed in 95% ethanol for 10 minutes, rinsed with water, counterstained with Harris' hematoxylin solution for 30 seconds, and rinsed with water once more.

Burst forming unit-erythroid (BFU-E) potential was evaluated in complete MethoCult methylcellulose-based medium containing 2-Mercaptoethanol, mSCF, mIL-3, hIL-6, and hEPO (MethoCult GF M3434, Stem Cell Technologies), further supplemented with 50ng/mL hTPO. Cultures were maintained for 7-10 days and analysed by staining with DAF as described above.

For evaluation of CFU-MK and BFU-E potentials in the FL studies in chapter 3, 200 bulk sorted cells of E10.5-E11.5 FL were plated per biological replicate.

For evaluation of CFU-GM and BFU-E potentials in the *Rag1*-Cre/*R26*R-EYFP studies in chapter 4, $40x10^4$ unfractionated cells of E14.5 FL were plated per biological replicate (Thermo Scientific) and YFP signal was evaluated with a fluorescence microscope, using wild-type littermate E14.5 FL cultures as a control for negative YFP signal.

2.5.4. Combined lineage potentials in switch-culture

Method used in chapter 3. Single cells were sorted by ACDU directly into wells with pre-plated monolayers of OP9 stromal cells and co-cultured for 5 days in Opti-MEM Glutamax medium supplemented with 10% culture-grade FCS, 100U/mL Penicillin, 0.1mg/mL Streptomycin, 25ng/mL mSCF, 25ng/mL hFlt3-L, and 20ng/mL hIL-7. Cultures were then

transferred to OP9-DL1 stroma and cultured for an additional 6 days in the same basic medium supplemented with 25ng/mL hFlt3-L.

2.6. Cytospins and cell morphology analysis

Method used in chapters 3, 4 and 5. Myeloid colonies grown *in vitro* were dissociated and collected by pipetting and transferred into 100-200µL of PBS with 20% FCS. Samples of 500-1000 myeloid cells from *Rag1*-Cre/*R26*R-EYFP E14.5 FL were sorted directly into 100-200µL of PBS with 20% FCS. Collected cells were centrifuged onto polylysine-coated microscope slides (VWR) by a Shandon Cytospin 4 Cytocentrifuge (Thermo Scientific). Slides were stained with May Grünwald (Sigma-Aldrich) and Giemsa (Fluka) solutions according to manufacturer's instructions, and mounted with Pertex (Cellpath). Morphology of stained cells was analysed with inverted bright field microscope.

2.7. Gene expression analysis

2.7.1. RNA sequencing

Samples were prepared for sequencing using the SMARTer Ultra Low RNA kit for Illumina Sequencing (Clontech) as previously described (Ramsköld et al., 2012). Samples of 70-100 cells were sorted through 85µm nozzle into PCR tubes containing freshly prepared lysis buffer (3.5µL/tube), consisting of 0.2% Triton X-100 and RNase inhibitor. Samples were centrifuged at 6000x*g* for 30 seconds, flash-frozen on dry ice and stored at -80°C until further processing. cDNA was generated using SMARTScribe Reverse Transcriptase (Clontech) and pre-amplified using Advantage 2 PCR Kit (Clontech). cDNA libraries were sheared using the Covaris AFA system. The NEBNext DNA Library Prep Reagent Set for

Illumina (New England Biolabs) was used to repair ends, adenylate 3' ends, ligate genomic adaptors and amplify fragments with Genomic DNA Sample Prep oligos (Illumina). Sample quality was tested with High Sensitivity DNA Analysis Kit for Agilent 2100 BioAnalyzer (Agilent Technologies, Inc). Sample concentration was measured with Qubit dsDNA HS Assay Kit (Thermo Fisher Scientific). For each flow cell lane, 5-6 samples with distinct index combinations were pooled at a final concentration of 2nM. Pooled samples were sequenced on HiSeq 2500 system (Illumina) at SciLifeLab, generating single-end 50 bp reads.

Short reads were aligned using Bowtie (Langmead et al., 2009) against the murine genome assembly (mm9) and against the murine transcriptome (Refseq and Ensembl, version from 31 Jul 2011 and 16 May 2011, respectively). Gene expression levels for Refseq transcripts were summarised as reads per kilobase of transcript per million mapped reads (RPKM) and read counts using Rpkmforgenes (Ramskold et al., 2012). RPKM values were used to evaluate expression of specific genes. Non-adjusted read counts for each gene were used for statistical calculation of global differential expression between the specified populations using the DESeq package (version 1.6.1) for R (version 2.14.2) (Anders and Huber, 2010). Genes that were significant at a 10% false discovery rate (calculated using a Benjamini-Hochberg adjusted p-value ≤0.05) were considered differentially expressed between populations. List of genes in lineage-affiliated transcriptional programs were selected from previously published literature (Luc et al., 2012).

2.7.2. Single cell RNA sequencing

Single cells were prepared for sequencing using Smart-seq2 protocol as previously described (Picelli et al., 2014). Single cells were sorted by ACDU through 85µm nozzle into 96-well PCR plates with freshly prepared lysis buffer (4µL/well) consisting of 0.2% Triton X-100 (Sigma-Aldrich), RNase inhibitor (Clontech), 2.5 mM dNTPs (Thermo Fisher Scientific) and 2.5 µM

oligo-$dT_{30}VN$ primer (Biomers.net). cDNA libraries were generated using SuperScript II (Invitrogen), pre-amplified using KAPA HiFi HotStart ReadyMix (KAPA Biosystems), and purified using Agencourt AMPure XP (Beckman Coulter). Tagmentation and library preparation was performed using the Nextera XT DNA Library Preparation Kit (Illumina). Sample quality was tested with High Sensitivity DNA Analysis Kit for Agilent 2100 BioAnalyzer (Agilent Technologies, Inc). Sample concentration was measured with Qubit dsDNA HS Assay Kit (Thermo Fisher Scientific). For each flow cell lane 17-48 samples (corresponding to single cells) with distinct index combinations were pooled at a final concentration of 2nM. Pooled samples were sequenced on a HiSeq 2500 system (Illumina) at SciLifeLab, generating single-end 50 bp reads.

Short reads were aligned using Tophat (version 2.0.10) (Kim et al., 2013) against the mouse genome (mm10 assembly). Non-uniquely mapped reads were discarded**.** Expression values were quantified as RPKM based on the RefSeq genes model using rpkmforgenes (Ramsköld et al., 2012). Differentially expressed genes analysis was performed using the nonparametric Wilcoxon test for the expression level and Fisher's exact test for the expressing cell frequency. P-values generated from both tests were then combined using Fisher's method, and were adjusted using Benjamini-Hochberg. Differentially expressed genes were selected using a cutoff at absolute log2 fold change ≥1 and adjusted p-values <0.05.

2.7.3. Multiplexed quantitative PCR

Multiplex quantitative PCR (qPCR) analysis was performed using the BioMark 48.48 or 96.96 Dynamic Array platform (Fluidigm) and TaqMan Gene Expression Assays (Thermo Fisher Scientific) as previously described (Tehranchi et al., 2010). Single cells were sorted by ACDU into 96-well PCR plates and bulk cells (25-50) were sorted into PCR tubes containing 5 or 10µL of RT/pre-amplification buffer, respectively. CellsDirect One-Step qRT-PCR kit (Invitrogen) was used for cDNA synthesis and pre-amplification of target genes. 10µl of pre-

amplification buffer consisted of 2.5µl Taqman assay mix containing all assays at 0.2x dilution, 5µL CellsDirect 2x Reaction mix (Invitrogen), 1.2µL CellsDirect RT/Taq mix (Invitrogen), 1.2µL TE buffer and 0.1µL SUPERase-In RNase Inhibitor (Ambion). Targetted cDNA pre-amplification was performed during 22 cycles and pre-amplified product was diluted 1:5 in TE buffer before processing with Dynamic Array protocol according to manufacturer specifications. TaqMan Gene Expression Assays used are listed in Table 2.4. No template controls and no RT controls were also analysed in each experiment, as well as positive control and negative control cell samples.

Mean fold-change of expression relative to Hypoxanthine Guanine Phosphoribosyltransferase 1 gene (*Hprt1*) was calculated as $2^{-\Delta Ct}$. Data presented in heatmaps (single cells and T cell cultures grown *in vitro*) was analysed using the ΔCt method, using the mean of housekeeping genes Hypoxanthine Guanine Phosphoribosyltransferase 1 (*Hprt1*) and Glyceraldehyde-3-Phosphate Dehydrogenase gene (*Gapdh*), or the mean of *Hprt1* and Beta-2-microglobulin gene (*B2m*) for normalization. Only cells expressing *Hprt1, Gapdh* and the proto-oncogene c-Kit gene (*c-Kit*) were included in single cell analysis. Only samples expressing *Hprt1, B2m,* and CD45 gene (*Ptcrp*) were included in T cell culture analysis.

2.8. Statistical analysis

The statistical significance of differences observed between experimental groups was calculated in Prism software (GraphPad Software, Inc). Two-tailed Student's t-test was used when comparing two experimental groups. One-way ANOVA followed by Tukey's multiple comparisons test (95% confidence interval, p-values adjusted for multiplicity) was used when comparing ≥3 experimental groups.

Table 2.4. Taqman assays used in multiplexed quantitative PCR.

Gene symbol	Gene name	Taqman assay ID
B2m	Beta-2-microglobulin	Mm00437762_m1
Bcl11b	B-cell leukemia/lymphoma 11B	Mm00480516_m1
Bmi1	Bmi1 polycomb ring finger oncogene	Mm03053308_g1
Ccr7	Chemokine (C-C motif) receptor 7	Mm01301785_m1
Ccr9	Chemokine (C-C motif) receptor 9	Mm02620030_s1
Cd4	CD4 antigen	Mm00442754_m1
Cd8a	CD8 antigen, alpha chain	Mm01182108_m1
Cd3d	CD3 antigen, delta polypeptide	Mm00442746_m1
Cd3e	CD3 antigen, epsilon polypeptide	Mm00599683_m1
Cd3g	CD3 antigen, gamma polypeptide	Mm00438095_m1
Cd19	CD19 antigen	Mm00515420_m1
Cd34	CD34 antigen	Mm00519283_m1
Cd79a / Mb1	CD79A antigen (immunoglobulin-associated alpha)	Mm00432423_m1
Cd86	CD86 antigen	Mm00444543_m1
Cebpa	CCAAT/enhancer binding protein (C/EBP), alpha	Mm00514283_s1
c-Kit	Proto-oncogene c-Kit	Mm00445212_m1
Csf1r	Colony stimulating factor 1 receptor	Mm01266652_m1
Csf2ra	Colony stimulating factor 2 receptor, alpha	Mm00438331_g1
Csf3r	Colony stimulating factor 3 receptor (granulocyte)	Mm00432735_m1
Ebf1	Early B cell factor 1	Mm00432948_m1
Epor	Erythropoietin receptor	Mm00438760_m1
Fhl1	Four and a half LIM domains 1	Mm04204611_g1
Fli1	Friend leukemia integration 1	Mm00484410_m1
Flt3	Fms-like tyrosine kinase 3	Mm00439016_m1
Gapdh	Glyceraldehyde-3-phosphate dehydrogenase	Mm99999915_g1
Gata1	GATA binding protein 1	Mm01352636_m1
Gata2	GATA binding protein 2	Mm00492301_m1
Gata3	GATA binding protein 3	Mm00484683_m1
Gfi1	Growth factor independent 1	Mm00515855_m1
Gfi1b	Growth factor independent 1B	Mm00492318_m1
Gfp	Green fluorescent protein	Mr03989638_mr
Hes1	Hairy and enhancer of split 1 (Drosophila)	Mm01342805_m1
Hk3	Hexokinase 3	Mm01341942_m1
Hlf	Hepatic leukemia factor	Mm00723157_m1
Hoxb4	Homeobox B4	Mm00657964_m1
Hprt1	Hypoxanthine guanine phosphoribosyl transferase 1	Mm01545399_m1
Igmh	Immunoglobulin heavy constant mu	Mm01718955_g1
Il2ra	Interleukin 2 receptor, alpha chain	Mm00434261_m1
Il7r	Interleukin 7 receptor	Mm00434295_m1
Itga2b / Cd41	Integrin alpha 2b	Mm00439741_m1
Klf1 / Eklf	Kruppel-like factor 1 (erythroid)	Mm04208330_g1

Table 2.4. Taqman assays used in multiplexed quantitative PCR (continued).

Gene symbol	Gene name	Taqman assay ID
Lat	Linker for activation of T cells	Mm00456761_m1
Lck	Lymphocyte protein tyrosine kinase	Mm00802897_m1
Lef1	Lymphoid enhancer binding factor 1	Mm00550265_m1
Lhx2	LIM homeobox protein 2	Mm00839783_m1
Lilrb3 / Pirb	Leukocyte immunoglobulin-like receptor, subfamily B	Mm01700366_m1
Ly6a / Sca-1	Lymphocyte antigen 6 complex, locus A	Mm00726565_s1
Ly6d	Lymphocyte antigen 6 complex, locus D	Mm00521959_m1
Mcl1	Myeloid cell leukemia sequence 1	Mm00725832_s1
Meis1	Meis homeobox 1	Mm00487664_m1
Mpl	Myeloproliferative leukemia virus oncogene	Mm00440310_m1
Mpo	Myeloperoxidase	Mm01298424_m1
Ms4a6b	Membrane-spanning 4-domains, subfamily A, member 6B	Mm00728225_m1
Notch1	Notch gene homolog 1 (Drosophila)	Mm00435249_m1
Pax5	Paired box gene 5	Mm00435501_m1
Pf4	Platelet factor 4	Mm00451315_g1
Ptcra	Pre T-cell antigen receptor alpha	Mm00478363_m1
Ptprc / Cd45	Protein tyrosine phosphatase, receptor type C	Mm01293577_m1
Rag1	Recombination activating gene 1 Forward primer: 5'-TGTGGAGCAAGGTAGCTTAGC-3' Reverse primer: 5'-TCATCGGGTGCAGAACTGAAG-3' Probe sequence: 5'-CATGGCTGCCTCCTTG-3'	Custom assay
Rag2	Recombination activating gene 2	Mm00501300_m1
Sdpr	Serum deprivation response	Mm00507087_m1
Selp	Selectin, platelet	Mm01295931_m1
Sfpi1 / PU.1	Spleen focus forming virus (SFFV) proviral integration oncogene	Mm00488142_m1
SIgh	Sterile Immunoglobulin heavy chain Forward primer: 5'-GGACTTTGGGATGGGTTTGGTT-3' Reverse primer: 5'-CCCTGGTCCTAGACATCAGAGTAAT-3' Probe sequence: 5'-CCCAGATGAAGGGCTAC'-3'	Custom assay
Slamf1 / Cd150	Signaling lymphocytic activation molecule family member 1	Mm00443316_m1
Tcf7	Transcription factor 7, T-cell specific	Mm00493445_m1
Tcrb	T cell receptor beta chain (constant regions 1 and 2) Forward primer: 5'-GCACAATCCTCGAAACCACT-3' Reverse primer: 5'-CCCTGATGATAGGATGCTGAA-3' Probe sequence: 5'-GTGGCCAGAGGGCTCACCCA-3'	Custom assay
Vwf	Von Willebrand factor homolog	Mm00550376_m1
Zfpm1	Zinc finger protein, multitype 1	Mm00494336_m1

CHAPTER 3: Lympho-myeloid haematopoietic progenitors in early foetal liver and yolk sac

3.1. Introduction

The classical model of bone marrow (BM) haematopoietic hierarchy postulates that downstream of multipotent haematopoietic stem cells (HSC) the first lineage fate decision is the segregation of lymphoid and myeloid/megakaryocyte/erythroid lineages, a dichotomy between common myeloid progenitor (CMP) and common lymphoid progenitor (CLP) (Kondo et al., 1997; Akashi et al., 2000a; Akashi et al., 2000b). In this model, the CMP is at the apex of all myeloid, megakaryocytic and erythroid cells, whereas the CLP precedes all lymphoid cells. An alternative model postulates that the first branching point of the haematopoietic hierarchy is instead the segregation of lymphoid/myeloid and myeloid/megakaryocyte/erythroid potentials through generation of a common myeloid/lymphoid progenitor (CMLP) and a CMP, respectively (Kawamoto, 2006; Arinobu et al., 2007; Iwasaki and Akashi, 2007a, b; Luc et al., 2008b; Kawamoto and Katsura, 2009) (see also chapter 1).

The existence of lympho-myeloid progenitors was first suggested by the results of several *in vitro* studies of the lineage potentials of intra-embryonic and extra-embryonic haematopoietic precursors (Cumano et al., 1992; Carlsson et al., 1995; Kawamoto et al., 1997; Lacaud et al., 1998; Katsura and Kawamoto, 2001; Mebius et al., 2001; Lu et al., 2002; Lin et al., 2014). A few years later, cells with combined myeloid/B/T cell potential but lacking megakaryocyte/erythroid (Mk/E) potential were prospectively isolated from adult BM (Adolfsson et al., 2005; Lai et al., 2005) and from foetal liver (FL) at embryonic day E14.5 (Mansson et al., 2007). These cells were named lymphoid-primed multipotent progenitors

(LMPP) and were phenotypically defined as Lin- Sca1+ c-Kit+ (LSK) with 25% highest expression of Fms-like tyrosine kinase 3 (Flt3, Flk2 or CD135). Subsequent studies on the cell surface expression of Flt3 within the LSK and Lin- Sca1- c-Kit+ (LK) compartments provided supporting evidence for the positioning of the LSK Flt3^{high} LMPP population parallel to CMP and upstream of CLP and granulocyte/macrophage progenitors (GMP) in the adult BM haematopoietic hierarchy (Lai and Kondo, 2006; Iwasaki and Akashi, 2007b; Karsunky et al., 2008; Heffner et al., 2011).

Although the LMPP has been identified in adult BM and E14.5 FL, it is not known if a similar hematopoietic hierarchy exists in early development. Mammalian embryonic haematopoiesis occurs in successive waves that involve multiple extra-embryonic and intra-embryonic sites (see also chapter 1). Definitive HSCs (dHSCs) emerge in the aorta-gonad-mesonephros (AGM) region around E10.5 (Medvinsky et al., 1993; Müller et al., 1994; Medvinsky and Dzierzak, 1996) and seed the FL around E11-E11.5 (Medvinsky et al., 1993; Sanchez et al., 1996; Kumaravelu et al., 2002). Prior to establishment of definitive haematopoiesis, haematopoietic potential is displayed by transient oligopotent progenitors (Godin and Cumano, 2005; Cumano and Godin, 2007; Medvinsky et al., 2011; Golub and Cumano, 2013; Lin et al., 2014).

To prospectively purify and study sub-populations in the hematopoietic hierarchy, in particular lymphoid progenitors, we make use of cell surface markers such as interleukin-7 receptor alpha (IL7Rα) and recombination activating gene 1 (*Rag1*). These are key regulators of early lymphoid commitment (Mombaerts et al., 1992; Peschon et al., 1994; Igarashi et al., 2002; Sitnicka et al., 2003; Yokota et al., 2003; Ikawa et al., 2004). Detection of lymphoid potential in the murine embryo, measured as the ability of tissue explants to produce CD45+ *Rag1*-GFP+ cells *in vitro*, has been reported as early as E8.5-E9.5 in yolk sac (YS) and para-

aortic splanchnopleura (P-Sp, prospective AGM region), but the specific progenitor cell of this lymphoid potential was not prospectively isolated (Yokota et al., 2006). The earliest *in vivo* expression of *Rag1*-GFP was detected in placenta, YS, and embryo proper around E10.5-E11.5 (Yokota et al., 2006), and the earliest *in vivo* expression of cell surface IL7Rα was also detected around E10.5-E11.5 in AGM, foetal blood (FB) and FL (Ikawa et al., 2004). Lympho-myeloid potential was reported from the Lin- c-Kit^{low} Sca1^{low} IL7Rα+ CLP equivalent in E14.5 FL (Mebius et al., 2001), but cell culture and gene expression data from Lin- c-Kit+ IL7Rα-expressing cells isolated from E12.5-E14.5 FL and FB suggested that these populations mainly consist of lymphoid-restricted progenitors (Kawamoto et al., 2000; Ikawa et al., 2004), implying that the first steps of lymphoid-commitment in the early embryo may not involve a lympho-myeloid compartment.

In this chapter, however, we identify lympho-myeloid progenitors in the early stages of embryonic lymphopoiesis, prospectively isolated from E9.5 YS, E10.5 FL, and E11.5 FL based on expression of the early lymphoid-affiliated genes *Il7r*, *Rag1* and *Flt3*. Similarly to the previously identified LMPP (Adolfsson et al., 2005; Mansson et al., 2007), we show that this population is transcriptionally lymphoid-primed and sustains both lymphoid and myeloid, but not Mk/E potentials at the single cell level.

Data presented in this chapter have been previously published (Böiers et al., 2013).

3.2. Results

3.2.1. Early embryonic progenitors with combined lymphoid and myeloid lineage potentials *in vitro*

We first investigated by flow cytometry the expression of IL7Rα and Flt3 lymphoid-affiliated cell surface markers in Lin- CD45+ c-Kit+ progenitor cells in E11.5 FL. We found that the majority of Lin- CD45+ c-Kit+ IL7Rα+ cells express Flt3 (71.46% ± 3.02, n=10 pools), and that the Lin- CD45+ c-Kit+ IL7Rα+ Flt3+ population (from now on referred to as IL7Rα+ Flt3+) constitutes 0.2% of FL cells (Figure 3.1A).

We also investigated expression of *Rag1*, another early lymphoid gene, in the E11.5 FL IL7Rα+ Flt3+ population of *Rag1*-GFP knock-in embryos (Kuwata et al., 1999), and we observed that *Rag1*-GFP is expressed by 91% of IL7Rα+ Flt3+ cells (Figure 3.1A). We noted that the enzymatic digestion methods used in the preparation of cell suspensions from E9.5 YS and E10.5 FL can affect Flt3 cell surface protein and hinder detection of Flt3 expression by flow cytometry, therefore we used *Rag1*-GFP as a substitute for Flt3 in the identification of the same cell population at earlier developmental stages (from now on referred to as IL7Rα+ *Rag1*-GFP+). We detected small populations of IL7Rα+ *Rag1*-GFP+ cells in E10.5 FL (0.05% of FL cells) and in E9.5 YS (0.02% of YS cells) (Figure 3.1B), but these cells are virtually absent from E8.5 conceptus, E9.5 placenta, and E9.5 P-Sp (Figure 3.1C).

For the subsequent study of lineage potentials we focused on the more abundant populations in E10.5 and E11.5 FL. Firstly we evaluated the *in vitro* lineage potentials of the E10.5 FL IL7Rα+ *Rag1*-GFP+ and E11.5 FL IL7Rα+ Flt3+ populations, comparing them to the E11.5 FL IL7Rα- Flt3- population and the IL7Rα^{high} and IL7Rα- sub-fractions of adult BM LMPP (Figure 3.2A). As expected based on their expression of lymphoid markers, IL7Rα+ *Rag1*-

GFP+ / IL7Rα+ Flt3+ FL cells show B cell (Figure 3.2B-C) and T cell potential (Figure 3.2D-E) when co-cultured with the OP9 (Nakano et al., 1994; Vieira and Cumano, 2004) and OP9-DL1 stromal cell lines (Schmitt and Zúñiga-Pflücker, 2002; de Pooter and Zúñiga-Pflücker, 2007; Holmes and Zúñiga-Pflücker, 2009), respectively. The B and T lymphoid potentials of single E11.5 FL IL7Rα+ Flt3+ cells are similar to those of single adult BM LMPPs.

Importantly, we also observed that E10.5-E11.5 FL IL7Rα+ *Rag1*-GFP+ / IL7Rα+ Flt3+ cells have substantial myeloid potential (Figure 3.2F), and we further confirmed that E11.5 FL IL7Rα+ Flt3+ cells can generate both granulocytes and monocytes/macrophages in culture (Figure 3.2G). Although the size of myeloid colonies varies between populations, total myeloid clonogenicity is not significantly different between single E10.5-E11.5 FL IL7Rα+ *Rag1*-GFP+ / IL7Rα+ Flt3+ cells and single adult BM LMPPs (Figure 3.2F).

We then evaluated the megakaryocyte and erythroid potentials of these FL progenitors, to test if they are similar to adult LMPPs. In stark contrast to IL7Rα- Flt3- cells, but similarly to adult BM LMPP, E10.5-E11.5 FL IL7Rα+ *Rag1*-GFP+ / IL7Rα+ Flt3+ show little or no megakaryocyte (<1%, Figure 3.2H) and erythroid potential (<1%, Figure 3.2I) in both single cell liquid cultures and bulk semi-solid cultures.

In order to determine if both lymphoid and myeloid potentials are present in the same individual cells within the IL7Rα+ Flt3+ FL progenitor population, we used a switch-culture system previously described for FL haematopoietic progenitors (Mansson et al., 2007). In this cell culture system single cells are firstly co-cultured for a short time with OP9 stroma, which is permissive of B cell and myeloid differentiation (without affecting future T cell potential), and then transferred to a co-culture with OP9-DL1 stroma, which is permissive of T cell differentiation. We observed that 26% of E11.5 FL IL7Rα+ Flt3+ cells produce lineage positive clones in switch-culture (Figure 3.2J). Consistently throughout different experiments, 37% of lineage positive clones contain both lymphoid (B and/or T) and myeloid

cells, and only 6% of clones contain lymphoid cells in the absence of myeloid cells (Figure 3.2K-L). At variable frequencies between experiments, seemingly unipotent clones were also generated in switch-culture. These clones either reflect true functional heterogeneity of progenitors within the IL7Rα+ Flt3+ population, or reflect the technical limitations of the *in vitro* assay used (sub-optimal efficiency in revealing all lineage potentials for all individual cells). To investigate the presence of more restricted progenitors within this compartment, it would be necessary to further sub-fractionate the compartment and prospectively isolate candidate progenitors for testing of combined lineage potentials. Nevertheless, even if it is not a pure compartment, our data show that the majority of E11.5 FL IL7Rα+ Flt3+ clonogenic cells are progenitors with robust combined lymphoid and myeloid potentials, but lacking megakaryocyte and erythroid potentials.

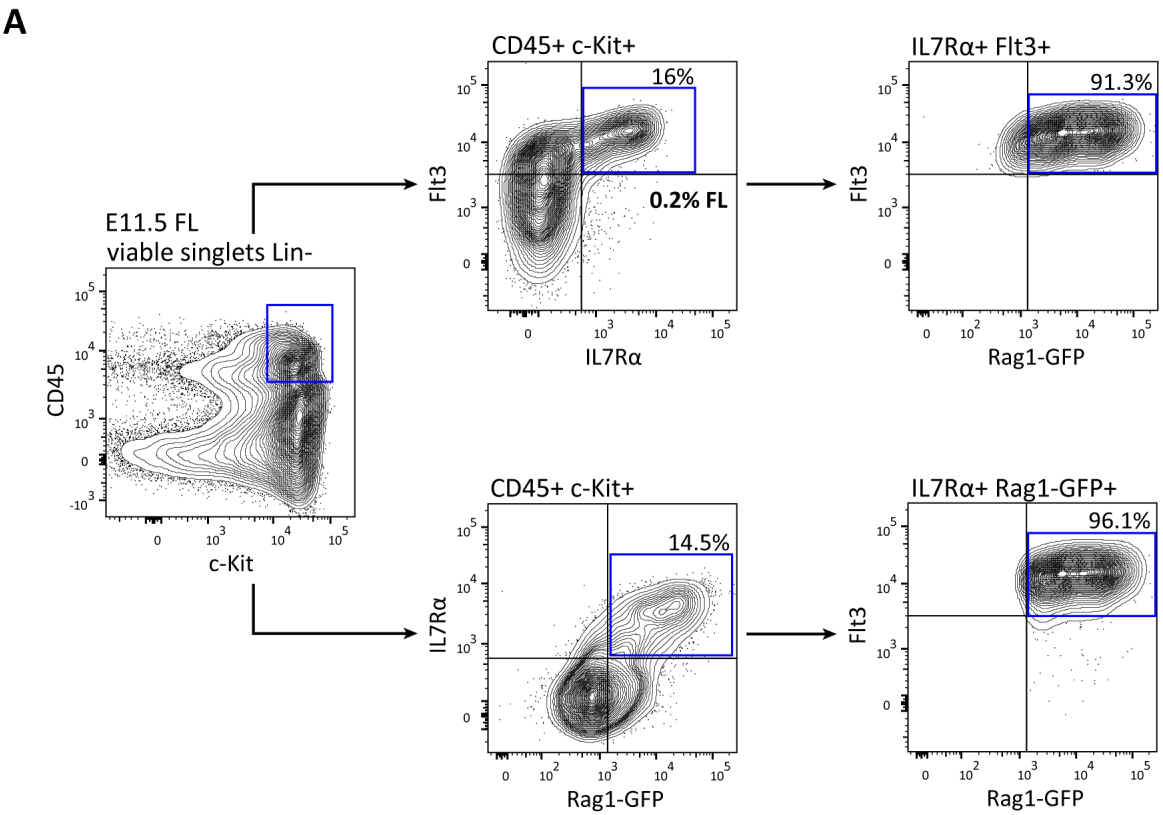
A
E11.5 FL
viable singlets Lin-
CD45
c-Kit
CD45+ c-Kit+
16%
0.2% FL
Flt3
IL7Rα
IL7Rα+ Flt3+
91.3%
Flt3
Rag1-GFP
CD45+ c-Kit+
14.5%
IL7Rα
Rag1-GFP
IL7Rα+ Rag1-GFP+
96.1%
Flt3
Rag1-GFP

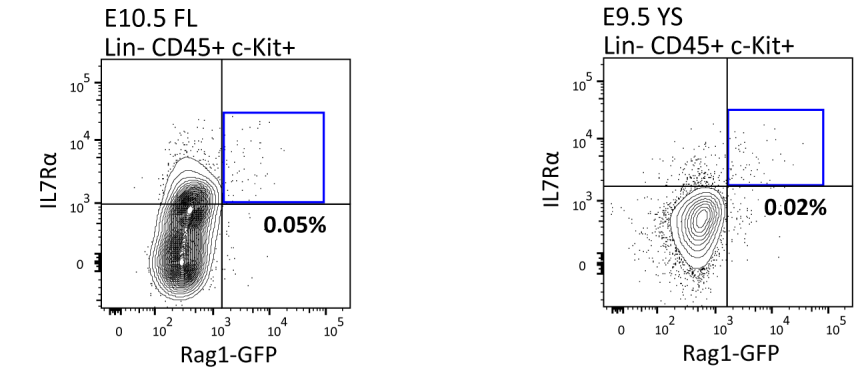
B
E10.5 FL
Lin- CD45+ c-Kit+
IL7Rα
0.05%
Rag1-GFP
E9.5 YS
Lin- CD45+ c-Kit+
IL7Rα
0.02%
Rag1-GFP

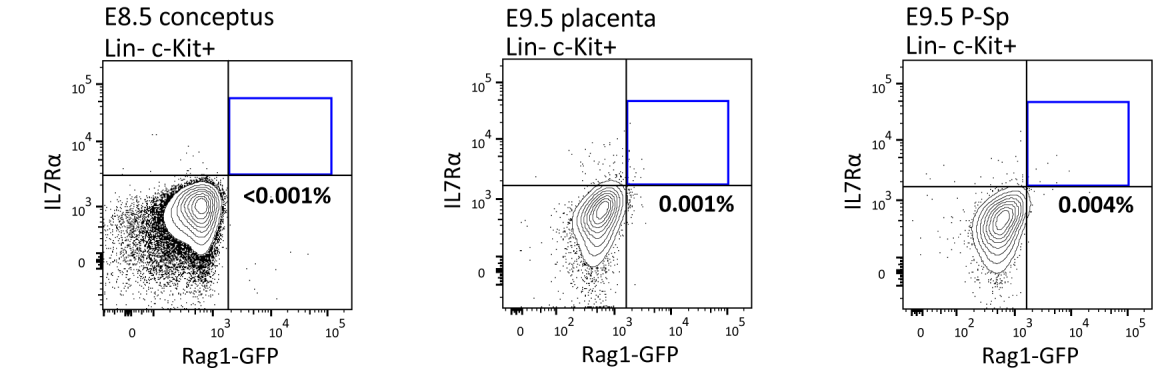
C
E8.5 conceptus
Lin- c-Kit+
IL7Rα
<0.001%
Rag1-GFP
E9.5 placenta
Lin- c-Kit+
IL7Rα
0.001%
Rag1-GFP
E9.5 P-Sp
Lin- c-Kit+
IL7Rα
0.004%
Rag1-GFP

Figure 3.1. Expression of lymphoid commitment markers in early embryonic CD45+ c-Kit+ progenitors.

Expression of IL7Rα and Flt3 lymphoid cell surface markers, and *Rag1* lymphoid gene in Lin- CD45+ c-Kit+ cells was analysed in foetal liver (FL), yolk sac (YS), para-aortic splanchnopleura (P-Sp), placenta, and whole conceptus of *Rag1*-GFP embryos at E8.5-E11.5.

(A) Gating strategy for flow cytometric analysis and sorting of Lin- CD45+ c-Kit+ IL7Rα+ Flt3+ (upper panels) and Lin- CD45+ c-Kit+ IL7Rα+ *Rag1*-GFP+ cells (lower panels) in E11.5 FL. Throughout this study IL7Rα+ Flt3+ E11.5 FL cells (upper middle panel) were sorted from C57BL/6J embryos, but the analysis of *Rag1*-GFP embryos is shown here to demonstrate co-expression of Flt3 and *Rag1*-GFP in virtually all Lin- CD45+ c-Kit+ IL7Rα+ cells. Mean % of cells in parent gate (n=12 *Rag1*-GFP FL) and in FL (n=10 C57BL/6J FL pools) is shown above and below the gates, respectively.

(B) Lin- CD45+ c-Kit+ IL7Rα+ *Rag1*-GFP+ cells in E10.5 FL (left panel, n=5 pools) and E9.5 YS (right panel, n=7 pools). Mean % of cells in each organ is shown below the gates.

(C) Lin- c-Kit+ IL7Rα+ *Rag1*-GFP+ cells (CD45+/-) in whole conceptus at E8.5 (left panel), in placenta at E9.5 (middle panel), and in P-Sp at E9.5 (right panel). Mean % of cells in each tissue is shown below the gates (n=3-4 pools for each).

Data presented in this figure were generated in collaboration with Dr. Charlotta Böiers, Dr. Michael Lutteropp, Dr. Marella de Bruijn, Dr. Emanuele Azzoni, and Joanna Green.

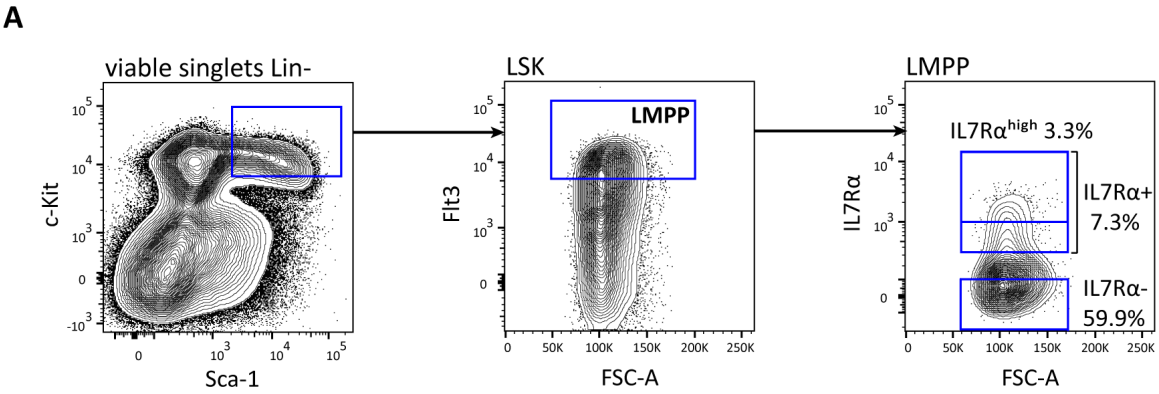
A
viable singlets Lin-
c-Kit
Sca-1
LSK
LMPP
Flt3
FSC-A
LMPP
IL7Rα^high 3.3%
IL7Rα+ 7.3%
IL7Rα- 59.9%
IL7Rα
FSC-A

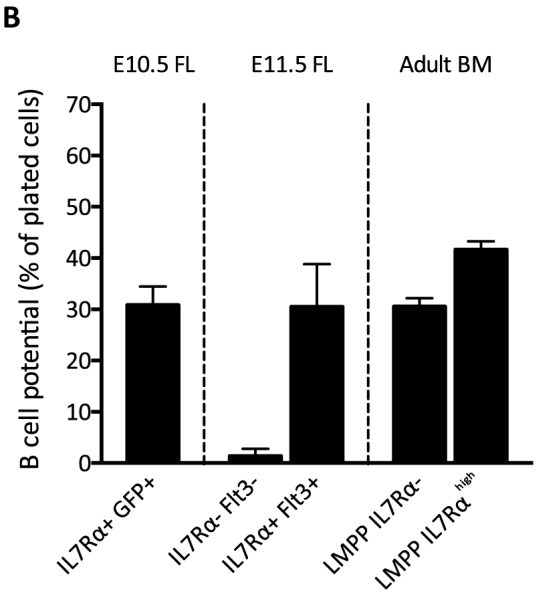
B
E10.5 FL
E11.5 FL
Adult BM
B cell potential (% of plated cells)
IL7Rα+ GFP+
IL7Rα- Flt3-
IL7Rα+ Flt3+
LMPP IL7Rα-
LMPP IL7Rα high

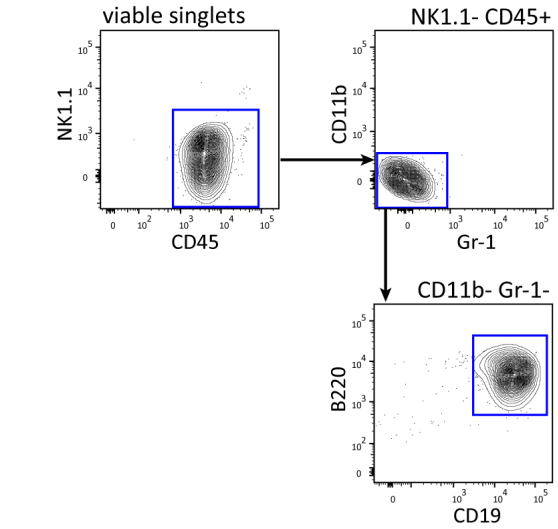
C
viable singlets
NK1.1
CD45
NK1.1- CD45+
CD11b
Gr-1
CD11b- Gr-1-
B220
CD19

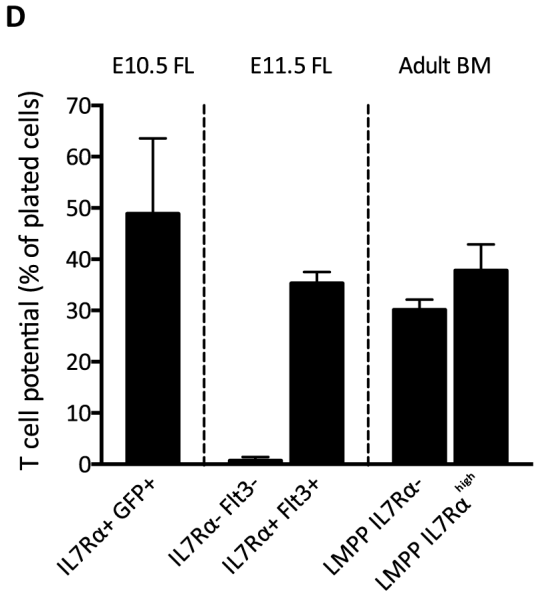
D
E10.5 FL
E11.5 FL
Adult BM
T cell potential (% of plated cells)
IL7Rα+ GFP+
IL7Rα- Flt3-
IL7Rα+ Flt3+
LMPP IL7Rα-
LMPP IL7Rα high

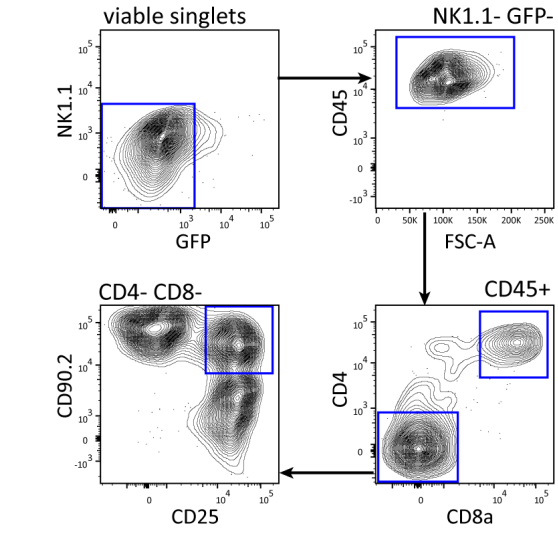
E
viable singlets
NK1.1
GFP
NK1.1- GFP-
CD45
FSC-A
CD4- CD8-
CD90.2
CD25
CD45+
CD4
CD8a

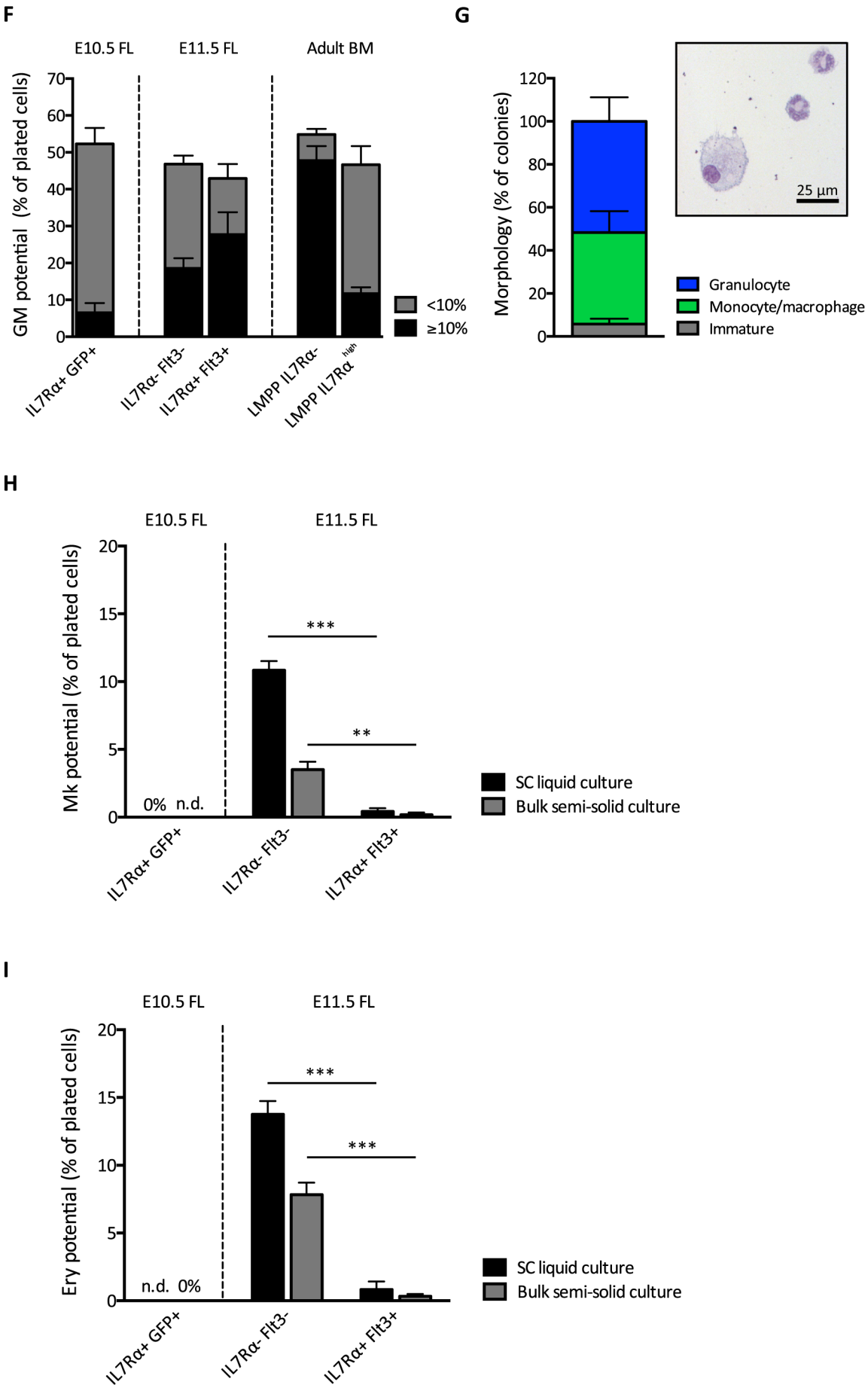
F
E10.5 FL
E11.5 FL
Adult BM
GM potential (% of plated cells)
70
60
50
40
30
20
10
0
<10%
≥10%
IL7Rα+ GFP+
IL7Rα- Flt3-
IL7Rα+ Flt3+
LMPP IL7Rα-
LMPP IL7Rα high
G
Morphology (% of colonies)
120
100
80
60
40
20
0
25 µm
Granulocyte
Monocyte/macrophage
Immature
H
E10.5 FL
E11.5 FL
Mk potential (% of plated cells)
20
15
10
5
0
***
**
0% n.d.
SC liquid culture
Bulk semi-solid culture
IL7Rα+ GFP+
IL7Rα- Flt3-
IL7Rα+ Flt3+
I
E10.5 FL
E11.5 FL
Ery potential (% of plated cells)
20
15
10
5
0
***
***
n.d. 0%
SC liquid culture
Bulk semi-solid culture
IL7Rα+ GFP+
IL7Rα- Flt3-
IL7Rα+ Flt3+

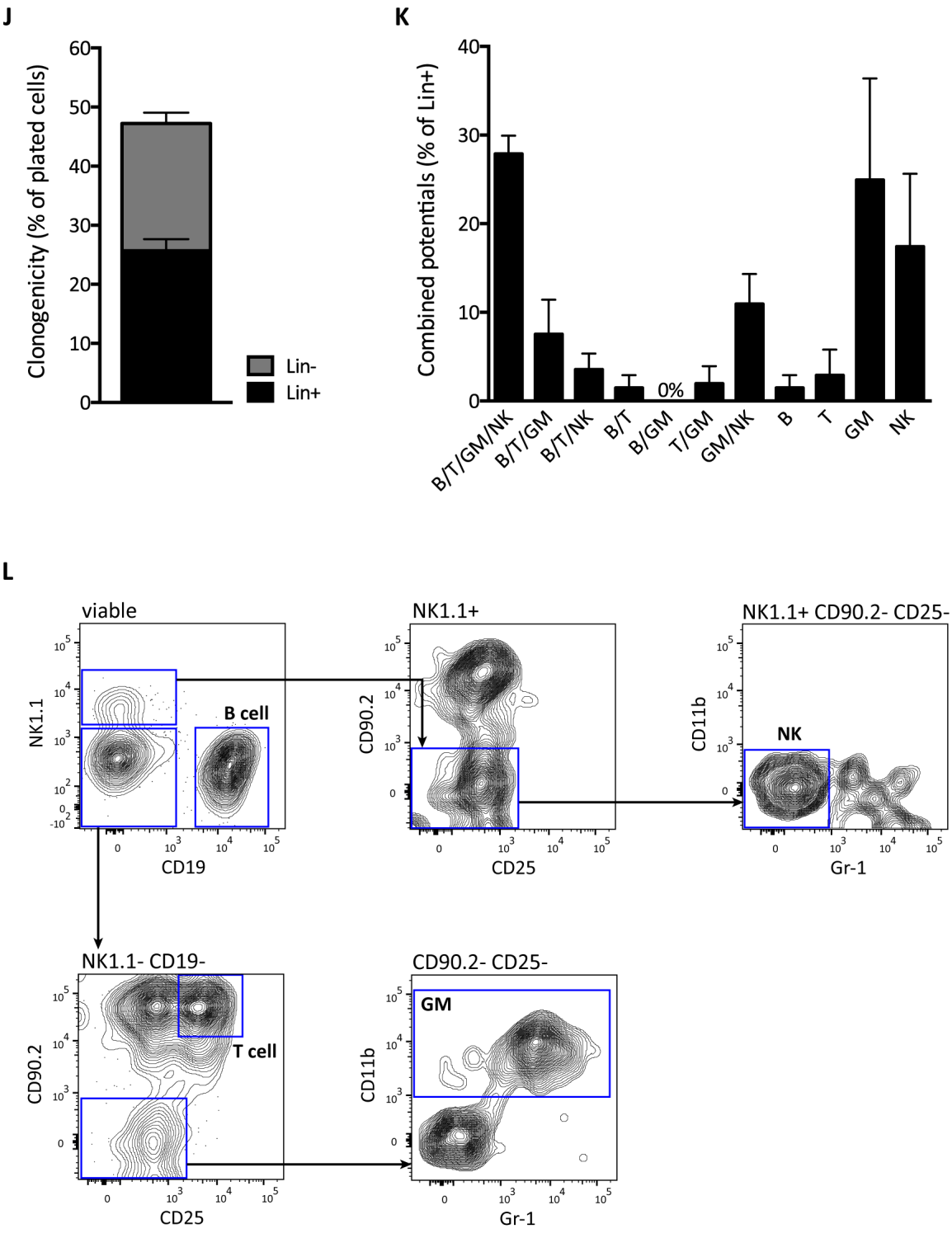
J
Clonogenicity (% of plated cells)
60
50
40
30
20
10
0
Lin-
Lin+
K
Combined potentials (% of Lin+)
40
30
20
10
0
0%
B/T/GM/NK
B/T/GM
B/T/NK
B/T
B/GM
T/GM
GM/NK
B
T
GM
NK
L
viable
NK1.1
CD19
B cell
NK1.1+
CD90.2
CD25
NK1.1+ CD90.2- CD25-
CD11b
Gr-1
NK
NK1.1- CD19-
CD90.2
CD25
T cell
CD90.2- CD25-
CD11b
Gr-1
GM

Figure 3.2. IL7Rα+ Flt3+ embryonic progenitors show lymphoid and myeloid potentials but lack megakaryocyte and erythroid potentials *in vitro*.

Lineage potentials of IL7Rα+ *Rag1*-GFP+ and IL7Rα- *Rag1*-GFP- cells from E10.5 FL and IL7Rα+ Flt3+ and IL7Rα- Flt3- cells from E11.5 FL were tested in cell culture assays *in vitro*, and compared to the IL7Rα+ and IL7Rα- sub-fractions of adult BM LMPP.

(A) Gating strategy for flow cytometric analysis and sorting of LMPP IL7Rα+ and IL7Rα- in adult BM. Mean % of parent gate is shown (n=3). Only the 3.3% of LMPPs with highest IL7Rα expression (LMPP IL7Rα^{high}) were sorted for cell culture assays.

(B) B cell lineage potential in OP9 co-culture. Cultured cells were evaluated by flow cytometry after 14 days. Mean % + SEM. E10.5 FL, >50 total plated wells from 3 biological replicates (4 cells/well). E11.5 FL, for each population >90 total plated wells from 3-4 biological replicates (1 cell/well). Adult BM, for each population >100 total plated wells from 3 biological replicates (1 cell/well).

(C) Gating strategy for flow cytometric analysis of B220+ CD19+ B cells grown *in vitro*.

(D) T cell lineage potential in OP9-DL1 co-culture. Cultured cells were evaluated by flow cytometry after 21 days. E10.5 FL, >50 total plated wells from 3 biological replicates (4 cells/well). E11.5 FL, for each population >90 total plated wells from 3-4 biological replicates (1 cell/well). Adult BM, for each population >100 total plated wells from 3 biological replicates (1 cell/well).

(E) Gating strategy for flow cytometric analysis of double positive (DP) CD4+ CD8+ and double-negative (DN) CD4- CD8- CD90.2+ CD25+ T cells grown *in vitro*. Only wells with ≥10 CD90.2+ CD25+ and/or CD4+ CD8+ clustered events were considered positive.

(F) Myeloid (GM) lineage potential of single cells in liquid culture. Cultures were evaluated after 7-11 days. E10.5 FL, >150 total plated wells from 3 biological replicates. E11.5 FL, for each population >350 total plated wells from 4 biological replicates. Adult BM, for each population >350 total plated wells from 3 biological replicates. Grey bars represent small

clones with cells covering <10% of the culture well, while black bars represent large clones with cells covering ≥10%.

(G) Morphological analysis of GM cells generated by 10 Lin- c-Kit+ IL7Rα+ Flt3+ E11.5 FL cells in liquid culture (granulocyte-specific cytokine conditions). Cultures derived from 3 biological replicates were evaluated after 6 days. Mean % + SEM (left panel). May-Grünwald/Giemsa staining of representative myeloid cells (right panel). Scale bar is 25µm.

(H) Megakaryocyte (Mk) potential of single cells in liquid culture and colony forming unit-megakaryocyte (CFU-Meg) potential of bulk cells in semi-solid culture. Cultures were evaluated after 7-11 days. Mean % + SEM. E10.5, n>150 total plated cells from 2 biological replicates in liquid culture, and semi-solid culture assay was not performed (not done, n.d.). E11.5, >450 total plated cells from 4 biological replicates in liquid culture and 600 total plated cells from 3 biological replicates in semi-solid culture.

(I) Erythroid (Ery) potential of single cells in liquid culture and burst colony forming unit-erythroid (BFU-E) potential of bulk cells in semi-solid culture. Clone growth was evaluated after 7-11 days of culture. Mean % + SEM. E10.5, liquid culture assay was not performed (not done, n.d.) and n>150 total plated cells from 2 biological replicates in semi-solid culture. E11.5, >450 total plated cells from 4 embryos in liquid culture and 600 total plated cells from 3 biological replicates in semi-solid culture.

(J) Total clonogenicity of E11.5 FL IL7Rα+ Flt3+ cells in a switch-culture system. Single cells were first incubated with OP9 stromal cells for 5 days, then transferred to OP9-DL1 stromal cells and cultured for another 6 days before flow cytometric analysis of cell surface markers of B cells, T cells, myeloid cells, and NK cells. Mean + SEM, n=237 total plated cells from 3 biological replicates. Grey bars represent lineage negative clones, while black bars represent all lineage positive clones (with B and/or T and/or myeloid and/or NK cells).

(K) Frequency of combined lineage potentials of single E11.5 FL IL7Rα+ Flt3+ cells in switch-culture. Mean % + SEM, n=112 lineage positive clones from 3 biological replicates.

(L) Representative profile of a combined B/T/GM/NK clone generated in switch-culture, with simultaneous detection of B cells (NK1.1- CD19+), T cells (NK1.1- CD19- CD90.2+ CD25+), myeloid cells (NK1.1- CD19- CD90.2- CD25- CD11b+ Gr-1+/-), and natural killer cells (NK1.1+ CD19- CD90.2- CD25- CD11b- Gr-1-) in the same clone.

One-way ANOVA followed by Tukey's multiple comparisons test, 95% confidence interval, p-values adjusted for multiplicity. Two-tailed Student's t-test used instead for Mk potential in semi-solid culture and Ery potential in liquid culture, due to comparison between only two experimental groups (E11.5 FL IL7Rα+ Flt3+ and IL7Rα- Flt3-). Non-significant (n.s.) $p>0.05$, * $p\leq0.05$, ** $p\leq0.01$, *** $p\leq0.001$.

Data presented in this figure were generated in collaboration with Dr. Charlotta Böiers, Dr. Sidinh Luc, Dr. Michael Lutteropp, and Dr. Adam Mead.

3.2.2. Transcriptional profile of embryonic lympho-myeloid progenitors

Next, to obtain molecular support for the lineage potentials we identified in culture, we performed gene expression analysis of IL7Rα+ *Rag1*-GFP+ progenitors from E9.5 YS and E10.5 FL and IL7Rα+ Flt3+ progenitors from E11.5 FL.

Firstly we performed global mRNA transcriptome analysis at the population level by RNA sequencing. We focused on previously described lineage-affiliated transcriptional programs (Luc et al., 2012) and compared the fold difference in gene expression between IL7Rα+ *Rag1*-GFP+ or IL7Rα+ Flt3+ cells and IL7Rα- *Rag1*-GFP- or IL7Rα- Flt3- cells, respectively. In agreement with our *in vitro* culture data, we found that the lymphoid transcriptional program is markedly up-regulated in IL7Rα+ *Rag1*-GFP+ and IL7Rα+ Flt3+ progenitors, while the Mk/E transcriptional program is down-regulated (Figure 3.3A-C). Consistent with the similar myeloid potential that we observed from IL7Rα+ Flt3+ cells and the IL7Rα- Flt3- control population, both cell types express a myeloid transcriptional program. The overall transcription priming of the IL7Rα+ Flt3+ progenitors is similar at all developmental stages analysed, but is most striking in E11.5 FL (Figure 3.3C).

We further investigated the gene expression profile of IL7Rα+ Flt3+ progenitors by multiplexed single cell qPCR, and confirmed that the majority of these cells (58-64%) co-express early lymphoid-affiliated genes (*Il7r*, *Flt3*, *Rag2*, *Ighm*, *Notch1*, *Hes1*, *Ccr9*, *Gata3*) and myeloid-affiliated genes (*Csf1r*, *Csf2r*, *Csf3r*), but do not express Mk/E-affiliated genes (*Gata1*, *Epor*, *Klf1*, *Vwf*) or lymphoid genes associated with late B cell commitment (*Ebf1*, *Pax5*) and late T cell commitment (*Ptcra*) (Figure 3.3D-F). Thus, the gene expression profile at the population level and single cell level supports our *in vitro* finding that E10.5-E11.5 FL IL7Rα+ *Rag1*-GFP+ / IL7Rα+ Flt3+ cells are lympho-myeloid restricted progenitors.

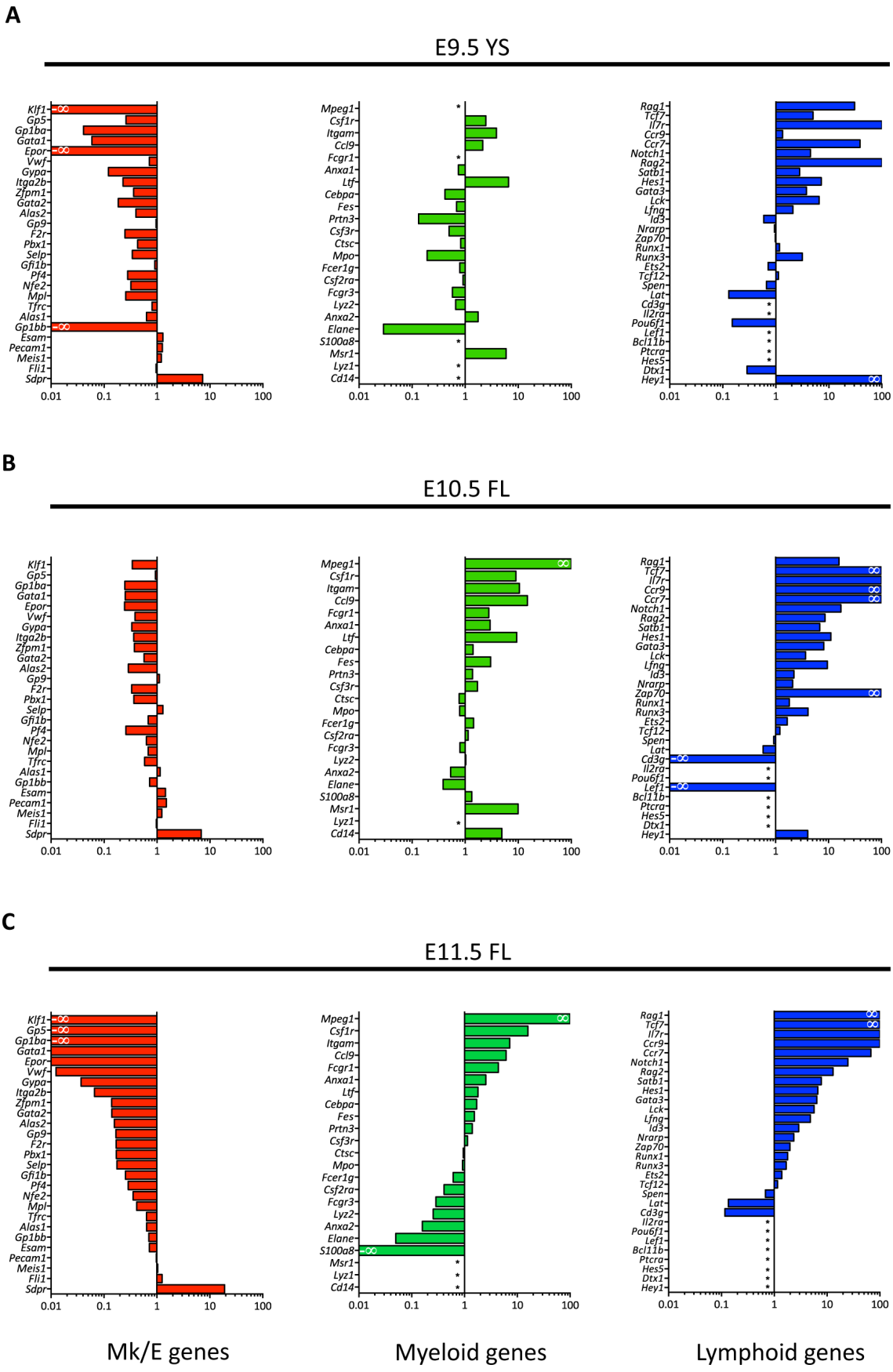
A
E9.5 YS
Klf1
Gp5
Gp1ba
Gata1
Epor
Vwf
Gypa
Itga2b
Zfpm1
Gata2
Alas2
Gp9
F2r
Pbx1
Selp
Gfi1b
Pf4
Nfe2
Mpl
Tfrc
Alas1
Gp1bb
Esam
Pecam1
Meis1
Fli1
Sdpr
Mpeg1
Csf1r
Itgam
Ccl9
Fcgr1
Anxa1
Ltf
Cebpa
Fes
Prtn3
Csf3r
Ctsc
Mpo
Fcer1g
Csf2ra
Fcgr3
Lyz2
Anxa2
Elane
S100a8
Msr1
Lyz1
Cd14
Rag1
Tcf7
Il7r
Ccr9
Ccr7
Notch1
Rag2
Satb1
Hes1
Gata3
Lck
Lfng
Id3
Nrarp
Zap70
Runx1
Runx3
Ets2
Tcf12
Spen
Lat
Cd3g
Il2ra
Pou6f1
Lef1
Bcl11b
Ptcra
Hes5
Dtx1
Hey1
0.01
0.1
1
10
100
B
E10.5 FL
C
E11.5 FL
Mk/E genes
Myeloid genes
Lymphoid genes

D

E9.5 YS

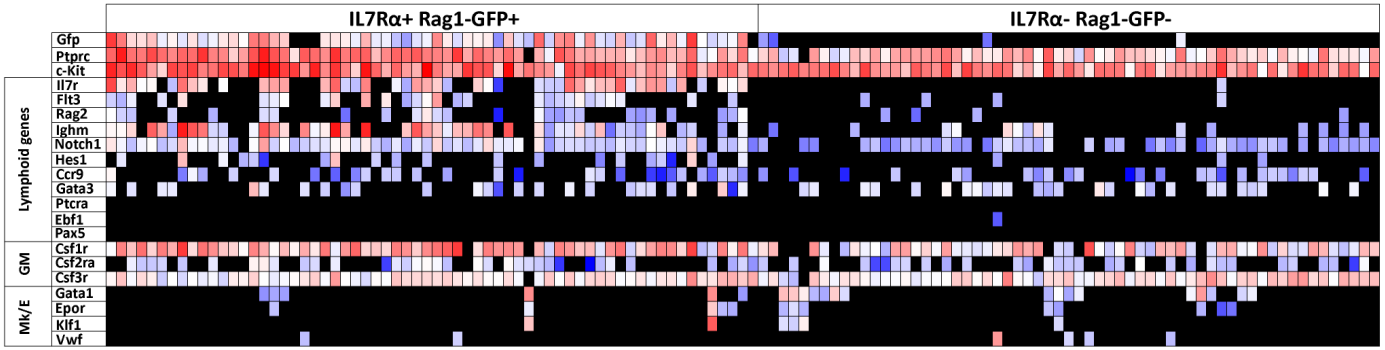

E

E11.5 FL

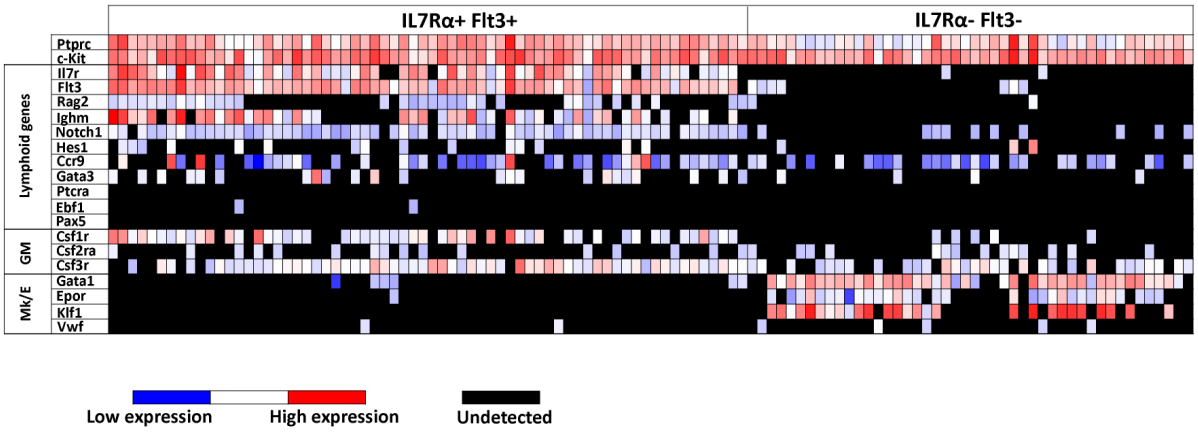

F

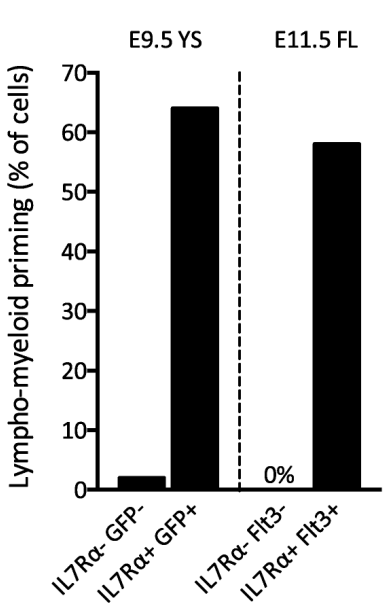

Figure 3.3. Transcriptional priming of lympho-myeloid embryonic progenitors.

Gene expression was analysed by sequencing of the global mRNA transcriptome of IL7Rα+ *Rag1*-GFP+ and IL7Rα- *Rag1*-GFP- cells sorted from *Rag1*-GFP E9.5 YS and E10.5 FL, and IL7Rα+ Flt3+ and IL7Rα- Flt3- cells sorted from C57BL/6 E11.5 FL (3 biological replicates per population, 70-100 cells per replicate). The expression profile of selected lineage-affiliated genes was further analysed at the single cell level by multiplexed qPCR (46-66 total single cells sorted from 3 biological replicates per population).

(A) Mean fold differences in the expression levels of lineage-affiliated genes between IL7Rα+ *Rag1*-GFP+ and IL7Rα- *Rag1*-GFP- cells from E9.5 YS, and **(B)** from E10.5 FL. **(C)** Mean fold differences in the expression levels of lineage-affiliated genes between IL7Rα+ Flt3+ and IL7Rα- Flt3- cells from E11.5 FL. mRNA sequencing data are presented as reads per kilobase of transcript per million mapped reads (RPKM), and values are presented on logarithmic scale. *, RPKM≤0.05 for both cell populations. ∞ indicates "infinite" fold difference due to RPKM=0 in the numerator or denominator population of the fold difference calculation.

(D) Heatmap of relative gene expression in IL7Rα+ *Rag1*-GFP+ (64 cells) and IL7Rα- *Rag1*-GFP- (61 cells) from E9.5 YS and in **(E)** IL7Rα+ Flt3+ (66 cells) and IL7Rα-Flt3- (46 cells) from E11.5 FL. Multiplexed qPCR data are presented as ΔCt normalised to the housekeeping gene *Hprt1.* Only samples with detectable levels of *Hprt1* and *c-Kit* were analysed, and we also confirmed expression of CD45 (*Ptprc*) and GFP. Each column corresponds to a single cell.

(F) Analysis of lineage priming in IL7Rα+ *Rag1*-GFP+ and IL7Rα- *Rag1*-GFP- cells from E9.5 YS, and IL7Rα+ Flt3+ and IL7Rα- Flt3- cells from E11.5 FL. % of cells expressing >3 early lymphoid genes (out of 8 analysed), ≥2 myeloid genes (out of 3 analysed), 0 Mk/E genes (out of 4 analysed) and 0 late lymphoid genes (out of 3 analysed).

Data presented in this figure were generated in collaboration with Dr. Michael Lutteropp. Bioinformatics analysis of RNA sequencing was performed by Dr. Petter Woll and Dr. Iain Macaulay.

3.2.3. Expression of paired immunoglobulin-like receptors in embryonic lympho-myeloid progenitors excludes B cell potential

Expression of paired immunoglobulin-like receptors (PIR) has been suggested to identify a sub-fraction of the c-Kit+ IL7Rα+ E12.5-E13.5 FL compartment that is also found in FB and might represent a thymus seeding progenitor with T cell, NK cell and dendritic cell (DC) restricted potentials. c-Kit+ IL7Rα+ PIR+ cells from E13.5 FL were found to not produce B cells *in vitro*, while c-Kit+ IL7Rα+ PIR- cells were found to not produce T cells, and therefore PIR was implicated as a marker for segregation of B and T cell potentials (Kubagawa et al., 1997; Masuda et al., 2005; Kubagawa et al., 2008). We found combined B and T cell potentials in the majority of single E11.5 FL IL7Rα+ Flt3+ progenitors, but also found some apparently unipotent B and T cell clones, as well as T/GM clones (Figure 3.2K). As previously discussed, it is unclear if these restricted clones only reflect technical limitations of the *in vitro* assay. We then investigated if expression of PIR in E11.5 FL IL7Rα+ Flt3+ progenitors would dissect heterogeneity of B and T cell potentials.

We found that a small fraction of IL7Rα+ Flt3+ cells expresses cell surface PIR (11%) (Figure 3.4A). We confirmed gene expression of *Pirb* by qPCR, and also noted up-regulation of *Il7r* and other early lymphoid transcripts (*sIgh*, *Rag1*, *Rag2*) in the PIR+ population when compared to the PIR- population (Figure 3.4B).

We then tested the *in vitro* lineage potentials of both PIR- and PIR+ sub-fractions of E11.5 FL IL7Rα+ Flt3+ cells, comparing them to the PIR- and PIR+ sub-fractions of total c-Kit+ IL7Rα+ compartment in E13.5 FL (Figure 3.4C), the population in which PIR was analysed in previous studies (Masuda et al., 2005). Contrary to what was previously described, we observed that both PIR- and PIR+ cells in E11.5 and E13.5 FL have myeloid potential (Figure 3.4D) and T cell

potential (Figure 3.4E). However, as previously reported, we did observe that the PIR+ populations in E11.5 and E13.5 FL have little or no B cell potential (Figure 3.4F).

Overall our data suggest that the small PIR+ sub-fraction of E11.5 FL IL7Rα+ Flt3+ cells are T cell/myeloid restricted progenitors that might replenish thymopoiesis.

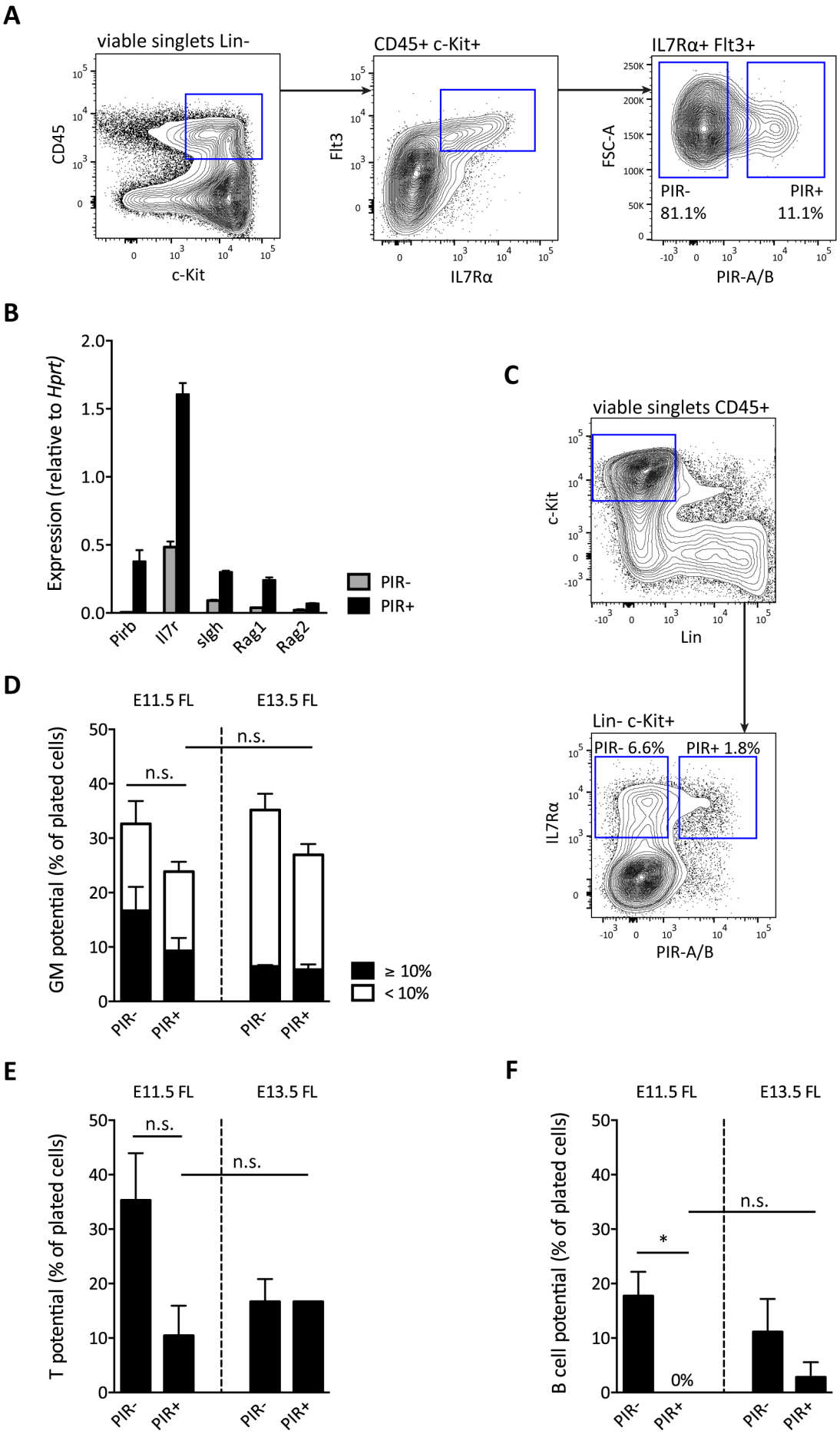
A
viable singlets Lin-
CD45+ c-Kit+
IL7Rα+ Flt3+
CD45
c-Kit
Flt3
IL7Rα
FSC-A
PIR-
81.1%
PIR+
11.1%
PIR-A/B
B
Expression (relative to Hprt)
PIR-
PIR+
Pirb
Il7r
sIgh
Rag1
Rag2
C
viable singlets CD45+
c-Kit
Lin
Lin- c-Kit+
PIR- 6.6%
PIR+ 1.8%
IL7Rα
PIR-A/B
D
E11.5 FL
E13.5 FL
n.s.
n.s.
GM potential (% of plated cells)
≥ 10%
< 10%
PIR-
PIR+
PIR-
PIR+
E
E11.5 FL
E13.5 FL
n.s.
n.s.
T potential (% of plated cells)
PIR-
PIR+
PIR-
PIR+
F
E11.5 FL
E13.5 FL
*
n.s.
B cell potential (% of plated cells)
0%
PIR-
PIR+
PIR-
PIR+

Figure 3.4. Paired immunoglobulin-like receptors in foetal liver progenitors.

In vitro lineage potentials of E11.5 FL IL7Rα+ Flt3+ cells and E13.5 FL IL7Rα+ cells sub-fractionated based on their cell surface expression of PIR-A/B were investigated (both isoforms are recognised by the same antibody clone).

(A) Gating strategy for flow cytometric analysis and sorting of E11.5 FL IL7Rα+ Flt3+ PIR+ and PIR- cells. Mean % of parent gate is shown (n=6 pools).

(B) Quantitative gene expression analysis of lymphoid transcripts by multiplexed qPCR of E11.5 FL Lin- c-Kit+ IL7Rα+ Flt3+ PIR+ and PIR- cells. Mean expression + SEM normalised to the housekeeping gene *Hprt1* (2 biological replicates of 25 cells per population).

(C) Gating strategy for flow cytometric analysis and sorting of E13.5 FL IL7Rα+ PIR+ and PIR- cells. Mean % of parent gate is shown (n=3).

(D) Myeloid (GM) lineage potential of single cells in liquid culture. Clone growth was evaluated after 11-12 days of culture. E11.5 FL, for each population >400 total plated wells from 5 biological replicates. E13.5 FL, for each population 360 total plated wells from 3 biological replicates. Grey bars represent small clones with cells covering <10% of the culture well, while black bars represent large clones with cells covering ≥10%.

(E) T cell lineage potential of single cells in OP9-DL1 co-culture. Clone identity was evaluated by flow cytometry after 21 days of co-culture (see Figure 3.2D for gating strategy). E11.5 FL, for each population >80 total plated wells from 4 biological replicates. E13.5 FL, for each population 72 total plated wells from 3 biological replicates.

(F) B cell lineage potential of single cells in OP9 co-culture. Clone identity was evaluated by flow cytometry after 14 days of co-culture (see Figure 3.2B for gating strategy). Mean % + SEM. E11.5 FL, for each population >90 total plated wells from 3-4 biological replicates. E13.5 FL, for each population 72 total plated wells from 3 biological replicates.

One-way ANOVA followed by Tukey's multiple comparisons test, 95% confidence interval, p-values adjusted for multiplicity. Non-significant (n.s.) $p>0.05$, * $p\leq0.05$.

3.3. Discussion

In this chapter we have demonstrated that lympho-myeloid immune-restriction is an early fate decision in embryonic haematopoiesis. We have shown that Lin- c-Kit+ IL7Rα+ Flt3+ cells co-expressing *Rag1*-GFP are found in FL as early as E10.5 (Figure 3.1) and have robust combined myeloid and T cell transcriptional priming and *in vitro* differentiation potential, but little or no Mk/E priming or potential (Figures 3.2-3.3).

Furthermore, we observed that 11% of the IL7Rα+ Flt3+ E11.5 FL compartment consists of PIR+ progenitors with T cell and myeloid potentials, but little or no B cell potential, while the remaining IL7Rα+ Flt3+ PIR- compartment retains T cell, B cell and myeloid potentials (Figure 3.4). We did not, however, test PIR+ cells for combined potentials at the single cell level or expression of T cell-restricted genes, and so we cannot conclude if individual cells in this population are T cell/myeloid-restricted.

IL7Rα+ PIR+ FL cells have previously been suggested to be a population of thymus seeding progenitors, although extra-thymic functions of these cells and the possibility that additional progenitor populations also migrate to the thymus were not excluded (Masuda et al., 2005; Kubagawa et al., 2008). Interestingly, in our global mRNA sequencing analysis we observed that the genes for chemokine (C-C motif) receptor 7 and 9 (*Ccr7* and *Ccr9*) – two proteins shown to be involved in the regulation of embryonic thymus colonisation (Liu et al., 2006; Calderon and Boehm, 2011) – are strongly up-regulated in E10.5-E11.5 FL IL7Rα+ *Rag*1-GFP+ / IL7Rα+ Flt3+ cells (Figure 3.3B-C). We also noted in our single cell qPCR analysis that 8% of E11.5 FL IL7Rα+ Flt3+ cells express high levels of *Ccr9* (Figure 3.3E), although we did not investigate co-expression of *Pira* or *Pirb* genes in these cells. Importantly, we demonstrated that both PIR- and PIR+ sub-fractions of the E11.5 FL IL7Rα+ Flt3+ compartment sustain myeloid potential (Figure 3.4D), which is in agreement with previous studies demonstrating

that adult thymus T cell progenitors still retain myeloid potential after loss of B cell potential (Bell and Bhandoola, 2008; Wada et al., 2008). However, the physiological relevance of intra-thymic myeloid potential in adult thymus continues to be debated, with conflicting conclusions being drawn from lineage tracing approaches (Schlenner et al., 2010; Schlenner and Rodewald, 2010) and knock-out mouse models (De Obaldia et al., 2013).

Conversely to adult thymus T cell progenitors, it has been demonstrated both *in vitro* and *in vivo* that the earliest neonatal thymus T cell progenitors not only possess myeloid potential but also B cell potential (Luc et al., 2012). These findings have been further confirmed by on-going studies of our research group regarding the initial seeding of embryonic thymus at E11-E11.5 (unpublished data). Another recent study agrees that combined T cell, B cell, and myeloid potentials are expressed by a second wave of embryonic thymus seeding progenitors, but suggest that the earliest wave of seeding consists only of T cell-restricted progenitors (Ramond et al., 2014). Thus, the complex process of embryonic and adult thymus seeding by multiple waves of haematopoietic progenitors with distinct lineage potentials remains unclear, and the models of extra-thymic lymphoid restriction or full T cell restriction are the subjects of continued debate (Bhandoola et al., 2007; Schlenner and Rodewald, 2010). Nevertheless, our data suggest that IL7Rα+ Flt3+ PIR+ and PIR- early FL progenitors warrant further investigation in regards to their possible ability to migrate to the embryonic thymus and express lympho-myeloid lineage potentials intra-thymically.

Although not described in this chapter, we identified E9.5 YS as the most likely site of emergence of IL7Rα+ *Rag1*-GFP+ lympho-myeloid progenitors (Böiers et al., 2013), thus preceding both the haematopoietic colonisation of FL around E11-E11.5 (Medvinsky et al., 1993; Sanchez et al., 1996; Kumaravelu et al., 2002) and the emergence of dHSCs in AGM around E10.5 (Medvinsky et al., 1993; Müller et al., 1994; Medvinsky and Dzierzak, 1996). Firstly, we detected a small IL7Rα+ *Rag1*-GFP+ population in E10.5 FL and E9.5 YS by flow

cytometry, but could not detect it in E9.5 placenta or P-Sp, or earlier in the whole E8.5 conceptus (Figure 3.1B-C). We then investigated by whole mount imaging the localisation of *Rag1*-GFP+ cells co-expressing the pan-haematopoietic marker CD45 and the endothelial marker CD31, and found that these cells are present in E9.5 YS but are rarely detected in the embryo proper (Böiers et al., 2013). However, circulation is already established by E8.25-E8.5 (Delassus and Cumano, 1996; McGrath et al., 2003), and it is possible that the *Rag1*-GFP+ cells detected in YS at E9.5 migrated there from another haematopoietic site. To determine if YS is the first emergence site of *Rag1*-expressing cells, we dissected YS and P-Sp from *Rag1*-GFP embryos pre-circulation, at E7.5-E8.5 (≤6 somite pairs), and cultured the explants *in vitro* for approximately 2 days. We performed whole mount imaging of the cultured explants and found that *Rag1*-GFP+ cells are detected in the majority of cultured YS explants, but cannot be detected in cultured P-Sp explants. These findings provide strong evidence that *Rag1*-GFP+ cells first emerge in the YS (Böiers et al., 2013), and contradict previous studies suggesting that lymphoid potential is exclusively found intra-embryonically before circulation (Cumano et al., 1996). An alternative experiment that could be performed to further confirm our findings is the analysis of NCX1 knock-out mice with a null mutation of the cardiac sodium-calcium (Na^+-Ca^{2+}) exchanger. NCX1 mice develop normally until E10 but circulation is not established due to absence of a heartbeat (Koushik et al., 2001), therefore this mouse model provides a circulation-free window of opportunity to separately analyze the haematopoietic potential of different extra-embryonic and intra-embryonic haematopoietic sites (Yoshimoto et al., 2008). Based on our findings, at E9.5 we would expect IL7Rα+ *Rag1*-GFP+ cells to be predominantly, if not completely, confined to the YS in NCX1 embryos. Which cell type in YS gives rises to early lympho-myeloid progenitors (haemogenic endothelium, pre-HSCs, or multipotent haematopoietic precursors) (Lancrin et al., 2009; Rybtsov et al., 2011; Yoshimoto et al., 2012; Golub and Cumano, 2013; Inlay et al., 2014), and how their emergence is regulated, are questions that remain for future study.

CHAPTER 4: Physiological contribution of lymphoid-primed haematopoietic progenitors to embryonic myelopoiesis

4.1. Introduction

The experimental data supporting both the lymphoid-primed multipotent progenitor (LMPP) model (Adolfsson et al., 2005; Lai and Kondo, 2006; Luc et al., 2007; Mansson et al., 2007; Doulatov et al., 2010) and the common myeloid progenitor (CMP) – common lymphoid progenitor (CLP) model (Galy et al., 1995; Kondo et al., 1997; Akashi et al., 2000a; Akashi et al., 2000b; Manz et al., 2002; Karsunky et al., 2008) of the haematopoietic hierarchy in adult and embryo, and in both mouse and human, have been largely generated by technically limited *in vitro* cultures and *in vivo* transplantation assays, which promote differentiation of purified populations in non-physiological conditions. Therefore, the physiological relevance of the two models of the haematopoietic hierarchy continues to be debated, and the first lineage fate decision steps of fully multipotent haematopoietic stem cells (HSC) remains an unresolved question (Forsberg et al., 2006; Kawamoto, 2006; Laiosa et al., 2006; Iwasaki and Akashi, 2007a, b; Ye and Graf, 2007; Luc et al., 2008b; Akashi, 2009; Kawamoto and Katsura, 2009; Schlenner et al., 2010; Boyer et al., 2012).

In vitro differentiation assays are powerful tools to reveal hidden lineage potentials and to demonstrate the plasticity of cell populations, but *in vitro* results may not always be predictive of the fulfilment of lineage potentials in normal *in vivo* conditions (Richie Ehrlich et al., 2011). The actualised lineage outputs of an isolated cell population can be better revealed through *in vivo* transplantation and *in vivo* genetic lineage tracing. While cell transplantation involves the induction of non-physiological signals within the recipient and

the transplanted cells themselves, genetic lineage tracing assays allow the tracking of a population's lineage outputs in steady-state conditions.

In chapter 3 we described the identification of a lympho-myeloid progenitor population in yolk sac (YS) at embryonic day E9.5, and in foetal liver (FL) at embryonic days E10.5 and E11.5 (Böiers et al., 2013), a compartment similar to the LMPP previously identified in E14.5 FL and adult BM (Adolfsson et al., 2005; Mansson et al., 2007). Through *in vitro* assays we demonstrated that these progenitors phenotypically defined as Lin- c-Kit+ IL7Rα+ Flt3+ (referred to as IL7Rα+ Flt3+), or equivalently as Lin- c-Kit+ IL7Rα+ *Rag1*-GFP+ (referred to as IL7Rα+ *Rag1*-GFP+), express a lymphoid-primed transcriptome and possess lymphoid and myeloid potentials but lack megakaryocyte and erythroid potentials.

In this chapter we use an *in vivo* lineage tracing approach to further confirm the lineage potentials of embryonic lympho-myeloid progenitors in physiological conditions. We showed in a *Rag1*-GFP knock-in mouse model (Kuwata et al., 1999) that *Rag1*-GFP expression highly correlates with Flt3 and IL7Rα expression in the Lin- c-Kit+ FL compartment, and in this study we used *Rag1*-Cre to drive YFP-labelling of all progeny of *Rag1*-expressing progenitors (McCormack et al., 2003a). Herein we demonstrate *in vivo* that *Rag1*-expressing progenitors contribute strongly to steady-state embryonic lymphopoiesis and myelopoiesis, and contribute minimally to megakaryopoiesis and erythropoiesis.

The data presented in this chapter has been previously published (Böiers et al., 2013).

4.2. Results

4.2.1. *Rag1*-expressing progenitors contribute robustly to embryonic myelopoiesis *in vivo*

To study the level of *in vivo* myeloid contribution of *Rag1*-expressing embryonic lymphoid-primed progenitors we traced cell labelling with enhanced yellow fluorescent protein (EYFP) in *Rag1*-Cre/*R26*R-EYFP mice (Srinivas et al., 2001a; McCormack et al., 2003a). In this Cre/Lox recombination system (Sauer and Henderson, 1988), the *EYFP* gene inserted into the ubiquitously expressed ROSA26 locus is preceded by a floxed transcriptional termination sequence. Cre recombinase-mediated excision of the floxed termination sequence allows for constitutive and irreversible expression of *EYFP*. Therefore, in the *Rag1*-Cre/*R26*R-EYFP reporter mice *Rag1*-expressing cells and their daughter cells are labelled with YFP signal, which can be detected by flow cytometry and microscopy.

We first analysed YFP labelling of CD11b+ myeloid cells, CD19+ B cells, CD150+ CD41+ megakaryocytes and TER119+ erythroid cells in E11.5 FL, E14.5 FL, and adult BM by flow cytometry (Figure 4.1A-C). Unspecific YFP labelling induced by sample processing for flow cytometry was assessed in CD45.1+ wild type BM cells mixed with CD45.2+ *Rag1*-Cre/*R26*R-EYFP samples. We found unspecific labelling in 0.33% of CD45.1+ control myeloid cells and 2.6% of CD45.1+ control B cells (Figure 4.1D).

As expected for *Rag-1*-expressing lymphoid-primed progenitors, all B cells are labelled at all developmental stages (Figure 4.1D). Also, YFP labelling is very low (<3%) in the megakaryocyte and erythroid lineages at all developmental stages (Figure 4.1E), in agreement with our previous transcriptional priming analysis and *in vitro* lineage potential assays for IL7Rα+ *Rag1*-GFP+ progenitors. Importantly, 36% and 17.5% of CD11b+ myeloid

cells are labelled by YFP in E11.5 FL and E14.5 FL, respectively, but only 2.4% are labelled in adult BM (Figure 4.1D). These results show that *Rag1*-expressing progenitors contribute robustly to early embryonic myelopoiesis. This contribution decreases with developmental age and is virtually lost in adult haematopoiesis (Figure 4.1D).

To demonstrate the myeloid nature of YFP labeled CD11b+ cells in the *Rag1*-Cre/*R26*R-EYFP reporter, we next analysed the morphology of sorted YFP+ and YFP- CD11b+ Gr1- and CD11b+ Gr1+ cells sorted from *Rag1*-Cre/*R26*R-EYFP E14.5 FL (Figure 4.2A-C). Through analysis of May-Grünwald/Giemsa-stained cytospins of these sorted cells we confirmed that YFP+ CD11b+ cells, similarly to YFP- CD11b+ cells, consist of mature and immature monocytes and granulocytes (Figure 4.2B-C).

Furthermore, we analysed YFP labelling of myeloid and erythroid colonies generated through *in vitro* culture of unfractionated *Rag1*-Cre/*R26*R-EYFP E14.5 FL in semi-solid media. In agreement with our lineage tracing results, we observed 9-20% of YFP+ myeloid colonies and <1% of YFP+ erythroid colonies derived from E14.5 FL (Figure 4.2D). Once again we confirmed the generation of both monocytes and granulocytes by *Rag1*-expressing progenitors through morphological analysis of YFP+ and YFP- myeloid colonies (Figure 4.2E).

This lineage tracing study with the *Rag1*-Cre/*R26*R-EYFP reporter strain confirms that the lineage potentials identified *in vitro* for embryonic IL7Rα+ *Rag1*-GFP+ progenitors (chapter 5) are realised *in vivo*, and further highlights the robust physiological contribution of *Rag1*-expressing lymphoid-primed progenitors to embryonic steady-state myelopoiesis.

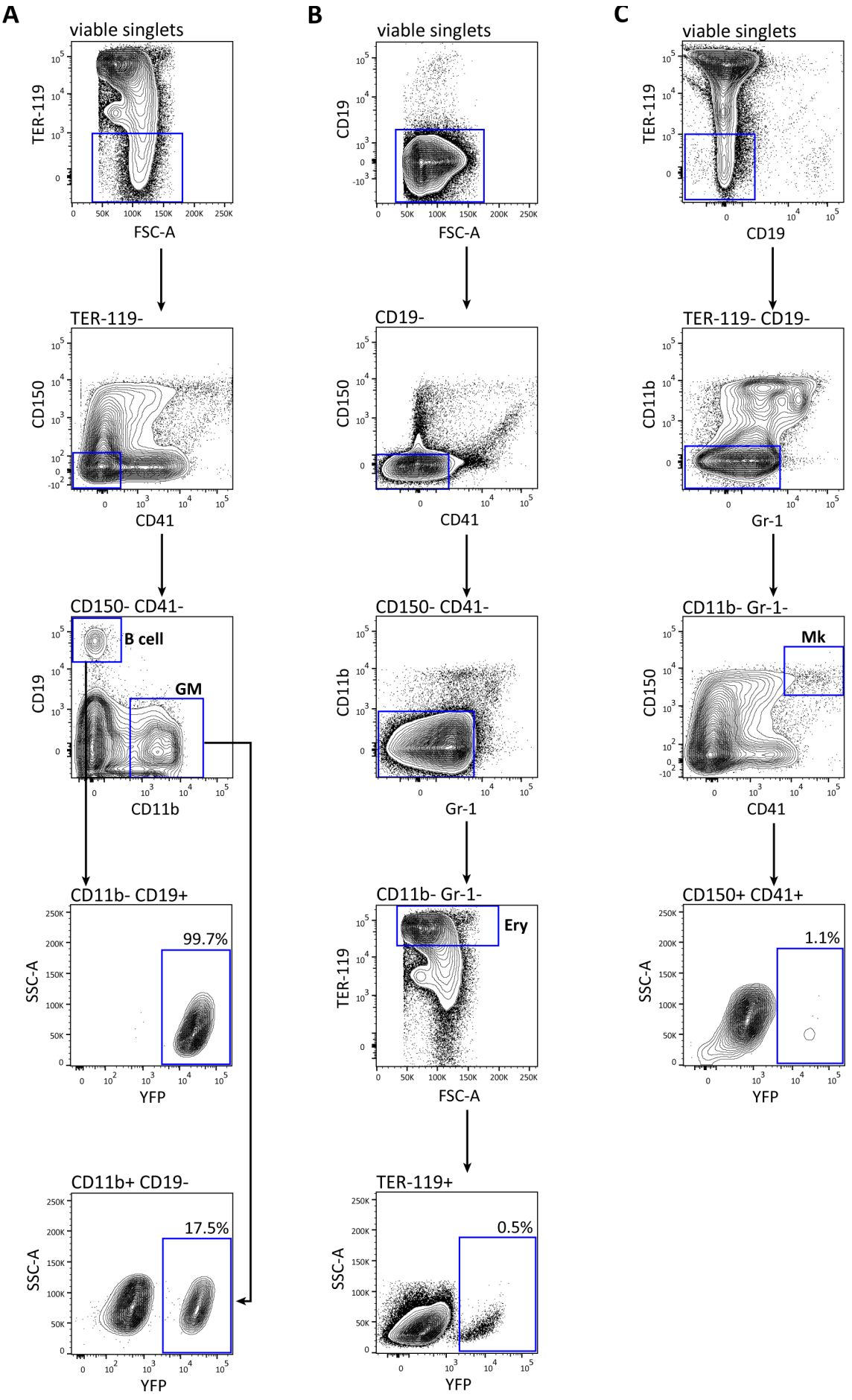
A
viable singlets
TER-119
FSC-A
TER-119-
CD150
CD41
CD150- CD41-
B cell
GM
CD19
CD11b
CD11b- CD19+
99.7%
SSC-A
YFP
CD11b+ CD19-
17.5%
SSC-A
YFP
B
viable singlets
CD19
FSC-A
CD19-
CD150
CD41
CD150- CD41-
CD11b
Gr-1
CD11b- Gr-1-
Ery
TER-119
FSC-A
TER-119+
0.5%
SSC-A
YFP
C
viable singlets
TER-119
CD19
TER-119- CD19-
CD11b
Gr-1
CD11b- Gr-1-
Mk
CD150
CD41
CD150+ CD41+
1.1%
SSC-A
YFP

D

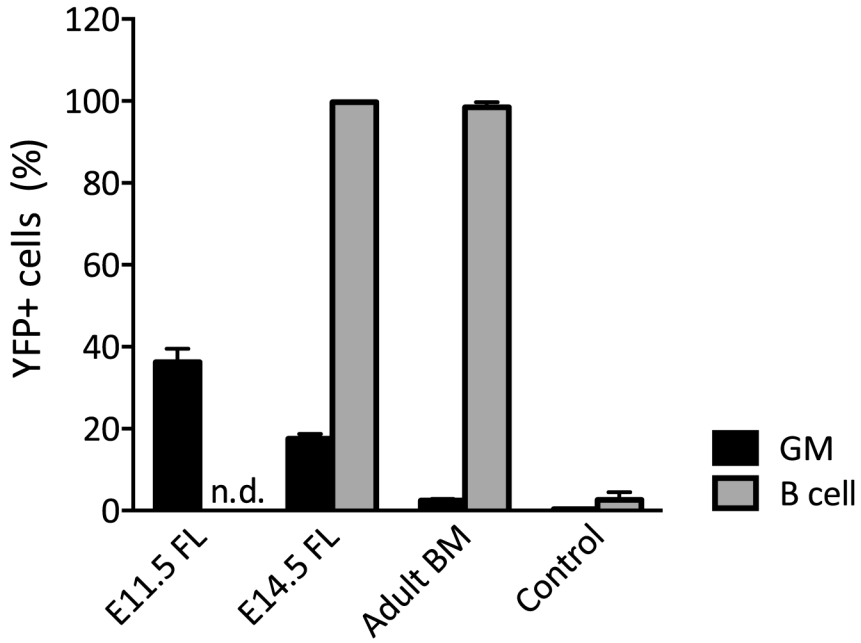
120
100
80
60
40
20
0
YFP+ cells (%)
n.d.
E11.5 FL
E14.5 FL
Adult BM
Control
GM
B cell

E

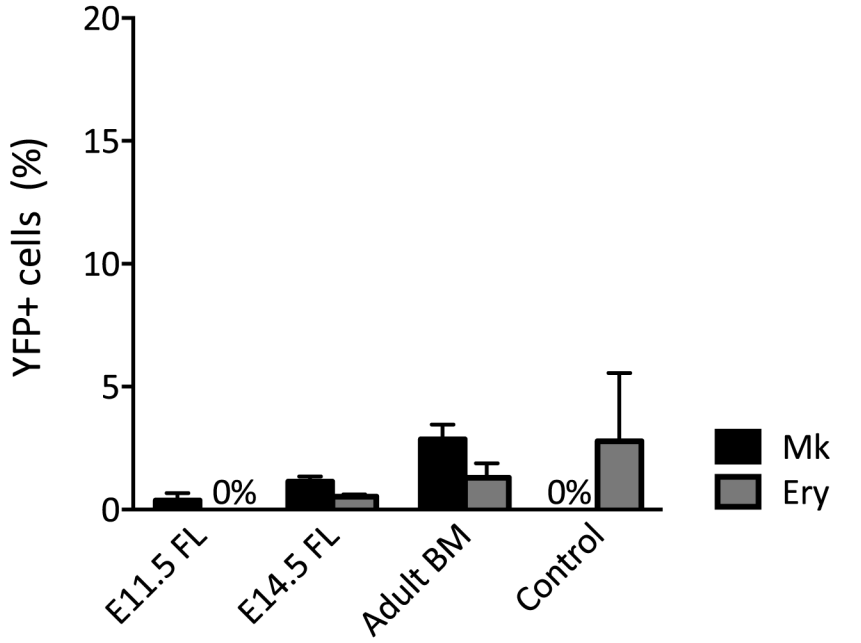
20
15
10
5
0
YFP+ cells (%)
0%
0%
E11.5 FL
E14.5 FL
Adult BM
Control
Mk
Ery

Figure 4.1. Lineage tracing in *Rag1*-Cre/*R26*R-EYFP embryos and adult mice.

Contribution of *Rag1*-expressing progenitors to E11.5 FL, E14.5 FL and adult BM lineages was quantified by flow cytometric analysis of YFP labelling of B cells, myeloid cells (GM), erythroid cells (Ery), and megakaryocytes (Mk) in *Rag1*-Cre/*R26*R-EYFP mice.

(A) Gating strategy for flow cytometric analysis of YFP labelling of B cells (TER119- CD150- CD41- CD11b- CD19+) and myeloid cells (TER119- CD150- CD41- CD11b+ CD19-). Representative plots from E14.5 FL. Mean % of parent gate is shown (n=12).

(B) Gating strategy for flow cytometric analysis of YFP labelling of erythroid cells (CD19- CD150- CD41- CD11b- Gr1- TER119+). Representative plots from E14.5 FL. Mean % of parent gate is shown (n=12).

(C) Gating strategy for flow cytometric analysis of YFP labelling of megakaryocytes (TER119- CD19- CD11b- Gr1- CD150+ CD41+). Representative plots from E14.5 FL. Mean % of parent gate is shown (n=12).

(D) Quantification of YFP labelling of myeloid cells in E11.5 FL (n=9), and quantification of myeloid cells and B cells in E14.5 FL (n=12), and adult BM (n=3). The CD19+ B cell population is very small in E11.5 FL and was not analysed (n.d.). Unspecific YFP labelling was quantified in wild-type CD45.1+ BM cells mixed with *Rag1*-Cre/*R26*R-EYFP CD45.2+ FL or BM cells (Control, n=6 mixed samples). Mean % + SEM. Unspecific labelling is 0.33% in myeloid cells and 2.61% in B cells.

(E) Quantification of YFP labelling of megakaryocytes and erythroid cells in E11.5 FL (n=9), E14.5 FL (n=12), and adult BM (n=3). Mean % + SEM. Unspecific labelling is 0% in megakaryocytes and 2.78% in erythroid cells. Note the y-axis scale: mean YFP labelling is below 3% in all populations.

The data presented in this figure was generated in collaboration with Dr. Michael Lutteropp.

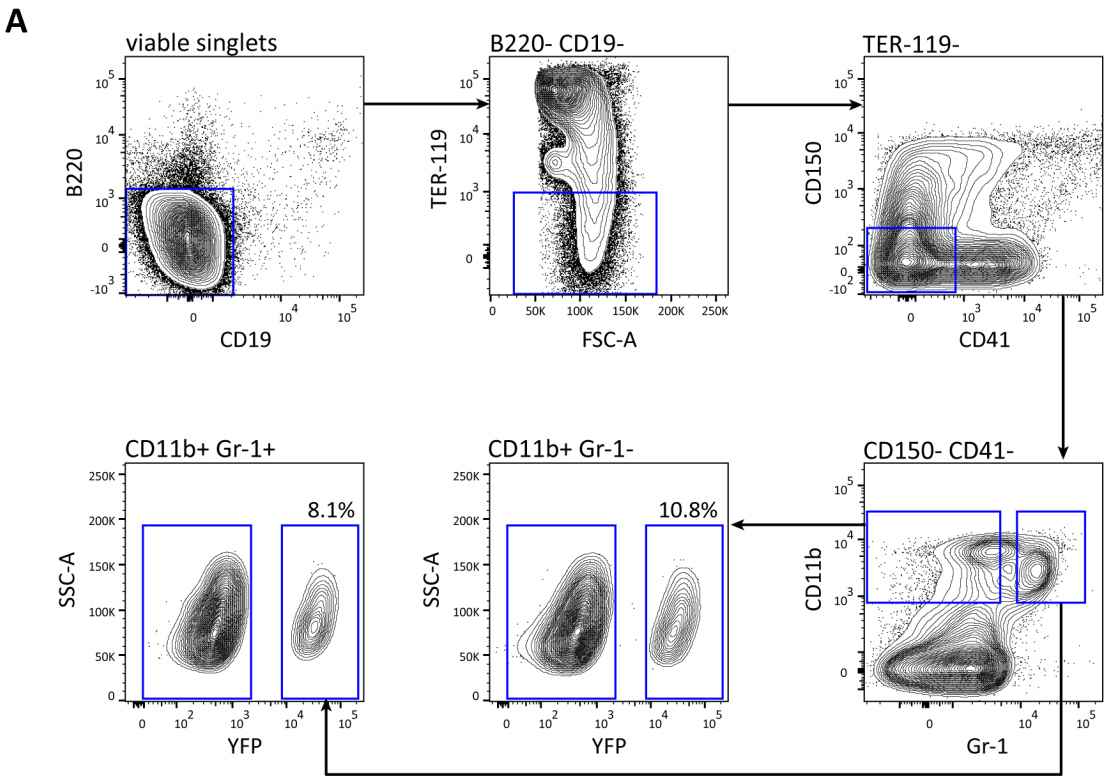
A
viable singlets
B220
CD19
B220- CD19-
TER-119
FSC-A
TER-119-
CD150
CD41
CD150- CD41-
CD11b
Gr-1
CD11b+ Gr-1+
8.1%
SSC-A
YFP
CD11b+ Gr-1-
10.8%
SSC-A
YFP

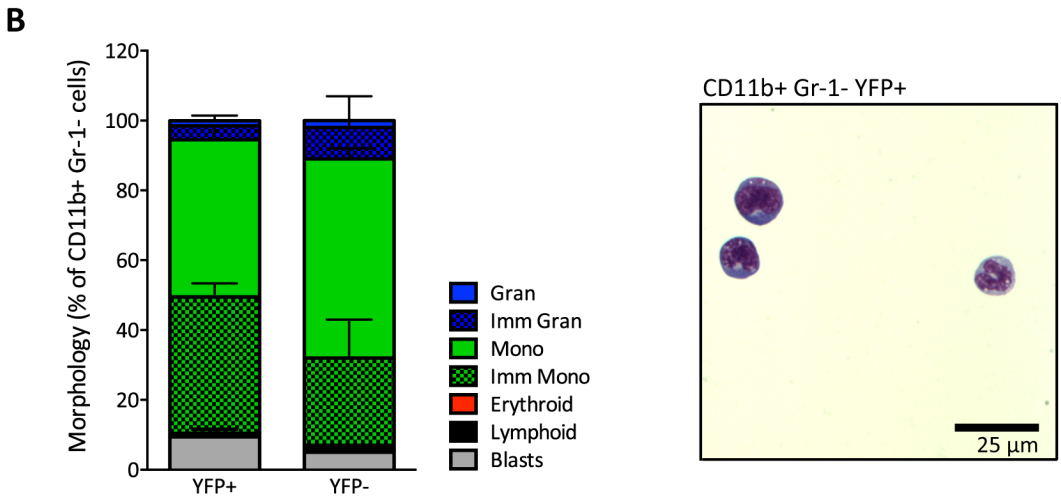
B
Morphology (% of CD11b+ Gr-1- cells)
YFP+
YFP-
Gran
Imm Gran
Mono
Imm Mono
Erythroid
Lymphoid
Blasts
CD11b+ Gr-1- YFP+
25 µm

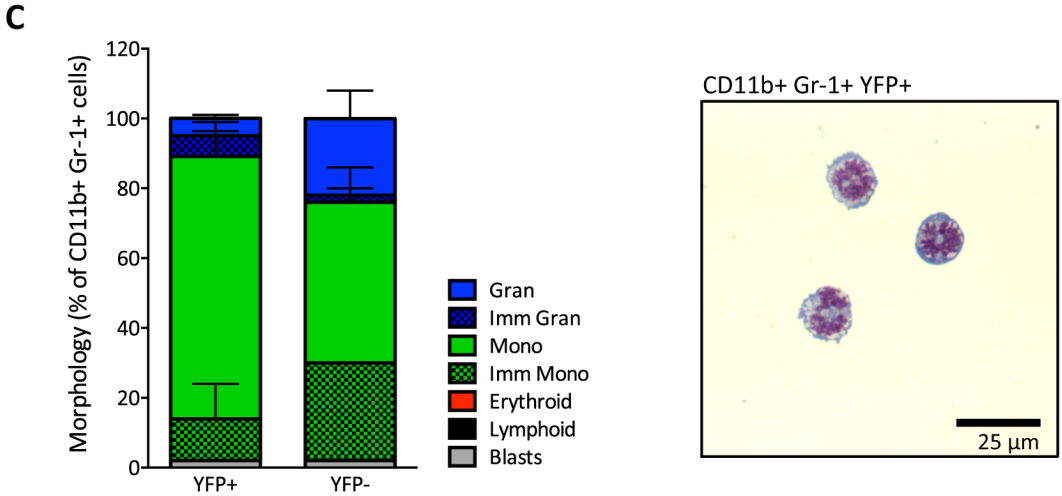
C
Morphology (% of CD11b+ Gr-1+ cells)
YFP+
YFP-
Gran
Imm Gran
Mono
Imm Mono
Erythroid
Lymphoid
Blasts
CD11b+ Gr-1+ YFP+
25 µm

D

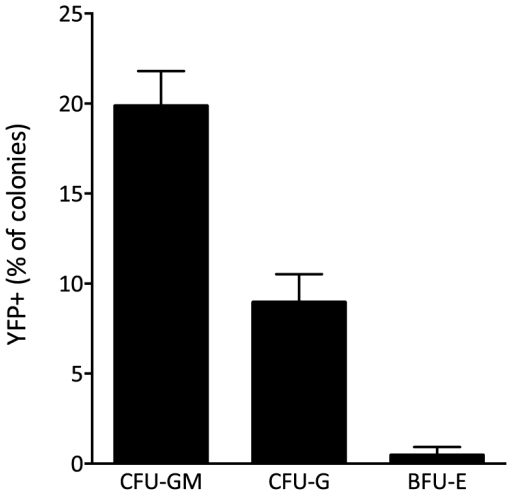

CFU-GM YFP+

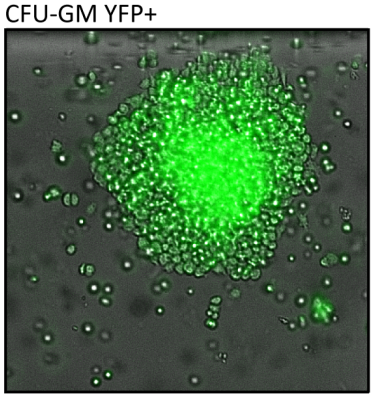

E

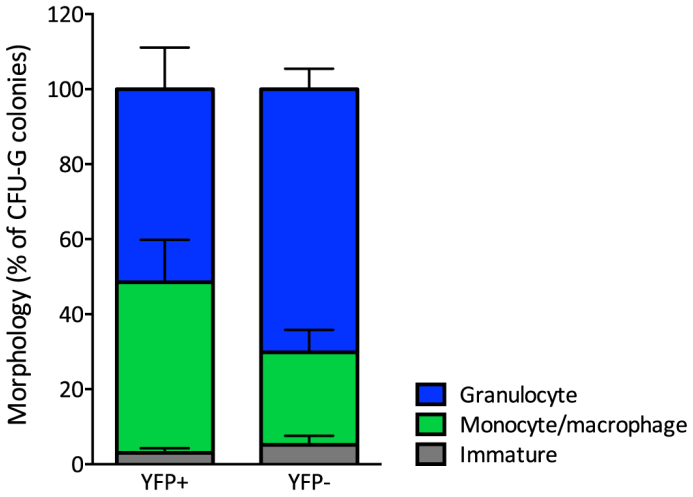

CFU-G YFP+

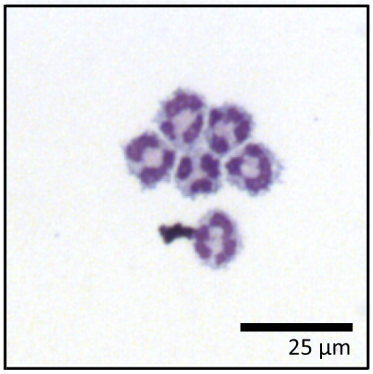

Figure 4.2. Embryonic *Rag1*-expressing progenitors generate both monocytes and granulocytes *in vivo* and *in vitro*.

Morphological analysis of YFP labelled sorted myeloid cells and *in vitro* myeloid colonies from *Rag1*-Cre/*R26*R-EYFP E14.5 FL.

(A) Gating strategy for sorting of YFP+ and YFP- CD11b+ Gr1- and CD11b+ Gr1+ myeloid cells. Mean % of parent gate is shown (n=4).

(B) Morphological analysis of sorted YFP+ and YFP- CD11b+ Gr1- myeloid cells (left panel). Mean % + SEM, n=2 for each population. May-Grünwald/Giemsa staining of representative CD11b+ Gr1- YFP+ myeloid cells (right panel). Scale bar is 25µm. "Imm", immature. "Gran", granulocyte. "Mono", monocyte/macrophage.

(C) Morphological analysis of sorted YFP+ and YFP- CD11b+ Gr1+ myeloid cells (left panel). Mean % + SEM, n=2 for each population. May-Grünwald/Giemsa staining of representative CD11b+ Gr1- YFP+ myeloid cells (right panel). Scale bar is 25µm.

(D) Quantification of YFP-labelling of colonies derived from unfractionated E14.5 FL cells in semi-solid cultures of colony forming unit-granulocyte/macrophage (CFU-GM), colony forming unit-granulocyte (CFU-G) and burst forming unit-erythroid (BFU-E) (left panel). Colonies were evaluated after 6 days of culture. Mean % + SEM. CFU-GM: n=1088 colonies from 12 embryos, CFU-G: n=380 colonies from 5 embryos, BFU-E: n=218 colonies from 9 embryos. CFU-GM and CFU-G colonies were generated through culture with different cytokine cocktails more permissive of the generation of monocytes/macrophages or granulocytes, respectively. YFP signal in a representative YFP+ CFU-GM colony (right panel).

(E) Morphological analysis of YFP+ and YFP- CFU-G colonies (left panel). Mean % + SEM, n=21-23 colonies from 5 embryos, 50-100 cells analysed per colony. May-Grünwald/Giemsa staining of representative CFU-G cells (right panel). Scale bar is 25µm.

The data presented in this figure was generated in collaboration with Dr. Charlotta Böiers, Dr. Michael Lutteropp, and Dr. Adam Mead.

4.2.2. Embryonic tissue-resident macrophages are mainly not derived from *Rag1*-expressing progenitors

Macrophages are one of the three types of phagocytic leucocytes in the innate immune system (macrophages, neutrophils, and dendritic cells), and are a very heterogeneous cell type widely distributed in body tissues. Tissue-resident macrophages play a variety of roles in clearance of cell debris, vascular and osteal development, metabolic regulation, and tissue homeostasis (Davies et al., 2013; Davies and Taylor, 2015).

Adult tissue-resident macrophages were originally thought to derive from BM monocytes, but recent lineage tracing studies suggest that these long-lasting macrophages are generated independently of HSC-derived definitive haematopoiesis. Published data suggests that these macrophages are instead derived from erythro-myeloid progenitors (EMP) in the YS, and then infiltrate other tissues during embryonic development (Ginhoux et al., 2010; Schulz et al., 2012; Yona et al., 2012; Gomez Perdiguero et al., 2013; Gomez Perdiguero et al., 2015). The emergence of two sequential waves of YS EMPs, which contribute separately to YS macrophages and FL monocytes and then generate distinct populations of tissue-resident macrophages, remains under debate (Bertrand et al., 2005; Hoeffel et al., 2012; Epelman et al., 2014; Hoeffel et al., 2015; Hoeffel and Ginhoux, 2015).

Our data suggests that *Rag1*-expressing lympho-myeloid progenitors first emerge in YS at E9.5 (Böiers et al., 2013). Considering the significant *in vivo* contribution of *Rag1*-expressing progenitors to early myelopoiesis in FL, we also investigated if *Rag1*-expressing progenitors play a role in the generation of tissue-resident macrophages. We analysed YFP labelling by flow cytometry in three populations of F4/80^{high} tissue-resident macrophages in *Rag1*-Cre/*R26*R-EYFP E14.5 embryos: brain microglia, liver Kupffer cells and epidermal Langerhans cells (Figure 4.3A-C). We found that all three populations were only marginally labeled by YFP (Figure 4.3D, <3% YFP+). These results suggests that the main generation pathway of

embryonic tissue-resident macrophages is independent from *Rag1*-expressing lympho-myeloid progenitors, which is in agreement with the proposed emergence of one or more YS EMP populations prior to the detection of IL7Rα+ *Rag1*-GFP+ progenitors in YS at E9.5 (Gomez Perdiguero et al., 2013; Hoeffel and Ginhoux, 2015).

A

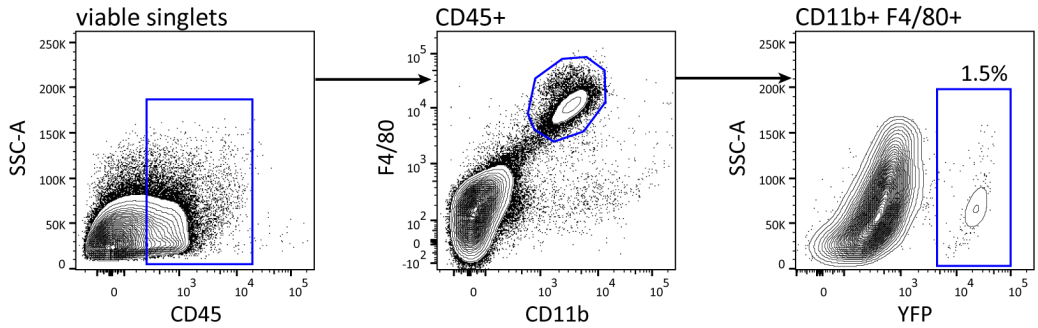
viable singlets
CD45+
CD11b+ F4/80+
SSC-A
CD45
F4/80
CD11b
1.5%
YFP

B

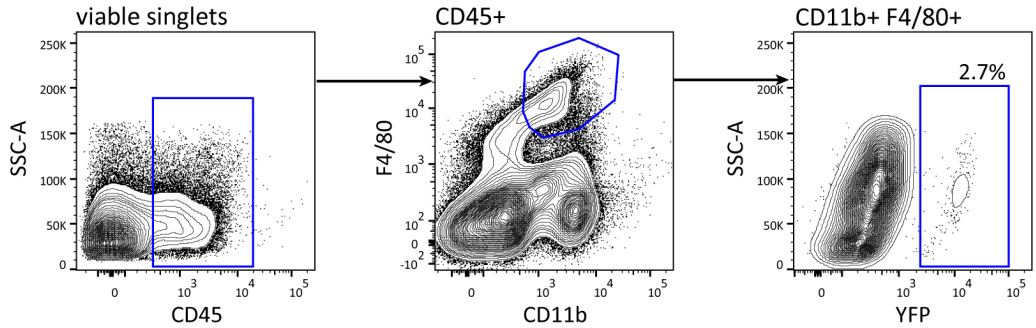
viable singlets
CD45+
CD11b+ F4/80+
SSC-A
CD45
F4/80
CD11b
2.7%
YFP

C

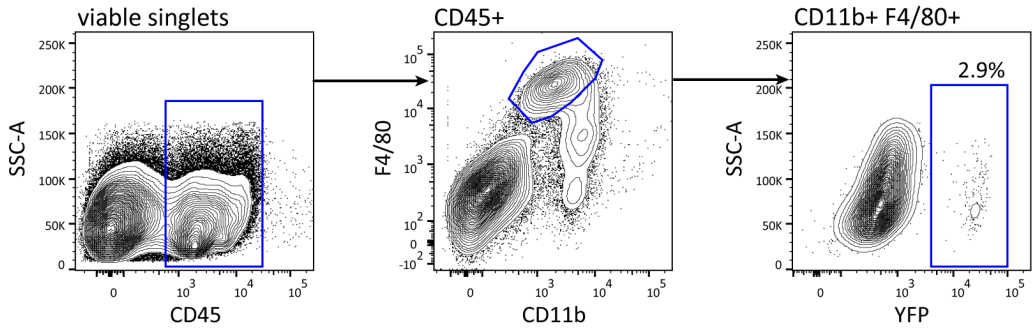
viable singlets
CD45+
CD11b+ F4/80+
SSC-A
CD45
F4/80
CD11b
2.9%
YFP

D

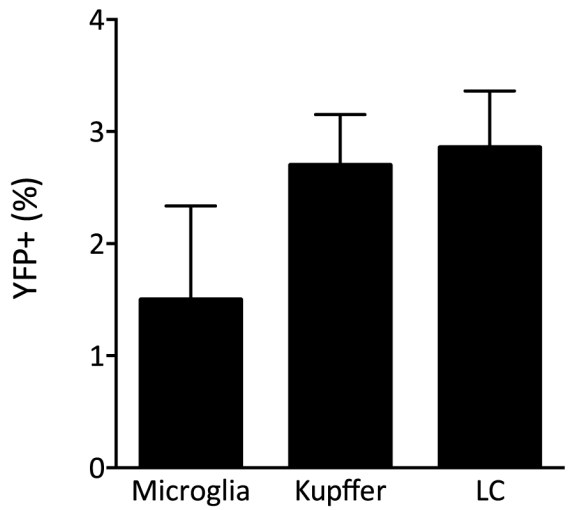
YFP+ (%)
Microglia
Kupffer
LC

Figure 4.3. Embryonic *Rag1*-expressing progenitors do not contribute significantly to tissue-resident macrophages.

Contribution of *Rag1*-expressing progenitors to foetal tissue-resident macrophages was quantified by flow cytometric analysis of YFP labelling of CD45+ CD11b^{low} F4/80^{high} cells in the brain, skin, and liver of *Rag1*-Cre/*R26*R-EYFP E14.5 embryos.

(A) Gating strategy for flow cytometric analysis of YFP labelling of microglia, F4/80^{high} brain resident macrophages. Mean % of parent gate is shown (n=7).

(B) Gating strategy for flow cytometric analysis of YFP labelling of Kupffer cells, F4/80^{high} liver resident macrophages. Mean % of parent gate is shown (n=7).

(C) Gating strategy for flow cytometric analysis of YFP labelling of epidermal Langerhans cells (LC), F4/80^{high} skin resident macrophage-like dendritic cells. Mean % of parent gate is shown (n=7).

(D) Quantification of YFP labelling of microglia, Kupffer cells, and epidermal Langerhans cells. Mean % + SEM, n=7 embryos. Note the y-axis scale: mean YFP labelling is below 3% for all populations.

The data presented in this figure was generated in collaboration with Dr. Elisa Gomez Perdiguero.

4.3. Discussion

The megakaryocyte and erythroid (Mk/E) potentials demonstrated by BM LMPPs phenotypically defined as LSK Flt3^{high} are minimal but not completely absent *in vitro* or *in vivo* (Adolfsson et al., 2005; Forsberg et al., 2006). This indicates that either all LMPPs exhibit low-level Mk/E potentials or the compartment is still heterogeneous, containing a majority of immune-restricted cells but also some multipotent cells. Further studies have provided data supporting the latter hypothesis, showing that BM LMPPs can be further fractionated into a gradient of sub-populations with increased restriction of lineage potentials (Forsberg et al., 2006; Lai and Kondo, 2006; Arinobu et al., 2007; Mansson et al., 2007; Luc et al., 2008a; Heffner et al., 2011).

Overall, many findings from different research groups support an hierarchical model of haematopoiesis in which loss of megakaryocyte/erythroid potential precedes loss of myeloid potential in the pathway of lymphoid lineage development in both adult and embryo (Adolfsson et al., 2005; Lai and Kondo, 2006; Iwasaki and Akashi, 2007a, b; Mansson et al., 2007; Akashi, 2009; Doulatov et al., 2010; Goardon et al., 2011).

One of the best approaches to analyse the physiological lineage outputs of a progenitor population is genetic lineage tracing *in vivo*. However, a major limitation of lineage tracing assays is the requirement for a distinct promoter that can be used to faithfully and specifically drive expression of Cre recombinase in the population of interest. For many populations such promoters have not yet been identified. Several lineage tracing studies that used Cre recombinase labelling systems dependent on the expression of *Flt3*, *Il7r* and *Rag1* have obtained results that question the *in vivo* physiological relevance of the LMPP model in adult haematopoiesis (Schlenner et al., 2010; Schlenner and Rodewald, 2010; Boyer et al., 2011; Boyer et al., 2012).

Although the LMPP compartment is phenotypically-defined by a high level of expression of the Flt3 cell surface marker (25% highest Flt3 expressing LSK cells), in adult BM the *Flt3* gene is lowly expressed already in the upstream multipotent HSC compartment (Christensen and Weissman, 2001; Buza-Vidas et al., 2011), and therefore the use of *Flt3*-Cre is not suitable for specific lineage tracing of LMPP progeny. Due to this early expression of *Flt3*, it is expected for the megakaryocyte and erythroid lineages to be labelled in a *Flt3*-Cre lineage tracing system as was reported (Boyer et al., 2011; Buza-Vidas et al., 2011; Boyer et al., 2012).

Il7r and *Rag1* are lymphoid-specific genes but only a small percentage of adult BM Flt3^{high} LMPPs express them, and higher expression of these genes correlates with higher expression of *Flt3* and lower myeloid clonogenicity within the LMPP compartment (Adolfsson et al., 2005; Luc et al., 2008a; Mansson et al., 2010). It is therefore not unexpected to find only low labelling of the myeloid lineage when performing lineage tracing experiments of adult haematopoiesis with *Il7r*-Cre (Schlenner et al., 2010; Schlenner and Rodewald, 2010) or *Rag1*-Cre mouse models (Welner et al., 2009). In these studies the faithfulness of *in vivo* lineage tracing of the progenitors of interest is compromised by the use of inadequate promoters, and thus they fail to properly address the lineage contributions of the LMPP compartment in adult haematopoiesis.

In chapter 3 we demonstrated that embryonic IL7Rα+ Flt3+ progenitors have lymphoid and myeloid potentials but minimal megakaryocyte and erythroid potentials *in vitro* (Böiers et al., 2013). In the current study we used a *Rag1*-Cre/*R26*R-EYFP reporter mouse line to analyse the lineage contribution of these LMPP-like progenitors in FL. In contrast to the adult BM LMPP studies mentioned above (Boyer et al., 2011; Boyer et al., 2012), the *Rag1*-Cre approach is appropriate for faithful lineage tracing of the progeny of embryonic lympho-myeloid progenitors. While <50% of adult LMPPs are *Rag1*-GFP+ in *Rag1*-GFP knock-in mice

(Luc et al., 2008a) and YFP+ in *Rag1*-Cre/*R26*R-EYFP mice (unpublished data), >90% of IL7Rα+ Flt3+ E11.5 FL lympho-myeloid progenitors are *Rag1*-GFP+ (Böiers et al., 2013).

In full agreement with our previous *in vitro* data, we found that *Rag1*-expressing progenitors contribute not only to *in vivo* lymphopoiesis but also contribute substantially to early embryonic myelopoiesis, generating both monocytes and granulocytes (Figures 4.1 and 4.2). We also confirmed that *Rag1*-expressing progenitors express minimal megakaryocyte and erythroid lineage potentials (Figure 4.1 and 4.2D).

Together our *in vitro* and *in vivo* findings in chapters 3 and 4 provide evidence of a very early LMPP-like population that arises in the YS, and seeds the FL before the establishment of HSC-driven definitive haematopoiesis. This population contributes to the generation of both myeloid and lymphoid lineages of the innate and adaptive immune systems in the embryo.

It is unclear how long myeloid contribution from YS-derived lympho-myeloid progenitors persists after the FL is seeded by definitive HSCs (dHSCs) around E11-E11.5 (Medvinsky et al., 1993; Sanchez et al., 1996; Kumaravelu et al., 2002). Our data shows that contribution by *Rag1*-expressing progenitors to myelopoiesis decreases with developmental age (Figure 4.1D). This suggests that this source of myeloid contribution is replaced by another progenitor population, and/or reflects the decrease of *Rag1* expression within the lympho-myeloid progenitor compartment throughout development, which compromises the relevance of the *Rag1*-Cre/*R26*R-EYFP reporter strain.

In E11.5 FL almost all LMPP-like IL7Rα+ Flt3+ cells co-express *Rag1*-GFP (91%) (Figure 3.1A) (Böiers et al., 2013), in E14.5 FL *Rag1*-GFP is expressed by 70% of LMPPs (data not shown), and in adult BM it is expressed by <50% of LMPPs (Luc et al., 2008a). *Rag1* expression in embryonic lympho-myeloid progenitors only drops by 20% between E11.5 and E14.5, while the YFP labelling of FL CD11b1+ cells in *Rag1*-Cre/*R26*R-EYFP embryos drops by 50%. So it appears that down-regulation of the *Rag1* gene in later lympho-myeloid progenitors is not

the only cause of the decrease in YFP labelling during embryonic development. At E11.5 definitive haematopoiesis is just starting to be established, but dHSCs expand very rapidly in the FL between E11.5 and E16.5 (Ema and Nakauchi, 2000; Mikkola and Orkin, 2006). It is likely that by E14.5 increased contribution of dHSC-derived myeloid progenitors has substituted some of the early myeloid contribution of lympho-myeloid progenitors and other YS-derived progenitors (McGrath and Palis, 2005; Lux et al., 2008; McGrath et al., 2015).

Distinguishing between YS-derived and dHSC-derived myeloid contribution in the FL is not trivial, and further studies would be necessary to identify appropriate genes for *in vivo* lineage tracing. The use of an inducible *Rag1*-Cre/*R26*R-EYFP reporter line for pulse-chase experiments in which Cre-driven YFP expression is activated at a specific time point and traced thereafter (Feil et al., 2009) is not suitable in this case ,due to the short time window between emergence of lympho-myeloid progenitors in the YS around E9.5 and emergence of dHSCs in the aorta-gonad-mesonephros region (AGM) around E10.5 – too short for common activation methods of inducible Cre/Lox lines (Reinert et al., 2012; Hoeffel and Ginhoux, 2015). Another possible approach is the use of a constitutive Cre-reporter mouse line allowing specific and efficient labelling of dHSCs and their progeny, without labelling also YS precursors and their progeny. However, the cell surface marker phenotype and respective transcriptome profile of the specific cell of origin of lympho-myeloid progenitors in YS is unknown, and lines such as *Pf4*-Cre (which is expressed by dHSCs and should not be expressed by YS precursors or YS-derived lympho-myeloid progenitors) have a very low labelling efficiency in FL compared to adult BM (Calaminus et al., 2012).

It is also unclear if any mature lineage contribution of YS-derived embryonic lympho-myeloid progenitors persists in the adult haematopoietic system. Lineage tracing of the contribution of extra-embryonic haematopoietic cells to adult haematopoiesis has been attempted with

an inducible *Runx1*-CreERT system. Runt related transcription factor 1 (*Runx1*) is expressed by all definitive haematopoietic cells and is first highly expressed in YS (Nottingham et al., 2007). With this approach, a small contribution (<10%) from *Runx1*-expressing cells to adult haematopoiesis was found (Samokhvalov et al., 2007). However, *Runx1* expression was suggested to not be exclusive to YS at the time of Cre induction in this study, which detracts from the conclusion of YS contribution (Dzierzak and Speck, 2008).

We observed that *Rag1*-expressing embryonic progenitors only contribute marginally to long-lived tissue-resident macrophage populations (brain microglia, liver Kupffer cells and epidermal Langerhans cells), but we did not test contribution to other types of cells with possible YS origin. As mentioned above, in order to trace the contribution of *Rag1*-expressing embryonic progenitors to adult haematopoiesis we could use an inducible *Rag1*-Cre/*R26*R-EYFP reporter line and perform pulse-chase experiments in which Cre-driven YFP expression activated in the embryo is later analysed in the adult mouse. Another possible experiment, although more technically challenging and less physiological, would be transplantation of *Rag1*-expressing progenitors from *Rag1*-Cre/*R26*R-EYFP embryos into recipient embryos or into neonates, again followed by tracing of YFP labelling in the adult mice (Liuba et al., 2009; Derderian et al., 2014).

CHAPTER 5: Functional and molecular characterisation of platelet-biased haematopoietic stem cells in adult bone marrow

5.1. Introduction

In chapters 3 and 4 we explored the early lineage commitment steps of the lymphoid/myeloid differentiation branch of the murine haematopoietic tree, namely the lymphoid/myeloid-priming of yolk sac (YS) and foetal liver (FL) progenitors. The data we presented in those chapters support the lympho-myeloid multipotent progenitor (LMPP) model of the haematopoietic hierarchy, in which the first bifurcation of lineage fates is the segregation of lymphoid/myeloid and myeloid/megakaryocyte/erythroid potentials. In the next two chapters we will conversely explore lineage bias and commitment in the opposite differentiation branch of the haematopoetic tree of the LMPP model: the myeloid/megakaryocyte/erythroid branch.

It has been shown, through single cell gene expression analysis, that a fraction of the adult bone marrow (BM) Lineage- Sca-1+ c-Kit+ (LSK) CD34- Flt3- phenotypic compartment, which includes long-term haematopoietic stem cells (LT-HSCs), is megakaryocyte/erythroid (Mk/E)-primed (Mansson et al., 2007). Furthermore, our group recently showed that the gene for von Willebrand factor (*Vwf)*, an Mk lineage affiliated gene, is expressed by approximately half of phenotypic LT-HSCs (LSK CD150+ CD48- CD34-) in the BM (Sanjuan-Pla et al., 2013).

Von Willebrand factor is a plasma multimeric glycoprotein with important roles in blood haemostasis. Through its interactions with platelet surface glycoproteins it mediates platelet recruitment and adhesion to sites of vascular injury. It is also a carrier and stabilizer of coagulation factor VIII, a protein essential for blood clotting. vWF protein biosynthesis and

secretion is limited to two mature cell types: endothelial cells and megakaryocytes/platelets. Endothelial cells synthesise vWF into Weibel-Palade bodies and then secret it to the plasma. Megakaryocytes synthesise vWF into α-granules that are inherited by the platelets they produce, and from which it is released upon appropriate stimulation (McGrath et al., 2010; Peyvandi et al., 2011).

Early expression of the Mk-associated *Vwf* gene in the LSK CD150+ CD48- CD34- BM compartment can be exploited as a discriminating marker to enrich for a thrombopoietin-dependent subtype of HSCs that preferentially reconstitutes platelets in short-term and long-term *in vivo* transplantation assays (Sanjuan-Pla et al., 2013). Although we have not studied vWF biosynthesis in LT-HSCs, we do not expect the protein to play a functional role in this haematopoietic population. This is supported by our observation that HSCs are present in normal numbers in the BM of *Vwf*-deficient mice, and lack any functional phenotype upon competitive transplantation (unpublished data, not shown).

In a parallel study, Yamamoto and colleagues identified within the LSK CD150+ CD34- compartment what they termed self-renewing progenitors with platelet/erythroid/myeloid-restricted, platelet/erythroid-restricted and platelet-restricted reconstitution behaviour when transplanted at the single cell level. They named these populations common myeloid repopulating progenitor (CMRP), megakaryocyte-erythroid repopulating progenitor (MERP) and megakaryocyte-repopulating progenitor (MkRP), respectively. Their findings in paired daughter cell assays (Ema et al., 2000; Nakauchi et al., 2001; Takano et al., 2004) indicate that MkRPs can derive directly from LT-HSCs without passing through intermediate progenitor stages (Yamamoto et al., 2013). Their study thus suggests that the properties of multipotentiality and long-term self-renewal ability are not always coupled together in the haematopoietic system, contrary to the prevailing view in the field.

Importantly, the biased and restricted cell populations identified in both studies mentioned above were not prospectively isolated, but only identified after retrospective analysis of *in vivo* reconstitution patterns. In our study *Vwf* expression enriched for – but did not purify – platelet-biased LT-HSCs (Sanjuan-Pla et al., 2013). In the study by Yamamoto and colleagues single cells were sorted from heterogeneous populations within the LSK CD34- compartment (Yamamoto et al., 2013). Future identification of specifically expressed genes and additional cell surface markers will be necessary for prospective purification of the cell populations currently identified only by their *in vivo* reconstitution behaviour.

In this chapter we present evidence that *Vwf* expression not only enriches for platelet-biased reconstitution behaviour in LT-HSCs, it also enriches for reconstitution patterns with lymphoid-exclusion, including a small percentage of cells that behave as platelet-restricted *in vivo*, similarly to the MkRPs described by Yamamoto and colleagues.

Furthermore, we describe here the biased haematopoietic hierarchies established by platelet-biased LT-HSCs and provide some insight into the mechanism of their establishment.

We also demonstrate that the *in vivo* restricted reconstitution behaviour of individual *Vwf*+ LT-HSCs does not reflect a true restriction of their lineage potentials.

Finally, we discuss preliminary data regarding the molecular characterisation of platelet-biased *Vwf+* LT-HSCs, and possible identification of new markers for their prospective isolation.

5.2. Results

5.2.1. Investigating the *in vivo* reconstitution behaviour of individual bone marrow *Vwf*+ long-term haematopoietic stem cells

Platelet-biased *Vwf*+ HSCs transplanted at the population level (5-50 cells) typically contribute considerably to myeloid lineages, whereas their lymphoid contribution is marginal (Sanjuan-Pla et al., 2013). Furthermore, considering the gating strategy used, It is likely that a fraction of the restricted reconstitution behaviours described by Yamamoto and colleagues (Yamamoto et al., 2013) derives from *Vwf*+ LT-HSCs. Together these observations suggest that lineage restriction may be a property of a subset of *Vwf*+ LT-HSCs, and so we sought to further investigate the functional properties of this population at the single cell level.

To study the *in vivo* reconstitution behaviour of individual adult BM *Vwf+* LT-HSCs we performed single cell transplantations using *Vwf*-tdTomato/*Gata1*-EGFP double fluorescent reporter mice as BM donors. In this mouse strain the fluorescent proteins are expressed under the control of the endogenous promoter and known regulatory elements of each gene (Figure 5.1A). The faithful correlation between *Vwf* and *Gata1* gene expression and respective fluorescent protein expression has been characterised by the group of Prof. Claus Nerlov (EMBL, Monterotondo and WIMM, Oxford) (unpublished data, not shown).

The most commonly used approach to distinguish donor-derived cells from recipient-derived cells in peripheral blood of transplanted mice relies on the use of congenic CD45 alleles, and we used this classic method to track donor-derived leucocytes. However, platelets and erythrocytes do not express CD45. Production of both these lineages can be easily traced by using *Vwf*-tdTomato/*Gata1*-EGFP mice as donors, since all platelets are *Vwf*+ *Gata1*- and all erythrocytes are *Vwf*+ *Gata1*+ (Figure 5.1B-C). The use of this double reporter mouse line is an improvement

on our previous studies, in which contribution of platelet-biased HSCs to the erythroid lineage was not assessed (Sanjuan-Pla et al., 2013).

Similarly to the previously published *Vwf*-EGFP reporter (Sanjuan-Pla et al., 2013), in the *Vwf*-tdTomato/*Gata1*-EGFP mouse approximately half of LT-HSCs are labelled by *Vwf*-tdTomato (Figure 5.1D). To avoid contamination by *Vwf*- cells when sorting purified LT-HSCs for single cell transplantation, on average only the 20% highest *Vwf*+ labelled LT-HSCs were selected, from now on referred to as *Vwf*^{high} (Figure 5.1E).

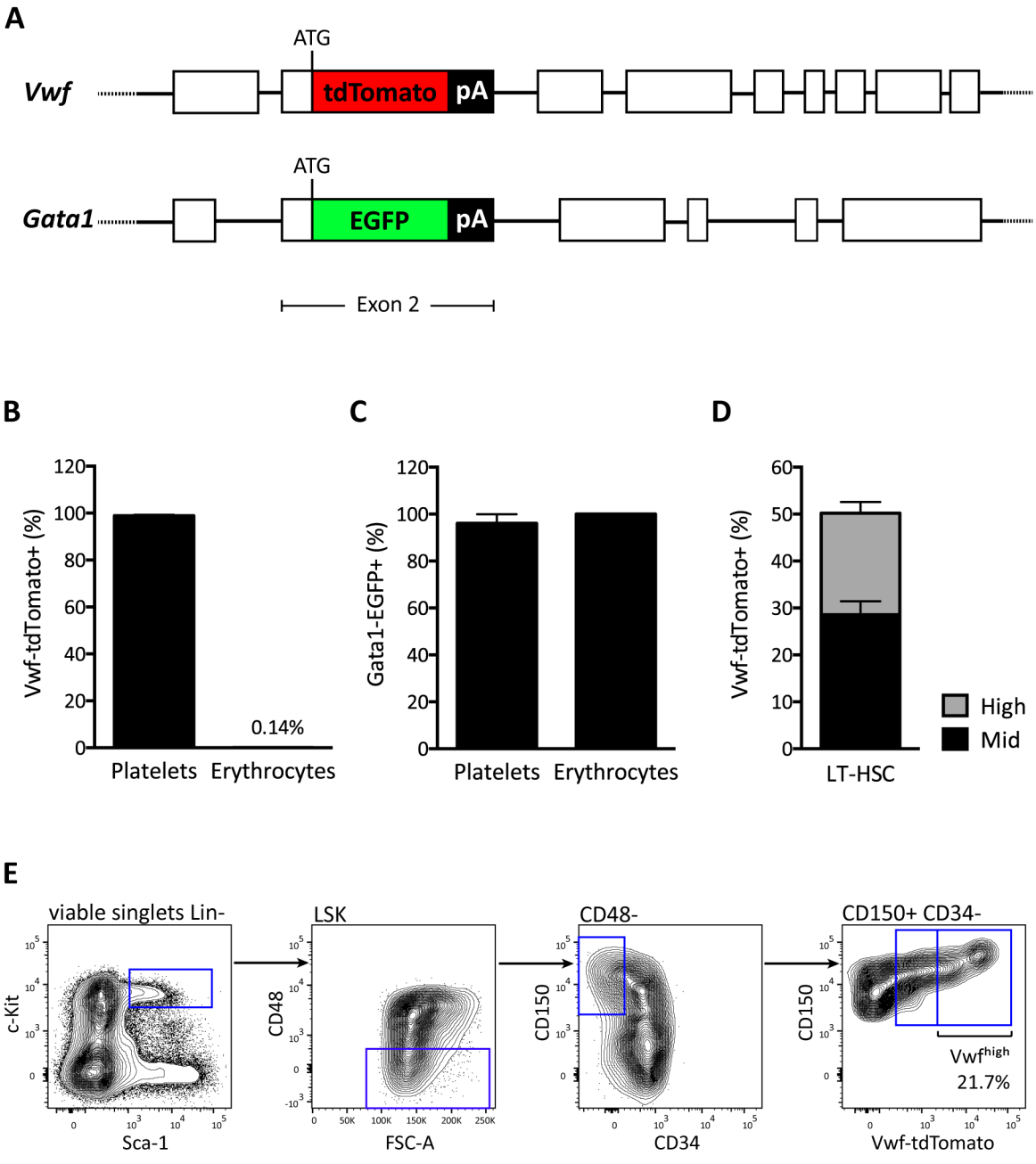

Figure 5.1. The Vwf-tdTomato/Gata1-EGFP double reporter mouse.

Vwf-tdTomato/*Gata1*-EGFP double fluorescent reporter mice were used as donors for single cell transplantations. This mouse strain enables sorting of *Vwf*+ LT-HSCs, as well as tracking of donor-derived platelets (*Vwf*+ *Gata1*+) and erythrocytes (*Vwf*- and *Gata1*+) in the blood of recipient mice.

(A) Structure of the *Vwf*-tdTomato and *Gata1*-EGFP constructs (not to scale). Bacterial artificial chromosomes were generated with the genomic region of each gene, and the coding sequence for fluorescent protein was inserted into the second exon. The two mouse lines were independently produced by intracytoplasmic sperm injection-mediated gene transfer, and crossed together to produce the *Vwf*-tdTomato/*Gata1*-EGFP double reporter line.

(B) Labelling of peripheral blood platelets (TER119- CD150+ CD41+) and erythrocytes (TER119+) in *Vwf*-tdTomato mice. Mean % + SEM, n=3.

(C) Labelling of peripheral blood platelets and erythrocytes in *Gata1*-EGFP mice. Mean % + SEM, n=3.

(D) Labelling of BM LT-HSCs (LSK CD150+ CD48- CD34-) in *Vwf*-tdTomato/*Gata1*-EGFP mice. Mean % + SEM, n=12.

(E) Gating strategy for sorting of *Vwf*+ LT-HSCs from *Vwf*-tdTomato/*Gata1*-EGFP donor mice. To avoid contamination by *Vwf*- cells, only the highest labelled LT-HSCs (Vwf^{high}) were sorted for single cell transplantation. Mean % of parent gate is shown (n=12).

Single cell transplantation of *Vwf*^{high} LT-HSCs and peripheral blood reconstitution analysis were performed as previously described (Sanjuan-Pla et al., 2013) (see also chapter 2). Briefly, single phenotypically defined *Vwf*^{high} LT-HSCs (LSK CD150+ CD48- CD34-) were sorted from *Vwf*-tdTomato/*Gata1*-EGFP CD45.2 donors and injected intravenously into lethally irradiated CD45.1 recipients, together with unfractionated BM cells from a CD45.1 *Kit*$^{W41/W41}$ mouse to ensure recipient survival. The CD45.1 *Kit*$^{W41/W41}$ strain was chosen as a donor of support cells because the partial loss of Kit function in *Kit*$^{W41/W41}$ HSCs provides an advantage to wild-type HSCs in competitive and non-competitive *in vivo* transplantation settings (Miller et al., 1997; Sharma et al., 2007; Thoren et al., 2008). It has been shown that the use of sub-lethally irradiated *Kit*$^{W41/W41}$ mice as recipients of BM cells yields similar results to wild-type recipients, with the advantage of eliminating the need for injection of additional support cells (Trevisan and Iscove, 1995; Trevisan et al., 1996; Miller and Eaves, 1997; Dykstra et al., 2007). However, *Kit*$^{W41/W41}$ mice suffer from moderate anaemia and reduced fertility (Sharma et al., 2007), and in our hands they also show higher mortality than wild-type CD45.1. Since our experimental design requires large cohorts of transplantable mice, we used wild-type CD45.1 as recipients due to their higher generation efficiency and more reliable long-term maintenance.

Peripheral blood reconstitution was analysed every 4 weeks between 8 and 18 weeks post-transplantation (8-10, 12-14, and 15-18 weeks), and some recipients were analysed at one or two additional time points up to 35 weeks post-transplantation. After the final peripheral blood analysis, reconstituted mice of interest were terminated for flow cytometric analysis of the donor contribution to the haematopoietic hierarchy in different tissues, for functional *in vitro* analysis of lineage potentials of donor-derived LSK cells, and for secondary transplantation of donor-derived HSCs (Figure 5.2A-D).

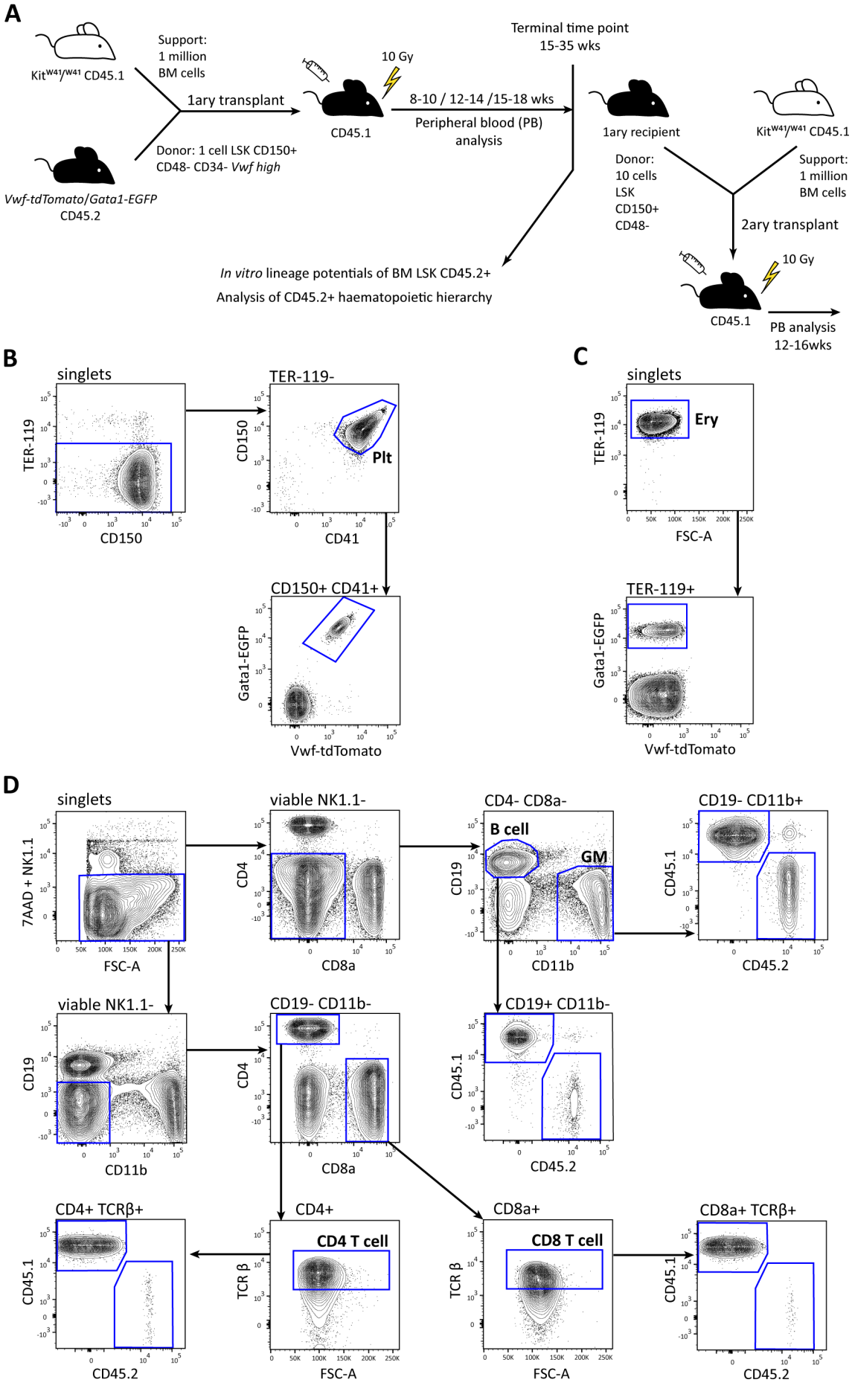
A
Kit^W41/W41 CD45.1
Support:
1 million
BM cells
1ary transplant
Donor: 1 cell LSK CD150+
CD48- CD34- Vwf high
Vwf-tdTomato/Gata1-EGFP
CD45.2
10 Gy
CD45.1
8-10 / 12-14 /15-18 wks
Peripheral blood (PB)
analysis
Terminal time point
15-35 wks
1ary recipient
Kit^W41/W41 CD45.1
Donor:
10 cells
LSK
CD150+
CD48-
Support:
1 million
BM cells
2ary transplant
10 Gy
CD45.1
PB analysis
12-16wks
In vitro lineage potentials of BM LSK CD45.2+
Analysis of CD45.2+ haematopoietic hierarchy
B
singlets
TER-119
CD150
TER-119-
CD150
CD41
Plt
CD150+ CD41+
Gata1-EGFP
Vwf-tdTomato
C
singlets
TER-119
Ery
FSC-A
TER-119+
Gata1-EGFP
Vwf-tdTomato
D
singlets
7AAD + NK1.1
FSC-A
viable NK1.1-
CD4
CD8a
CD4- CD8a-
CD19
B cell
GM
CD11b
CD19- CD11b+
CD45.1
CD45.2
viable NK1.1-
CD19
CD11b
CD19- CD11b-
CD4
CD8a
CD19+ CD11b-
CD45.1
CD45.2
CD4+ TCRβ+
CD45.1
CD45.2
CD4+
CD4 T cell
TCR β
FSC-A
CD8a+
CD8 T cell
TCR β
FSC-A
CD8a+ TCRβ+
CD45.1
CD45.2

Figure 5.2. Single cell transplantation of bone marrow *Vwf*^{high} long-term haematopoietic stem cells and peripheral blood analysis by flow cytometry.

Vwf^{high} LT-HSCs were transplanted at the single cell level and the long-term reconstitution of peripheral blood lineages was carefully analysed over time by flow cytometry. Detection of donor-derived platelets and erythrocytes was based on fluorescence, while detection of donor-derived white blood cells was based on CD45 congenic markers.

(A) Experimental design of single cell transplantation of LT-HSCs and peripheral blood analysis.

(B) Gating strategy for flow cytometric analysis of donor-derived peripheral blood platelets (TER119- CD150+ CD41+ *Vwf*+ *Gata1*+).

(C) Gating strategy for flow cytometric analysis of donor-derived peripheral blood erythrocytes (TER119+ *Vwf*- *Gata1*+).

(D) Gating strategy for flow cytometric analysis of donor-derived CD45.2+ myeloid cells (NK1.1- CD4- CD8a- CD19- CD11b+), B cells (NK1.1- CD4- CD8a- CD11b- CD19+), CD4 T cells (NK1.1- CD19- CD11b- CD8a- CD4+ TCRβ+) and CD8 T cells (NK1.1- CD19- CD11b- CD4- CD8a+ TCRβ+) in peripheral blood of transplantation recipients.

5.2.2. *In vivo* lineage outputs of single *Vwf*^{high} LT-HSCs follow a systematic and predictable pattern

In this study we transplanted a total of 263 mice with single *Vwf*^{high} LT-HSCs, but excluded from analysis the 15 recipients that did not survive the full period of follow-up post-transplantation. Long-term reconstituted mice represented 39% of the 248 transplanted mice analysed (Figure 5.3A), which is comparable to recent publications using the same experimental approach (Sanjuan-Pla et al., 2013; Yamamoto et al., 2013). However, transplantation of purified HSCs has several technical caveats: cells may perish or be induced to differentiate during sorting and pre-injection preparations; they may remain attached to the collection plate or syringe; or they may be lost due to technical error during the injection procedure. The percentage of long-term reconstituted mice is, therefore, likely to be an underestimation of the real number of transplantable long-term self-renewing HSCs within the LSK CD150+ CD48- CD34- *Vwf*^{high} compartment.

Long-term reconstituted mice were retrospectively assigned to different categories of reconstitution behaviour based on the level of donor contribution to each peripheral blood lineage, as detailed in Table 5.1. Biased reconstitution is defined here as a lineage reconstitution level ≥ 5-fold higher than the next highest reconstituted lineage, and observable at least in the last two consecutive time points of peripheral blood analysis. Importantly, in this study we focused only on long-term reconstitution that is continuously detectable after 8 weeks post-transplantation. In previous analyses we observed that cases of transient and/or delayed reconstitutions from *Vwf*^{high} LT-HSCs are rare (data not shown), and in the current study our analysis parameters deliberately excluded such cases. Furthermore, the criteria chosen to categorize restricted patterns were purposefully strict to more accurately represent the lineage potentials of each single transplanted cell, and to highlight instances of apparent lineage

restriction (Table 5.1). In several cases of platelet/erythroid-restricted and platelet/erythroid/myeloid-restricted reconstitution with platelet-bias, donor contribution to erythrocytes and/or myeloid cells was only detectable at a single time point of analysis and/or was very low compared to platelets (>1000-fold lower than donor-derived platelets). These cases are very close to being categorised as platelet-restricted, but the convincing – even if extremely low – detection of any donor contribution to the erythroid and/or myeloid lineages demonstrates that the single *Vwf*^{high} LT-HSC transplanted does possess additional lineage potentials and, thus, is not lineage-restricted.

In agreement with our previously published data (Sanjuan-Pla et al., 2013), we observed that the *in vivo* reconstitution behaviour of individual *Vwf*^{high} LT-HSCs is highly platelet-dominated. Out of 97 long-term reconstituted mice analysed, 66% developed reconstitution patterns with platelet-bias, platelet/erythroid-bias or platelet/erythroid/myeloid-bias (Figure 5.3B). Importantly, only one case of lymphoid/erythroid-bias, and no cases of lymphoid/platelet-bias or lymphoid/myeloid-bias, were observed. These findings highlight the strong skewing of *Vwf*^{high} LT-HSCs away from lymphoid potential. Indeed, although the majority of reconstituted mice showed multilineage reconstitution patterns (71%), a significant fraction showed lymphoid-excluding reconstitution (28%) characterised by <0.01% donor contribution to B and T cells at all time points of blood analysis (Figure 5.3C). Cells with balanced *in vivo* lineage outputs, which may be considered to be the classically defined long-term HSCs, represented only 23% of multilineage *Vwf*^{high} LT-HSCs (Figure 5.3D). Both within the group of multilineage reconstitutions and the group of lymphoid-excluding reconstitutions, platelet/erythroid/myeloid-bias is the most prevalent type of bias (Figure 5.3D-E).

Interestingly, we found that some individual *Vwf*^{high} LT-HSCs generate completely platelet-restricted reconstitution patterns, in which donor-contribution to platelets is ≥0.01% and donor-

contribution to all other blood lineages is <0.01% at all time points of analysis. Only four long-term cases of platelet-restricted reconstitution were observed, representing 15% of lymphoid-excluding reconstitutions (and only 4% of all reconstitutions) (Figure 5.3E). Importantly, with our experimental conditions, stable long-term uni-lineage reconstitution was not observed for any blood lineage other than platelets.

The reconstitution of blood lineages in mice transplanted with single *Vwf*^{high} LT-HSCs can gradually change over time before reaching a stable pattern (Figure 5.3F). Throughout this gradual change, detection of donor contribution to the different blood lineages follows a specific and predictable order: first platelets, then erythrocytes, myeloid cells, B cells, and lastly T cells.

Consistent with the low frequency of platelet/erythroid-restricted patterns observed, erythrocyte reconstitution is usually closely followed by myeloid cell reconstitution. Interestingly, B cell reconstitution often appears uncoupled from T cell reconstitution. Compared to the other lineages, detection of donor-derived CD4 and CD8 T cells is often delayed, and many cases of non-balanced multilineage patterns include lymphoid-reconstitution consisting only of donor-derived B cells. This systematic order of reconstitution detection allows for accurate deduction regarding the presence of reconstituted lineages. For example, when donor-derived myeloid cells are detected, the additional presence of platelet and erythroid reconstitution can be accurately inferred. Likewise, the detection of donor-derived B cells allows inference that platelet, erythroid, and myeloid reconstitution will also be present.

This order of lineage detection could be the result of preferential generation, by HSCs, of the progenitor sub-sets upstream of the different mature lineages, with generation of progenitors of the platelet lineage being favoured by *Vwf*^{high} HSCs. Alternatively, or concomitantly, it might also reflect different kinetics of mature cell production from progenitors downstream of HSCs, with the differentiation pathway of platelets being the fastest and the differentiation pathway of lymphocytes being the slowest.

Table 5.1. Donor-derived reconstitution biases and patterns derived from single cell transplantation of *Vwf*^{high} long-term haematopoietic stem cells.

Lineage bias		**Bias description**
Platelet-bias		Donor-derived platelets ≥ 5x donor-derived erythrocytes, myeloid and lymphoid cells (both T and B)
Platelet/erythroid-bias		Donor-derived platelets and erythrocytes ≥5x donor-derived myeloid and lymphoid cells (both T and B) Fold difference of reconstitution between platelets and erythrocytes <5x
Platelet/erythroid/myeloid-bias		Donor-derived platelets, erythrocytes and myeloid cells ≥5x donor-derived lymphoid cells (both T and B) Fold difference of reconstitution between platelets, erythrocytes and myeloid cells <5x
Lymphoid/erythroid-bias		Donor-derived lymphoid cells (both B and T) and erythrocytes ≥5x donor-derived platelets and myeloid cells Fold difference of reconstitution between B cells, T cells and erythrocytes <5x
Reconstitution patterns		**Pattern description**
Multilineage	**Balanced**	Platelets, erythrocytes, myeloid cells and lymphoid cells (both T and B) reconstituted Fold difference of reconstitution between all lineages <5x
	Non-balanced	Platelets, erythrocytes, myeloid cells and lymphoid cells (T and/or B) reconstituted Fold difference of reconstitution between some or all lineages ≥5x
Lymphoid-excluding	**Platelet/erythroid/myeloid-restricted**	Platelets, erythrocytes and myeloid cells reconstituted. Lymphoid cells (both T and B) not reconstituted
	Platelet/erythroid-restricted	Platelets and erythrocytes reconstituted. Myeloid cells and lymphoid cells (both T and B) not reconstituted
	Platelet-restricted	Platelets reconstituted. Erythrocytes, myeloid cells and lymphoid cells (both T and B) not reconstituted
Other		Reconstitution patterns outside the defined categories

Donor-derived reconstitution of peripheral blood lineages (platelets, erythrocytes, myeloid cells, B cells, T cells) was analysed at 8-10, 12-14 and 16-18 weeks post-transplantation, and for some mice at 1-2 additional time points up to 35 weeks post-transplantation. A lineage was considered to be reconstituted when donor-derived contribution was ≥0.01% with ≥10 clustered donor-derived events observed by flow cytometry. The conditions described for each lineage bias were observed at least in the last 2 consecutive time points of analysis. Fold-difference <5x between all lineages in balanced multilineage patterns was observed at least in the last time point of analysis. The non-balanced multilineage category encompasses all cases of long-term multilineage reconstitution with ≥5x difference between some or all lineages. Although it is common for platelet/erythroid-restricted and platelet/erythroid/myeloid-restricted patterns to appear platelet-restricted at some time points, a pattern was only considered to be truly restricted when the absent lineages were absent at every time point of analysis.

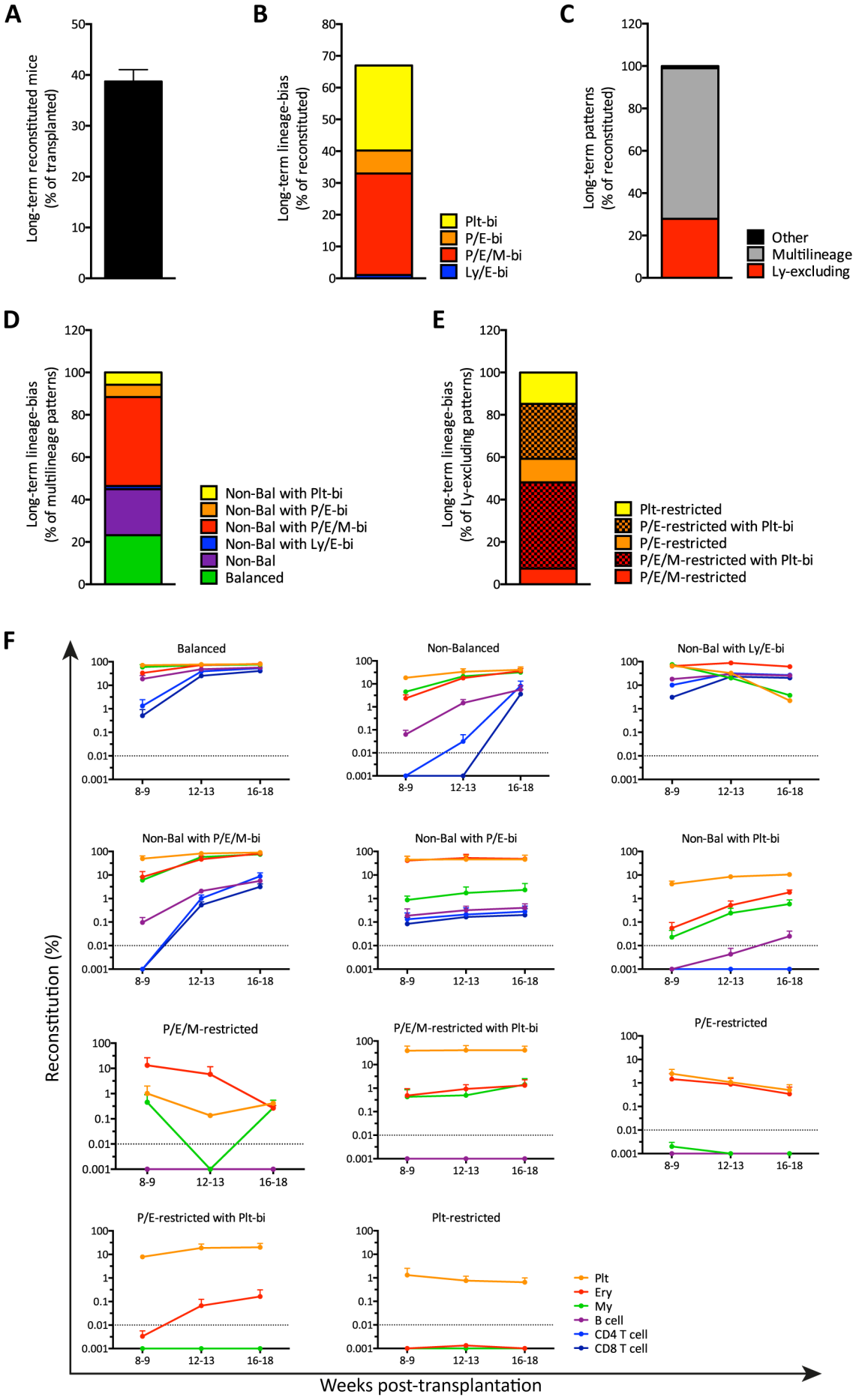
A
Long-term reconstituted mice (% of transplanted)
B
Long-term lineage-bias (% of reconstituted)
Plt-bi
P/E-bi
P/E/M-bi
Ly/E-bi
C
Long-term patterns (% of reconstituted)
Other
Multilineage
Ly-excluding
D
Long-term lineage-bias (% of multilineage patterns)
Non-Bal with Plt-bi
Non-Bal with P/E-bi
Non-Bal with P/E/M-bi
Non-Bal with Ly/E-bi
Non-Bal
Balanced
E
Long-term lineage-bias (% of Ly-excluding patterns)
Plt-restricted
P/E-restricted with Plt-bi
P/E-restricted
P/E/M-restricted with Plt-bi
P/E/M-restricted
F
Balanced
Non-Balanced
Non-Bal with Ly/E-bi
Non-Bal with P/E/M-bi
Non-Bal with P/E-bi
Non-Bal with Plt-bi
P/E/M-restricted
P/E/M-restricted with Plt-bi
P/E-restricted
P/E-restricted with Plt-bi
Plt-restricted
Reconstitution (%)
Weeks post-transplantation
8-9
12-13
16-18
Plt
Ery
My
B cell
CD4 T cell
CD8 T cell

Figure 5.3. Restriction of lineage outputs in mice reconstituted by single *Vwf*^{high} long-term haematopoietic stem cells follows a systematic and predictable order.

Single cell transplantation of adult BM *Vwf*^{high} LT-HSCs enriches for strongly platelet-dominated blood reconstitution patterns, and for reconstitution patterns with a complete lack of lymphoid reconstitution. The criteria for long-term reconstitution and for the biases and patterns quantified in this figure are detailed in Table 5.1.

(A) Long-term reconstituted mice transplanted with a single *Vwf*^{high} LT-HSC. Mean % + SEM of 10 independent experiments, n=248 transplanted mice.

(B) Long-term lineage-biased reconstitutions observed. Reconstituted mice, n=97.

(C) Broad categorisation of the reconstitution patterns observed, with emphasis on the presence or absence of lymphoid reconstitution. Reconstituted mice, n=97.

(D) Relative frequency of lineage-biases observed within multilineage reconstitution patterns (n=69) and **(E)** within lymphoid-excluding reconstitution patterns (n=27).

(F) Reconstitution kinetics of representative recipient mice. Mean % + SEM presented on logarithmic scale. For each plot n=3, with two exceptions: only two cases of platelet/erythroid/myeloid-restricted reconstitution and only one case of non-balanced multilineage reconstitution with lymphoid/erythroid-bias were observed and are presented in the respective plots.

5.2.3. Platelet-biased peripheral blood reconstitution patterns reflect equally biased haematopoietic hierarchies

Next we evaluated donor contribution to different compartments of the haematopoietic hierarchy, in order to gain insight into the differentiation pathway through which individual platelet-biased LT-HSCs generate platelet-dominant reconstitution patterns.

Firstly, to confirm the levels of lymphoid reconstitution in blood, we analysed donor contribution to mature B and T cells in the spleen (Figure 5.4A). Unlike myeloid cells, lymphoid cells are very long-lived. Donor-derived contribution to lymphoid cells could conceivably be found in blood and spleen for an extended period of time even when donor-derived lymphopoiesis is no longer active. To investigate this, we analysed the reconstitution of B cell progenitors in BM (Figure 5.4B) and T cell progenitors in thymus (Figure 5.4C).

We also analysed reconstitution levels of myeloid, megakaryocyte and erythroid progenitors in BM (Figure 5.4D) (Pronk et al., 2007). And, finally, we investigated the ability of donor-derived LT-HSCs to repopulate the LSK compartment, namely HSCs (LSK CD150+ CD48-), early multipotent progenitors (eMPP, LSK CD150+ CD48+), and Flt3+ MPPs (LSK Flt3+) (Figure 5.4E) (Wilson et al., 2008; Oguro et al., 2013; Pietras et al., 2015). Importantly, due to the variability of population sizes in different reconstituted mice, it was not possible to adequately and consistently gate on the 25% highest level of Flt3 within BM LSK, which corresponds to lymphoid-primed multipotent progenitors (LMPP, LSK Flt3^{high}) (Adolfsson et al., 2005). Therefore, the total LSK Flt3+ compartment, containing LMPPs, was analysed.

The results of flow cytometric analysis of the donor-derived haematopoietic hierarchy are summarised in Table 5.2. Reconstitution levels of each population were normalised to the reconstitution of platelets in each recipient. For instance, a normalised reconstitution level of 2x indicates that donor-contribution to that population was 2-fold higher than the contribution to platelets.

In patterns with mild platelet-bias (platelet reconstitution 5-25x above the second most reconstituted lineage), the normalised reconstitution levels of BM pre-granulocyte/macrophage progenitors (Pre-GM), granulocyte/macrophage progenitors (GMP), pre-megakaryocyte/erythroid progenitors (Pre-MegE), and pre-colony forming unit-erythroid progenitors (Pre-CFU-E) are all low compared to platelet reconstitution (0.14-0.35x). However, donor contribution to these progenitors is 2.5-3x higher than contribution to blood erythrocytes and myeloid cells, which suggests that there is a myeloid/erythroid differentiation block and/or the contribution of these progenitors is skewed to megakaryocyte lineage rather than myeloid and erythroid lineages.

Furthermore, in patterns with mild platelet-bias reconstitution of megakaryocyte progenitors (MkP) is 1.8x higher then their upstream Pre-MegE progenitors, but only 0.35x compared to platelets. This suggests that Pre-MegE progenitors might not be the only contributors to MkP production, and that MkPs might also not be the only contributors to platelet production. The phenotypically defined Pre-MegE and common myeloid progenitors (CMP, progenitor of both Pre-GM and Pre-MegE) are known to be heterogeneous at the single cell level (Akashi et al., 2000b; Pronk et al., 2007; Rieger et al., 2009b; Mansson et al., 2010), and platelet-biased HSCs might preferentially generate Mk-biased or Mk-restricted subsets within these progenitor compartments. Alternatively, or simultaneously, in platelet-biased hierarchies the differentiation rate between donor-derived Pre-MegE, MkP and platelets may be too fast to be accurately represented by the single time point captured by flow cytometry.

In patterns with strong platelet-bias (platelet reconstitution >1000x above the second most reconstituted lineage) the above findings are even more prominent. In these cases reconstitution of all progenitor compartments is almost completely absent, except for HSC,

eMPP, and MkP. This indicates that increased restriction in mature lineage outputs is driven by decreased diversity of progenitors generated by HSCs.

When platelet-bias is stronger MkPs are much more highly reconstituted than their upstream Pre-MegE progenitors (9.5x), and much more lowly reconstituted than platelets (0.18x). The greater discrepancy between reconstitution levels of Pre-MegE, MkPs, and platelets in these patterns with stronger platelet-bias further supports the conclusion that platelet production by platelet-biased HSCs does not depend solely on the canonical Mk differentiation pathway that includes the Pre-MegE and MkP progenitor compartments.

Interestingly, in platelet/erythroid/myeloid-biased patterns the reconstitution level of BM Flt3+ MPPs correlates well with the reconstitution level of platelet, myeloid, and erythroid cells and respective BM progenitors, despite low reconstitution of mature lymphoid cells in blood and committed lymphoid progenitors in spleen, thymus, and BM. In mice with platelet-biased reconstitution, in which erythroid and myeloid reconstitution is low, the reconstitution of LSK Flt3+ MPPs is decreased, and it decreases further with increased platelet-bias. It appears that if any donor-derived LSK Flt3+ MPPs are generated by platelet/erythroid/myeloid-biased and platelet-biased HSCs, they are skewed towards myeloid production and/or blocked from lymphoid differentiation.

The most striking observation regarding donor-derived platelet-biased haematopoietic hierarchies (mild and strong platelet-bias) is that HSCs and eMPPs are the only compartments reconstituted at levels similar or higher than platelets. HSC reconstitution is the highest in these hierarchies (1.4-3.5x compared to platelets), indicating that platelet-biased HSCs self-renew very efficiently. eMPPs have the second highest reconstitution level: 0.5-1.4x compared to platelets, and 3-5x higher than MkP reconstitution. These findings are

consistent with a model of megakaryopoiesis in which platelet-biased HSCs differentiate through a non-canonical pathway that involves a subset of eMPPs but not Pre-MegEs or MkPs. It is also possible that platelet-biased HSCs, or a subset of these cells, are able to differentiate straight into megakaryocytes/platelets without intermediate progenitor steps, but our data do not provide direct evidence of this.

Overall our flow cytometry data suggest that platelet-biased reconstitution patterns are not created at the terminal stages of haematopoietic differentiation, but are instead a result of a strongly biased progenitor hierarchy established by highly self-renewing platelet-biased HSCs. The data also suggest that when a few BM progenitors of the erythroid, myeloid, and lymphoid lineages are generated by platelet-biased HSCs, their normal lineage outputs may be blocked and their lineage potential skewed towards platelet production. To clarify the function of these lowly reconstituted progenitors (Flt3+ MPP, Pre-GM, GMP, Pre-MegE) it will be necessary to isolate them from mice reconstituted with balanced and platelet-biased patterns to quantify the skewing of their lineage potentials *in vitro*, and to investigate their gene expression profile for the presence of specific lineage priming. To investigate the role of the few MkPs generated by platelet-biased HSCs we will also compare them to MkPs derived from balanced HSCs, in regards to their Mk potency and speed of Mk production *in vitro*.

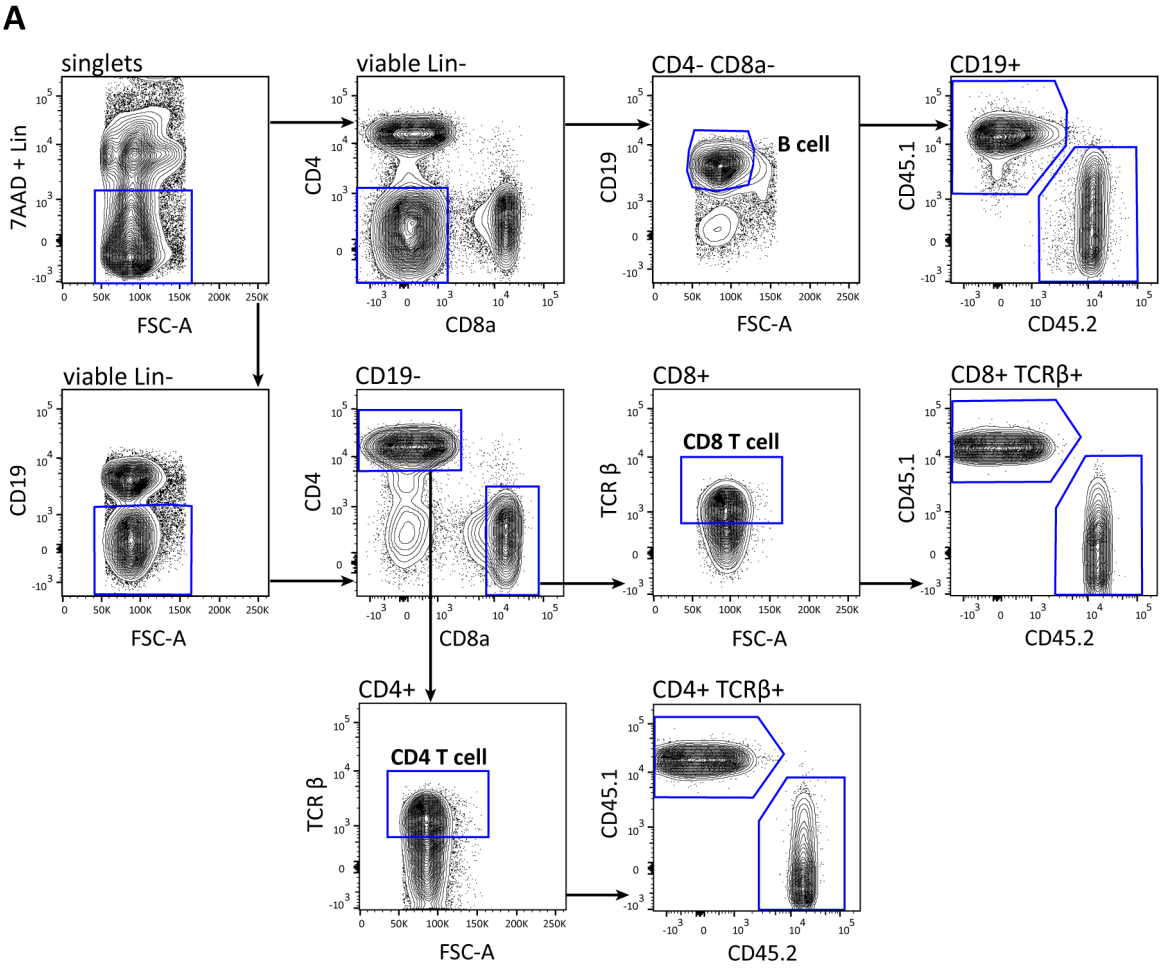
A
singlets
7AAD + Lin
FSC-A
viable Lin-
CD4
CD8a
CD4- CD8a-
B cell
CD19
FSC-A
CD19+
CD45.1
CD45.2
viable Lin-
CD19
FSC-A
CD19-
CD4
CD8a
CD8+
CD8 T cell
TCR β
FSC-A
CD8+ TCRβ+
CD45.1
CD45.2
CD4+
CD4 T cell
TCR β
FSC-A
CD4+ TCRβ+
CD45.1
CD45.2

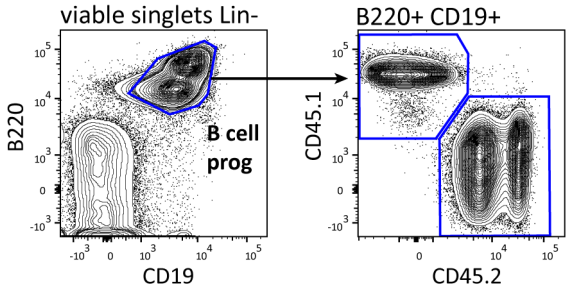
B
viable singlets Lin-
B220
B cell
prog
CD19
B220+ CD19+
CD45.1
CD45.2

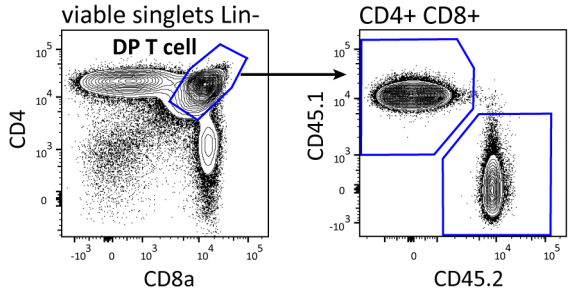
C
viable singlets Lin-
DP T cell
CD4
CD8a
CD4+ CD8+
CD45.1
CD45.2

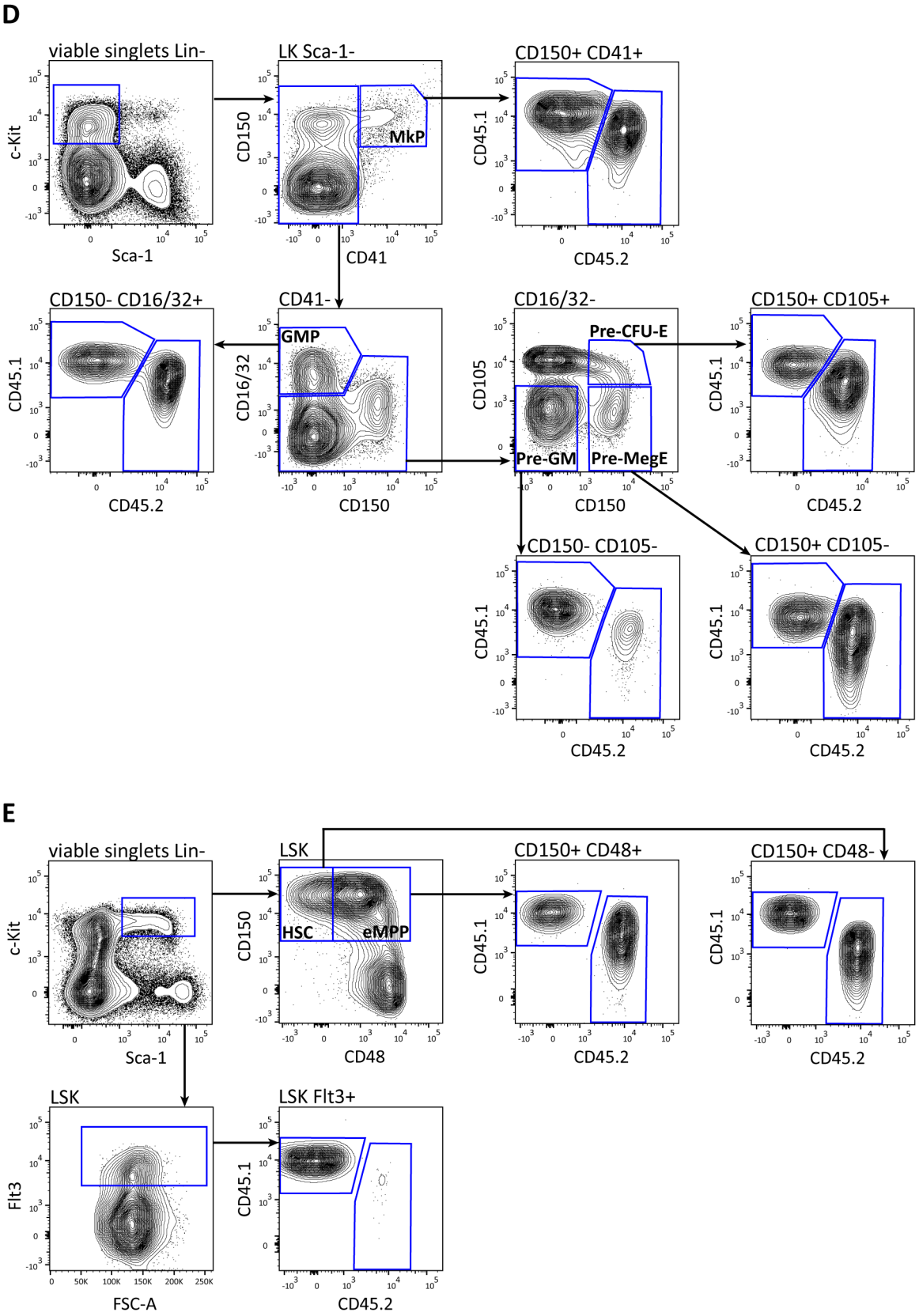
D
viable singlets Lin-
c-Kit
Sca-1
LK Sca-1-
CD150
MkP
CD41
CD150+ CD41+
CD45.1
CD45.2
CD150- CD16/32+
CD45.1
CD45.2
CD41-
GMP
CD16/32
CD150
CD16/32-
Pre-CFU-E
CD105
Pre-GM
Pre-MegE
CD150
CD150+ CD105+
CD45.1
CD45.2
CD150- CD105-
CD45.1
CD45.2
CD150+ CD105-
CD45.1
CD45.2
E
viable singlets Lin-
c-Kit
Sca-1
LSK
CD150
HSC
eMPP
CD48
CD150+ CD48+
CD45.1
CD45.2
CD150+ CD48-
CD45.1
CD45.2
LSK
Flt3
FSC-A
LSK Flt3+
CD45.1
CD45.2

Figure 5.4. Flow cytometric analysis of the donor-derived haematopoietic hierarchy in recipients of single *Vwf*^{high} long-term haematopoietic stem cells.

Reconstitution analysis of haematopoietic compartments in spleen, thymus, and BM were performed for selected recipients at 16-35 weeks post-transplantation. See also Table 5.2.

(A) Gating strategy for flow cytometric analysis of donor-derived CD45.2+ B cells (Lin- CD4- CD8a- CD19+), CD4+ T cells (Lin- CD19- CD8a- CD4+ TCRβ+), and CD8+ T cells (Lin- CD19- CD4- CD8a+ TCRβ+) in the spleen of transplantation recipients.

(B) Gating strategy for flow cytometric analysis of donor-derived CD45.2+ B cell progenitors in the BM of transplantation recipients (Lin- B220+ CD19+).

(C) Gating strategy for flow cytometric analysis of donor-derived CD45.2+ double positive (DP) T cells (Lin- CD4+ CD8a+) in the thymus of transplantation recipients.

(D) Gating strategy for flow cytometric analysis of donor-derived CD45.2+ myeloid, erythroid and megakaryocytic progenitors in the BM of transplantation recipients. MkP, LK Sca-1- CD150+ CD41+. GMP, Lin- c-Kit+ Sca-1- CD41- CD150- CD16/32+. Pre-GM, LK Sca-1- CD41- CD16/32- CD150- CD105-. Pre-MegE, LK Sca-1- CD41- CD16/32- CD150+ CD105-. Pre-CFU-E, LK Sca-1- CD41- CD16/32- CD150+ CD105+.

(E) Gating strategy for flow cytometric analysis of donor-derived CD45.2+ stem and progenitor cells in the BM LSK compartment of transplantation recipients. HSC, LSK CD150+ CD48-. eMPP, LSK CD150+ CD48+. Flt3+ MPP (including LMPP), LSK Flt3+.

Table 5.2. Reconstitution of haematopoietic cell compartments in blood, spleen, thymus and bone marrow of recipients of single *Vwf*^{high} long-term haematopoietic stem cells.

Tissue	Population	Balanced	P/E/M-bias	Mild Plt-bias	Strong Plt-bias
Blood	**Platelets**	**1x**	**1x**	**1x**	**1x**
	Erythrocytes	1.21 ± 0.17	1.27 ± 0.30	0.05 ± 0.01	<0.01
	Myeloid cells	1.12 ± 0.17	0.96 ± 0.36	0.06 ± 0.02	<0.01
	B cells	0.93 ± 0.22	0.08 ± 0.03	<0.01	<0.01
	CD4 T cells	0.83 ± 0.22	0.08 ± 0.05	<0.01	<0.01
	CD8 T cells	0.64 ± 0.19	0.03 ± 0.02	<0.01	<0.01
Spleen	**B cells**	0.83 ± 0.22	0.05 ± 0.02	<0.01	<0.01
	CD4 T cells	0.81 ± 0.22	0.06 ± 0.04	<0.01	<0.01
	CD8 T cells	0.79 ± 0.22	0.05 ± 0.03	<0.01	<0.01
Thymus	**DP T cells**	1.07 ± 0.27	0.33 ± 0.24	<0.01	<0.01
Bone marrow	**B cell prog**	0.89 ± 0.25	0.12 ± 0.05	<0.01	<0.01
	Pre-GM	1.03 ± 0.27	1.19 ± 0.43	0.20 ± 0.07	<0.01
	GMP	1.14 ± 0.17	1.27 ± 0.46	0.14 ± 0.06	<0.01
	Pre-MegE	1.18 ± 0.16	1.30 ± 0.33	0.19 ± 0.06	0.02 ± 0.01
	Pre-CFU-E	1.21 ± 0.17	1.40 ± 0.38	0.19 ± 0.06	0.01 ± 0.00
	MkP	1.01 ± 0.12	0.95 ± 0.13	0.35 ± 0.04	0.18 ± 0.10
	HSC	0.43 ± 0.23	0.65 ± 0.19	2.36 ± 0.61	2.45 ± 1.08
	eMPP	0.62 ± 0.17	0.89 ± 0.12	1.10 ± 0.31	0.83 ± 0.28
	Flt3+ MPP	1.15 ± 0.14	0.79 ± 0.18	0.13 ± 0.04	<0.01

Terminal reconstitution in haematopoietic compartments of recipient mice at 16-35 weeks post-transplantation. Mean fold-difference ± SEM. Fold-difference is defined as the reconstitution level of a population relatively to the reconstitution level of platelets in the same mouse, with platelet level always normalizing to 1x. The non-normalised level of platelet reconstitution in these mice was 3% to 99.6%. Balanced patterns, n=5. Platelet/erythroid/myeloid-biased patterns, n=5. Mild platelet-biased patterns (platelet reconstitution 5-25x above the second most reconstituted lineage), n=5. Strong platelet-biased patterns (platelet reconstitution >1000x above the second most reconstituted lineage), n=3.

5.2.4. *Vwf*+ haematopoietic stem cells and early multipotent progenitors are expanded in the LSK compartment of platelet-biased hierarchies

In agreement with previous studies (Sanjuan-Pla et al., 2013), we have confirmed that single cell transplantation of single *Vwf*^{high} HSCs strongly enriches for platelet-biased long-term peripheral blood reconstitution. We have also shown that platelet-biased peripheral blood reconstitution patterns result from platelet-biased donor-derived haematopoietic hierarchies, with relative progenitor reconstitution levels being highest within the LSK compartment. In order to gain insight into the first steps of establishment of platelet-biased hierarchies, we further investigated the composition of the donor-derived LSK compartment.

We analysed *Vwf* and *Gata1* gene expression within donor-derived HSCs and eMPPs by flow cytometry (Figure 5.5A). In mice with platelet-biased reconstitution there is an increase in the proportion of donor-derived *Vwf*+ HSCs, particularly *Vwf*+ *Gata1*- HSCs, when compared to mice with balanced reconstitution (Figure 5.5B-C). Although it is not statistically significant, there is a tendency for the *Vwf*+ *Gata1*- HSC population to be further expanded when platelet-bias is stronger (Figure 5.5C).

In mice with platelet-biased reconstitution there is also an increase in the proportion of *Vwf*+ eMPPs, particularly *Vwf*+ *Gata1*+ eMPPs, when compared to mice with balanced reconstitution (Figure 5.5D-E). When platelet-bias is stronger there is a statistically significant tendency for *Vwf*+ *Gata1*+ eMPPs to be further increased (Figure 5.5E).

Together these data show that platelet-biased reconstitution patterns established by *Vwf*^{high} LT-HSCs are characterised by preferred production of *Vwf*+ *Gata1*- HSCs and *Vwf*+ *Gata1*+ eMPPs, which suggests that these progenitor populations may be the mediators of platelet-bias.

We then investigated the serial reconstitution ability of a low cell number of donor-derived HSC sub-populations generated by a single *Vwf*^{high} HSC (Table 5.3). The rare *Vwf*+ sub-population of donor-derived HSCs from a mouse with balanced reconstitution mainly propagates balanced multilineage reconstitution, while the much more abundant donor-derived *Vwf*- HSCs propagate only lymphoid-biased reconstitution. This suggests that the majority of *Vwf*+ HSCs derived from a single balanced *Vwf*+ HSC are also balanced, although it must be highlighted that cells from only one donor with balanced reconstitution were tested. Since secondary transplantation was not performed at the single cell level, the multilineage patterns observed could also be a composite of the outputs of different lineage-biased HSCs. Therefore, the next experimental step to clarify these results will be to also perform secondary transplantations of single donor-derived HSCs.

The *Vwf*+ *Gata1*- sub-population of donor-derived HSCs from mice with platelet-biased lymphoid-excluding reconstitution propagates platelet-biased reconstitution in secondary recipients: in a total of 10 mice transplanted with 10 donor-derived *Vwf*+ *Gata1*- HSCs, 8 mice were reconstituted and all developed platelet-biased patterns. In contrast, the potency of *Vwf*+ *Gata1*+ HSCs is very low: in a total of 10 mice transplanted with 10 donor-derived *Vwf+ Gata1+* HSCs, only 2 mice were reconstituted and only 1 developed a platelet-biased reconstitution pattern.

Interestingly, the *Vwf*- sub-fraction of donor-derived HSCs from mice with platelet-biased lymphoid-excluding reconstitution appears to be completely incapable of repopulating secondary recipients: no reconstitution was observed when 8 mice were transplanted with 10 donor-derived *Vwf*- HSCs. This suggests that *Vwf*- HSCs derived from balanced *Vwf*^{high} HSCs – but not from platelet-biased lymphoid-excluding *Vwf*^{high} HSCs – actively contribute to lymphoid reconstitution.

Therefore, in recipient mice with platelet-biased lymphoid-excluding reconstitution, the *Vwf*+ *Gata1*- sub-population appears to be the only donor-derived HSC sub-population with a very high frequency of long-term serial repopulating HSCs, although a limiting dilution analysis using multiple donors will be necessary for an accurate estimate of this frequency (Hu and Smyth, 2009). Overall, our findings indicate that platelet-biased reconstitution is established by *Vwf*+ *Gata1*- HSCs.

Donor-derived lymphoid cells can be detected in secondary recipients of unfractionated BM from a mouse with lymphoid-excluding reconstitution (Table 5.3, mouse "platelet-biased 4"). Reconstitution of lineages that were not previously detected in the primary recipient is rare when re-transplanting a low cell number of donor-derived HSCs, but can also occur. Donor-derived *Vwf*+ *Gata1*- HSCs sorted from a mouse with platelet/erythroid-restricted reconstitution with platelet-bias (Table 5.3, mouse "platelet-biased 3") were able to reconstitute myeloid cells in one of the secondary recipients and T cells in another (data not shown). These findings pertain to only two distinct donors, but they suggest that single *Vwf*^{high} HSCs that give rise to restricted reconstitution patterns in primary recipients are not fully restricted in their lineage potentials, and still retain the ability to produce all other lineages.

A

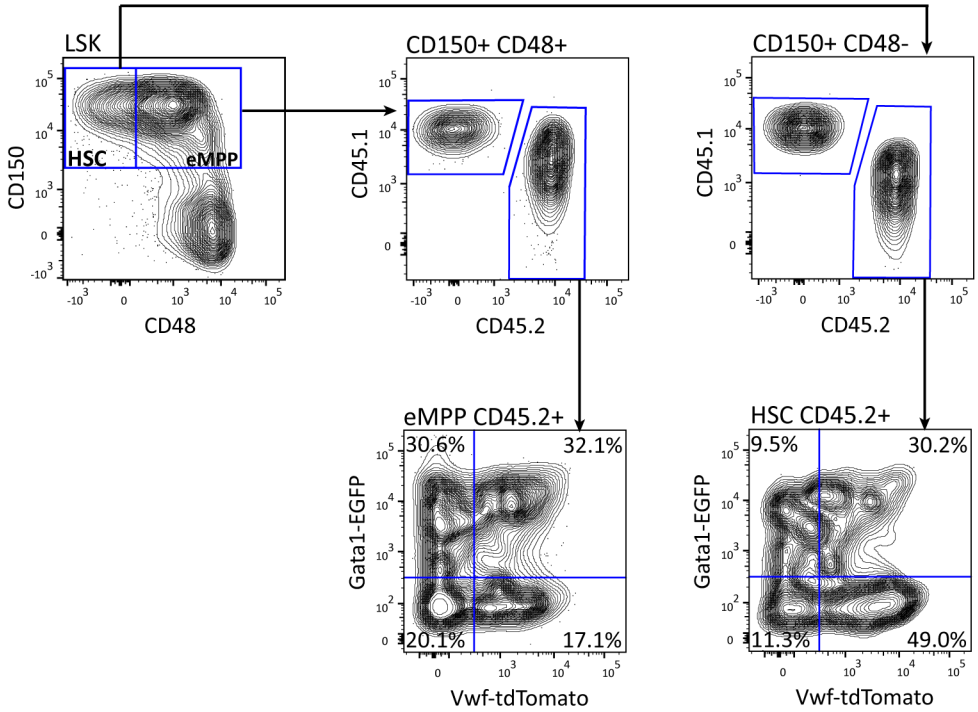
LSK
HSC
eMPP
CD150
CD48
CD150+ CD48+
CD45.1
CD45.2
CD150+ CD48-
CD45.1
CD45.2
eMPP CD45.2+
30.6%
32.1%
20.1%
17.1%
Gata1-EGFP
Vwf-tdTomato
HSC CD45.2+
9.5%
30.2%
11.3%
49.0%
Gata1-EGFP
Vwf-tdTomato

B

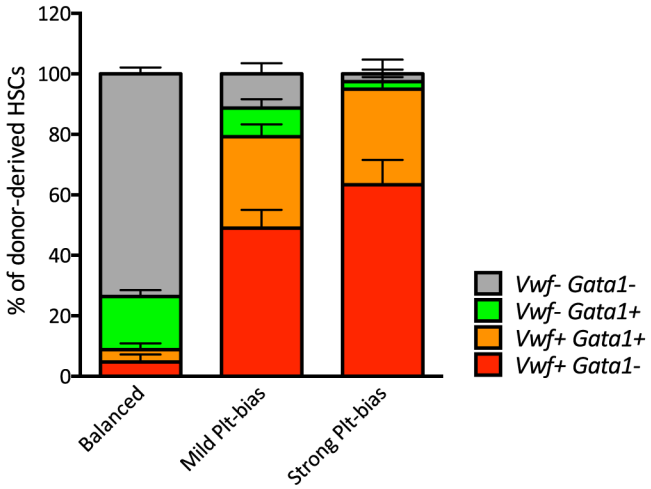
% of donor-derived HSCs
120
100
80
60
40
20
0
Balanced
Mild Plt-bias
Strong Plt-bias
Vwf- Gata1-
Vwf- Gata1+
Vwf+ Gata1+
Vwf+ Gata1-

C

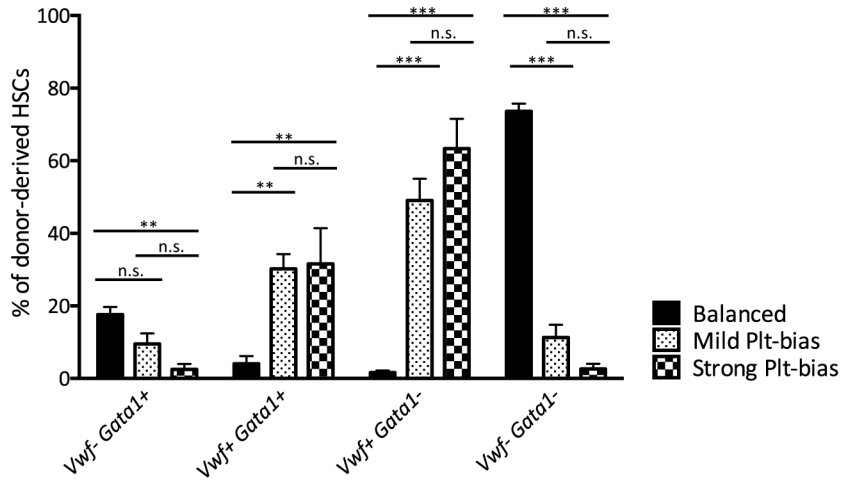
% of donor-derived HSCs
100
80
60
40
20
0
***
n.s.
***
***
n.s.
***
**
n.s.
**
**
n.s.
n.s.
Vwf- Gata1+
Vwf+ Gata1+
Vwf+ Gata1-
Vwf- Gata1-
Balanced
Mild Plt-bias
Strong Plt-bias

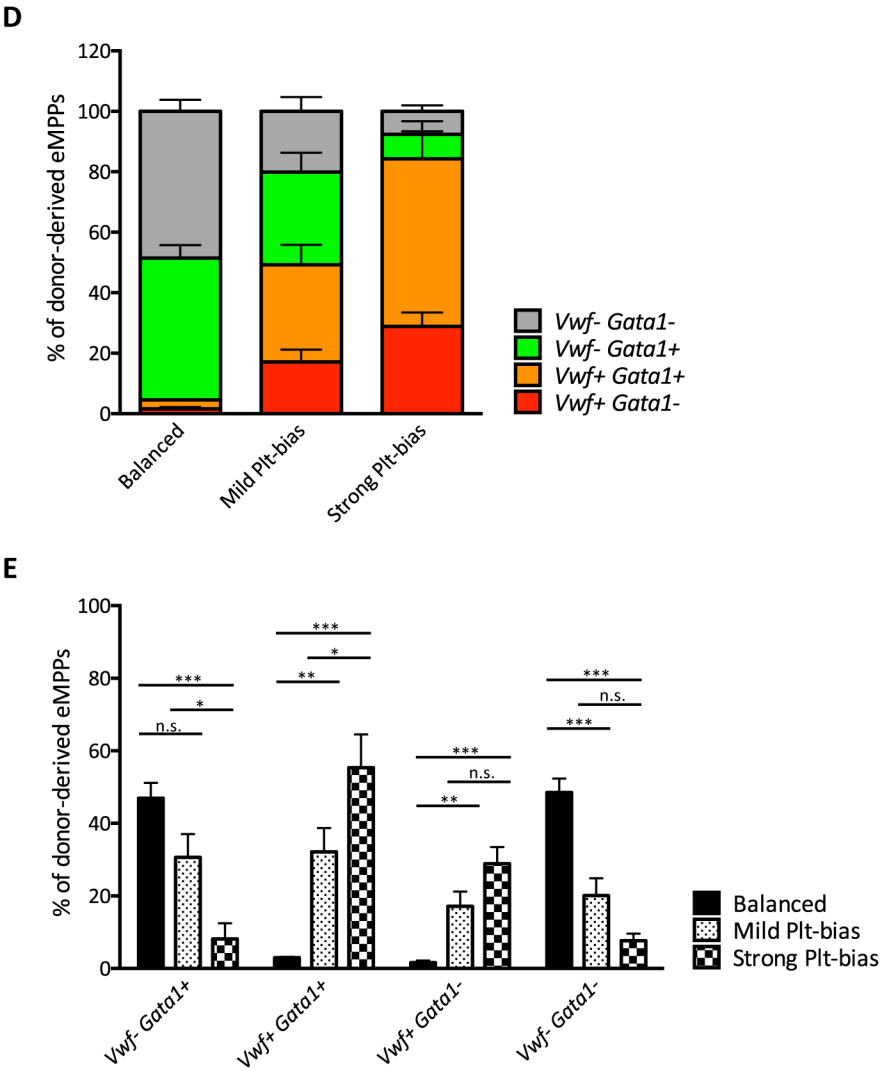

Figure 5.5. *Vwf*+ haematopoietic stem cells and early multipotent progenitors are expanded in the donor-derived Lin- Sca-1+ c-Kit+ compartment of mice with platelet-biased reconstitution patterns.

Vwf-tdTomato and *Gata1*-EGFP signals were analysed within the donor-derived LSK compartment of recipients of single Vwf^{high} LT-HSCs with balanced reconstitution, mild platelet-biased reconstitution (platelet reconstitution 5-25x above the second most reconstituted lineage) and strong platelet-biased reconstitution (platelet reconstitution >1000x above the second most reconstituted lineage).

(A) Gating strategy for flow cytometric analysis of donor-derived CD45.2+ HSCs and eMPPs. Representative plots from mice with mild platelet-biased reconstitution. Mean % of parent gate is shown (n=6).

(B-C) Distribution of *Vwf*-tdTomato and *Gata1*-EGFP signals within the donor-derived HSC compartment (LSK CD150+ CD48- CD45.2+) and **(D-E)** within the donor-derived eMPP compartment (LSK CD150+ CD48+ CD45.2+). Mean % + SEM. Balanced, n=6. Mild platelet-bias, n=6. Strong platelet-bias, n=4. One-way ANOVA for each population across the 3 patterns, followed by Tukey's multiple comparisons test, 95% confidence interval, p-values adjusted for multiplicity. Non-significant (n.s.) $p>0.05$, * $p\leq0.05$, ** $p\leq0.01$, *** $p\leq0.001$.

Table 5.3. Propagation of platelet-biased reconstitution in secondary transplantation.

Donor patterns	Populations transplanted	Cell number	Reconstituted mice	Balanced multilineage	Non-balanced multilineage	Platelet biased	Lymphoid biased
Balanced	HSC *Vwf+*	10 cells	100% (4/4)	75% (3/4)	0% (0/4)	0% (0/4)	25% (1/4)
	HSC *Vwf-*	10 cells	75% (3/4)	0% (0/3)	0% (0/3)	0% (0/3)	100% (3/3)
Platelet-biased 1	HSC *Vwf+*	10 cells	100% (3/4)	0% (0/3)	0% (0/3)	0% (0/3)	0% (0/3)
	HSC *Vwf-*	10 cells	0% (0/4)	-	-	-	-
Platelet-biased 2	HSC *Vwf+ Gata1-*	10 cells	66.67% (4/6)	0% (0/4)	0% (0/4)	100% (4/4)	0% (0/4)
	HSC *Vwf+ Gata1+*	10 cells	0% (0/6)	-	-	-	-
Platelet-biased 3	HSC *Vwf+ Gata1-*	10 cells	100% (4/4)	0% (0/4)	0% (0/4)	100% (4/4)	0% (0/4)
	HSC *Vwf+ Gata1+*	10 cells	50% (2/4)	0% (0/2)	0% (0/2)	50% (1/2)	50% (1/2)
	HSC *Vwf-*	10 cells	0% (0/4)	-	-	-	-
Platelet-biased 4	Unfractionated BM	3.5×10^6 cells	100% (4/4)	25% (1/4)	50% (2/4)	0% (0/4)	25% (1/4)

Secondary transplantation of donor-derived HSC sub-populations and unfractionated BM sorted from five distinct primary recipients of a single *Vwf*^{high} HSC with balanced or platelet-biased lymphoid-excluding reconstitution. Peripheral blood reconstitution analysis was performed at 12-16 weeks post-transplantation. Reconstituted recipients are presented as % of total transplanted mice. Reconstitution patterns are presented as % of reconstituted mice. Absolute numbers of transplanted and reconstituted mice are also indicated in parentheses.

5.2.5. Long-term haematopoietic stem cells lacking lymphoid output *in vivo* show lymphoid potential *in vitro*

Transplantation of single *Vwf*^{high} HSCs not only enriches for platelet-biased reconstitution, it often also results in lineage-restricted long-term peripheral blood reconstitution patterns. These lineage-restricted patterns are mainly lymphoid-excluding, but lymphoid/myeloid-excluding and, more rarely, lymphoid/myeloid/erythroid-excluding are also observed (Figure 5.3).

The appearance, in one case, of detectable myeloid and lymphoid reconstitution upon secondary transplantation of donor-derived *Vwf+ Gata1-* HSCs from a mouse with platelet/erythroid-restricted reconstitution led us to further investigate if the *in vivo* lineage-restricted output behaviours observed in primary recipients are intrinsically and irreversibly determined, or if HSCs with lineage-restricted behaviours *in vivo* can produce the originally missing lineage outputs under appropriate *in vitro* culture conditions.

An exploitable characteristic of single cell transplantations is the fact that all donor-derived cells in a reconstituted mouse originate from a single original HSC for which long-term lineage output behaviour becomes known. Furthermore, we have shown that donor-derived *Vwf*+ HSCs maintain the lineage-bias of their ancestor *Vwf*+ HSC (Table 5.3). We then analysed donor-derived LSK cells as an indirect approach to study the *in vitro* lineage potentials of apparently lineage-restricted HSCs, reasoning that the differentiation ability of HSPCs derived from a single transplanted HSC reflect the lineage potentials of that original single cell.

We sorted donor-derived LSK cells from mice with lymphoid-excluding reconstitution patterns and evaluated their *in vitro* T cell potential in co-culture with the BM-derived OP9-

DL1 stromal cell line (de Pooter and Zúñiga-Pflücker, 2007; Holmes and Zúñiga-Pflücker, 2009). CD4- CD8- CD90.2+ CD25+ T cell precursors (corresponding to thymocyte DN2 stage) were generated *in vitro* by all samples of donor-derived LSK cells sorted from mice with different reconstitution patterns, except in the one platelet-restricted case tested. Less immature CD4+ CD8+ T cell precursors (corresponding to thymocyte DP stage) were frequently, but not always, simultaneously generated in the same co-cultures (Figure 5.6A).

T cell precursors grown *in vitro* were identified by flow cytometry (Figure 5.6B), and their T cell commitment was further confirmed by gene expression analysis (Figure 5.6C). Both CD4+ CD8+ and more immature CD90.2+ CD25+ cultures expressed lymphoid genes (such as *Lat*, *Tcf7*, and *Il2ra*) and T cell-specific cell surface marker genes (such as *Cd3d*, *Cd3e*, *Cd3g*, and *Tcrb*) in patterns comparable to their wild-type counterparts in thymus (Figure 5.6C).

Overall our OP9-DL1 co-culture data demonstrate that the majority of single HSCs lacking detectable *in vivo* T cell output nevertheless possess considerable T cell potential that can be revealed *in vitro*. The results obtained with cells sorted from mice with platelet/erythroid/myeloid-restricted reconstitution suggest that any cells with no T cell potential should be limited to the groups of *in vivo* platelet/erythroid-restricted and platelet-restricted patterns. Additional testing of donor-derived cells sorted from more mice with platelet/erythroid-restricted and platelet-restricted patterns will be required to further strengthen this conclusion, and to provide an estimate of the frequency of LT-HSCs lacking both T cell output *in vivo* and *in vitro*.

A

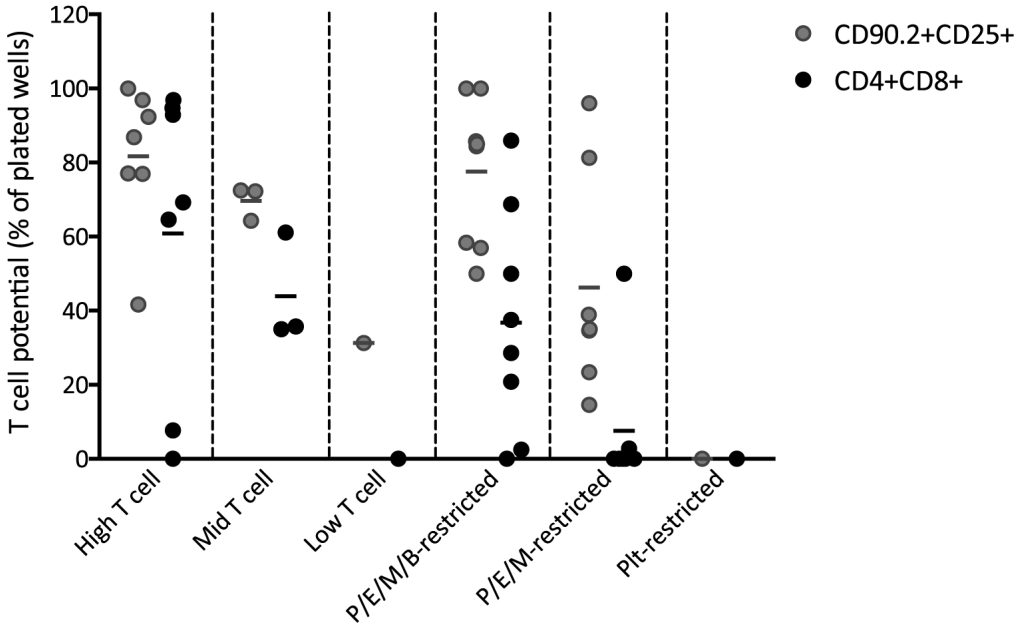
T cell potential (% of plated wells)
120
100
80
60
40
20
0
CD90.2+CD25+
CD4+CD8+
High T cell
Mid T cell
Low T cell
P/E/M/B-restricted
P/E/M-restricted
Plt-restricted

B

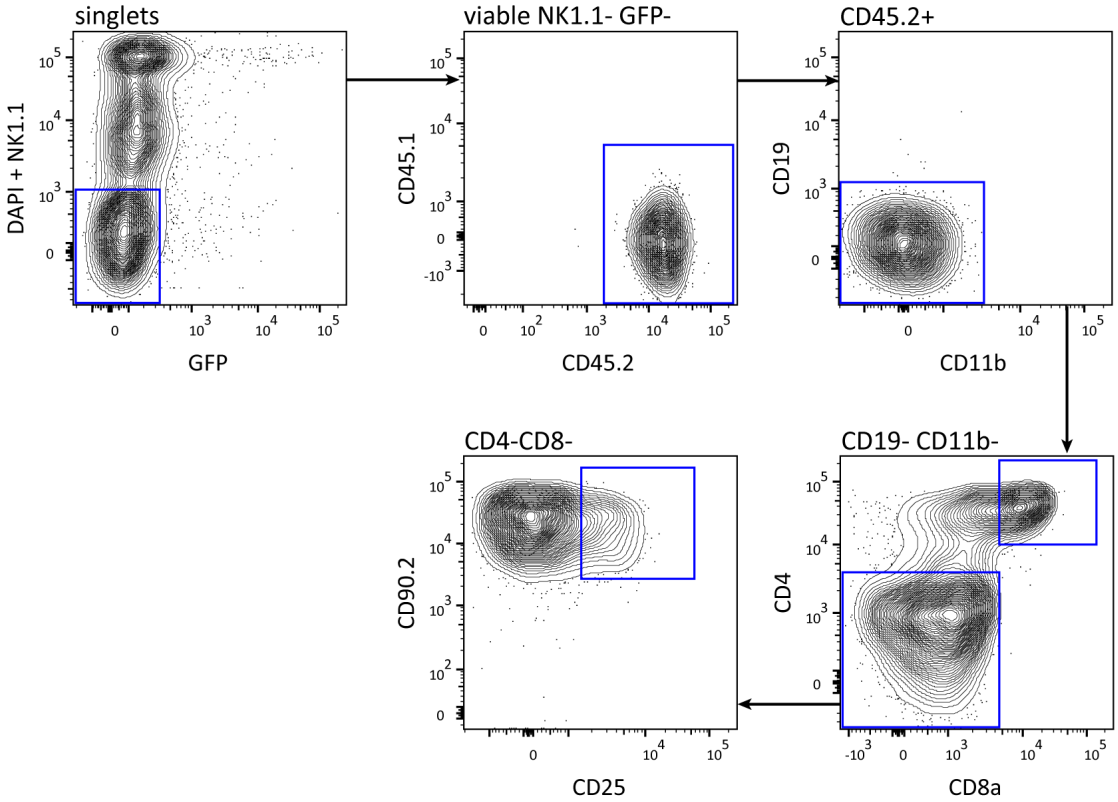
singlets
DAPI + NK1.1
GFP
viable NK1.1- GFP-
CD45.1
CD45.2
CD45.2+
CD19
CD11b
CD4-CD8-
CD90.2
CD25
CD19- CD11b-
CD4
CD8a

C

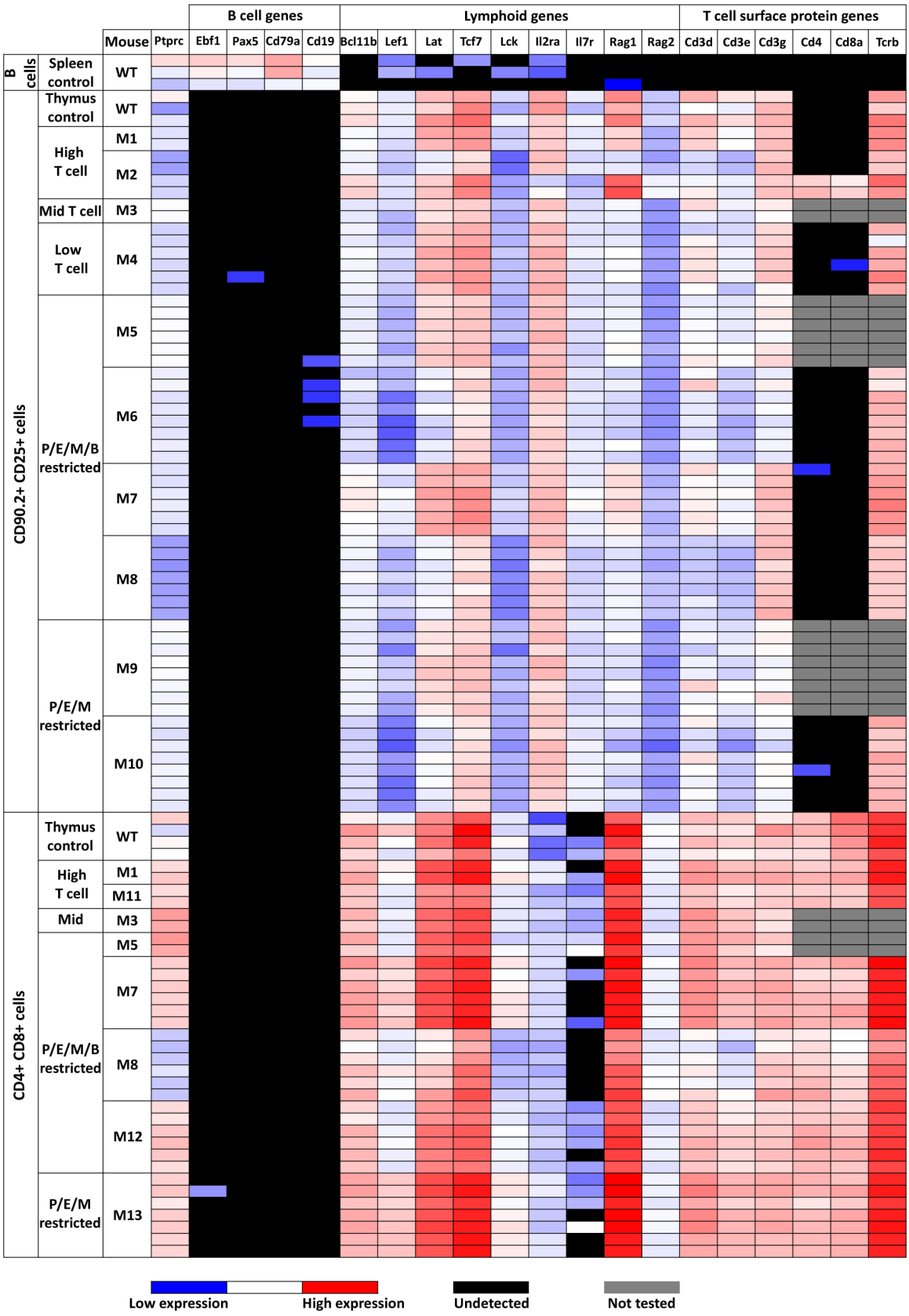
B cell genes
Lymphoid genes
T cell surface protein genes
Mouse
Ptprc
Ebf1
Pax5
Cd79a
Cd19
Bcl11b
Lef1
Lat
Tcf7
Lck
Il2ra
Il7r
Rag1
Rag2
Cd3d
Cd3e
Cd3g
Cd4
Cd8a
Tcrb
B cells
Spleen control
WT
CD90.2+ CD25+ cells
Thymus control
High T cell
Mid T cell
Low T cell
P/E/M/B restricted
P/E/M restricted
M1
M2
M3
M4
M5
M6
M7
M8
M9
M10
CD4+ CD8+ cells
Mid
M11
M12
M13
Low expression
High expression
Undetected
Not tested

Figure 5.6. Haematopoietic stem cells lacking T cell output *in vivo* show T cell potential *in vitro.*

To evaluate the T cell potential of a single transplanted *Vwf*^{high} LT-HSC, donor-derived LSK CD45.2+ cells were sorted from reconstituted mice at 20-35 weeks post-transplantation and co-cultured *in vitro* with OP9-DL1 stromal cells.

(A) T cell lineage potential of 5-20 LSK CD45.2+ cells in OP9-DL1 co-cultures. Identity of the cells in culture was evaluated by flow cytometry after 26-37 days of co-culture. Individual % (dots) and mean % (bar), 7-72 wells plated per mouse. Grey dots represent cultures with CD4- CD8- CD90.2+ CD25+ DN2-like cells, and black dots represent cultures with CD4+ CD8+ DP-like cells. "High T cell" group consists of mice with 20-85% CD4 T cell reconstitution in blood (n=7). "Mid T cell" group consists of mice with 0.4-10% CD4 T cell reconstitution in blood (n=3). "Low T cell" group consists of one mouse with 0.02% CD4 T cell reconstitution in blood (n=1). "P/E/M/B-restricted" (n=8), "P/E/M-restricted" (n=7) and "Plt-restricted" (n=1) groups consist of mice with no T cell reconstitution in blood at all time points of analysis.

(B) Gating strategy for flow cytometric analysis and sorting of donor-derived CD45.2+ T cell precursors generated in culture. OP9-DL1 stromal cells express GFP; hence the exclusion of GFP+ cells in this gating strategy. Only wells with ≥10 CD90.2+ CD25+ and/or CD4+ CD8+ grouped events were considered positive.

(C) Heatmap of gene expression in T cell cultures. Multiplexed qPCR data are presented as ΔCt between each gene and the average of the housekeeping genes *Hprt1* and *B2m.* Only samples with detectable levels of *Hprt*, *B2m* and *Ptprc* (*Cd45*) were analysed. Each row corresponds to one sample (10-50 sorted cells). Cells from 2-8 different culture wells were sorted for each of 13 reconstituted mice (M1 to M13).

5.2.6. Long-term haematopoetic stem cells lacking myeloid output *in vivo* show myeloid potential *in vitro*

Similarly to the previously described *in vitro* T cell culture approach, we also sought to challenge *in vitro* the myeloid potential of donor-derived cells with *in vivo* myeloid-excluding reconstitution behaviours (which are always lymphoid/myeloid-excluding).

We observed that donor-derived LSK cells sorted from mice with different reconstitution patterns generated large myeloid clones *in vitro* (cells covering ≥10% of the culture well), with the exception of the single case of platelet-restricted reconstitution tested (Figure 5.7A). Donor-derived LSK cells sorted from the mouse with platelet-restricted reconstitution produced mainly small clones (cells covering <10% of the culture well) and only 0.8% of large clones (1 clone in 125 plated wells).

Presence of both granulocytes and macrophages in clones generated by donor-derived LSK cells from mice with very low *in vivo* myeloid reconstitution (0.01-0.02%) and from a mouse with platelet/erythroid-restricted reconstitution was confirmed by morphological analysis of stained cytospins (Figure 5.7B-C). The clones generated by cells from a mouse with platelet-restricted reconstitution were mainly comprised of megakaryocytes and immature precursor cells, but although rare, the presence of granulocytes was also confirmed upon more detailed morphological analysis of stained cytospins (Figure 5.7D).

Overall, these data demonstrate that the majority of HSCs lacking detectable myeloid output *in vivo* still possess significant myeloid potential. However, tracking of *in vitro* clone morphology over time (9 to 21 days) indicates that the kinetics of myeloid cell differentiation is considerably slower for HSCs that show little or no myeloid output *in vivo* (data not shown). LSK cells from non-transplanted wild-type mice and donor-derived LSK

cells from transplanted mice with balanced multilineage reconstitution generate large quantities of mature granulocytes before 9-10 days of culture, and macrophages completely dominate the cultures by day 12-13. In comparison, donor-derived LSK cells from mice with low or undetectable myeloid reconstitution show 3 to 5 days delay in both granulocyte and macrophage differentiation.

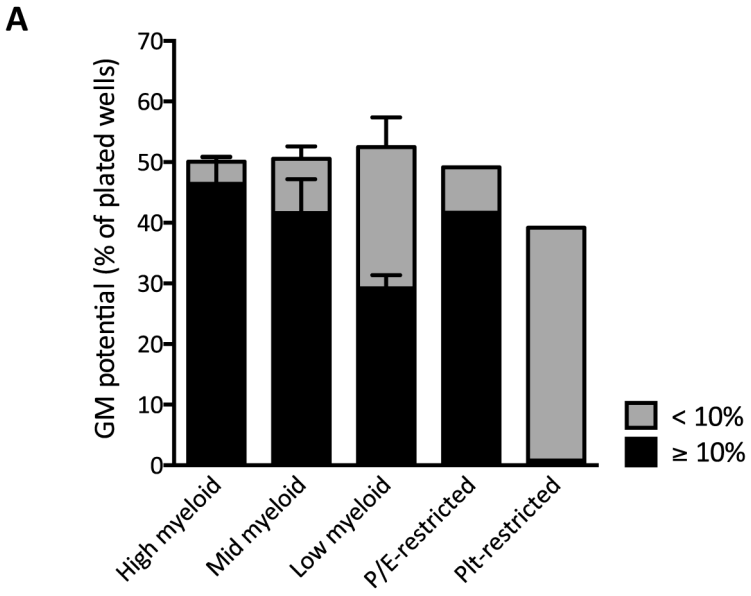
A
GM potential (% of plated wells)
70
60
50
40
30
20
10
0
< 10%
≥ 10%
High myeloid
Mid myeloid
Low myeloid
P/E-restricted
Plt-restricted

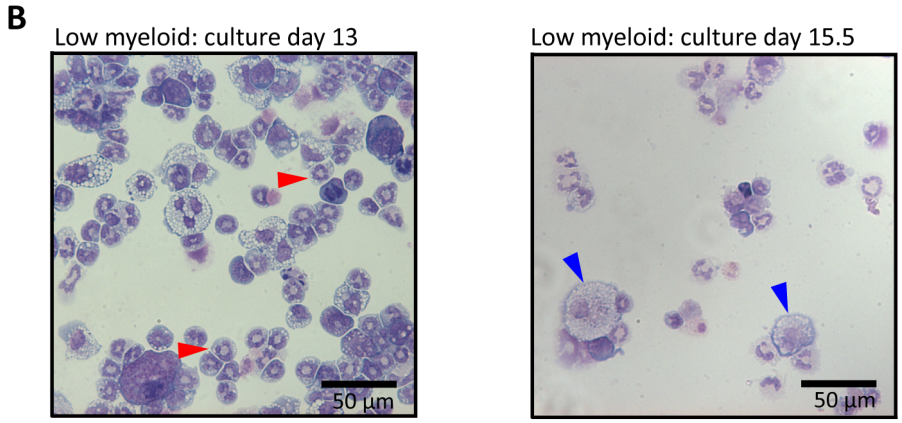
B
Low myeloid: culture day 13
50 µm
Low myeloid: culture day 15.5
50 µm

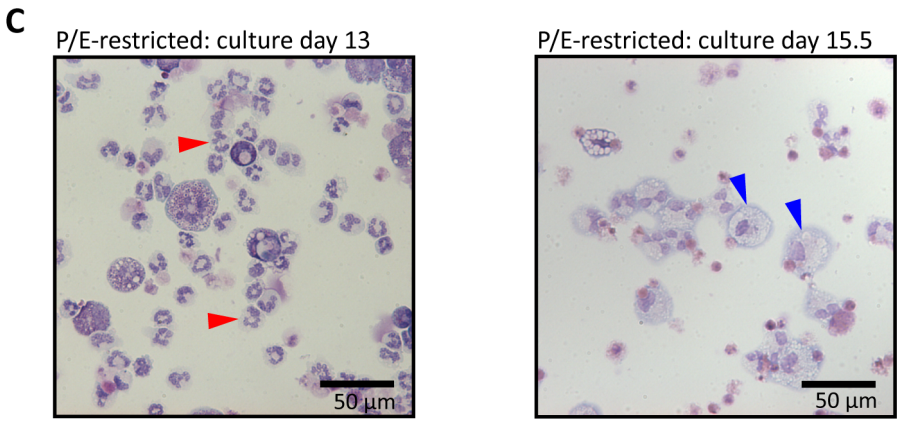
C
P/E-restricted: culture day 13
50 µm
P/E-restricted: culture day 15.5
50 µm

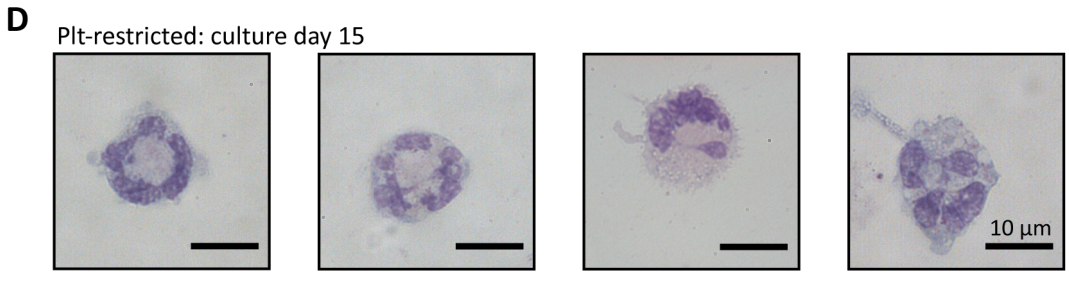
D
Plt-restricted: culture day 15
10 µm

Figure 5.7. Haematopoietic stem cells lacking myeloid output *in vivo* show myeloid potential *in vitro.*

To evaluate the myeloid potential of a single transplanted *Vwf*^{high} LT-HSC, donor-derived LSK CD45.2+ cells were sorted from reconstituted mice at 20-35 weeks post-transplantation and cultured *in vitro*.

(A) Myeloid (GM) lineage potential of single LSK CD45.2+ cells in liquid culture. Clonal growth was quantified after 10-13 days of culture, and cell morphology was also investigated at several time points between day 9 and 21. Mean % + SEM, 120-240 wells plated per mouse. Grey bars represent small clones with cells covering <10% of the culture well, while black bars represent large clones with cells covering ≥10%. "High myeloid" group consists of mice with 60-95% myeloid reconstitution in blood (n=4). "Mid myeloid" group consists of mice with 1-2.5% myeloid reconstitution in blood (n=3). "Low myeloid" group consists of mice with 0.01-0.02% myeloid reconstitution in blood (n=3). "P/E-restricted" (n=1) and "Plt-restricted" (n=1) groups consist of mice with undetectable myeloid reconstitution in blood at all time points of analysis. The platelet-restricted mouse included in this figure is the same individual in Figure 5.5A, from which donor-derived LSK CD45.2+ cells did not generate *in vitro* T cell growth.

(B) Granulocytes (red arrowheads, left panel) and macrophages (blue arrowheads, right panel) generated by donor-derived LSK cells from a mouse in the "Low myeloid" group and **(C)** from a mouse with platelet/erythroid-restricted reconstitution. May-Grünwald/Giemsa staining of cytospins of single large clones at culture day 13 and 15.5. Scale bar is 50μm.

(D) Rare granulocytes produced by donor-derived LSK cells from a mouse with platelet-restricted reconstitution. May-Grünwald/Giemsa staining of cytospins of pooled clones at culture day 15. No macrophages were identified in these cytospins. Scale bar is 10μm.

5.2.7. Gene expression profile of platelet-biased haematopoetic stem cells

Our single cell transplantation approach allows for enrichment of platelet-biased LT-HSCs, but we have only been able to identify these cells retrospectively based on their reconstitution behaviour. We therefore set out to identify viable markers for prospective isolation of platelet-biased LT-HSCs, and to gain insight into the mechanisms of gene regulation involved in the establishment of platelet-biased behaviour.

We sequenced, at the single cell level (Picelli et al., 2014), the global mRNA transcriptome of donor-derived *Gata1*- HSCs sorted from the BM of recipients of single *Vwf*^{high} LT-HSCs with balanced multilineage reconstitution, platelet/erythroid/myeloid-biased reconstitution, and platelet-biased/restricted reconstitution (Figure 5.5A). Similarly to our approach in the *in vitro* lineage potential assays, we analysed the phenotypic HSCs derived from a single transplanted HSC as an indirect method of assessing the properties of the original transplanted cell. We selected the *Gata1*- fraction of HSCs for analysis due to our previous unpublished data showing that *Gata1*+ HSCs are not functional *in vivo*, and showing the exclusive ability of *Vwf*+ *Gata1*- HSCs to robustly propagate platelet-biased reconstitution (Figure 5.5 and Table 5.3).

A three-way comparison of the most differently expressed (DE) genes shows that the gene expression profile of strongly platelet-biased HSCs is distinct from the profile of balanced multilineage and platelet/erythroid/myeloid-biased HSCs (Figure 5.8). Not unexpectedly, expression of several genes is concomitantly up-regulated or down-regulated in both platelet-biased and platelet/erythroid/myeloid-biased HSCs compared to balanced HSCs (including *Mt1*, *Mycn*, *Erdr1*). However, a few genes are specifically up-regulated (*Mmrn1*, *Isl1, Pam*) or down-regulated (*Cd34, Myc, Cd27*) in platelet-biased HSCs compared to both

balanced and platelet/erythroid/myeloid-biased HSCs. Literature regarding specific functions in haematopoietic cells is absent or scarce for some of the genes identified, but speculation can be made based on their proposed functions in other cell types.

N-Myc and c-Myc have been reported to be expressed at similar levels in HSCs (Laurenti et al., 2008), however, in platelet-biased HSCs expression of the N-Myc gene (*Mycn*) is up-regulated while expression of the c-Myc gene (*Myc*) is down-regulated. Moreover, the majority of platelet-biased HSCs do not express *Cd34* (Osawa et al., 1996; Goodell et al., 1997; Matsuoka, 2001), and show high expression of erythroid differentiation regulator 1 (*Erdr1*) and metallothionein (*Mt1*), which have proposed roles in the regulation of apoptosis and cell differentiation (Dormer et al., 2004; Jung et al., 2011; Takahashi, 2012). Overall, the expression profile of several genes suggests that platelet-biased HSCs have a distinctive regulation mechanism of quiescence, self-renewal, differentiation, and survival, which may be shared in part with platelet/erythroid/myeloid-biased HSCs. N-Myc and c-Myc are also known to be regulated post-transcriptionally, a factor to be considered when studying the involvement of expression of these genes in the regulation of HSCs (Wilson et al., 2004; Laurenti et al., 2008; Delgado and Léon, 2010).

Furthermore, specific expression of the Multimerin 1 gene (*Mmrn1)* (Hayward et al., 1998; Jeimy et al., 2008) and the ISL LIM Homeobox 1 gene (*Isl1)* (Moretti et al., 2006) in platelet-biased HSCs proposes possible transcriptional similarities between these cells and vascular endothelial cells, which will be investigated further. Deficiency of peptidylglycine alpha-amidating monooxygenase (*Pam*) (Eipper et al., 1993) has also been implicated in cardiovascular defects during embryonic development (Czyzyk et al., 2005), and is another gene to investigate.

Interestingly, expression of *Cd27*, the gene coding for a cell surface marker recently proposed for identification of LT-HSCs (Vazquez et al., 2015), is down-regulated in platelet-biased HSCs, and is therefore a candidate negative selection marker for further testing in the prospective isolation of these cells. We will sort single HSCs based on expression of candidate cell surface markers and/or fluorescent labelling in mouse lines that report expression of genes found to be specifically expressed in platelet-biased HSCs, and through quantitative PCR analysis we will seek to confirm the gene expression profile obtained by mRNA sequencing. We will then test *in vivo* if HSCs isolated based on the novel validated cell sorting strategy exclusively generate platelet-biased reconstitution patterns upon single cell transplantation.

The expression pattern of the top DE genes between the three HSC sub-types appears to predominantly convey the primitiveness of the platelet-biased HSC sub-type. Insight into key mediators of platelet-bias and suppressors of other lineage potentials in these cells will require a more detailed analysis of additional DE genes. Moreover, we will also analyse the gene expression profile of donor-derived *Vwf+ Gata1+* eMPPs from mice with different reconstitution patterns, since our data indicate that these populations might represent candidate platelet-biased or restricted MPPs directly downstream of platelet-biased HSCs (Figure 5.5D-E). The function of any candidate regulator genes identified will be further studied *in vivo* through genetic experiments of knock-down, knock-out and overexpression in HSCs.

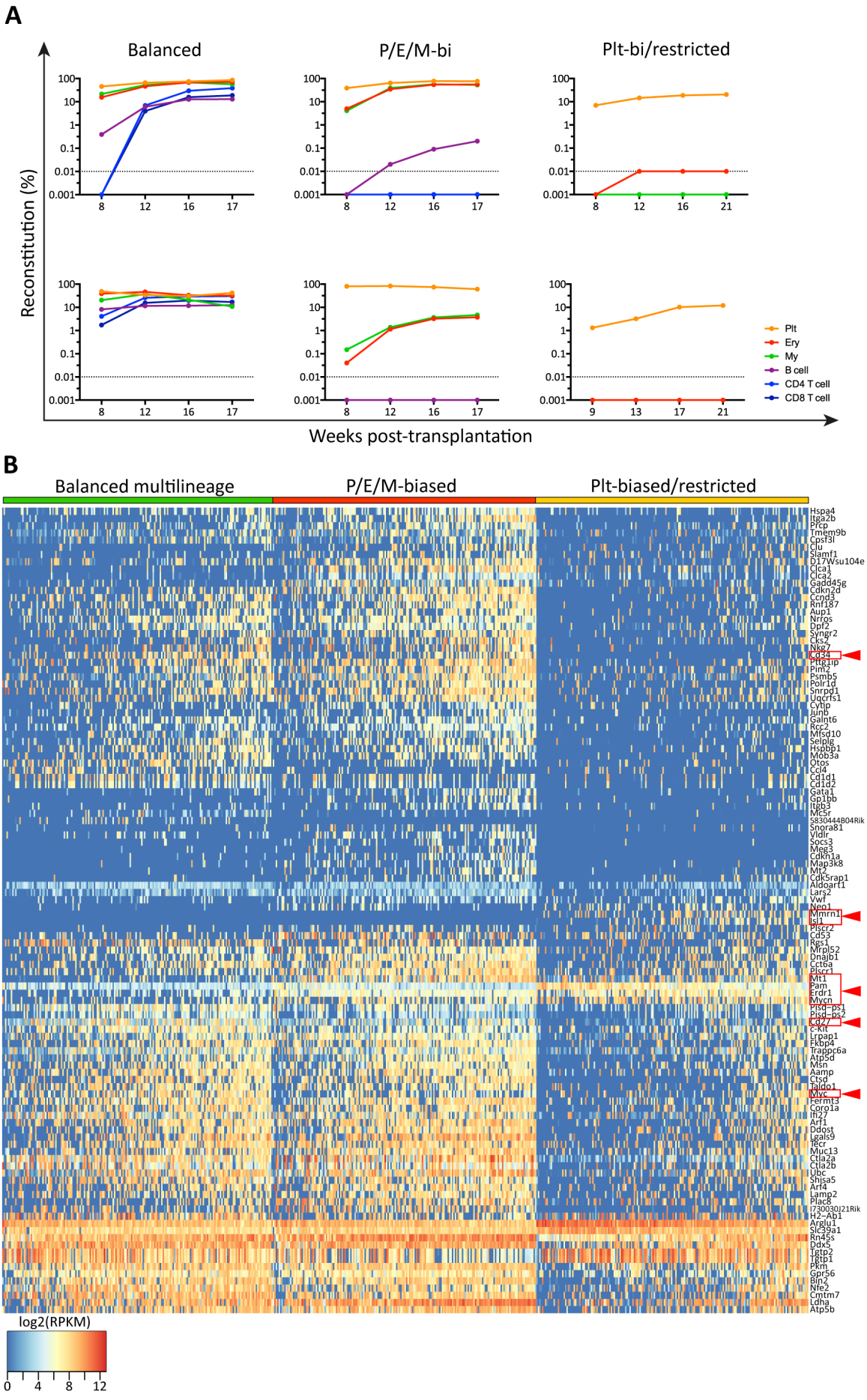
A
Balanced
P/E/M-bi
Plt-bi/restricted
Reconstitution (%)
Weeks post-transplantation
Plt
Ery
My
B cell
CD4 T cell
CD8 T cell
B
Balanced multilineage
P/E/M-biased
Plt-biased/restricted
log2(RPKM)
0
4
8
12

Figure 5.8. Gene expression profile of platelet-biased haematopoetic stem cells by single cell RNA sequencing.

At 17-21 weeks after primary transplantation, donor-derived HSCs (LSK CD150+ CD48- CD45.2+) were sorted from donors with different reconstitution patterns, and subjected to global mRNA transcriptome analysis by single cell RNA sequencing.

(A) Peripheral blood reconstitution kinetics of the cell donors for RNA sequencing. Balanced multilineage reconstitution patterns (left panels), platelet/erythroid/myeloid-biased reconstitution patterns (middle panels), and platelet-biased/restricted reconstitution patterns (right panels).

(B) Heatmap of differentially expressed genes (DE) obtained by single cell sequencing of the global mRNA transcriptome of donor-derived HSCs. Selected genes of interest are highlighted with red arrowheads. List of DE genes was obtained from combined lists of the top 50 DE genes in a three-way comparison between donor-derived *Gata1*- HSCs from recipient mice with balanced (n=188 cells from 2 mice), platelet/erythroid/myeloid-biased (n=185 cells from 2 mice), and platelet-biased reconstitution (n=190 cells from 2 mice). Expression values were quantified as reads per kilobase of transcript per million mapped reads (RPKM). DE genes were selected using a cut-off at absolute log2 fold-change ≥1 and adjusted p-value <0.05 for each comparison.

Data presented in this figure were generated in collaboration with Dr. Adriana Gambardella, and bioinformatics analysis was performed by Dr. Supat Thongjuea.

5.3. Discussion

In this chapter we presented data demonstrating that high *Vwf* expression in individual LT-HSCs enriches not only for platelet-biased reconstitution behaviour *in vivo* – in agreement with previously published data (Sanjuan-Pla et al., 2013) – but also for reconstitution patterns with complete absence of lymphoid output (28% of reconstituted mice). In the subset of lymphoid-excluding reconstitutions, platelet/erythroid/myeloid-restricted and platelet/erythroid-restricted patterns are the most common, but we also identified rare cases of platelet-restricted patterns (4% of reconstituted mice).

We observed that erythroid output is most often accompanied by similar levels of myeloid output and, therefore, platelet/erythroid-biased behaviour is uncommon. In contrast to 32% of platelet/erythroid/myeloid-biased patterns, only 7% of reconstituted mice show platelet/erythroid-biased reconstitution. No cases of platelet/erythroid/myeloid-restricted reconstitution with platelet/erythroid-bias were observed. Moreover, when a reconstitution pattern is platelet/erythroid-restricted, platelet-bias is twice as frequent as absence of platelet-bias (Figure 5.5E). Taken together, these data suggest that the differentiation pathway of platelets generated by *Vwf*^{high} LT-HSCs diverges from erythroid and myeloid differentiation, but the latter two lineages are predominantly linked to each other. The low frequency of megakaryocyte-erythroid repopulating progenitor (MERP) observed by Yamamoto and colleagues, compared to common myeloid repopulating progenitor (CMRP) and megakaryocyte-repopulating progenitor (MkRP), is in agreement with our findings (Yamamoto et al., 2013). Overall, these observations are consistent with a platelet-biased differentiation pathway separate from the common myeloid progenitor (CMP) pathway.

Consistent with the observations described above, we further showed that platelet-biased peripheral blood reconstitution patterns result from the establishment of platelet-biased progenitor hierarchies derived from the original transplanted HSC. In these donor-derived hierarchies, the low reconstitution level of a mature blood lineage is a reflection of the low reconstitution of upstream progenitors (Table 5.2). This finding is also consistent with the results of Yamamoto and colleagues regarding lymphoid, myeloid and megakaryocyte BM progenitors, although their study did not specify or correlate the relative reconstitution levels of mature blood cells and progenitor compartments (Yamamoto et al., 2013).

We also found that, in platelet-biased BM hierarchies, *Vwf+ Gata1-* HSCs comprise the majority of the donor-derived HSC compartment (Figure 5.5B-C). Moreover, in secondary transplantation only this donor-derived HSC fraction is able to consistently propagate platelet-biased reconstitution (Table 5.3). *Vwf+ Gata1+* eMPPs are the most abundant sub-fraction of donor-derived eMPPs in platelet-biased BM hierarchies and, similarly to *Vwf+ Gata1-* HSCs, expansion of these eMPPs correlates with increased platelet-bias (Figure 5.5D-E). Together these observations suggest that platelet-bias is a stable phenotype propagated only by *Vwf+ Gata1-* HSCs and mediated by *Vwf+ Gata1+* eMPPs, which might represent an early commitment step in a fast track megakaryopoiesis differentiation pathway.

However, further *in vitro* and *in vivo* investigation is required to clarify the role of eMPP sub-fractions in the establishment of platelet-biased haematopoietic hierarchies. In differentiation assays *in vitro* we would expect donor-derived *Vwf+ Gata1+* eMPPs to produce mainly or only megakaryocyte colonies, and to generate megakaryocytes much faster and more abundantly than the other eMPP sub-fractions. In secondary transplantation assays *in vivo* we would expect donor-derived *Vwf+ Gata1+* eMPPs, but not other eMPP sub-fractions, to be able to propagate platelet-biased or restricted reconstitution similarly to *Vwf+ Gata1-* HSCs, albeit only transiently, according to the limited

reconstituting potential previously reported for LSK CD150+CD48+ progenitors (Oguro et al., 2013).

Our *in vivo* and *in vitro* observations suggest that *Vwf*^{high} LT-HSCs that behave restrictively *in vivo* are still multipotent, and that the lineage potentials lacking *in vivo* can be incited by appropriate environmental conditions. We find that detection of lineage reconstitution in secondary recipients that was not previously detected in primary recipients is rare, but does occur. Furthermore, by culturing donor-derived LSK cells sorted from reconstituted mice, we can show indirectly that single transplanted LT-HSC lacking myeloid and/or lymphoid output *in vivo* are still able to produce myeloid and lymphoid cells *in vitro*. These results highlight the importance of further *in vitro* and *in vivo* testing – in addition to reconstitution analysis – in the study of lineage restriction.

Considering the absence of *in vitro* lymphoid potential and very low level of myeloid potential observed for LSK cells derived from a *Vwf*^{high} LT-HSC with platelet-restricted behaviour *in vivo* (Figures 5.6 and 5.7), it is possible that some *Vwf*^{high} LT-HSCs might not be multipotent and indeed be very close to true platelet-restriction. Alternatively, the culture conditions used may have not been optimal for this extremely platelet-biased cell type. Additional *in vitro* analysis of donor-derived cells sorted from mice with platelet/erythroid-restricted and platelet-restricted patterns – including testing of different culture conditions for myeloid and lymphoid differentiation – will be required to further clarify these results.

We also investigated the B cell potential of donor-derived LSK cells using standard OP9 co-culture conditions (Nakano et al., 1994; Vieira and Cumano, 2004), which in our hands works well with wild-type LMPPs and HSCs. With this assay we were able to generate B cells from donor-derived LSK cells sorted from some (but not all) mice with balanced multilineage reconstitution. However, we have not yet been able to consistently obtain B cell differentiation from LSK cells sorted from mice with other reconstitution patterns. Our detection of B cell potential *in vitro* has been very low or absent even for donor-derived LSK

cells obtained from mice with detectable B cell reconstitution *in vivo*, and for which we can observe both myeloid and T cell potential *in vitro*. This suggests that the absence of B cell differentiation from reconstituted cells is a technical issue, and indicates the need for further optimisation of OP9 culture conditions for these cells.

It is also important to demonstrate that cryptic lineage potentials can be revealed under appropriate conditions *in vivo*. We will test if it is possible to change an *in vivo* platelet-biased reconstitution pattern established by *Vwf*^{high} LT-HSCs by injecting mice with very platelet-biased reconstitution with cytokines that promote myelopoiesis and lymphopoiesis (for example, GM-CSF and IL-7, respectively). We will also test the ability of platelet-biased donor-derived LSK cells to increase their *in vivo* lymphoid output when re-transplanted into *Rag1* knock-out secondary recipients lacking endogenous mature B and T lymphoid cells (Mombaerts et al., 1992; Thompson, 1992). Inflammation, infection, or leucopenia can also be induced in reconstituted mice to investigate modulation of platelet-biased behaviour.

A recent study by Yamamoto and colleagues (Yamamoto et al., 2013) suggested that within the LSK CD150+ CD34- compartment there is a high percentage of myeloid-restricted progenitors with repopulating activity (MyRPs), including platelet/erythroid/myeloid-restricted progenitors lacking lymphoid potential (CMRP), platelet/erythroid-restricted progenitors lacking myeloid and lymphoid potentials (MERP), and platelet-restricted progenitors lacking erythroid, myeloid and lymphoid potentials (MkRP). In total, they determined that MyRPs account for 55-80% of reconstitution patterns obtained from single cell transplantation of LSK CD150+ CD34- (CD41- or CD41+) cells. In contrast, our data suggest that lymphoid-excluding *Vwf*^{high} LT-HSCs (LSK CD150+ CD48- CD34-) account for only 28% of all reconstitution patterns. Interestingly, Yamamoto and colleagues did not find any LT-HSC activity in the LSK CD34- CD150+ CD41+ compartment, which is unexpected based on our data and other previously published findings (Gekas and Graf, 2013). This result could be

in part due to the use of CD41 antibody clone MWReg30, which has been shown to affect the long-term repopulation ability of HSCs (Gekas and Graf, 2013).

A major difference between our study and the one by Yamamoto and colleagues is the FACS strategy used to isolate single cells for transplantation. While they sorted three sub-fractions within the LSK CD34- compartment (CD150+ CD41-, CD150+ CD41+, and CD150- CD41-), we sorted phenotypic LT-HSCs expressing *Vwf* (LSK CD150+ CD48- CD34- *Vwf*^{high}). *Vwf* and CD41 are co-expressed in phenotypic LT-HSCs (Sanjuan-Pla et al., 2013), and we can estimate that >93% of the *Vwf*^{high} LT-HSCs cells we transplanted were part of the LSK CD150+ CD41+ compartment. Moreover, we transplanted only CD48- cells, while Yamamoto and colleagues did not use CD48 as a marker in their sorting strategy. Based on these two markers we would conclude that Yamamoto and colleagues investigated more types of cells in their transplantations than we did. However, we transplanted cells with a much broader spectrum of Sca-1 cell surface expression than Yamamoto and colleagues, and they might have excluded some of our *Vwf*^{high} LT-HSCs from their analysis due to the strict Lin- c-Kit+ Sca-1^{high} gating strategy applied. Overall it seems that, in addition to CD41- and CD48+ cells that we did not study, Yamamoto and colleagues only transplanted a subset of our *Vwf*^{high} LT-HSCs. Conversely, we only analysed the CD48- fraction of the Lin- c-Kit+ Sca-1^{high} CD150+ CD41+ compartment transplanted by Yamamoto and colleagues, but also analysed Lin- c-Kit+ Sca-1^{mid} CD150+ CD41+ cells that they did not transplant. It is, therefore, not possible to directly compare the data from these two studies.

Considering the low levels of total reconstitution detected, and lack of reconstitution sustainability at the later time points of analysis and in secondary transplantation, it is disputable if the reconstitution patterns that Yamamoto and colleagues attributed to MyRPs can be considered a product of long-term self-renewal. It appears more likely that the majority of the patterns they observed were produced by short-term and intermediate-term

progenitors, which might be compartments downstream of the platelet-biased LT-HSCs that we identified. Moreover, the low levels of total reconstitution obtained detract from the conclusion that a given transplanted cell is lineage-restricted, since it is possible that the missing blood lineages are also reconstituted but at even lower levels, and thus undetectable in flow cytometric analysis of peripheral blood.

Arguably the strongest observations of platelet restriction by Yamamoto and colleagues were obtained in their paired daughter cell (PDC) micro-manipulation experiments, in which single LSK CD150+ CD41- cells were cultured *in vitro* during one cell division and then each daughter cell was transplanted at single cell level. Their results in these experiments suggest that MkRPs can be generated directly by LT-HSCs without passing through an intermediate multipotent progenitor stage. These results are consistent with our own observations that LT-HSCs that behave as platelet-restricted *in vivo* appear to use a fast track for megakaryocyte commitment. However, Yamamoto and colleagues obtained these data from LSK CD150+ CD41- cells, which equate to only a small fraction of the *Vwf*^{high} cells that we focused on.

As described above, our *in vitro* differentiation data show that missing lineage outputs can be revealed under the appropriate *in vitro* conditions for the majority of cells that behave restrictively *in vivo* (Figures 5.6 and 5.7), which demonstrates that these cells are not truly restricted in their lineage potentials. Yamamoto and colleagues did not test the *in vitro* potentials of cells derived from the MyRPs they identified. By replicating their sorting strategy we intend to reproduce the restricted reconstitution patterns they observed, and then test the *in vitro* potentials of donor-derived LSK cells isolated from the mice reconstituted with such patterns. If the cells identified by Yamamoto and colleagues are long-term self-renewing HSCs, as the *Vwf*^{high} cells we studied, we expect them to still be multipotent and express all lineage potentials *in vitro*. If multipotentiality is not revealed *in*

vitro, the cells identified by Yamamoto and colleagues might instead represent short-term stem-like progenitors that act as intermediates in the biased differentiation pathways driven by distinct sub-populations of lineage-biased HSCs. The latter interpretation would be more consistent with the results of our study and with our assessment that the self-renewal potential shown for MyRPs is limited.

Overall our findings regarding platelet-biased hierarchies established by platelet-biased HSCs are in agreement with the recent proposal of a new model of the haematopoietic hierarchy in which generation of blood lineages is regulated at the level of functionally distinct MPP subsets (Pietras et al., 2015). This study suggests that distinct biased MPPs are produced independently from the HSC compartment, and that one MPP subset is not able to generate another. Furthermore, LSK Flt3- CD150+ CD48+ MPPs (MPP2) were platelet/erythroid/myeloid-biased, LSK Flt3- CD150- CD48+ cells (MPP3) were myeloid/erythroid-biased, and LSK Flt3+ CD150- CD48+ cells (MPP4) were lymphoid/myeloid-biased.

Two other recent studies have also proposed a unipotent pathway of megakaryopoiesis derived from platelet-biased HSCs in steady-state or emergency haematopoiesis. One group suggested that a branch of Mk-restricted differentiation that runs parallel to the Pre-MegE pathway is mediated by LSK CD41+ progenitors downstream of platelet-biased HSCs (Nishikii et al., 2015). Within the BM LSK compartment all CD41+ cells are CD150+ Flt3-, but no additional cell surface markers were used to define the population in question, therefore it must include a mixture of CD48- HSCs and CD48+ eMPPs. Another group identified a sub-population of the phenotypic HSC compartment as stem-like megakaryocyte committed progenitors (SL-MkPs, LSK CD150+ CD48- $CD41^{high}$), which constitute an inflammation-responsive unipotent progenitor pool. The phenotypic $CD41^{high}$ population does not exist in steady-state BM, but up-regulation of CD41 is induced in the HSC compartment by inflammation. The transient platelet-restricted repopulation ability of SL-MkPs *in vivo* (Haas

et al., 2015) is consistent with a model in which *Vwf*+ LT-HSCs express platelet-restriction during emergency haematopoiesis through preferential production of downstream SL-MkPs.

Reconciling all of our findings with the recently published data briefly described above, we propose a model in which steady-state platelet-biased LT-HSCs (P-HSC, a not yet purified sub-fraction of the LSK Flt3- CD150+ CD48- CD34- CD41+ *Vwf*+ *Gata1*- population) preferentially generate platelet-biased eMPPs (P-MPP, possibly LSK Flt3- CD150+ CD48+ CD34+ CD41+ *Vwf*+ *Gata1*+), which in turn produce megakaryocytes very efficiently through a fast track differentiation pathway that largely bypasses Pre-MegE progenitors (LK Sca-1- CD41- CD16/32- CD150+ CD105-) and MkP progenitors (LK Sca-1- CD150+ CD41+). The level of platelet-restriction in the proposed P-MPP compartment is unknown, therefore this pathway might or not involve an additional Mk-restricted downstream progenitor compartment (Figure 5.9). This proposal revises the LMPP-CMP model of the haematopoietic hierarchy by adding a distinct branch of megakaryocyte lineage differentiation separate from the CMP branch (see also chapter 1).

We noted that if a reconstitution pattern generated by a single *Vwf*^{high} LT-HSC changes over time (any kind of pattern), detection of lineage reconstitution always occurs in a systematic and predictable order – first platelets, then erythrocytes, myeloid cells, B cells, and lastly T cells. Furthermore, in all but few exceptions, the level of platelet reconstitution remains the highest of all lineages throughout time. This suggests that platelet-biased/restricted MPPs might always be the first sub-type of MPP generated by all *Vwf*^{high} LT-HSCs, even if not platelet-biased. This is in agreement with the recent finding that LSK Flt3- CD150+ CD48+ cells (MPP2) have faster generation kinetics than other biased MPPs (Pietras et al., 2015). Alternatively, a *Vwf*^{high} LT-HSC that is not platelet-biased might generate all MPP sub-types

equally, but the kinetics of platelet output from the platelet-biased/restricted MPPs might be much faster than the output of other lineages from other MPP compartments.

Furthermore, we have found that a few *Vwf*+ HSCs are platelet-restricted *in vivo*, and our data do not exclude the possibility that these cells might be able to differentiate into megakaryocytes directly without cell division, as has been previously suggested by *in vitro* culture data (Roch et al., 2015). Perhaps the expansion of the $CD41^{high}$ sub-fraction of phenotypic HSCs (SL-MkPs, LSK Flt3- CD150+ CD48- CD34- $CD41^{high}$) observed during inflammation (Haas et al., 2015) is associated with such a direct megakaryopoiesis mechanism. During emergency haematopoiesis, platelet-restricted *Vwf*+ HSCs might expand and up-regulate CD41, and then directly differentiate into megakaryocytes. The few platelet-restricted reconstitution patterns that we observed in single cell transplantations could then correspond to pre-expansion inflammation-responsive platelet-restricted HSCs. It does not seem likely that the platelet-restricted reconstitution patterns we described result directly from dormant SL-MkPs in BM, since the repopulation ability of these cells (after induction by inflammation) appears to be very limited (Haas et al., 2015). Platelet-restricted *Vwf*+ HSCs are not necessarily only involved in emergency haematopoiesis, but it is unknown if they normally contribute to steady-state haematopoiesis or are predominantly dormant.

The platelet-biased *in vivo* reconstitution behaviour of LT-HSCs is most probably determined by interplay between intrinsic and extrinsic factors. A possible regulatory mechanism of platelet-bias and platelet-restriction is a positive feedback loop in which LT-HSCs with intrinsic platelet-bias (determined by their Mk-primed transcriptome) are selectively drawn to distinct BM niches (Kiel and Morrison, 2008; Anthony and Link, 2014; Morrison and Scadden, 2014) that produce factors that reinforce the bias. The micro-environmental factors at specific BM sites could instructively reinforce platelet-bias through modulation of

lineage-specific receptor levels, thus boosting the efficiency of response to pro-megakaryopoiesis cues and eliminating the ability of response to other differentiation cues (Shah et al., 2015).

Although platelet-bias is largely maintained in secondary transplantation, we noted that some secondary platelet-biased reconstitution patterns become less restricted than the pattern observed in the primary recipient. A mixed intrinsic/extrinsic mechanism of lineage-bias fits better with these pattern variations in secondary transplantation than a purely intrinsic mechanism. It would be expected for intrinsically platelet-primed HSCs to often, but not always, re-establish themselves in BM niches that reinforce their bias when re-transplanted. Therefore, it would be expected for the re-transplanted cells to often, but not always, continue to behave as restrictively as in the primary recipient. Furthermore, variations in the degree of restriction of lineage outputs may also be influenced by variations in the concentration of extrinsic factors produced by the natural BM niche of platelet-biased HSCs.

Through global transcriptome analysis of the HSC compartment derived from platelet-biased HSCs, and from our candidate platelet-biased eMPP, we hope to identify cell surface receptors, transcription factors, and overall signalling pathways that are distinctly expressed by platelet-biased HSCs, and which may indicate a specific or increased sensitivity of these cells to particular extrinsic factors.

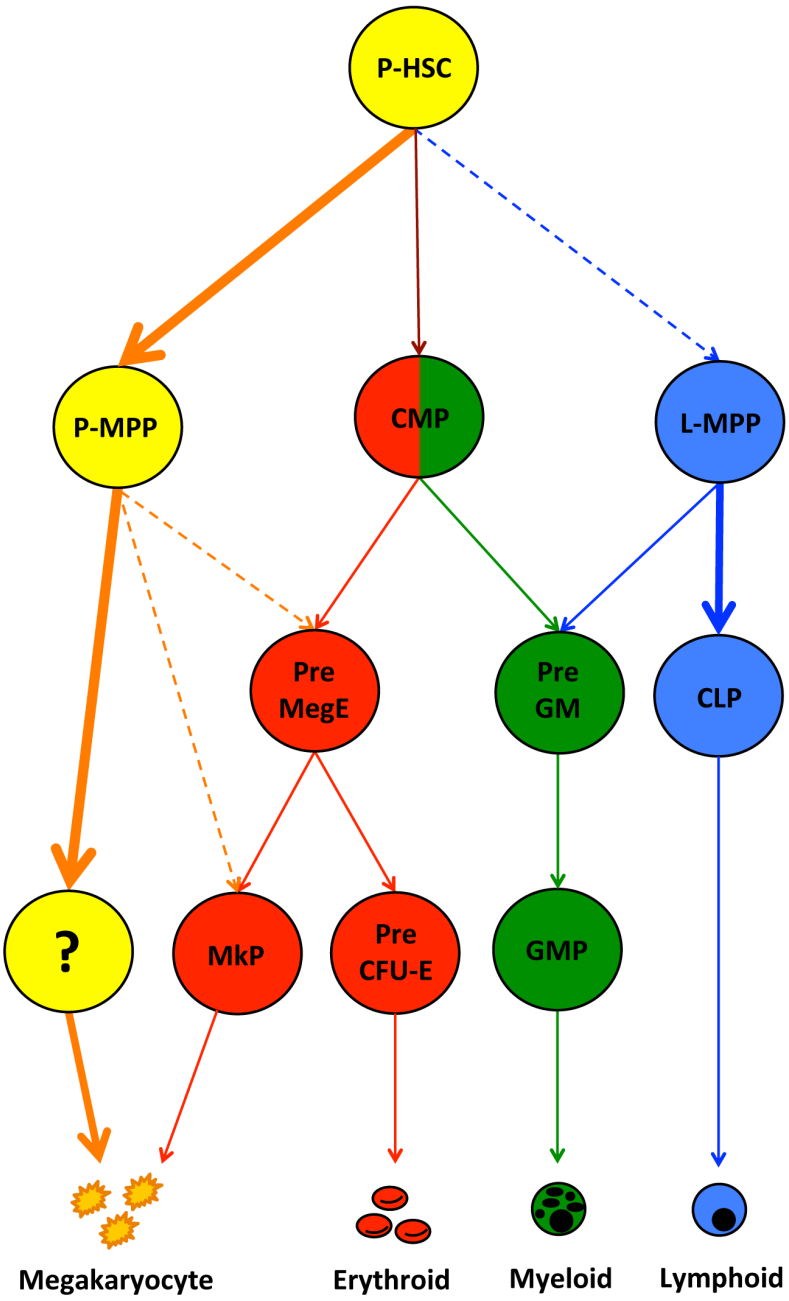

Figure 5.9. Proposed model for the establishment of platelet-biased hierarchies by *Vwf*+ haematopoetic stem cells through a novel branch of megakaryocyte lineage differentiation.

Platelet-biased HSCs (P-HSC) preferentially generate platelet-biased or restricted MPPs (P-MPP), which efficiently produce megakaryocytes through a fast track differentiation pathway that mainly bypasses Pre-MegE and MkP progenitors, and might or not involve an additional unknown progenitor compartment.

CHAPTER 6: Identification of rare platelet-biased haematopoietic stem cells in foetal liver

6.1. Introduction

In this chapter we sought to investigate if the platelet-biased haematopoietic stem cells (HSC) that we identified in adult bone marrow (BM) are also present in foetal liver (FL), the main embryonic haematopoietic site. The study of platelet-biased HSCs in the early embryo is especially relevant because the production of megakaryocytes and platelets is crucial for normal embryonic development. In addition to their protective function in response to vascular injuries, platelets are required during embryonic angiogenesis for the separation of the nascent lymphatic vasculature from blood vessels (Carramolino et al., 2010; Uhrin et al., 2010).

Myeloid-biased HSCs (α-HSCs) have previously been identified in E14.5 and E18.5 FL through single cell transplantation approaches, and these cells were found to be rare compared to much more abundant balanced (β-HSCs) and lymphoid-biased (γ/δ-HSCs) HSCs (Benz et al., 2012; Babovic and Eaves, 2014). In these studies, however, the platelet and erythroid outputs of transplanted FL HSCs were not investigated.

In the current study we applied the same single cell transplantation approach to FL HSCs as described in chapter 5 for adult BM *Vwf*+ HSCs. To allow tracking of both platelets and erythrocytes in peripheral blood of recipients, we used *Vwf*-EGFP and *Vwf*-tdtomato/*Gata1*-EGFP embryos as donors in single cell transplantations. Our results suggest that, unlike in BM, platelet-biased reconstitution behaviour is not prevalent in FL HSCs.

6.2. Results

6.2.1. *Vwf* expression in E14.5 foetal liver haematopoietic stem cells

Firstly we analysed *Vwf* expression by flow cytometry in FL HSCs at embryonic day E14.5. For this analysis we used a similar combination of cell surface markers and a similar gating strategy to the one used for adult BM HSCs. However, since FL HSCs are more proliferative than adult BM HSCs and all express CD34 (Matsuoka, 2001), we did not include this cell surface-marker in our FL HSC gating strategy.

In agreement with our previously published results (Sanjuan-Pla et al., 2013), and in contrast to adult BM HSCs, virtually all E14.5 FL HSCs (LSK CD150+ CD48-) were labelled by *Vwf*-EGFP and *Vwf*-tdTomato in reporter mice (Figure 6.1A).

Interestingly, when analysed by quantitative PCR (qPCR), sorted *Vwf*-EGFP+ E14.5 FL HSCs show a much wider range of *Vwf* transcript expression than *Vwf*-EGFP+ BM HSCs (Figure 6.1B). This difference could be explained, at least in part, by the gating strategy used. In adult BM there is wider spread of *Vwf*-EGFP signal (compared to FL HSCs), therefore only the 40% highest labelled adult HSCs were sorted (out of the total 65.7% *Vwf*-EGFP+ HSCs) to avoid contamination by *Vwf*-EGFP- cells. In contrast, in E14.5 FL the 88% highest labeled HSCs were sorted (out of 100% *Vwf*-EGFP+ HSCs).

Vwf transcript expression was undetectable in comparable fractions of FL and adult BM HSCs sorted as *Vwf*-EGFP+ (Figure 6.1B): 22.54% of *Vwf*-EGFP+ E14.5 FL HSCs (16 of 71 cells) and 16.67% of *Vwf*-EGFP+ BM HSCs (3 of 18 cells). This could be due to contamination by *Vwf*-EGFP- cells, although it seems unlikely considering the strict gating strategy used, especially for adult HSCs. This discrepancy is more likely to be due to experimental error, insufficient assay sensitivity for detection of very low *Vwf* transcript levels, or a lag between down-regulation of *Vwf* expression and turnover of EGFP protein in some HSCs.

Gene expression analysis revealed that megakaryocytic (Mk) lineage priming is weaker and myeloid lineage priming is stronger in E14.5 FL HSCs than in *Vwf*-EGFP+ adult BM HSCs (Figure 6.1C). 16.9% of E14.5 FL HSCs express megakaryocyte–associated genes and 42.3% express myeloid-associated genes, in contrast to 66.7% and 22.2% of adult BM HSCs, respectively. This difference is stronger when comparing the two-thirds of cells with highest *Vwf* expression level (48 foetal cells and 12 adult cells), and even stronger when comparing only the one-third of cells with highest *Vwf* expression level (24 foetal cells and 6 adult cells). Therefore, the difference in lineage priming is independent from the different strictness of foetal and adult *Vwf*-EGFP+ gating strategies, and expression of *Vwf* transcripts is not positively correlated to Mk priming in E14.5 FL HSCs. Overall our gene expression data show that, unlike in adult BM, Mk lineage priming is not characteristic of *Vwf*-EGFP+ E14.5 FL HSCs.

A

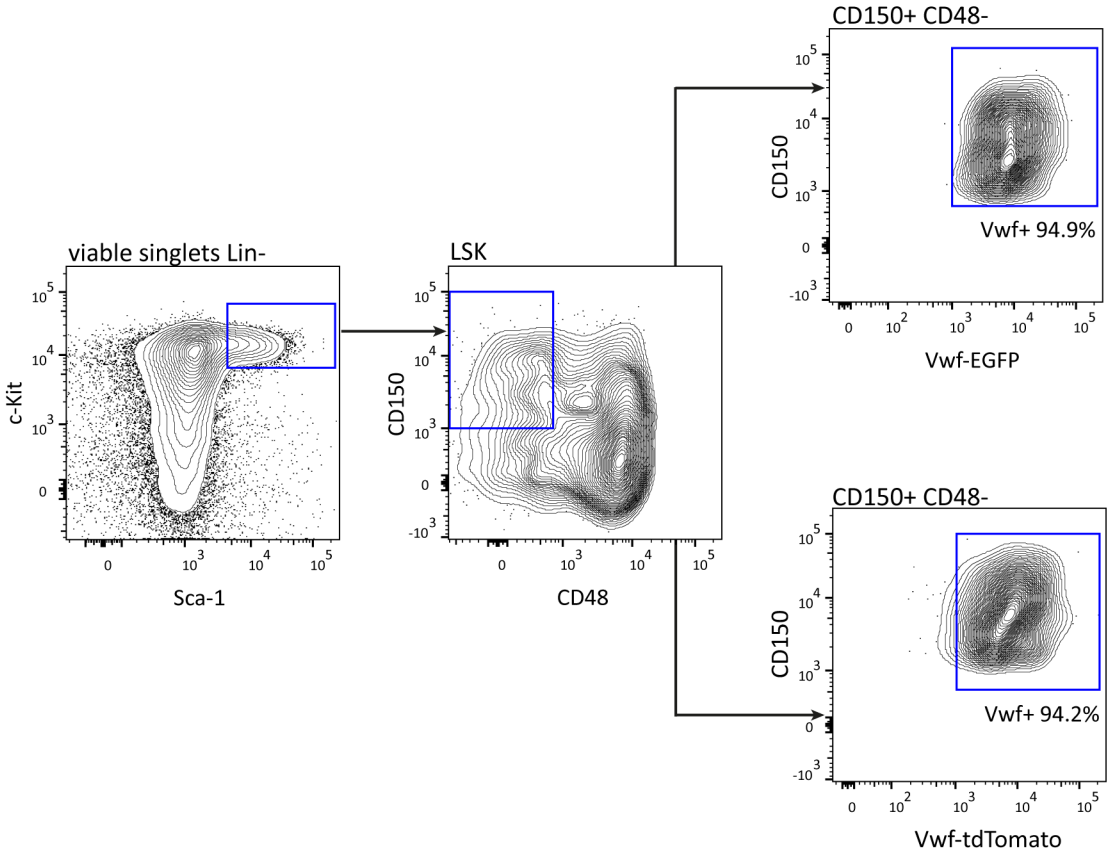
viable singlets Lin-
c-Kit
Sca-1
LSK
CD150
CD48
CD150+ CD48-
CD150
Vwf+ 94.9%
Vwf-EGFP
CD150+ CD48-
CD150
Vwf+ 94.2%
Vwf-tdTomato

B

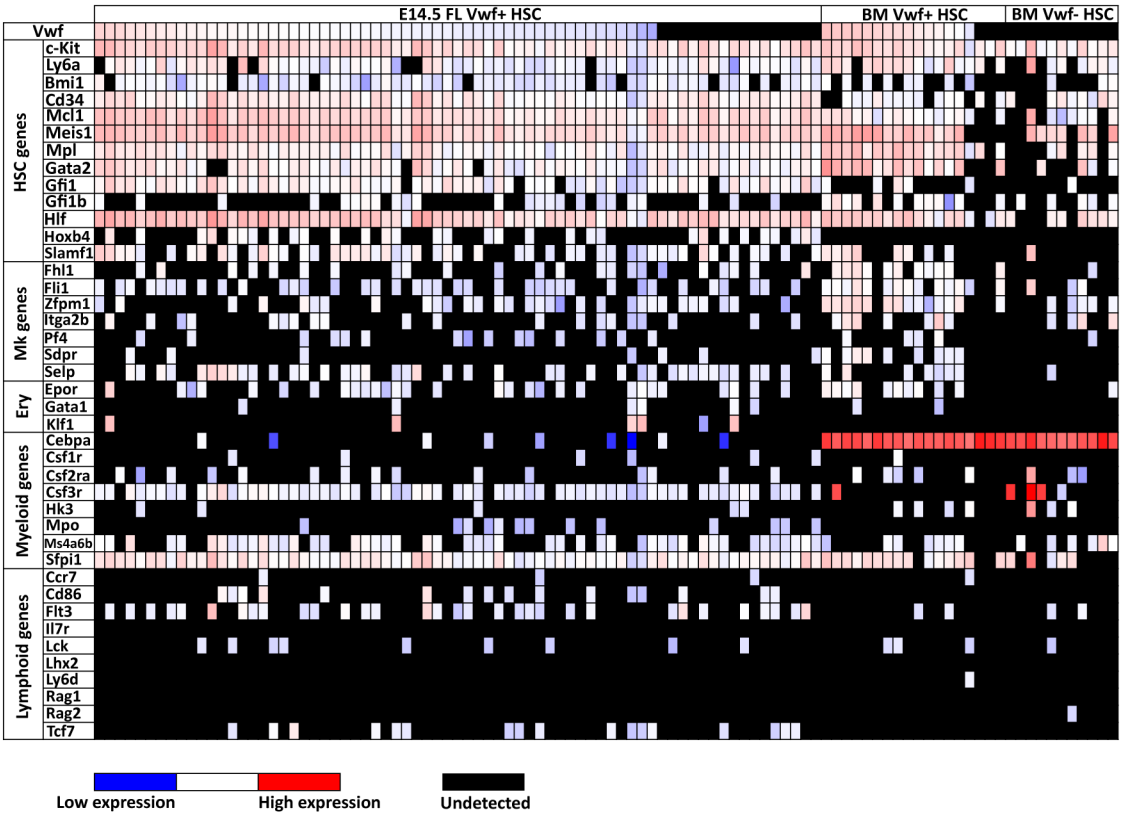
E14.5 FL Vwf+ HSC
BM Vwf+ HSC
BM Vwf- HSC
Vwf
HSC genes
c-Kit
Ly6a
Bmi1
Cd34
Mcl1
Meis1
Mpl
Gata2
Gfi1
Gfi1b
Hlf
Hoxb4
Slamf1
Mk genes
Fhl1
Fli1
Zfpm1
Itga2b
Pf4
Sdpr
Selp
Ery
Epor
Gata1
Klf1
Myeloid genes
Cebpa
Csf1r
Csf2ra
Csf3r
Hk3
Mpo
Ms4a6b
Sfpi1
Lymphoid genes
Ccr7
Cd86
Flt3
Il7r
Lck
Lhx2
Ly6d
Rag1
Rag2
Tcf7
Low expression
High expression
Undetected

C

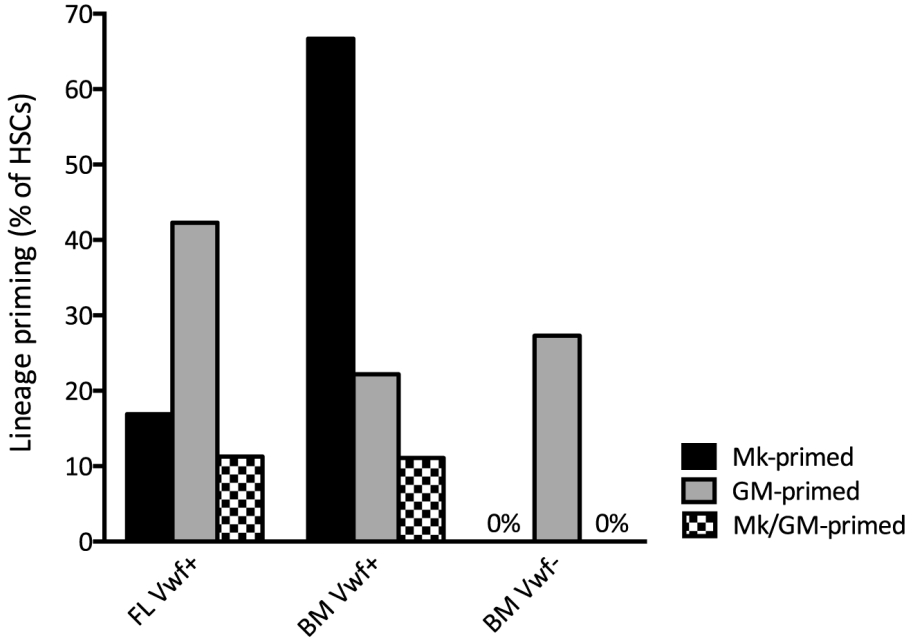

Figure 6.1. *Vwf* expression in E14.5 foetal liver haematopoietic stem cells.

Analysis of *Vwf* expression by flow cytometry and multiplexed qPR in E14.5 FL HSCs of *Vwf*-EGFP and *Vwf*-tdTomato/*Gata1*-EGFP embryos.

(A) Gating strategy for analysis and sorting of E14.5 FL *Vwf*+ HSCs. All E14.5 FL HSCs are labelled by EGFP in *Vwf*-EGFP mice (upper panel, n=6 pools) and by tdTomato in *Vwf*-tdTomato/*Gata1*-EGFP mice (lower panel, n=4 pools). Mean % of parent gate is shown.

(B) Heatmap of relative gene expression in FL HSCs (LSK CD150+ CD48-) and BM HSCs (LSK CD150+ CD48- CD34-) sorted from *Vwf*-EGFP mice. Multiplexed qPCR data are presented as ΔCt normalised to the housekeeping gene *Hprt1*. Only samples with detectable levels of *Hprt1* and *c-Kit* were analysed. Each column represents a single cell, and cells for each HSC population are ordered from highest to lowest *Vwf* expression (first row). *Vwf*-EGFP+ E14.5 FL HSCs, n=71 cells from 2 pooled samples. *Vwf*-EGFP+ and *Vwf*-EGFP- BM HSCs, n=18 cells and n=11 cells respectively, all from 1 pooled sample.

(C) Mk and GM lineage priming in E14.5 FL and adult BM HSCs, as detected by qPCR. % of HSCs analysed expressing >3 Mk-associated genes (out of 7 analysed) and/or >3 GM-associated genes (out of 8 analysed).

6.2.2. Haematopoietic stem cells with *in vivo* platelet-biased behaviour are rare in E14.5 foetal liver

Based on the low Mk lineage priming of *Vwf*+ E14.5 FL HSCs, we predicted that the *in vivo* reconstitution behaviour of these cells should differ from that of *Vwf*+ adult BM HSCs. To address this question we performed single cell transplantations of E14.5 FL HSCs from *Vwf*-EGFP and *Vwf*-tdTomato/*Gata1*-EGFP embryos, in the same manner previously detailed in chapter 5 for adult BM HSCs (Figure 5.2).

Peripheral blood reconstitution was analysed at 6-9 weeks and 16 weeks post-transplantation, and some recipients were analysed at an additional time point at 24-32 weeks post-transplantation. The reconstitution threshold, the definition of bias, and the different categories of reconstitution behaviour used in this chapter are similar to those previously described in chapter 5 (Table 5.1). However, since the majority of recipients of E14.5 FL HSCs were only analysed at two time points post-transplantation (6-9 and 16 weeks) – instead of the three time points of analysis performed for adult BM HSCs (8-9, 12-13, and 16-18) – the criteria applied in the classification of lineage-biased patterns in this study are not as strict as was used for adult BM HSCs. Namely, reconstitution patterns are considered balanced or biased when the conditions described in Table 5.1 were observed at least at the last time point of analysis, but not necessarily at other time points.

Reconstitution of platelets, erythrocytes and leucocytes was analysed whenever using *Vwf*-tdTomato/*Gata1*-EGFP embryos as donors, but erythrocytes could not be tracked in peripheral blood when using *Vwf*-EGFP embryos as donors. Furthermore, flow cytometric analysis of T cells in peripheral blood of recipients of single E14.5 FL HSCs was less exhaustive than previously described for the adult BM HSC study in chapter 5 (Figure 5.2). In the BM HSC study we investigated reconstitution of CD4 and CD8 T cells separately, and also

included TCRβ as a marker for increased specificity. In this FL study we defined T cells simply as CD4+ and/or CD8+, and pooled these cell surface markers in the same fluorescence channel for flow cytometric analysis. This less detailed analysis of T cell reconstitution did not, however, impact negatively on our ability to investigate the presence of platelet-biased HSCs in FL.

We transplanted 27 mice with single *Vwf*-EGFP+ E14.5 FL HSCs and 83 mice with single *Vwf*-tdTomato+ E14.5 FL HSCs. A total of 3 recipients did not survive the full period of follow-up post-transplantation, and were therefore excluded from analysis. Long-term reconstituted mice represented 29% of the total 107 transplanted mice analysed (Figure 6.2A). When transplanting single *Vwf*-EGFP+ or *Vwf*-tdTomato+ E14.5 FL HSCs, 52% of total reconstituted recipients develop balanced reconstitution patterns or multilineage reconstitution patterns without a specific lineage bias, while 34.5% develop lymphoid-biased or lymphoid-restricted patterns (Figure 6.2B-C). Only 14% of total recipients of *Vwf*+ E14.5 FL HSCs developed reconstitution patterns with platelet-bias or platelet/myeloid-bias (Figure 6.2B-C), in stark contrast to the 66% of recipients of single adult BM *Vwf*^{high} HSCs (Figure 5.3B). The low level of platelet-biased and platelet/myeloid-biased reconstitution observed is in agreement with the low percentage of myeloid-biased HSCs (α-HSCs) reported by earlier FL studies in which platelet reconstitution analysis was omitted (Benz et al., 2012; Babovic and Eaves, 2014).

Out of the total 29 mice reconstituted by *Vwf*+ E14.5 FL HSCs only one pattern with lymphoid-exclusion was observed (platelet/erythroid/myeloid-restricted with platelet-bias, Figure 6.2B-C), while 28% of reconstitution patterns generated by adult BM *Vwf*^{high} HSCs are characterised by lymphoid-exclusion (Figure 5.3C). Overall these data demonstrate that, unlike adult BM HSCs, *Vwf* expression identified by flow cytometry in E14.5 FL HSCs does not enrich for lymphoid-exclusion or platelet-biased reconstitution behaviour *in vivo*.

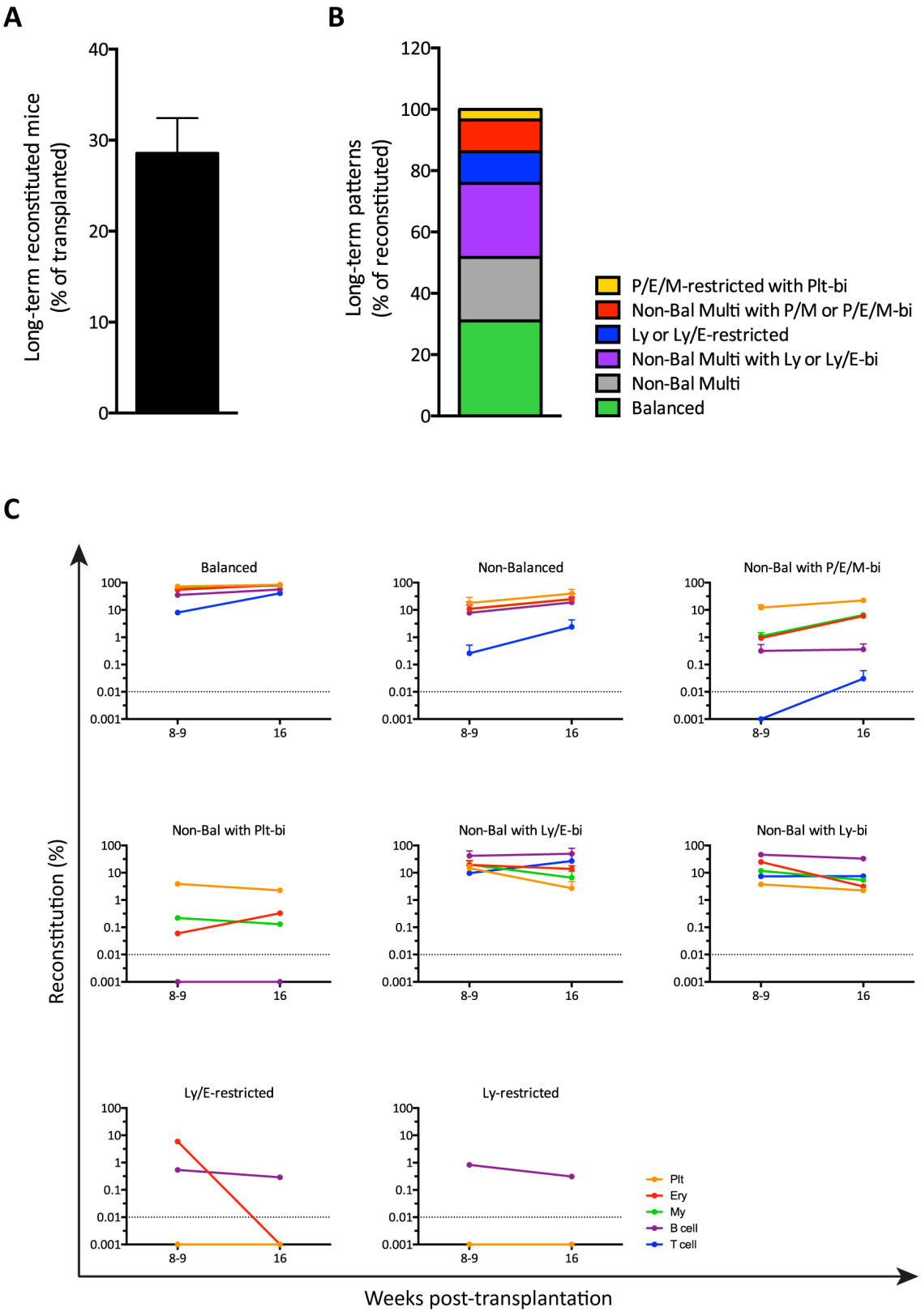
A
Long-term reconstituted mice
(% of transplanted)
40
30
20
10
0
B
Long-term patterns
(% of reconstituted)
120
100
80
60
40
20
0
P/E/M-restricted with Plt-bi
Non-Bal Multi with P/M or P/E/M-bi
Ly or Ly/E-restricted
Non-Bal Multi with Ly or Ly/E-bi
Non-Bal Multi
Balanced
C
Balanced
Non-Balanced
Non-Bal with P/E/M-bi
Non-Bal with Plt-bi
Non-Bal with Ly/E-bi
Non-Bal with Ly-bi
Ly/E-restricted
Ly-restricted
100
10
1
0.1
0.01
0.001
8-9
16
Reconstitution (%)
Weeks post-transplantation
Plt
Ery
My
B cell
T cell

Figure 6.2. Platelet-biased haematopoietic stem cells are rare in E14.5 foetal liver.

Unlike BM HSCs, single cell transplantation of E14.5 FL *Vwf*+ HSCs does not enrich for lymphoid-exclusion or for platelet-dominated blood reconstitution patterns.

(A) Long-term reconstituted mice transplanted with a single *Vwf*-EGFP+ or *Vwf*-tdTomato+ E14.5 FL HSC. Mean % + SEM of 6 independent experiments, n=107 transplanted mice.

(B) Long-term reconstitution patterns observed when transplanting single *Vwf*-EGFP+ or *Vwf*-tdTomato+ E14.5 FL HSCs. Reconstituted mice, n=29.

(C) Reconstitution kinetics in representative recipients of single *Vwf*-tdTomato+ E14.5 FL HSCs. Mean % + SEM presented in logarithmic scale. Balanced multilineage reconstitution, n=1. Non-balanced multilineage reconstitution, n=3. Non-balanced multilineage reconstitution with platelet/erythroid/myeloid-bias, n=2. Non-balanced multilineage reconstitution with platelet-bias, n=1. Non-balanced multilineage reconstitution with lymphoid/erythroid-bias, n=2. Non-balanced multilineage reconstitution with lymphoid-bias, n=5. Lymphoid/erythroid-restricted reconstitution, n=1. Lymphoid-restricted reconstitution, n=1.

6.2.3. Balanced foetal liver haematopoietic stem cells generate bone marrow platelet-biased haematopoietic stem cells

We showed that in E14.5 FL platelet-biased HSCs are rare, while balanced and non-specifically biased multilineage HSCs are the most abundant. We then investigated the repopulation ability of adult BM HSCs derived from a single balanced E14.5 FL HSC.

The proportion of *Vwf+* donor-derived HSCs in primary adult recipients of balanced E14.5 FL HSCs is low (Figure 6.3). This is relatively similar to the donor-derived HSC compartment of recipients of single balanced *Vwf*^{high} adult BM HSCs (Figure 5.5B).

We previously demonstrated that the rare *Vwf*+ HSCs derived from a single *Vwf*+ adult BM HSC that behaved as balanced in primary recipients continue to behave as balanced when transplanted into secondary recipients. We also observed that *Vwf*+ adult BM HSCs derived from a single platelet-biased *Vwf*+ HSC propagate platelet-biased reconstitution (Table 5.3). Interestingly, we found that *Vwf*+ BM HSCs derived from balanced *Vwf*+ E14.5 FL HSCs behave differently from their precursor, generating platelet/myeloid-biased reconstitution patterns – with and without lymphoid-exclusion – when serially transplanted (Table 6.1 and Figure 6.3). Although it will be necessary to generate more serial transplantation data from multiple donors, the results obtained so far indicate that, in contrast to FL, platelet bias is readily established in adult *Vwf*+ HSCs. This change could be intrinsic to adult-like HSCs, but perhaps also mediated by the adult BM micro-environment.

Table 6.1. Platelet-biased reconstitution behaviour upon secondary transplantation of balanced foetal liver–derived haematopoietic stem cells.

Donor pattern	Balanced		
Populations transplanted	Unfractionated BM	*Vwf+*	*Vwf-*
Cell number	10 x 10^6 cells	1 cell	5 cells
Reconstituted mice	100% (4/4)	14.71% (5/34)	10% (1/10)
Balanced multilineage	25% (1/4)	0% (0/5)	0% (0/1)
Non-balanced multilineage	75% (3/4)	20% (1/5)	0% (0/1)
Platelet/myeloid-biased	0% (0/4)	80% (4/5)	0% (0/1)
Lymphoid-biased	0% (0/4)	0% (0/5)	100% (1/1)

Secondary transplantation of unfractionated BM and donor-derived HSC sub-populations sorted from a primary recipient of a single *Vwf*-EGFP+ E14.5FL HSC with balanced reconstitution. Peripheral blood analysis was performed at 14 weeks post-transplantation.

Reconstituted recipients are presented as % of total transplanted mice. Reconstitution patterns are presented as % of reconstituted mice. Absolute numbers of transplanted and reconstituted mice are also indicated in parentheses.

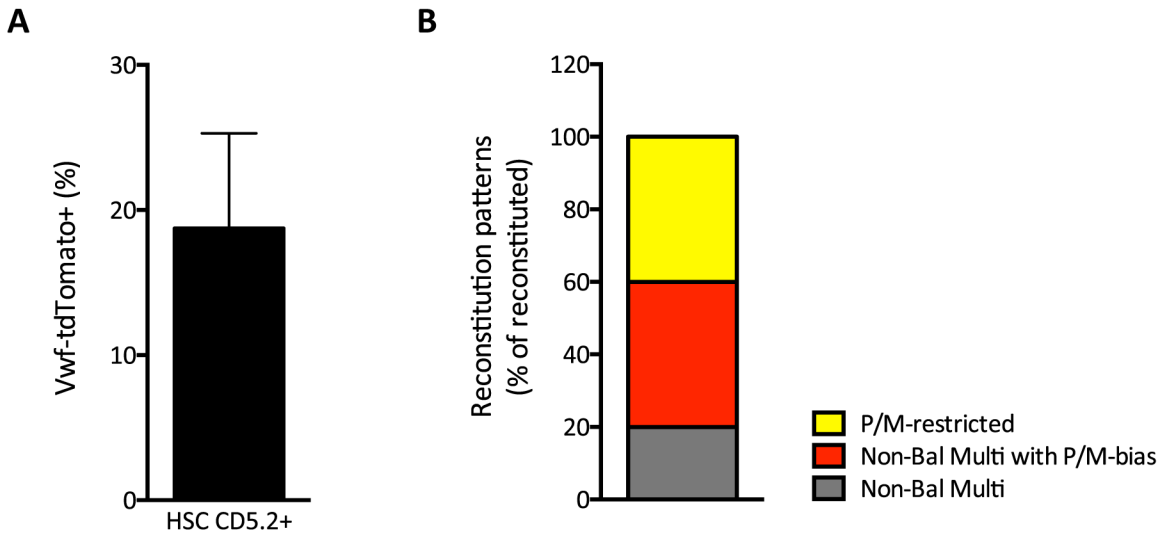

Figure 6.3. Platelet-biased reconstitution behaviour by adult bone marrow *Vwf+* foetal liver-derived haematopoietic stem cells.

Adult BM *Vwf*+ HSCs derived from a single balanced *Vwf*+ E14.5 FL HSC behave differently from their FL precursor, mainly generating platelet/myeloid-biased reconstitution patterns in secondary transplantation.

(A) Donor-derived *Vwf*-EGFP+ or *Vwf*-tdTomato+ HSCs in BM of recipients of a single E14.5 FL *Vwf*+ balanced HSC. Mean % + SEM, n=6.

(B) Long-term reconstitution patterns observed when re-transplanting a single donor-derived adult BM *Vwf*-EGFP+ HSC generated by a single balanced E14.5 FL HSC. Single donor-derived BM HSCs were sorted from one donor with balanced reconstitution and transplanted into 34 secondary recipients. Reconstituted mice, n=5.

6.2.4. Platelet-biased reconstitution activity in early foetal liver

Definitive HSCs (dHSCs) have been found to be first generated in the aorta-gonad-mesonephros (AGM) region of the embryo around E10.5 (Medvinsky et al., 1993; Müller et al., 1994; Medvinsky and Dzierzak, 1996), and to subsequently seed the FL around E11-E11.5 (Medvinsky et al., 1993; Sanchez et al., 1996; Kumaravelu et al., 2002). Definitive multilineage HSCs have been defined in the literature as being capable of long-term repopulation of myeloid and lymphoid lineages upon transplantation into adult recipient mice. Contribution to the platelet and erythroid lineages was not previously investigated, and it is therefore possible that early FL is also seeded by platelet-biased or non-multilineage HSCs.

We demonstrated that lymphoid-exclusion and platelet-bias, although not completely absent, are rarely seen in the outputs of E14.5 FL HSCs (Figure 6.2). We then investigated the presence of platelet-biased reconstitution activity at earlier embryonic ages, E10-E12.

Both platelets and erythrocytes express *Gata1* and are labelled in *Gata1* fluorescent reporter mice, and therefore we used *Gata1*-EGFP embryos as transplantation donors to allow tracking of these lineages. We transplanted into adult recipients whole unfractionated *Gata1*-EGFP FLs collected just before FL seeding by dHSCs (E10-E10.5) and during the period of FL seeding (E11-E12). We also transplanted $5x10^5$ unfractionated cells from E14.5 FLs as a positive control for multilineage reconstitution.

We did not detect reconstitution of any blood lineage when transplanting whole E10-10.5 FLs (Table 6.2). This is in agreement with the classic studies of FL seeding, and suggests that at this time point there are no potent HSCs in FL, neither multilineage nor platelet-biased.

When transplanting whole E11-12 FLs we detected mainly balanced and lymphoid-biased reconstitution. Interestingly, we also detected one case of platelet-restricted reconstitution

with a low level of donor-derived platelets (Table 6.2 and Figure 6.4). This finding demonstrates that some E11-E12 FL haematopoietic cells have fast kinetics of platelet production. However, we did not test lineage reconstitution levels beyond 8 weeks in the single platelet-restricted pattern observed, and further study is required to determine if rare HSCs with long-term platelet-biased/restricted reconstitution activity seed the FL or are otherwise promptly generated by the first FL seeding HSCs. In future whole FL transplantation experiments long-term reconstitution analysis will be performed to clarify if platelet-biased/restricted reconstitution is merely transient or long-lasting, and if robust reconstitution of other blood lineages surfaces later.

Table 6.2. Reconstitution patterns obtained from transplantation of early foetal livers.

Embryo age	E10-10.5	E11-12	E14.5
Reconstituted mice	0% (0/4)	45% (9/20)	100% (8/8)
Balanced multilineage	-	55.56% (5/9)	100% (8/8)
Platelet-biased	-	11.11% (1/9)	0% (0/8)
Lymphoid-biased	-	33.33% (3/9)	0% (0/8)

Transplantation of whole unfractionated *Gata1*-EGFP E10-E12 FL and $5x10^5$ cells of E14.5 FL into adult recipient mice. Peripheral blood analysis was performed at 8 weeks post-transplantation. Reconstituted recipients are shown as a percentage of total transplanted mice. Reconstitution patterns are shown as a percentage of reconstituted mice. Absolute numbers of transplanted and reconstituted mice are also shown in parentheses. See also Figure 6.3.

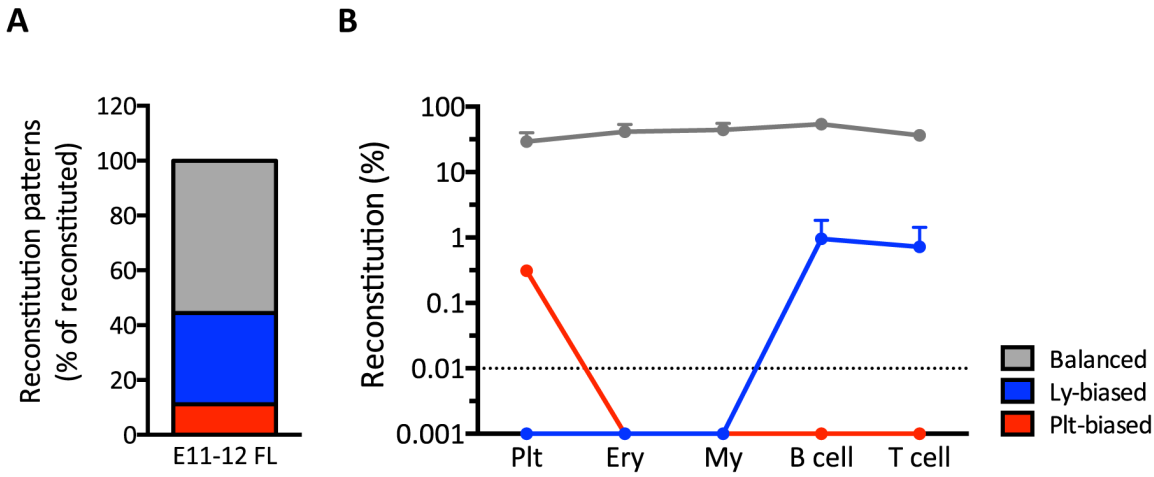

Figure 6.4. Platelet-biased repopulation activity in early foetal liver.

Early foetal liver platelet-biased repopulation activity was investigated through transplantation of whole unfractionated *Gata1*-EGFP E11-E12 FLs.

(A) Reconstitution patterns observed after transplantation of whole *Gata1*-EGFP E11-12 FLs. Peripheral blood reconstitution analysis was performed at 8 weeks post-transplantation. N=9 reconstituted mice out of 20 transplanted mice in 3 independent experiments. See also Table 6.2.

(B) Reconstitution level of each blood lineage in the reconstitution patterns obtained from transplantation of E11-12 *Gata1*-EGFP FLs. Mean % + SEM presented in logarithmic scale. Balanced patterns, n=5. Lymphoid-biased patterns, n=3. Platelet-biased patterns, n=1.

6.3. Discussion

In this chapter we showed that all E14.5 FL HSCs are labelled by *Vwf*-EGFP and *Vwf*-tdTomato in reporter mice, in contrast to only half of adult BM HSCs. Also unlike BM, individual *Vwf*+ E14.5 FL HSCs rarely exhibit platelet-biased reconstitution behaviour upon transplantation. This reconstitution behaviour may be explained by the fact that, compared to adult BM *Vwf*^{high} HSCs, the great majority of FL HSCs possess a low level of *Vwf* transcripts and have a gene expression profile less primed for the Mk lineage.

Endothelial cells express *Vwf*, and if the definitive HSCs that seed FL are indeed generated from haemogenic endothelium or other endothelial-related processes, as suggested by many previous studies (Cumano and Godin, 2007; Medvinsky et al., 2011), it is not unexpected that all FL HSCs initially express *Vwf*. However, it appears that by E14.5 many of these HSCs have down-regulated *Vwf* expression. There might be a lag between down-regulation of *Vwf* expression in HSCs and turnover of EGFP in *Vwf*-EGFP reporter mice. This is not, however, a satisfying explanation considering the fast self-renewing and proliferation ability of FL HSCs, since one would expect a rapid expansion of *Vwf*-EGFP- following the initial down-regulation of *Vwf*. Alternatively, it might be that the minimum level of *Vwf* transcript expression required for EGFP expression in the fluorescent reporter mice may be too low to be detected by our qPCR assay.

Previous studies, in which the contribution to platelet and erythroid lineages was not analysed, concluded that all adult HSC subtypes are also detected in foetal and neonatal life (Dykstra et al., 2007; Benz et al., 2012; Babovic and Eaves, 2014). Our observation that E14.5 FL HSCs most commonly generate multilineage and lymphoid-biased reconstitution patterns is in agreement with those previous studies. However, we did not detect platelet/erythroid-

restricted or platelet-restricted reconstitution patterns derived from single E14.5 FL HSCs, which we detect when transplanting adult BM HSCs. Considering the low frequency of adult BM HSCs with these strictly restricted behaviours, additional FL transplantations will be required to confirm if exclusion of myeloid output is exclusive to adult BM HSCs.

Overall we currently do not have enough data to conclude that the full array of functional phenotypes that we observe for individual adult BM HSCs does not also exist in E14.5 FL HSCs, as has been suggested by previous studies (Babovic and Eaves, 2014). We can conclude that the composition of the HSC compartment, in regards to relative frequency of functional subtypes, is different in these two developmental stages. FL HSCs are more homogeneously multilineage and less primed for production of specific blood lineages than adult BM HSCs. The differentiation plasticity of foetal and adult HSCs, and how such plasticity is regulated and responds to specific environmental cues, is an important topic for further investigation.

The differential survival, self-renewal ability, and differentiation properties of foetal and adult HSCs is probably, at least in part, determined by exposure to fine-tuned combinations of cytokines, chemokines, and other micro-environmental factors (Challen et al., 2010; Challen et al., 2012; Copley et al., 2013; Mallaney et al., 2014; Matatall et al., 2014; Wohrer et al., 2014). Differential maintenance and regulation of HSCs and more restricted haematopoietic progenitors is also likely to be influenced by the distinct cellular niches these populations occupy in adult BM (Ding and Morrison, 2013). Previous studies noted that the first changes in the functional composition of the heterogeneous foetal HSC compartment – namely an increase of myeloid-biased HSC frequency – overlap with the migration of haematopoiesis from FL to foetal BM at E18.5 (Babovic and Eaves, 2014).

We find that E14.5 FL HSCs rarely generate reconstitution patterns with platelet-bias (5%) and platelet/myeloid-bias (10%), but we observe a great increase in the frequency of

platelet/myeloid-biased behaviour (80%) when re-transplanting donor-derived BM HSCs from a primary adult recipient of a single balanced E14.5 FL HSC. Transplanted BM *Vwf*+ HSCs give rise to more *Vwf*+ HSCs that maintain the bias of the primary reconstitution pattern. In contrast, E14.5 FL *Vwf*+ HSCs transplanted into an adult BM niche produce *Vwf*+ HSCs that no longer behave like their FL precursor, and instead display the platelet/myeloid-biased behaviour characteristic of adult BM *Vwf*+ HSCs. These data do not exclude the possibility that development of platelet-bias is coupled to intrinsic changes that occur during the transition of FL HSCs to adult HSCs, but it is also compatible with the possibility that interactions with the BM niche play a role in the establishment of platelet-biased and platelet/myeloid-biased reconstitution behaviours.

As discussed in chapter 5, overall our findings are compatible with a model in which platelet-biased HSCs are regulated by interplay between both intrinsic (transcriptional) and extrinsic (niche) factors. In comparison to adult BM niches (Kiel and Morrison, 2008; Anthony and Link, 2014; Morrison and Scadden, 2014) not much is currently known about the FL niches that support HSC expansion and differentiation (Mikkola and Orkin, 2006; Chou et al., 2013; Khan et al., 2015). It is possible that the extrinsic factors available in foetal liver micro-environments are not able to reinforce intrinsic platelet-bias in HSCs (see also discussion in chapter 5).

CHAPTER 7: Conclusions

7.1. Immune-restricted embryonic progenitors

In the studies presented in chapter 3 and 4 we have prospectively isolated the earliest known immune-restricted progenitor sustaining combined lymphoid and myeloid potential but little or no megakaryocyte/erythroid potential. We demonstrated through *in vivo* lineage tracing that this progenitor compartment contributes robustly to embryonic myelopoiesis under physiological conditions, therefore demonstrating that the myeloid potential sustained by lymphoid-primed progenitors has a functional role.

Our findings are of especial relevance for childhood leukaemias that are associated with *in utero* pre-leukemic translocations occurring in yet unidentified progenitors (Greaves and Wiemels, 2003), and that can result in mixed lineage phenotypes with markers of both lymphoid and myeloid lineages, but often not megakaryocyte or erythroid lineages (Bene, 2009; Matutes et al., 2011). Embryonic lympho-myeloid progenitors constitute candidate cells of origin for these types of leukaemia. Interestingly, a leukaemic LMPP-like compartment has recently been identified in acute myeloid leukaemia in the adult (Goardon et al., 2011).

7.2. Platelet-biased/restricted haematopoietic stem cells

In the studies presented in chapter 5 we showed that the adult bone marrow long-term repopulating HSC compartment includes a high frequency of HSCs that have completely down-regulated the *in vivo* expression of their lymphoid potential. We also identified platelet-restricted HSCs with robust long-term repopulating activity. Based on our findings we have proposed a revised model of the haematopoietic hierarchy, in which megakaryocyte lineage commitment from HSCs represents a very primitive lineage fate decision that can be carried out independently of known bone marrow myeloid/megakaryocyte/erythroid progenitors.

In contrast, our studies in chapter 6 demonstrated that the foetal liver HSC compartment is predominantly balanced, and foetal liver platelet-biased HSCs are very rare. It is possible that our proposed branch of megakaryocyte-lineage differentiation from HSCs is exclusive to adult haematopoiesis.

What might be the functional significance of adult HSCs so strongly dedicated to platelet production? Our hypothesis is that different subsets of HSCs might be selectively responsive to specific stimuli, and selectively accomplish distinct purposes in the fulfilment of haematopoietic needs. A haematopoietic hierarchy in which there is division of labour between distinct subsets of HSCs might be more efficient during emergency haematopoiesis. For example, if two incidents such as haemorrhaging and acute inflammation occur simultaneously – one requiring increased platelet production and the other increased granulocyte production, respectively – it might be detrimental for the organism if the HSC compartment were to respond homogenously and non-specifically to the two conflicting stimuli. Rather than mobilizing a broad, non-targeted and weak response, the specific activation of specialized sub-types of HSCs through distinct activation pathways might conceivably result in a much faster and stronger reaction to each incident.

BIBLIOGRAPHY

Adolfsson, J., Borge, O.J., Bryder, D., Theilgaard-Mönch, K., Astrand-Grundström, I., Sitnicka, E., Sasaki, Y., and Jacobsen, S.E. (2001). Upregulation of Flt3 Expression within the BM LSK SC compartment is Accompanied by Loss of Self-Renewal Capacity. Immunity *15*, 659-669.

Adolfsson, J., Mansson, R., Buza-Vidas, N., Hultquist, A., Liuba, K., Jensen, C.T., Bryder, D., Yang, L., Borge, O.J., Thoren, L.A.*, et al.* (2005). Identification of Flt3+ lympho-myeloid stem cells lacking erythro-megakaryocytic potential a revised road map for adult blood lineage commitment. Cell *121*, 295-306.

Akashi, K. (2009). Lymphoid lineage fate decision of hematopoietic stem cells. Ann N Y Acad Sci *1176*, 18-25.

Akashi, K., Reya, T., Dalma-Weiszhausz, D., and Weissman, I. (2000a). Lymphoid precursors. Curr Opin Immunol *12*, 144–150.

Akashi, K., Traver, D., Miyamoto, T., and Weissman, I. (2000b). A clonogenic common myeloid progenitor that gives rise to all myeloid lineages. Nature *404*, 193-197.

Akashi, K., Traver, D., and Zon, L.I. (2005). The complex cartography of stem cell commitment. Cell *121*, 160-162.

Alvarez-Silva, M., Belo-Diabangouaya, P., Salaun, J., and Dieterlen-Lievre, F. (2003). Mouse placenta is a major hematopoietic organ. Development *130*, 5437-5444.

Anders, S., and Huber, W. (2010). Differential expression analysis for sequence count data. Genome Biol *11*, R106.

Anthony, B.A., and Link, D.C. (2014). Regulation of hematopoietic stem cells by bone marrow stromal cells. Trends Immunol *35*, 32-37.

Arinobu, Y., Mizuno, S., Chong, Y., Shigematsu, H., Iino, T., Iwasaki, H., Graf, T., Mayfield, R., Chan, S., Kastner, P.*, et al.* (2007). Reciprocal activation of GATA-1 and PU.1 marks initial specification of hematopoietic stem cells into myeloerythroid and myelolymphoid lineages. Cell Stem Cell *1*, 416-427.

Audet, J., Miller, C.L., Eaves, C.J., and Piret, J.M. (2002). Common and distinct features of cytokine effects on hematopoietic stem and progenitor cells revealed by dose-response surface analysis. Biotechnol Bioeng *80*, 393-404.

Babovic, S., and Eaves, C.J. (2014). Hierarchical organization of fetal and adult hematopoietic stem cells. Exp Cell Res *329*, 185-191.

Back, J., Allman, D., Chan, S., and Kastner, P. (2005). Visualizing PU.1 activity during hematopoiesis. Exp Hematol *33*.

Barnes, D.W.H., and Loutit, J.F. (1954). What is the recovery factor in spleen? Nucleonics *12*, 68-71.

Baron, M.H. (2013). Early Embryonic Erythropoiesis ... Not so Primitive After All. Stem Cells 10.1002/stem.1342.

Baum, C.M., Weissman, I., Tsukamoto, A., Buckle, A.-M., and Peault, B. (1992). Isolation of a candidate human hematopoietic stem cell population. Proc Natl Acad Sci U S A *89*, 2804-2808.

Becker, A.J., McCulloch, E.A., and Till, J.E. (1963). Cytological demonstration of the clonal nature of spleen colonies derived from transplanted mouse marrow cells. Nature *197*, 452-454.

Beerman, I., Bhattacharya, D., Zandi, S., Sigvardsson, M., Weissman, I.L., Bryder, D., and Rossi, D.J. (2010). Functionally distinct hematopoietic stem cells modulate hematopoietic lineage potential during aging by a mechanism of clonal expansion. Proc Natl Acad Sci U S A *107*, 5465-5470.

Bell, J.J., and Bhandoola, A. (2008). The earliest thymic progenitors for T cells possess myeloid lineage potential. Nature *452*, 764-767.

Bellantuono, I. (2004). Haemopoietic stem cells. Int J Biochem Cell Biol *36*, 607-620.

Belteki, G., Haigh, J., Kabacs, N., Haigh, K., Sison, K., Costantini, F., Whitsett, J., Quaggin, S.E., and Nagy, A. (2005). Conditional and inducible transgene expression in mice through the combinatorial use of Cre-mediated recombination and tetracycline induction. Nucleic Acids Res *33*, e51.

Bene, M.C. (2009). Biphenotypic, bilineal, ambiguous or mixed lineage: strange leukemias! Haematologica *94*, 891-893.

Benveniste, P., Frelin, C., Janmohamed, S., Barbara, M., Herrington, R., Hyam, D., and Iscove, N.N. (2010). Intermediate-term hematopoietic stem cells with extended but time-limited reconstitution potential. Cell Stem Cell *6*, 48-58.

Benz, C., Copley, M.R., Kent, D.G., Wohrer, S., Cortes, A., Aghaeepour, N., Ma, E., Mader, H., Rowe, K., Day, C*., et al.* (2012). Hematopoietic stem cell subtypes expand differentially during development and display distinct lymphopoietic programs. Cell Stem Cell *10*, 273-283.

Bertoncello, I., Hodgson, G.S., and Bradley, T.R. (1985). Multiparameter analysis of transplantable hemopoietic stem cells: I. The separation and enrichment of stem cells homing to marrow and spleen on the basis of rhodamine-123 fluorescence. Exp Hematol *13*, 999-1006.

Bertrand, J.Y., Jalil, A., Klaine, M., Jung, S., Cumano, A., and Godin, I. (2005). Three pathways to mature macrophages in the early mouse yolk sac. Blood *106*, 3004-3011.

Bhandoola, A., von Boehmer, H., Petrie, H.T., and Zúñiga-Pflücker, J.C. (2007). Commitment and developmental potential of extrathymic and intrathymic T cell precursors: plenty to choose from. Immunity *26*, 678-689.

Bhatia, M., Wang, J.C., Kapp, U., Bonnet, D., and Dick, J.E. (1997). Purification of primitive human hematopoietic cells capable of repopulating immune-deficient mice. Proc Natl Acad Sci U S A *94*, 5320-5325.

Böiers, C., Carrelha, J., Lutteropp, M., Luc, S., Green, J.C., Azzoni, E., Woll, P.S., Mead, A.J., Hultquist, A., Swiers, G*., et al.* (2013). Lymphomyeloid contribution of an immune-restricted progenitor emerging prior to definitive hematopoietic stem cells. Cell Stem Cell *13*, 535-548.

Boyer, S.W., Beaudin, A.E., and Forsberg, E.C. (2012). Mapping differentiation pathways from hematopoietic stem cells using Flk2/Flt3 lineage tracing. Cell Cycle *11*, 3180-3188.

Boyer, S.W., Schroeder, A.V., Smith-Berdan, S., and Forsberg, E.C. (2011). All hematopoietic cells develop from hematopoietic stem cells through Flk2/Flt3-positive progenitor cells. Cell Stem Cell *9*, 64-73.

Bradley, T.R., and Metcalf, D. (1966). The growth of mouse bone marrow cells in vitro. J Exp Biol Med Sci *44*, 287-299.

Broudy, V.C., Lin, N.L., Priestley, G.V., Nocka, K., and Wolf, N.S. (1996). Interaction of stem cell factor and its receptor c-kit mediates lodgment and acute expansion of hematopoietic cells in the murine spleen. Blood *88*, 75-81.

Bryder, D., Rossi, D.J., and Weissman, I.L. (2006). Hematopoietic stem cells: the paradigmatic tissue-specific stem cell. Am J Pathol *169*, 338-346.

Busch, K., Klapproth, K., Barile, M., Flossdorf, M., Holland-Letz, T., Schlenner, S.M., Reth, M., Hofer, T., and Rodewald, H.R. (2015). Fundamental properties of unperturbed haematopoiesis from stem cells in vivo. Nature *518*, 542-546.

Buza-Vidas, N., Woll, P., Hultquist, A., Duarte, S., Lutteropp, M., Bouriez-Jones, T., Ferry, H., Luc, S., and Jacobsen, S.E. (2011). FLT3 expression initiates in fully multipotent mouse hematopoietic progenitor cells. Blood *118*, 1544-1548.

Bystrykh, L.V., de Haan, G., and Verovskaya, E. (2014). Barcoded vector libraries and retroviral or lentiviral barcoding of hematopoietic stem cells. Methods Mol Biol *1185*, 345-360.

Bystrykh, L.V., Verovskaya, E., Zwart, E., Broekhuis, M., and de Haan, G. (2012). Counting stem cells: methodological constraints. Nat Methods *9*, 567-574.

Calaminus, S.D.J., Guitart, A.V., Sinclair, A., Schachtner, H., Watson, S.P., Holyoake, T.L., Kranc, K.R., and Machesky, L.M. (2012). Lineage tracing of Pf4-Cre marks hematopoietic stem cells and their progeny. PLoS One *7*, e51361.

Calderon, L., and Boehm, T. (2011). Three chemokine receptors cooperatively regulate homing of hematopoietic progenitors to the embryonic mouse thymus. Proc Natl Acad Sci U S A *108*, 7517-7522.

Camargo, F., Chambers, S.M., Drew, E., McNagny, K.M., and Goodell, M.A. (2006). Hematopoietic stem cells do not engraft with absolute efficiencies. Blood *107*, 501-507.

Carlsson, L., Candéias, S., Staerz, U., and Keller, G. (1995). Expression of FcgRIII defines distinct subpopulations of fetal liver B cell and myeloid precursors. Eur J Immunol *25*, 2308-2317.

Carramolino, L., Fuentes, J., Garcia-Andres, C., Azcoitia, V., Riethmacher, D., and Torres, M. (2010). Platelets play an essential role in separating the blood and lymphatic vasculatures during embryonic angiogenesis. Circ Res *106*, 1197-1201.

Challen, G.A., Boles, N.C., Chambers, S.M., and Goodell, M.A. (2010). Distinct hematopoietic stem cell subtypes are differentially regulated by TGF-beta1. Cell Stem Cell *6*, 265-278.

Challen, G.A., Sun, D., Jeong, M., Luo, M., Jelinek, J., Berg, J.S., Bock, C., Vasanthakumar, A., Gu, H., Xi, Y.*, et al.* (2012). Dnmt3a is essential for hematopoietic stem cell differentiation. Nat Genet *44*, 23-31.

Cho, R.H., and Müller-Sieburg, C.E. (2000). High frequency of long-term culture-initiating cells retain in vivo repopulation and self-renewal capacity. Exp Hematol *28*, 1080-1086.

Chou, S., Chu, P., Hwang, W., and Lodish, H. (2010). Expansion of human cord blood hematopoietic stem cells for transplantation. Cell Stem Cell *7*, 427-428.

Chou, S., Flygare, J., and Lodish, H.F. (2013). Fetal Hepatic Progenitors Support Long-term Expansion of Hematopoietic Stem Cells. Exp Hematol *41*, 479-490.

Christensen, J., and Weissman, I. (2004). Circulation and chemotaxis of fetal hematopoietic stem cells. PLoS Biol *2*, E75.

Christensen, J.L., and Weissman, I.L. (2001). Flk-2 is a marker in hematopoietic stem cell differentiation: a simple method to isolate long-term stem cells. Proc Natl Acad Sci U S A *98*, 14541-14546.

Copley, M.R., Babovic, S., Benz, C., Knapp, D.J., Beer, P.A., Kent, D.G., Wohrer, S., Treloar, D.Q., Day, C., Rowe, K.*, et al.* (2013). The Lin28b-let-7-Hmga2 axis determines the higher self-renewal potential of fetal haematopoietic stem cells. Nat Cell Biol *15*, 916-925.

Copley, M.R., Beer, P.A., and Eaves, C.J. (2012). Hematopoietic stem cell heterogeneity takes center stage. Cell Stem Cell *10*, 690-697.

Corbel, C., Salaun, J., Belo-Diabangouaya, P., and Dieterlen-Lièvre, F. (2007). Hematopoietic potential of the pre-fusion allantois. Dev Biol *301*, 478-488.

Cumano, A., Dieterlen-Lièvre, F., and Godin, I. (1996). Lymphoid potential, probed before circulation in mouse, is restricted to caudal intraembryonic splanchnopleura. Cell *86*, 907-916.

Cumano, A., Ferraz, J.C., Klaine, M., Di Santo, J.P., and Godin, I. (2001). Intraembryonic, but not yolk sac hematopoietic precursors, isolated before circulation, provide long-term multilineage reconstitution. Immunity *15*, 477-485.

Cumano, A., and Godin, I. (2001). Pluripotent hematopoietic stem cell development during embryogenesis. Curr Opin Immunol *13*, 166-171.

Cumano, A., and Godin, I. (2007). Ontogeny of the hematopoietic system. Annu Rev Immunol *25*, 745-785.

Cumano, A., Paige, C.J., Iscove, N.N., and Brady, G. (1992). Bipotential precursors of B cells and macrophages in murine fetal liver. Nature *356*, 612-615.

Curry, J.L., and Trentin, J.J. (1967a). Hemopoietic spleen colony studies. I. Growth and differentiation. Dev Biol *15*, 395-413.

Curry, J.L., and Trentin, J.J. (1967b). Hemopoietic spleen colony studies. IV. Phytohemagglutinin and hemopoietic regeneration. J Exp Med *126*, 819-832.

Czyzyk, T.A., Ning, Y., Hsu, M.S., Peng, B., Mains, R.E., Eipper, B.A., and Pintar, J.E. (2005). Deletion of peptide amidation enzymatic activity leads to edema and embryonic lethality in the mouse. Dev Biol *287*, 301-313.

Davies, L.C., Jenkins, S.J., Allen, J.E., and Taylor, P.R. (2013). Tissue-resident macrophages. Nat Immunol *14*, 986-995.

Davies, L.C., and Taylor, P.R. (2015). Tissue-resident macrophages: then and now. Immunology *144*, 541-548.

de Boer, J., Williams, A., Skavdis, G., Harker, N., Coles, M., Tolaini, M., Norton, T., Williams, K., Roderick, K., Potocnik, A.J.*, et al.* (2003). Transgenic mice with hematopoietic and lymphoid specific expression of Cre. Eur J Immunol *33*, 314-325.

de Graaf, C.A., and Metcalf, D. (2011). Thrombopoietin and hematopoietic stem cells. Cell Cycle *10*, 1582-1589.

De Obaldia, M.E., Bell, J.J., and Bhandoola, A. (2013). Early T-cell progenitors are the major granulocyte precursors in the adult mouse thymus. Blood *121*, 64-71.

de Pooter, R., and Zúñiga-Pflücker, J.C. (2007). T-cell potential and development in vitro: the OP9-DL1 approach. Curr Opin Immunol *19*, 163-168.

Delassus, S., and Cumano, A. (1996). Circulation of Hematopoietic Progenitors in the Mouse Embryo. Immunity *4*, 97-106.

Delgado, M.D., and Léon, J. (2010). Myc roles in hematopoiesis and leukemia. Genes Cancer *1*, 605-616.

Derderian, S.C., Togarrati, P.P., King, C., Moradi, P.W., Reynaud, D., Czechowicz, A., Weissman, I.L., and MacKenzie, T.C. (2014). In utero depletion of fetal hematopoietic stem cells improves engraftment after neonatal transplantation in mice. Blood *124*, 973-980.

Dick, J.E., Magli, M.C., Huszar, D., Phillips, R.A., and Bernstein, A. (1985). Introduction of a Selectable Gene into Primitive Stem Cells Capable of Long-Term Reconstitution of the Hemopoietic System of W/Wv Mice. Cell *42*, 71-79.

Ding, L., and Morrison, S.J. (2013). Haematopoietic stem cells and early lymphoid progenitors occupy distinct bone marrow niches. Nature *495*, 231-235.

Domen, J., and Weissman, I. (1999). Self-renewal, differentiation or death: regulation and manipulation of hematopoietic stem cell fate. Mol Med Today *5*, 201-208.

Dormer, P., Spitzer, E., and Moller, W. (2004). EDR is a stress-related survival factor from stroma and other tissues acting on early haematopoietic progenitors (E-Mix). Cytokine *27*, 47-57.

Doulatov, S., Notta, F., Eppert, K., Nguyen, L.T., Ohashi, P.S., and Dick, J.E. (2010). Revised map of the human progenitor hierarchy shows the origin of macrophages and dendritic cells in early lymphoid development. Nat Immunol *11*, 585-593.

Doulatov, S., Notta, F., Laurenti, E., and Dick, J.E. (2012). Hematopoiesis: a human perspective. Cell Stem Cell *10*, 120-136.

Dykstra, B., Kent, D., Bowie, M., McCaffrey, L., Hamilton, M., Lyons, K., Lee, S.J., Brinkman, R., and Eaves, C. (2007). Long-term propagation of distinct hematopoietic differentiation programs in vivo. Cell Stem Cell *1*, 218-229.

Dzierzak, E., and Medvinsky, A. (2008). The discovery of a source of adult hematopoietic cells in the embryo. Development *135*, 2343-2346.

Dzierzak, E., and Speck, N.A. (2008). Of lineage and legacy: the development of mammalian hematopoietic stem cells. Nat Immunol *9*, 129-136.

Eilken, H.M., Nishikawa, S., and Schroeder, T. (2009). Continuous single-cell imaging of blood generation from haemogenic endothelium. Nature *457*, 896–900.

Eipper, B.A., Milgram, S.L., Husten, E.J., Yun, H.-Y., and Mains, R.E. (1993). Peptidylglycine alpha-amidating monooxygenase: A multifunctional protein with catalytic, processing, and routing domains. Protein Science *2*, 489-497.

Ema, H., Morita, Y., and Suda, T. (2014). Heterogeneity and hierarchy of hematopoietic stem cells. Exp Hematol *42*, 74-82 e72.

Ema, H., and Nakauchi, H. (2000). Expansion of hematopoietic stem cells in the developing liver of a mouse embryo. Blood *95*, 2284-2288.

Ema, H., Takano, H., Sudo, K., and Nakauchi, H. (2000). In Vitro Self-Renewal Division of Hematopoietic Stem Cells. J Exp Med *192*, 1281-1288.

Epelman, S., Lavine, K.J., Beaudin, A.E., Sojka, D.K., Carrero, J.A., Calderon, B., Brija, T., Gautier, E.L., Ivanov, S., Satpathy, A.T.*, et al.* (2014). Embryonic and adult-derived resident cardiac macrophages are maintained through distinct mechanisms at steady state and during inflammation. Immunity *40*, 91-104.

Feil, S., Valtcheva, N., and Feil, R. (2009). Inducible Cre mice. Methods Mol Biol *530*, 343-363.

Ferreira, R., Ohneda, K., Yamamoto, M., and Philipsen, S. (2005). GATA1 function, a paradigm for transcription factors in hematopoiesis. Mol Cell Biol *25*, 1215-1227.

Ford, C.E., Hamerton, J.L., Barnes, D.W.H., and Loutit, J.F. (1956). Cytological identification of radiation-chimeras. Nature *177*, 452-454.

Forsberg, E.C., Serwold, T., Kogan, S., Weissman, I.L., and Passegue, E. (2006). New evidence supporting megakaryocyte-erythrocyte potential of Flk2/Flt3+ multipotent hematopoietic progenitors. Cell *126*, 415-426.

Frame, J.M., McGrath, K.E., and Palis, J. (2013). Erythro-myeloid progenitors: "definitive" hematopoiesis in the conceptus prior to the emergence of hematopoietic stem cells. Blood Cells Mol Dis *51*, 220-225.

Galy, A., Travis, M., Cen, D., and Chen, B. (1995). Human T, B, natural killer, and dendritic cells arise from a common bone marrow progenitor cell subset. Immunity *3*, 459-473.

Gekas, C., and Graf, T. (2013). CD41 expression marks myeloid-biased adult hematopoietic stem cells and increases with age. Blood *121*, 4463-4472.

Georgiades, P., Ogilvy, S., Duval, H., Licence, D.R., Charnock-Jones, D.S., Smith, S.K., and Print, C.G. (2002). VavCre transgenic mice: a tool for mutagenesis in hematopoietic and endothelial lineages. Genesis *34*, 251-256.

Gerrits, A., Dykstra, B., Kalmykowa, O.J., Klauke, K., Verovskaya, E., Broekhuis, M., De Haan, G., and Bystrykh, L.V. (2010). Cellular barcoding tool for clonal analysis in the hematopoietic system. Blood *115*, 2610-2618.

Ginhoux, F., Greter, M., Leboeuf, M., Nandi, S., See, P., Gokhan, S., Mehler, M.F., Conway, S.J., Ng, L.G., Stanley, E.R.*, et al.* (2010). Fate mapping analysis reveals that adult microglia derive from primitive macrophages. Science *330*, 841-845.

Glotzbach, J.P., Januszyk, M., Vial, I.N., Wong, V.W., Gelbard, A., Kalisky, T., Thangarajah, H., Longaker, M.T., Quake, S.R., Chu, G.*, et al.* (2011). An Information Theoretic, Microfluidic-Based Single Cell Analysis Permits Identification of Subpopulations among Putatively Homogeneous Stem Cells. PLoS One *6*, e21211.

Goardon, N., Marchi, E., Atzberger, A., Quek, L., Schuh, A., Soneji, S., Woll, P., Mead, A., Alford, K.A., Rout, R.*, et al.* (2011). Coexistence of LMPP-like and GMP-like leukemia stem cells in acute myeloid leukemia. Cancer Cell *19*, 138-152.

Godin, I., and Cumano, A. (2005). Of birds and mice: hematopoietic stem cell development. Int J Dev Biol *49*, 251-257.

Golub, R., and Cumano, A. (2013). Embryonic hematopoiesis. Blood Cells Mol Dis *51*, 226-231.

Gomez Perdiguero, E., Klapproth, K., Schulz, C., Busch, K., Azzoni, E., Crozet, L., Garner, H., Trouillet, C., de Bruijn, M.F., Geissmann, F*., et al.* (2015). Tissue-resident macrophages originate from yolk-sac-derived erythro-myeloid progenitors. Nature *518*, 547-551.

Gomez Perdiguero, E., Schulz, C., and Geissmann, F. (2013). Development and homeostasis of "resident" myeloid cells: The case of the microglia. Glia *61*, 112-120.

Gonzalez-Murillo, A., Lozano, M.L., Montini, E., Bueren, J.A., and Guenechea, G. (2008). Unaltered repopulation properties of mouse hematopoietic stem cells transduced with lentiviral vectors. Blood *112*, 3138-3147.

Goodell, M.A., Brose, K., Paradis, G., Conner, A.S., and Mulligan, R.C. (1996). Isolation and Functional Properties of Murine Hematopoietic Stem Cells that are Replicating In Vivo. J Exp Med *183*, 1797-1806.

Goodell, M.A., Rosenzweig, M., Kim, H., Marks, D.F., DeMaria, M., Paradis, G., Grupp, S.A., Sieff, C.A., Mulligan, R.C., and Johnson, R.P. (1997). Dye efflux studies suggest that hematopoietic stem cells expressing low or undetectable levels of CD34 antigen exist in multiple species. Nat Med *3*, 1337-1345.

Greaves, M.F., and Wiemels, J. (2003). Origins of chromosome translocations in childhood leukaemia. Nat Rev Cancer *3*, 639-649.

Grosselin, J., Sii-Felice, K., Payen, E., Chretien, S., Roux, D.T., and Leboulch, P. (2013). Arrayed lentiviral barcoding for quantification analysis of hematopoietic dynamics. Stem Cells *31*, 2162-2171.

Haas, S., Hansson, J., Klimmeck, D., Loeffler, D., Velten, L., Uckelmann, H., Wurzer, S., Prendergast, A.M., Schnell, A., Hexel, K*., et al.* (2015). Inflammation-induced emergency megakaryopoiesis driven by hematopoietic stem cell-like megakaryocyte progenitors. Cell Stem Cell *17*, 422-434.

Hamanaka, S., Ooehara, J., Morita, Y., Ema, H., Takahashi, S., Miyawaki, A., Otsu, M., Yamaguchi, T., Onodera, M., and Nakauchi, H. (2013). Generation of transgenic mouse line expressing Kusabira Orange throughout body, including erythrocytes, by random segregation of provirus method. Biochem Biophys Res Commun *435*, 586-591.

Harrison, D.E. (1980). Competitive repopulation: a new assay for long-term stem cell functional capacity. Blood *55*, 77-81.

Harrison, D.E., Jordan, C.T., Zhong, R.K., and Astle, C.M. (1993). Primitive hemopoietic stem cells: direct assay of most productive populations by competitive repopulation with simple binomial, correlation and covariance calculations. Exp Hematol *21*, 206-219.

Hayashi, S., and McMahon, A.P. (2002). Efficient recombination in diverse tissues by a tamoxifen-inducible form of Cre: a tool for temporally regulated gene activation/inactivation in the mouse. Dev Biol *244*, 305-318.

Hayward, C., Cramer, E.M., Song, Z., Zheng, S., Fung, R., Massé, J., Stead, R.H., and Podor, T.J. (1998). Studies of multimerin in human endothelial cells. Blood *91*, 1304-1317.

Heffner, G.C., Clutter, M.R., Nolan, G.P., and Weissman, I.L. (2011). Novel hematopoietic progenitor populations revealed by direct assessment of GATA1 protein expression and cMPL signaling events. Stem Cells *29*, 1774-1782.

Hepworth, M.R., and Sonnenberg, G.F. (2014). Regulation of the adaptive immune system by innate lymphoid cells. Curr Opin Immunol *27*, 75-82.

Hobeika, E., Thiemann, S., Storch, B., Jumaa, H., Nielsen, P.J., Pelanda, R., and Reth, M. (2006). Testing gene function early in the B cell lineage in mb1-cre mice. Proc Natl Acad Sci U S A *103*, 13789-13794.

Hock, H. (2010). Some hematopoietic stem cells are more equal than others. J Exp Med *207*, 1127-1130.

Hoeffel, G., Chen, J., Lavin, Y., Low, D., Almeida, F.F., See, P., Beaudin, A.E., Lum, J., Low, I., Forsberg, E.C.*, et al.* (2015). C-Myb+ erythro-myeloid progenitor-derived fetal monocytes give rise to adult tissue-resident macrophages. Immunity *42*, 665-678.

Hoeffel, G., and Ginhoux, F. (2015). Ontogeny of tissue-resident macrophages. Front Immunol *6*, 486.

Hoeffel, G., Wang, Y., Greter, M., See, P., Teo, P., Malleret, B., Leboeuf, M., Low, D., Oller, G., Almeida, F.*, et al.* (2012). Adult Langerhans cells derive predominantly from embryonic fetal liver monocytes with a minor contribution of yolk sac-derived macrophages. J Exp Med *209*, 1167-1181.

Holmes, R., and Zúñiga-Pflücker, J.C. (2009). The OP9-DL1 system: generation of T-lymphocytes from embryonic or hematopoietic stem cells in vitro. Cold Spring Harb Protoc *2009*, pdb prot5156.

Hu, Y., and Smyth, G.K. (2009). ELDA: Extreme limiting dilution analysis for comparing depleted and enriched populations in stem cell and other assays. J Immunol Methods *347*, 70-78.

Hume, D.A. (2011). Applications of myeloid-specific promoters in transgenic mice support in vivo imaging and functional genomics but do not support the concept of distinct macrophage and dendritic cell lineages or roles in immunity. J Leukoc Biol *89*, 525-538.

Igarashi, H., Gregory, S.C., Yokota, T., Sakaguchi, N., and Kincade, P.W. (2002). Transcription from the RAG1 Locus Marks the Earliest Lymphocyte Progenitors in Bone Marrow. Immunity *17*, 117-130.

Ikawa, T., Masuda, K., Lu, M., Minato, N., Katsura, Y., and Kawamoto, H. (2004). Identification of the earliest prethymic T-cell progenitors in murine fetal blood. Blood *103*, 530-537.

Inlay, M.A., Bhattacharya, D., Sahoo, D., Serwold, T., Seita, J., Karsunky, H., Plevritis, S.K., Dill, D.L., and Weissman, I.L. (2009). Ly6d marks the earliest stage of B-cell specification and identifies the branchpoint between B-cell and T-cell development. Genes Dev *23*, 2376-2381.

Inlay, M.A., Serwold, T., Mosley, A., Fathman, J.W., Dimov, I.K., Seita, J., and Weissman, I.L. (2014). Identification of multipotent progenitors that emerge prior to hematopoietic stem cells in embryonic development. Stem Cell Reports *2*, 457-472.

Iwama, A., Oguro, H., Negishi, M., Kato, Y., Morita, Y., Tsukui, H., Ema, H., Kamijo, T., Katoh-Fukui, Y., Koseki, H.*, et al.* (2004). Enhanced self-renewal of hematopoietic stem cells mediated by the polycomb gene product Bmi-1. Immunity *21*, 843-851.

Iwasaki, A., and Medzhitov, R. (2015). Control of adaptive immunity by the innate immune system. Nat Immunol *16*, 343-353.

Iwasaki, H., and Akashi, K. (2007a). Hematopoietic developmental pathways: on cellular basis. Oncogene *26*, 6687-6696.

Iwasaki, H., and Akashi, K. (2007b). Myeloid lineage commitment from the hematopoietic stem cell. Immunity *26*, 726-740.

Iwasaki, H., Mizuno, S., Arinobu, Y., Ozawa, H., Mori, Y., Shigematsu, H., Takatsu, K., Tenen, D.G., and Akashi, K. (2006). The order of expression of transcription factors directs hierarchical specification of hematopoietic lineages. Genes Dev *20*, 3010-3021.

Iwasaki, H., Mizuno, S., Wells, R., Cantor, A., Watanabe, S., and Akashi, K. (2003). GATA-1 Converts Lymphoid and Myelomonocytic Progenitors into the Megakaryocyte/Erythrocyte Lineages. Immunity *19*, 451-462.

Iwasaki, H., Mizuno, S.I., Mayfield, R., Shigematsu, H., Arinobu, Y., Seed, B., Gurish, M.F., Takatsu, K., and Akashi, K. (2005a). Identification of eosinophil lineage-committed progenitors in the murine bone marrow. J Exp Med *201*, 1891-1897.

Iwasaki, H., Somoza, C., Shigematsu, H., Duprez, E.A., Iwasaki-Arai, J., Mizuno, S., Arinobu, Y., Geary, K., Zhang, P., Dayaram, T*., et al.* (2005b). Distinctive and indispensable roles of PU.1 in maintenance of hematopoietic stem cells and their differentiation. Blood *106*, 1590-1600.

Iwasaki-Arai, J., Iwasaki, H., Miyamoto, T., Watanabe, S., and Akashi, K. (2003). Enforced granulocyte/macrophage colony-stimulating factor signals do not support lymphopoiesis, but instruct lymphoid to myelomonocytic lineage conversion. J Exp Med *197*, 1311-1322.

Jacobson, L.O., Marks, E.K., Gaston, E.O., and Zirkle, R.E. (1949). Effect of spleen protection on mortality following X-irradiation. J Lab Clin Med *34*, 1538-1543.

Jacobson, L.O., Simmons, E.L., Marks, E.K., and Eldredge, J.H. (1951). Recovery from radiation injury. Science *113*, 510-511.

Jeimy, S.B., Tasneem, S., Cramer, E.M., and Hayward, C.P. (2008). Multimerin 1. Platelets *19*, 83-95.

Johns, J.L., and Christopher, M.M. (2012). Extramedullary hematopoiesis: a new look at the underlying stem cell niche, theories of development, and occurrence in animals. Vet Pathol *49*, 508-523.

Jones, R.J., Wagner, J.E., Celano, P., Zicha, M.S., and Sharkis, S.J. (1990). Separation of pluripotent haematopoietic stem cells from spleen colony-forming cells. Nature *347*, 188-189.

Jordan, C.T., and Lemischka, I.R. (1990). Clonal and systemic analysis of long-term hematopoiesis in the mouse. Genes Dev *4*, 220-232.

Jung, M.K., Park, Y., Song, S.B., Cheon, S.Y., Park, S., Houh, Y., Ha, S., Kim, H.J., Park, J.M., Kim, T.S*., et al.* (2011). Erythroid differentiation regulator 1, an interleukin 18-regulated gene, acts as a metastasis suppressor in melanoma. J Invest Dermatol *131*, 2096-2104.

Just, U., Stocking, C., Spooncer, E., Dexter, T.M., and Ostertag, W. (1991). Expression of the GM-CSF gene after retroviral transfer in hematopoietic stem cell lines induces synchronous granulocyte–macrophage differentiation. Cell *64*, 1163-1173.

Karsunky, H., Inlay, M.A., Serwold, T., Bhattacharya, D., and Weissman, I.L. (2008). Flk2+ common lymphoid progenitors possess equivalent differentiation potential for the B and T lineages. Blood *111*, 5562-5570.

Katsura, Y., and Kawamoto, H. (2001). Stepwise lineage restriction of progenitors in lympho-myelopoiesis. Intern Rev Immunol *20*, 1-20.

Kaushansky, K. (2006). Lineage-Specific Hematopoietic Growth Factors. N Engl J Med *354*, 2034-2045.

Kawamoto, H. (2006). A close developmental relationship between the lymphoid and myeloid lineages. Trends Immunol *27*, 169-175.

Kawamoto, H., Ikawa, T., Ohmura, K., Fujimoto, S., and Katsura, Y. (2000). T Cell Progenitors Emerge Earlier Than B Cell Progenitors in the Murine Fetal Liver. Immunity *12*, 441-450.

Kawamoto, H., and Katsura, Y. (2009). A new paradigm for hematopoietic cell lineages: revision of the classical concept of the myeloid-lymphoid dichotomy. Trends Immunol *30*, 193-200.

Kawamoto, H., Ohmura, K., and Katsure, Y. (1997). Direct evidence for the commitment of hematopoietic stem cells to T, B and myeloid lineages in murine fetal liver. Int Immunol *9*, 1011-1019.

Kawamoto, H., Wada, H., and Katsura, Y. (2010). A revised scheme for developmental pathways of hematopoietic cells: the myeloid-based model. Int Immunol *22*, 65-70.

Kent, D.G., Copley, M.R., Benz, C., Wohrer, S., Dykstra, B.J., Ma, E., Cheyne, J., Zhao, Y., Bowie, M.B., Gasparetto, M.*, et al.* (2009). Prospective isolation and molecular characterization of hematopoietic stem cells with durable self-renewal potential. Blood *113*, 6342-6350.

Khan, J.A., Mendelson, A., Kunisaki, Y., Birbrair, A., Kou, Y., Arnal-Estapé, A., Ma'ayan, A., Bergman, A., Merad, M., and Frenette, P.S. (2015). Fetal liver hematopoietic stem cell niches associate with portal vessels. Science 10.1126/science.aad0084.

Kiel, M.J., and Morrison, S.J. (2008). Uncertainty in the niches that maintain haematopoietic stem cells. Nat Rev Immunol *8*, 290-301.

Kiel, M.J., Yilmaz, O.H., Iwashita, T., Terhorst, C., and Morrison, S.J. (2005). SLAM family receptors distinguish hematopoietic stem and progenitor cells and reveal endothelial niches for stem cells. Cell *121*, 1109-1121.

Kieusseian, A., Brunet de la Grange, P., Burlen-Defranoux, O., Godin, I., and Cumano, A. (2012). Immature hematopoietic stem cells undergo maturation in the fetal liver. Development *139*, 3521-3530.

Kim, D., Pertea, G., Trapnell, C., Pimentel, H., Kelley, R., and Salzberg, S. (2013). TopHat2: accurate alignment of transcriptomes in the presence of insertions, deletions and gene fusions. Genome Biology *14*, R36.

Kincade, P.W., Owen, J.J., Igarashi, H., Kouro, T., Yokota, T., and Rossi, M.I. (2002). Nature or nurture? Steady-state lymphocyte formation in adults does not recapitulate ontogeny. Immunol Rev *187*, 116.

Kokkaliaris, K.D., Loeffler, D., and Schroeder, T. (2012). Advances in tracking hematopoiesis at the single-cell level. Curr Opin Hematol *19*, 243-249.

Kondo, M., Scherer, D.C., Miyamoto, T., King, A.G., Akashi, K., and Sugamura, K. (2000). Cell-fate conversion of lymphoid-committed progenitors by instructive actions of cytokines. Nature *407*, 383–386.

Kondo, M., Weissman, I., and Akashi, K. (1997). Identification of clonogenic common lymphoid progenitors in mouse bone marrow. Cell *91*, 661-672.

Koushik, S.V., Wang, J., Rogers, R., Moskophidis, D., Lambert, N.A., Creazzo, T.L., and Conway, S.J. (2001). Targeted inactivation of the sodium-calcium exchanger (Ncx1) results in the lack of a heartbeat and abnormal myofibrillar organization. FASEB J *15*, 1209-1211.

Krieger, T., and Simons, B.D. (2015). Dynamic stem cell heterogeneity. Development *142*, 1396-1406.

Kubagawa, H., Burrows, P.D., and Cooper, M.D. (1997). A novel pair of immunoglobulin-like receptors expressed by B cells and myeloid cells. Proc Natl Acad Sci U S A *94*, 5261-5266.

Kubagawa, H., Chen, C.-C., Torii, I., Cooper, M., Masuda, K., Katsura, Y., and Kawamoto, H. (2008). Recent progress on paired immunoglobulin-like receptors. In How the Immune System Recognizes Self and Nonself, D. Kitamura, ed. (Springer Japan), pp. 83-98.

Kumaravelu, P., Hook, L., Morrison, A.M., Ure, J., Zhao, S., Zuyev, S., Ansell, J., and Medvinsky, A. (2002). Quantitative developmental anatomy of definitive haematopoietic stem cells/long-term repopulating units (HSC/RUs): role of the aorta-gonad-mesonephros (AGM) region and the yolk sac in colonisation of the mouse embryonic liver. Development *129*, 4891-4899.

Kuwata, N., Igarashi, H., Ohmura, T., Aizawa, S., and Sakaguchi, N. (1999). Cutting Edge: Absence of expression of RAG1 in peritoneal B-1 cells detected by knocking into RAG1 locus with green fluorescent protein gene. J Immunol *163*, 6355-6359.

Lacaud, G., Carlsson, L., and Keller, G. (1998). Identification of a fetal hematopoietic precursor with B cell, T cell, and macrophage potential. Immunity *9*, 827-838.

Lai, A.Y., and Kondo, M. (2006). Asymmetrical lymphoid and myeloid lineage commitment in multipotent hematopoietic progenitors. J Exp Med *203*, 1867-1873.

Lai, A.Y., Lin, S.M., and Kondo, M. (2005). Heterogeneity of Flt3-Expressing Multipotent Progenitors in Mouse Bone Marrow. The Journal of Immunology *175*, 5016-5023.

Laiosa, C.V., Stadtfeld, M., and Graf, T. (2006). Determinants of lymphoid-myeloid lineage diversification. Annu Rev Immunol *24*, 705-738.

Lancrin, C., Sroczynska, P., Stephenson, C., Allen, T., Kouskoff, V., and Lacaud, G. (2009). The haemangioblast generates haematopoietic cells through a haemogenic endothelium stage. Nature *457*, 892-895.

Langmead, B., Trapnell, C., Pop, M., and Salzberg, S.L. (2009). Ultrafast and memory-efficient alignment of short DNA sequences to the human genome. Genome Biol *10*, R25.

Laurenti, E., Varnum-Finney, B., Wilson, A., Ferrero, I., Blanco-Bose, W.E., Ehninger, A., Knoepfler, P.S., Cheng, P.F., MacDonald, H.R., Eisenman, R.N.*, et al.* (2008). Hematopoietic stem cell function and survival depend on c-Myc and N-Myc activity. Cell Stem Cell *3*, 611-624.

Lemischka, I.R., Raulet, D.H., and Mulligan, R.C. (1986). Developmental Potential and Dynamic Behavior of Hematopoietic Stem Cells. Cell *45*, 917-927.

Lin, Y., Yoder, M.C., and Yoshimoto, M. (2014). Lymphoid progenitor emergence in the murine embryo and yolk sac precedes stem cell detection. Stem Cells Dev *23*, 1168-1177.

Liu, C., Saito, F., Liu, Z., Lei, Y., Uehara, S., Love, P., Lipp, M., Kondo, S., Manley, N., and Takahama, Y. (2006). Coordination between CCR7- and CCR9-mediated chemokine signals in prevascular fetal thymus colonization. Blood *108*, 2531-2539.

Liuba, K., Pronk, C., Stott, S.R., and Jacobsen, S.E. (2009). Polyclonal T-cell reconstitution of X-SCID recipients after in utero transplantation of lymphoid-primed multipotent progenitors. Blood *113*, 4790-4798.

Lorenz, E., Uphoff, E.D., Reid, T.R., and Shelton, E. (1951). Modification of acute irradiation injury in mice and guinea pigs by bone marrow injection. Radiology *58*, 863-877.

Lotem, J., and Sachs, L. (2002). Cytokine control of developmental programs in normal hematopoiesis and leukemia. Oncogene *21*, 3284-3294.

Lu, L.-S., Wang, S.-J., and Auerbach, R. (1996). In vitro and in vivo differentiation into B cells, T cells, and myeloid cells of primitive yolk sac hematopoietic precursor cells expanded >100-fold by coculture with a clonal yolk sac endothelial cell line. PNAS *93*, 14782-14787.

Lu, M., Kawamoto, H., Katsube, Y., Ikawa, T., and Katsura, Y. (2002). The Common Myelolymphoid Progenitor: A Key Intermediate Stage in Hemopoiesis Generating T and B Cells. J Immunol *169*, 3519-3525.

Lu, R., Neff, N.F., Quake, S.R., and Weissman, I.L. (2011). Tracking single hematopoietic stem cells in vivo using high-throughput sequencing in conjunction with viral genetic barcoding. Nat Biotechnol *29*, 928-933.

Luc, S., Anderson, K., Kharazi, S., Buza-Vidas, N., Böiers, C., Jensen, C.T., Ma, Z., Wittmann, L., and Jacobsen, S.E. (2008a). Down-regulation of Mpl marks the transition to lymphoid-primed multipotent progenitors with gradual loss of granulocyte-monocyte potential. Blood *111*, 3424-3434.

Luc, S., Buza-Vidas, N., and Jacobsen, S.E. (2007). Biological and molecular evidence for existence of lymphoid-primed multipotent progenitors. Ann N Y Acad Sci *1106*, 89-94.

Luc, S., Buza-Vidas, N., and Jacobsen, S.E. (2008b). Delineating the cellular pathways of hematopoietic lineage commitment. Semin Immunol *20*, 213-220.

Luc, S., Luis, T.C., Boukarabila, H., Macaulay, I.C., Buza-Vidas, N., Bouriez-Jones, T., Lutteropp, M., Woll, P.S., Loughran, S.J., Mead, A.J.*, et al.* (2012). The earliest thymic T cell progenitors sustain B cell and myeloid lineage potential. Nat Immunol *13*, 412-419.

Lux, C.T., Yoshimoto, M., McGrath, K., Conway, S.J., Palis, J., and Yoder, M.C. (2008). All primitive and definitive hematopoietic progenitor cells emerging before E10 in the mouse embryo are products of the yolk sac. Blood *111*, 3435-3438.

Maehle, A.H. (2011). Ambiguous cells: the emergence of the stem cell concept in the nineteenth and twentieth centuries. Notes and Records of the Royal Society *65*, 359-378.

Majeti, R., Park, C.Y., and Weissman, I.L. (2007). Identification of a hierarchy of multipotent hematopoietic progenitors in human cord blood. Cell Stem Cell *1*, 635-645.

Mallaney, C., Kothari, A., Martens, A., and Challen, G.A. (2014). Clonal-level responses of functionally distinct hematopoietic stem cells to trophic factors. Exp Hematol *42*, 317-327 e312.

Mansson, R., Hultquist, A., Luc, S., Yang, L., Anderson, K., Kharazi, S., Al-Hashmi, S., Liuba, K., Thoren, L., Adolfsson, J.*, et al.* (2007). Molecular evidence for hierarchical transcriptional lineage priming in fetal and adult stem cells and multipotent progenitors. Immunity *26*, 407-419.

Mansson, R., Zandi, S., Welinder, E., Tsapogas, P., Sakaguchi, N., Bryder, D., and Sigvardsson, M. (2010). Single-cell analysis of the common lymphoid progenitor compartment reveals functional and molecular heterogeneity. Blood *115*, 2601-2609.

Manz, M.G., Miyamoto, T., Akashi, K., and Weissman, I.L. (2002). Prospective isolation of human clonogenic common myeloid progenitors. Proc Natl Acad Sci U S A *99*, 11872-11877.

Masuda, K., Kubagawa, H., Ikawa, T., Chen, C.C., Kakugawa, K., Hattori, M., Kageyama, R., Cooper, M.D., Minato, N., Katsura, Y.*, et al.* (2005). Prethymic T-cell development defined by the expression of paired immunoglobulin-like receptors. EMBO J *24*, 4052-4060.

Matatall, K.A., Shen, C.C., Challen, G.A., and King, K.Y. (2014). Type II interferon promotes differentiation of myeloid-biased hematopoietic stem cells. Stem Cells *32*, 3023-3030.

Matsuoka, S. (2001). CD34 expression on long-term repopulating hematopoietic stem cells changes during developmental stages. Blood *97*, 419-425.

Matutes, E., Pickl, W.F., van't Veer, M., Morilla, R., Swansbury, J., Strobl, H., Attarbaschi, A., Hopfinger, G., Ashley, S., Bene, M.C*., et al.* (2011). Mixed-phenotype acute leukemia: clinical and laboratory features and outcome in 100 patients defined according to the WHO 2008 classification. Blood *117*, 3163-3171.

McCormack, M.P., Forster, A., Drynan, L., Pannell, R., and Rabbitts, T.H. (2003a). The LMO2 T-cell oncogene is activated via chromosomal translocations or retroviral insertion during gene therapy but has no mandatory role in normal T-cell development. Molecular and Cellular Biology *23*, 9003-9013.

McCormack, M.P., Forster, A., Drynan, L., Pannell, R., and Rabbitts, T.H. (2003b). The LMO2 T-cell oncogene is activated via chromosomal translocations or retroviral insertion during gene therapy but has no mandatory role in normal T-cell development. Mol Cell Biol *23*, 9003-9013.

McGrath, K.E., Frame, J.M., Fegan, K.H., Bowen, J.R., Conway, S.J., Catherman, S.C., Kingsley, P.D., Koniski, A.D., and Palis, J. (2015). Distinct sources of hematopoietic progenitors emerge before HSCs and provide functional blood cells in the mammalian embryo. Cell Rep *11*, 1892-1904.

McGrath, K.E., Koniski, A.D., Malik, J., and Palis, J. (2003). Circulation is established in a stepwise pattern in the mammalian embryo. Blood *101*, 1669-1676.

McGrath, K.E., and Palis, J. (2005). Hematopoiesis in the yolk sac: more than meets the eye. Exp Hematol *33*, 1021-1028.

McGrath, R.T., McRae, E., Smith, O.P., and O'Donnell, J.S. (2010). Platelet von Willebrand factor - structure, function and biological importance. Br J Haematol *148*, 834-843.

McKenna, H.J., Stocking, K.L., Miller, R.E., Brasel, K., De Smedt, T., Maraskovsky, E., Maliszewski, C.R., Lynch, D.H., Smith, J., Pulendran, B*., et al.* (2000). Mice lacking flt3 ligand have deficient hematopoiesis affecting hematopoietic progenitor cells, dendritic cells, and nature killer cells. Blood *95*, 3489-3497.

McKinney-Freeman, S.L., Naveiras, O., Yates, F., Loewer, S., Philitas, M., Curran, M., Park, P.J., and Daley, G.Q. (2009). Surface antigen phenotypes of hematopoietic stem cells from embryos and murine embryonic stem cells. Blood *114*, 268-278.

Mebius, R.E., Miyamoto, T., Christensen, J., Domen, J., Cupedo, T., Weissman, I., and Akashi, K. (2001). The Fetal Liver Counterpart of Adult Common Lymphoid Progenitors Gives Rise to All Lymphoid Lineages, CD45+ CD4+ CD3- Cells, As Well As Macrophages. J Immunol *166*, 6593-6601.

Medvinsky, A., and Dzierzak, E. (1996). Definitive hematopoiesis is autonomously initiated by the AGM region. Cell *86*, 897-906.

Medvinsky, A., Rybtsov, S., and Taoudi, S. (2011). Embryonic origin of the adult hematopoietic system: advances and questions. Development *138*, 1017-1031.

Medvinsky, A., Samoylina, N.L., Müller, A.M., and Dzierzak, E. (1993). An early pre-liver intra-embryonic source of CFU-S in the developing mouse. Nature *364*, 64-67.

Medvinsky, A., Taoudi, S., Mendes, S., and Dzierzak, E. (2008). Analysis and manipulation of hematopoietic progenitor and stem cells from murine embryonic tissues. Curr Protoc Stem Cell Biol *Chapter 2*, Unit 2A 6.

Mercer, E.M., Lin, Y.C., and Murre, C. (2011). Factors and networks that underpin early hematopoiesis. Semin Immunol *23*, 317-325.

Mikkola, H.K., and Orkin, S.H. (2006). The journey of developing hematopoietic stem cells. Development *133*, 3733-3744.

Mildner, A., and Jung, S. (2014). Development and function of dendritic cell subsets. Immunity *40*, 642-656.

Miller, C.L., and Eaves, C.J. (1997). Expansion in vitro of adult murine hematopoietic stem cells with transplantable lympho-myeloid reconstituting ability. PNAS *94*, 13648-13653.

Miller, C.L., Rebel, V.I., Helgason, C.D., Lansdorp, P.M., and Eaves, C.J. (1997). Impaired Steel Factor responsiveness differentially affects the detection and long-term maintenance of fetal liver hematopoietic stem cells in vivo. Blood *89*, 1214-12223.

Miller, J.P., and Allman, D. (2005). Linking age-related defects in B lymphopoiesis to the aging of haematopoietic stem cells. Semin Immunol *17*, 321-329.

Miller, R.G., and Phillips, R.A.J. (1969). Separation of cells by velocity sedimentation. Cell Physiol *73*, 191-201.

Miltenyi, S., Müller, W., Weichel, W., and Radbruch, A. (1990). High gradient magnetic cell separation with MACS. Cytometry *11*, 231-238.

Mombaerts, P., Iacomini, J., Johnson, R.S., Herrup, K., Tonegawa, S., and Papaioannou, V.E. (1992). RAG-1-deficient mice have no mature B and T lymphocytes. Cell *68*, 869-877.

Moore, M.A., and Metcalf, D. (1970). Ontogeny of the Haemopoietic System: Yolk Sac Origin of In Vivo and In Vitro Colony Forming Cells in the Developing Mouse Embryo. Br J Haematol *18*, 279-296.

Moreira, P.N., Pozueta, J., Giraldo, P., Gutiérrez-Adán, A., and Montoliu, L. (2006). Generation of yeast artificial chromosome transgenic mice by intracytoplasmic sperm injection. Methods Mol Biol *349*, 151-161.

Moretti, A., Caron, L., Nakano, A., Lam, J.T., Bernshausen, A., Chen, Y., Qyang, Y., Bu, L., Sasaki, M., Martin-Puig, S.*, et al.* (2006). Multipotent embryonic isl1+ progenitor cells lead to cardiac, smooth muscle, and endothelial cell diversification. Cell *127*, 1151-1165.

Morita, Y., Ema, H., and Nakauchi, H. (2010). Heterogeneity and hierarchy within the most primitive hematopoietic stem cell compartment. J Exp Med *207*, 1173-1182.

Morrison, S.J., Hemmati, H.D., Wandycz, A.M., and Weissman, I. (1995). The purification and characterization of fetal liver hematopoietic stem cells. Proc Natl Acad Sci U S A *92*, 10302–10306.

Morrison, S.J., and Scadden, D.T. (2014). The bone marrow niche for haematopoietic stem cells. Nature *505*, 327-334.

Morrison, S.J., Wandycz, A.M., Akashi, K., Globerson, A., and Weissman, I. (1996). The aging of hematopoietic stem cells. Nat Med *2*, 1011-1016.

Morrison, S.J., Wandycz, A.M., Hemmati, H.D., Wright, D.E., and Weissman, I. (1997). Identification of a lineage of multipotent hematopoietic progenitors. Development *124*, 1929-1939.

Morrison, S.J., and Weissman, I. (1994). The Long-Term Repopulating Subset of Hematopoietic Stem Cells Is Deterministic and Isolatable by Phenotype. Immunity *1*, 661-673.

Morstyn, G., Nicola, N., and Metcalf, D. (1980). Purification of hemopoietic progenitor cells from human marrow using a fucose-binding lectin and cell sorting. Blood *56*, 798-805.

Müller, A.M., Medvinsky, A., Strouboulis, J., Grosveld, F., and Dzierzak, E. (1994). Development of hematopoietic stem cell activity in the mouse embryo. Immunity *1*, 291-301.

Müller-Sieburg, C.E., Cho, R.H., Karlsson, L., Huang, J.F., and Sieburg, H.B. (2004). Myeloid-biased hematopoietic stem cells have extensive self-renewal capacity but generate diminished lymphoid progeny with impaired IL-7 responsiveness. Blood *103*, 4111-4118.

Müller-Sieburg, C.E., Cho, R.H., Thoman, M., Adkins, B., and Sieburg, H.B. (2002). Deterministic regulation of hematopoietic stem cell self-renewal and differentiation. Blood *100*, 1302-1309.

Müller-Sieburg, C.E., Sieburg, H.B., Bernitz, J.M., and Cattarossi, G. (2012). Stem cell heterogeneity: implications for aging and regenerative medicine. Blood *119*, 3900-3907.

Müller-Sieburg, C.E., Whitlock, C.A., and Weissman, I. (1986). Isolation of Two Early B Lymphocyte Progenitors from Mouse Marrow: A Committed Pre-Pre-B Cell and a Clonogenic Thy-1lo Hematopoietic Stem Cell. Cell *44*, 653-662.

Murphy, K., ed. (2014). Janeway's Immunobiology, 8th edition (Garland Science, New York).

Na Nakorn, T., Traver, D., Weissman, I.L., and Akashi, K. (2002). Myeloerythroid-restricted progenitors are sufficient to confer radioprotection and provide the majority of day 8 CFU-S. J Clin Invest *109*, 1579-1585.

Nakano, T., Kodama, H., and Honjo, T. (1994). Generation of lymphohematopoietic cells from embryonic stem cells in culture. Science *265*, 1098-1101.

Nakauchi, H., Sudo, K., and Ema, H. (2001). Quantitative Assessment of the Stem Cell Self-Renewal Capacity. Ann NY Acad Sci *938*, 18-25.

Nicola, N.A. (1989). Hemopoietic cell growth factors and their receptors. Annu Rev Biochem *58*, 45-77.

Nijhof, W., Goris, H., Dontje, B., Dresz, J., and Loeffler, M. (1993). Optimal erythroid cell production during erythropoietin treatment of mice occurs by exploiting the splenic microenvironment. Exp Hematol *21*, 496-501.

Nishikii, H., Kanazawa, Y., Umemoto, T., Goltsev, Y., Matsuzaki, Y., Matsushita, K., Yamato, M., Nolan, G.P., Negrin, R., and Chiba, S. (2015). Unipotent megakaryopoietic pathway bridging hematopoietic stem cells and mature megakaryocytes. Stem Cells *33*, 2196-2207.

Nottingham, W.T., Jarratt, A., Burgess, M., Speck, C.L., Cheng, J.F., Prabhakar, S., Rubin, E.M., Li, P.S., Sloane-Stanley, J., Kong, A.S.J*., et al.* (2007). Runx1-mediated hematopoietic stem-cell emergence is controlled by a Gata/Ets/SCL-regulated enhancer. Blood *110*, 4188-4197.

Nowell, P.C., Cole, P.J., Habermeyer, J.G., and Roan, P.L. (1956). Growth and continued function of rat marrow cells in x-radiated mice. Cancer Res *16*, 258–261.

Ogawa, M. (1993). Differentiation and proliferation of hematopoietic stem cells. Blood *81*, 2844-2853.

Ogawa, M. (2002). Changing phenotypes of hematopoietic stem cells. Exp Hematol *30*, 3-6.

Oguro, H., Ding, L., and Morrison, S.J. (2013). SLAM family markers resolve functionally distinct subpopulations of hematopoietic stem cells and multipotent progenitors. Cell Stem Cell *13*, 102-116.

Orkin, S.H. (2000). Diversification of haematopoietic stem cells to specific lineages. Nat Rev Genet *1*, 57-64.

Orkin, S.H., and Zon, L.I. (2008). Hematopoiesis: an evolving paradigm for stem cell biology. Cell *132*, 631-644.

Osawa, M., Hanada, K.-I., Hamada, H., and Nakauchi, H. (1996). Long-Term Lymphohematopoietic Reconstitution by a Single CD34-Low/Negative Hematopoietic Stem Cell. Science *273*, 242-245.

Ottersbach, K., and Dzierzak, E. (2005). The murine placenta contains hematopoietic stem cells within the vascular labyrinth region. Dev Cell *8*, 377-387.

Ottersbach, K., and Dzierzak, E. (2010). The placenta as a haematopoietic organ. Int J Dev Biol *54*, 1099-1106.

Ottersbach, K., Smith, A., Wood, A., and Gottgens, B. (2010). Ontogeny of haematopoiesis: recent advances and open questions. Br J Haematol *148*, 343-355.

Palis, J., Robertson, S., Kennedy, M., Wall, C., and Keller, G. (1999). Development of erythroid and myeloid progenitors in the yolk sac and embryo proper of the mouse. Development *126*, 5073-5084.

Palis, J., and Yoder, M.C. (2001). Yolk-sac hematopoiesis: The first blood cells of mouse and man. Exp Hematol *29*, 927-936.

Paul, F., Arkin, Y.a., Giladi, A., Jaitin, Diego A., Kenigsberg, E., Keren-Shaul, H., Winter, D., Lara-Astiaso, D., Gury, M., Weiner, A*., et al.* (2015). Transcriptional Heterogeneity and Lineage Commitment in Myeloid Progenitors. Cell 10.1016/j.cell.2015.11.013.

Pereira, C., Clarke, E., and Damen, J. (2007). Hematopoietic Colony-Forming Cell Assays. Methods Mol Biol *407*, 177-208.

Peschon, J.J., Morrissey, P.J., Grabstein, K.H., Ramsdell, F.J., Maraskovsky, E., Gliniak, B.C., Park, L.S., Ziegler, S.F., Williams, D.E., Ware, C.B*., et al.* (1994). Early lymphocyte expansion is severely impaired in interleukin 7 receptor-deficient mice. J Exp Med *180*, 1955-1960.

Peyvandi, F., Garagiola, I., and Baronciani, L. (2011). Role of von Willebrand factor in the haemostasis. Blood Transfus *9 Suppl 2*, s3-8.

Picelli, S., Faridani, O.R., Björklund, Å.K., Winberg, G., Sagasser, S., and Sandberg, R. (2014). Full-length RNA-seq from single cells using Smart-seq2. Nat Protoc *9*, 171-181.

Pietras, E.M., Reynaud, D., Kang, Y.A., Carlin, D., Calero-Nieto, F.J., Leavitt, A.D., Stuart, J.M., Gottgens, B., and Passegue, E. (2015). Functionally distinct subsets of lineage-biased multipotent progenitors control blood production in normal and regenerative conditions. Cell Stem Cell *17*, 35-46.

Pina, C., Fugazza, C., Tipping, A.J., Brown, J., Soneji, S., Teles, J., Peterson, C., and Enver, T. (2012). Inferring rules of lineage commitment in haematopoiesis. Nat Cell Biol *14*, 287-294.

Pluznick, D.H., and Sachs, L.J. (1965). The cloning of normal "mast" cells in tissue culture. Cell Physiol *66*, 319-324.

Pronk, C.J., and Bryder, D. (2011). Flow cytometry-based identification of immature myeloerythroid development. Methods Mol Biol *699*, 275-293.

Pronk, C.J., Rossi, D.J., Mansson, R., Attema, J.L., Norddahl, G.L., Chan, C.K., Sigvardsson, M., Weissman, I.L., and Bryder, D. (2007). Elucidation of the phenotypic, functional, and molecular topography of a myeloerythroid progenitor cell hierarchy. Cell Stem Cell *1*, 428-442.

Purton, L.E., and Scadden, D.T. (2007). Limiting factors in murine hematopoietic stem cell assays. Cell Stem Cell *1*, 263-270.

Ramalho-Santos, M., and Willenbring, H. (2007). On the origin of the term "stem cell". Cell Stem Cell *1*, 35-38.

Ramond, C., Berthault, C., Burlen-Defranoux, O., de Sousa, A.P., Guy-Grand, D., Vieira, P., Pereira, P., and Cumano, A. (2014). Two waves of distinct hematopoietic progenitor cells colonize the fetal thymus. Nat Immunol *15*, 27-35.

Ramsköld, D., Luo, S., Wang, Y.C., Li, R., Deng, Q., Faridani, O.R., Daniels, G.A., Khrebtukova, I., Loring, J.F., Laurent, L.C*., et al.* (2012). Full-length mRNA-Seq from single-cell levels of RNA and individual circulating tumor cells. Nat Biotechnol *30*, 777-782.

Reinert, R.B., Kantz, J., Misfeldt, A.A., Poffenberger, G., Gannon, M., Brissova, M., and Powers, A.C. (2012). Tamoxifen-induced Cre-loxP recombination Is prolonged in pancreatic islets of adult mice. PLoS One *7*, e33529.

Reya, T., Morrison, S.J., Clarke, M.F., and Weissman, I. (2001). Stem cells, cancer, and cancer stem cells. Nature *414*, 105-111.

Rhodes, K.E., Gekas, C., Wang, Y., Lux, C.T., Francis, C.S., Chan, D.N., Conway, S., Orkin, S.H., Yoder, M.C., and Mikkola, H.K. (2008). The emergence of hematopoietic stem cells is initiated in the placental vasculature in the absence of circulation. Cell Stem Cell *2*, 252-263.

Richie Ehrlich, L.I., Serwold, T., and Weissman, I. (2011). In vitro assays misrepresent in vivo lineage potentials of murine lymphoid progenitors. Blood *117*, 2618-2624.

Rickert, R.C., Roes, J., and Rajewsky, K. (1997). B lymphocyte-specific, Cre-mediated mutagenesis in mice. Nuc Acid Research *25*, 1317-1318.

Rieger, M.A., Hoppe, P.S., Smejkal, B.M., Eitelhuber, A.C., and Schroeder, T. (2009a). Hematopoietic cytokines can instruct lineage choice. Science *325*, 217-218.

Rieger, M.A., Smejkal, B.M., and Schroeder, T. (2009b). Improved prospective identification of megakaryocyte–erythrocyte progenitor cells. Br J Haematol *144*, 448-451.

Robb, L. (2007). Cytokine receptors and hematopoietic differentiation. Oncogene *26*, 6715-6723.

Roch, A., Trachsel, V., and Lutolf, M.P. (2015). Single cell analysis reveals cell division-independent emergence of megakaryocytes from phenotypic hematopoietic stem cells. Stem Cells 10.1002/stem.2106.

Rybtsov, S., Sobiesiak, M., Taoudi, S., Souilhol, C., Senserrich, J., Liakhovitskaia, A., Ivanovs, A., Frampton, J., Zhao, S., and Medvinsky, A. (2011). Hierarchical organization and early hematopoietic specification of the developing HSC lineage in the AGM region. J Exp Med *208*, 1305-1315.

Samokhvalov, I.M., Samokhvalova, N.I., and Nishikawa, S. (2007). Cell tracing shows the contribution of the yolk sac to adult haematopoiesis. Nature *446*, 1056-1061.

Sanchez, M., Holmes, A., Miles, C., and Dzierzak, E. (1996). Characterization of the first definitive hematopoietic stem cells in the AGM and liver of the mouse embryo. Immunity *5*, 513-525.

Sanjuan-Pla, A., Macaulay, I.C., Jensen, C.T., Woll, P.S., Luis, T.C., Mead, A., Moore, S., Carella, C., Matsuoka, S., Jones, T.B*., et al.* (2013). Platelet-biased stem cells reside at the apex of the haematopoietic stem-cell hierarchy. Nature *502*, 232-236.

Sauer, B., and Henderson, N. (1988). Site-specific DNA recombination in mammalian cells by the Cre recombinase of bacteriophage P1. Proc Natl Acad Sci USA *85*, 5166-5170.

Sauvageau, G., Iscove, N.N., and Humphries, R.K. (2004). In vitro and in vivo expansion of hematopoietic stem cells. Oncogene *23*, 7223-7232.

Schlenner, S.M., Madan, V., Busch, K., Tietz, A., Laufle, C., Costa, C., Blum, C., Fehling, H.J., and Rodewald, H.R. (2010). Fate mapping reveals separate origins of T cells and myeloid lineages in the thymus. Immunity *32*, 426-436.

Schlenner, S.M., and Rodewald, H.R. (2010). Early T cell development and the pitfalls of potential. Trends Immunol *31*, 303-310.

Schmitt, T., and Zúñiga-Pflücker, J.C. (2002). Induction of T Cell Development from Hematopoietic Progenitor Cells by Delta-like-1 In Vitro. Immunity *17*, 749-756.

Schroeder, T. (2005). Tracking hematopoiesis at the single cell level. Ann N Y Acad Sci *1044*, 201-209.

Schroeder, T. (2010). Hematopoietic stem cell heterogeneity: subtypes, not unpredictable behavior. Cell Stem Cell *6*, 203-207.

Schroeder, T. (2011). Long-term single-cell imaging of mammalian stem cells. Nat Methods *8*, S30-35.

Schulz, C., Gomez Perdiguero, E., Chorro, L., Szabo-Rogers, H., Cagnard, N., Kierdorf, K., Prinz, M., Wu, B., Jacobsen, S.E., Pollard, J.W.*, et al.* (2012). A lineage of myeloid cells independent of Myb and hematopoietic stem cells. Science *336*, 86-90.

Seita, J., Ema, H., Ooehara, J., Yamazaki, S., Tadokoro, Y., Yamasaki, A., Eto, K., Takaki, S., Takatsu, K., and Nakauchi, H. (2007). Lnk negatively regulates self-renewal of hematopoietic stem cells by modifying thrombopoietin-mediated signal transduction. Proc Natl Acad Sci U S A *104*, 2349-2354.

Seita, J., and Weissman, I.L. (2010). Hematopoietic stem cell: self-renewal versus differentiation. Wiley Interdiscip Rev Syst Biol Med *2*, 640-653.

Semerad, C.L., Poursine-Laurent, J., Liu, F., and Link, D.C. (1999). A role for G-CSF receptor signaling in the regulation of hematopoietic cell function but not lineage commitment ordifferentiation. Immunity *11*, 153-161.

Shah, N.A., Levesque, M.J., Raj, A., and Sarkar, C.A. (2015). Robust hematopoietic progenitor cell commitment in the presence of a conflicting cue. J Cell Sci *128*, 3009-3017.

Sharma, Y., Astle, C.M., and Harrison, D.E. (2007). Heterozygous Kit mutants with little or no apparent anemia exhibit large defects in overall hematopoietic stem cell function. Exp Hematol *35*, 214-220.

Sieburg, H.B., Cho, R.H., Dykstra, B., Uchida, N., Eaves, C.J., and Müller-Sieburg, C.E. (2006). The hematopoietic stem compartment consists of a limited number of discrete stem cell subsets. Blood *107*, 2311-2316.

Siegemund, S., Shepherd, J., Xiao, C., and Sauer, K. (2015). hCD2-iCre and Vav-iCre mediated gene recombination patterns in murine hematopoietic cells. PLoS One *10*, e0124661.

Siminovitch, L., McCulloch, E.A., and Till, J.E. (1963). The distribution of colony-forming cells among spleen colonies. J Cell Comp Physiol *62*, 327-336.

Siminovitch, L., Till, J.E., and McCulloch, E.A. (1964). Decline in colony-forming ability of marrow cells subjected to serial transplantation into irradiated mice. J Cell Comp Physiol *144*, 23-31.

Sitnicka, E., Brakebusch, C., Martensson, I.L., Svensson, M., Agace, W.W., Sigvardsson, M., Buza-Vidas, N., Bryder, D., Cilio, C.M., Ahlenius, H.*, et al.* (2003). Complementary signaling through flt3 and interleukin-7 receptor alpha is indispensable for fetal and adult B cell genesis. J Exp Med *198*, 1495-1506.

Sitnicka, E., Bryder, D., Theilgaard-Monch, K., Buza-Vidas, N., Adolfsson, J., and Jacobsen, S.E. (2002). Key Role of flt3 Ligand in Regulation of the Common Lymphoid Progenitor but Not in Maintenance of the Hematopoietic Stem Cell Pool. Immunity *17*, 463-472.

Sitnicka, E., Buza-Vidas, N., Ahlenius, H., Cilio, C.M., Gekas, C., Nygren, J.M., Mansson, R., Cheng, M., Jensen, C.T., Svensson, M.*, et al.* (2007). Critical role of FLT3 ligand in IL-7 receptor independent T lymphopoiesis and regulation of lymphoid-primed multipotent progenitors. Blood *110*, 2955-2964.

Spangrude, G., Heimfeld, S., and Weissman, I. (1988). Purification and characterization of mouse Hematopoietic Stem Cells. Science *241*, 58-62.

Spangrude, G.J., and Johnson, G.R. (1990). Resting and activated subsets of mouse multipotent haematopoietic stem cells. PNAS *87*, 7433-7437.

Spits, H., and Cupedo, T. (2012). Innate lymphoid cells: emerging insights in development, lineage relationships, and function. Annu Rev Immunol *30*, 647-675.

Srinivas, S., Watanabe, T., Lin, C.-S., William, C.M., Tanabe, Y., Jessel, T.M., and Costantini, F. (2001a). Cre reporter strains produced by targeted insertion of EYFP and ECFP into the ROSA26 locus. BMC Developmental Biology *1*.

Srinivas, S., Watanabe, T., Lin, C.S., William, C.M., Tanabe, Y., Jessell, T.M., and Costantini, F. (2001b). Cre reporter strains produced by targeted insertion of EYFP and ECFP into the ROSA26 locus. BMC Dev Biol *1*, 4.

Stadtfeld, M., Varas, F., and Graf, T. (2005). Fluorescent protein-cell labeling and its application in time-lapse analysis of hematopoietic differentiation. Methods Mol Med *105*, 395-412.

Stoffel, R., Ziegler, S., Ghilardi, N., Ledermann, B., de Sauvage, F.J., and Skoda, R.C. (1999). Permissive role of thrombopoietin and granulocyte colony-stimulating factor receptors in hematopoietic cell fate decisions in vivo. PNAS *96*, 698-702.

Suda, J., Suda, T., and Ogawa, M. (1984). Analysis of differentiation of mouse hemopoietic stem cells in culture by sequential replating of paired progenitors. Blood *64*, 393-399.

Suda, T., Suda, J., and Ogawa, M. (1983). Single-cell origin of mouse hemopoietic colonies expressing multiple lineages in variable combinations. PNAS *80*, 6689-9663.

Sun, J., Ramos, A., Chapman, B., Johnnidis, J.B., Le, L., Ho, Y.J., Klein, A., Hofmann, O., and Camargo, F.D. (2014). Clonal dynamics of native haematopoiesis. Nature 10.1038/nature13824.

Sutherland, H.J., Eaves, C.J., Eaves, A.C., Dragowska, W., and Lansdrop, P.M. (1989). Characterization and Partial Purification of Human Marrow Cells Capable of Initiating Long-Term Hematopoiesis In Vitro. Blood *74*, 1563-1570.

Takahashi, S. (2012). Molecular functions of metallothionein and its role in hematological malignancies. J Hematol Oncol *5*, 41.

Takano, H., Ema, H., Sudo, K., and Nakauchi, H. (2004). Asymmetric division and lineage commitment at the level of hematopoietic stem cells: inference from differentiation in daughter cell and granddaughter cell pairs. J Exp Med *199*, 295-302.

Takeuchi, M., Sekiguchi, T., Hara, T., Kinoshita, T., and Miyajima, A. (2002). Cultivation of aorta-gonad-mesonephros–derived hematopoietic stem cells in the fetal liver microenvironment amplifies long-term repopulating activity and enhances engraftment to the bone marrow. Blood *99*, 1190-1196.

Takizawa, H., Boettcher, S., and Manz, M.G. (2012). Demand-adapted regulation of early hematopoiesis in infection and inflammation. Blood *119*, 2991-3002.

Taniguchi, H., Toyoshima, T., Fukao, K., and Nakauchi, H. (1996). Presence of hematopoietic stem cells in the adult liver. Nat Med *2*, 198-203.

Tehranchi, R., Woll, P., Anderson, M., Buza-Vidas, N., Mizukami, T., Mead, A., Astrand-Grundstrom, I., Strombeck, B., Horvat, A., Ferry, H.*, et al.* (2010). Persistent Malignant Stem Cells in del(5q) Myelodysplasia in Remission. N Engl J Med *363*, 1025-1037.

Thompson, C. (1992). RAG knockouts deliver a one/two punch. Current Biology *2*, 180-182.

Thoren, L., Liuba, K., Bryder, D., Nygren, J., Jensen, C.T., Qian, H., Antonchuk, J., and Jacobsen, S.E. (2008). Kit regulates maintenance of quiescent hematopoietic stem cells. J Immunol *180*, 2045-2053.

Tiedt, R., Schomber, T., Hao-Shen, H., and Skoda, R.C. (2007). Pf4-Cre transgenic mice allow the generation of lineage-restricted gene knockouts for studying megakaryocyte and platelet function in vivo. Blood *109*, 1503-1506.

Till, J.E., and McCulloch, E.A. (1961). A Direct Measurement of the Radiation Sensitivity of Normal Mouse Bone Marrow Cells. Radiation Research *14*, 213-222.

Till, J.E., McCulloch, E.A., and Siminovitch, L. (1964). A stochastic model of stem cell proliferation, based on the growth of spleen colony forming cells. PNAS *51*, 29-36.

Tober, J., Koniski, A., McGrath, K.E., Vemishetti, R., Emerson, R., de Mesy-Bentley, K.K., Waugh, R., and Palis, J. (2007). The megakaryocyte lineage originates from hemangioblast precursors and is an integral component both of primitive and of definitive hematopoiesis. Blood *109*, 1433-1441.

Trevisan, M., and Iscove, N. (1995). Phenotypic analysis of murine long-term hemopoietic reconstituting cells quantitated competitively in vivo and comparison with more advanced colony-forming progeny. J Exp Med *181*, 93-103.

Trevisan, M., Yan, X., and Iscove, N. (1996). Cycle initiation and colony formation in culture by murine marrow cells with long-term reconstituting potential in vivo. Blood *88*, 4149-4158.

Uchida, N., Dykstra, B., Lyons, K.J., Leung, F.Y.K., and Eaves, C.J. (2003). Different in vivo repopulating activities of purified hematopoietic stem cells before and after being stimulated to divide in vitro with the same kinetics. Exp Hematol, 1338–1347.

Uhrin, P., Zaujec, J., Breuss, J.M., Olcaydu, D., Chrenek, P., Stockinger, H., Fuertbauer, E., Moser, M., Haiko, P., Fassler, R.*, et al.* (2010). Novel function for blood platelets and podoplanin in developmental separation of blood and lymphatic circulation. Blood *115*, 3997-4005.

Vazquez, S.E., Inlay, M.A., and Serwold, T. (2015). CD201 and CD27 identify hematopoietic stem and progenitor cells across multiple murine strains independently of Kit and Sca-1. Exp Hematol *43*, 578-585.

Verovskaya, E., Broekhuis, M.J., Zwart, E., Ritsema, M., van Os, R., de Haan, G., and Bystrykh, L.V. (2013). Heterogeneity of young and aged murine hematopoietic stem cells revealed by quantitative clonal analysis using cellular barcoding. Blood 10.1182/blood-2013-01-481135.

Verovskaya, E., Broekhuis, M.J., Zwart, E., Weersing, E., Ritsema, M., Bosman, L.J., van Poele, T., de Haan, G., and Bystrykh, L.V. (2014). Asymmetry in skeletal distribution of mouse hematopoietic stem cell clones and their equilibration by mobilizing cytokines. J Exp Med *211*, 487-497.

Vieira, P., and Cumano, A. (2004). Differentiation of B lymphocytes from hematopoietic stem cells. Methods Mol Biol *271*, 67-76.

Vos, O., Davids, J.A.G., Weyzen, W.W.H., and van Bekkum, D.W. (1956). Evidence for cellular hypothesis in radiation protection by bone marrow cells. Acta Physiol Pharmacol Neerl *4*, 482–486.

Wada, H., Masuda, K., Satoh, R., Kakugawa, K., Ikawa, T., Katsura, Y., and Kawamoto, H. (2008). Adult T-cell progenitors retain myeloid potential. Nature *452*, 768-772.

Walker, J.A., Barlow, J.L., and McKenzie, A.N. (2013). Innate lymphoid cells - how did we miss them? Nat Rev Immunol *13*, 75-87.

Weissman, I. (2006). Stem Cells: Biology, Transplantation, and Political Ethics. Proc Am Phil Soc *150*, 121-147.

Weissman, I., Papaioannou, V., and Gardner, R. (1978). Fetal hematopoietic origins of the adult hemolymphoid system. In Differentiation of normal and neoplastic cells, B. Clarkson, P. Mark, and J.E. Till, eds. (New York: Cold Spring Harbour), pp. 33-47.

Weissman, I.L., and Shizuru, J.A. (2008). The origins of the identification and isolation of hematopoietic stem cells, and their capability to induce donor-specific transplantation tolerance and treat autoimmune diseases. Blood *112*, 3543-3553.

Welner, R.S., Esplin, B.L., Garrett, K.P., Pelayo, R., Luche, H., Fehling, H.J., and Kincade, P.W. (2009). Asynchronous RAG-1 expression during B lymphopoiesis. J Immunol *183*, 7768-7777.

Whitlock, C.A., and Witte, O.N. (1982). Long-term culture of B lymphocytes and their precursors from murine bone marrow. PNAS *79*, 3608-3612.

Wickrema, A., and Kee, B., eds. (2009). Molecular Basis of Hematopoiesis, 1st edition (Springer, New York).

Wilson, A., Laurenti, E., Oser, G., van der Wath, R.C., Blanco-Bose, W., Jaworski, M., Offner, S., Dunant, C.F., Eshkind, L., Bockamp, E.*, et al.* (2008). Hematopoietic stem cells reversibly switch from dormancy to self-renewal during homeostasis and repair. Cell *135*, 1118-1129.

Wilson, A., Murphy, M.J., Oskarsson, T., Kaloulis, K., Bettess, M.D., Oser, G.M., Pasche, A.-C., Knabenhans, C., MacDonald, H.R., and Trumpp, A. (2004). c-Myc controls the balance between hematopoietic stem cell self-renewal and differentiation. Genes Dev *18*, 2747-2763.

Wilson, N.K., Kent, D.G., Buettner, F., Shehata, M., Macaulay, I.C., Calero-Nieto, F.J., Sanchez Castillo, M., Oedekoven, C.A., Diamanti, E., Schulte, R.*, et al.* (2015). Combined Single-Cell Functional and Gene Expression Analysis Resolves Heterogeneity within Stem Cell Populations. Cell Stem Cell *16*, 712-724.

Wohrer, S., Knapp, D.J., Copley, M.R., Benz, C., Kent, D.G., Rowe, K., Babovic, S., Mader, H., Oostendorp, R.A., and Eaves, C.J. (2014). Distinct stromal cell factor combinations can separately control hematopoietic stem cell survival, proliferation, and self-renewal. Cell Rep *7*, 1956-1967.

Wolf, N.S., and Trentin, J.J. (1968). Hemopoietic colony studies. V. Effect of hemopoietic organ stroma on differentiation of pluripotent stem cells. J Exp Med *127*, 205-214.

Worton, R.G., McCulloch, E.A., and Till, J.E. (1969a). Physical separation of hemopoietic stem cells differing in their capacity for self-renewal. J Exp Med *130*, 91-103.

Worton, R.G., McCulloch, E.A., and Till, J.E. (1969b). Physical separation of hemopoietic stem cells from cells forming colonies in culture. Cell Physiol *74*, 171-182.

Wu, A.M., Till, J.E., Siminovitch, L., and McCulloch, E.A. (1968). Cytological evidence for a relationship between normal hematopoietic colony-forming cells and cells of the lymphoid system. J Exp Med *127*, 455-467.

Wu, M., Kwon, H.Y., Rattis, F., Blum, J., Zhao, C., Ashkenazi, R., Jackson, T.L., Gaiano, N., Oliver, T., and Reya, T. (2007). Imaging hematopoietic precursor division in real time. Cell Stem Cell *1*, 541-554.

Yamamoto, R., Morita, Y., Ooehara, J., Hamanaka, S., Onodera, M., Rudolph, K.L., Ema, H., and Nakauchi, H. (2013). Clonal analysis unveils self-renewing lineage-restricted progenitors generated directly from hematopoietic stem cells. Cell *154*, 1112-1126.

Yang, L., Bryder, D., Adolfsson, J., Nygren, J., Mansson, R., Sigvardsson, M., and Jacobsen, S.E. (2005). Identification of Lin(-)Sca1(+)kit(+)CD34(+)Flt3- short-term hematopoietic stem cells capable of rapidly reconstituting and rescuing myeloablated transplant recipients. Blood *105*, 2717-2723.

Ye, M., and Graf, T. (2007). Early decisions in lymphoid development. Curr Opin Immunol *19*, 123-128.

Yokota, T., Huang, J., Tavian, M., Nagai, Y., Hirose, J., Zúñiga-Pflücker, J.C., Peault, B., and Kincade, P.W. (2006). Tracing the first waves of lymphopoiesis in mice. Development *133*, 2041-2051.

Yokota, T., Kouro, T., Hirose, J., Igarashi, H., Garrett, K.P., Gregory, S.C., Sakaguchi, N., Owen, J., and Kincade, P.W. (2003). Unique Properties of Fetal Lymphoid Progenitors Identified According to RAG1 Gene Expression. Immunity *19*, 365-375.

Yokota, T., Oritani, K., Butz, S., Ewers, S., Vestweber, D., and Kanakura, Y. (2012). Markers for Hematopoietic Stem Cells: Histories and Recent Achievements. In Advances in Hematopoietic Stem Cell Research, R. Pelayo, ed. (InTech).

Yona, S., Kim, K.W., Wolf, Y., Mildner, A., Varol, D., Breker, M., Strauss-Ayali, D., Viukov, S., Guilliams, M., Misharin, A*., et al.* (2012). Fate mapping reveals origins and dynamics of monocytes and tissue macrophages under homeostasis. Immunity *38*, 79-91.

Yoshida, T., Ng, S.Y., Zúñiga-Pflücker, J.C., and Georgopoulos, K. (2006). Early hematopoietic lineage restrictions directed by Ikaros. Nat Immunol *7*, 382-391.

Yoshimoto, M., Porayette, P., Glosson, N.L., Conway, S.J., Cardoso, A.A., Kaplan, M.H., and Yoder, M.C. (2012). Autonomous murine T cell progenitor production in the extra-embryonic yolk sac before HSC emergence. Blood *119*, 5706-5714.

Yoshimoto, M., Porayette, P., and Yoder, M.C. (2008). Overcoming obstacles in the search for the site of hematopoietic stem cell emergence. Cell Stem Cell *3*, 583-586.

Yu, H.M., Liu, B., Chiu, S.Y., Costantini, F., and Hsu, W. (2005). Development of a unique system for spatiotemporal and lineage-specific gene expression in mice. Proc Natl Acad Sci U S A *102*, 8615-8620.

Zanatta, D.B., Tsujita, M., Borelli, P., Aguiar, R.B., Ferrari, D.G., and Strauss, B.E. (2014). Genetic barcode sequencing for screening altered population dynamics of hematopoietic stem cells transduced with lentivirus. Mol Ther Methods Clin Dev *1*, 14052.

Zeigler, B., Sugiyama, D., Chen, M., Guo, Y., Downs, K.M., and Speck, N.A. (2006). The allantois and chorion, when isolated before circulation or chorioallantoic
fusion, have hematopoietic potential. Development *133*, 4183-4192.

Zhu, J., and Emerson, S.G. (2002). Hematopoietic cytokines, transcription factors and lineage commitment. Oncogene *21*, 3295-3313.

Zon, L.I. (1995). Developmental Biology of Hematopoiesis. Blood *86*, 2876-2891.